

Charging of Electric Vehicles at Commercial Buildings

A thesis submitted for the degree of
Doctor of Philosophy

Charalampos Marmaras

March 2017

**Cardiff University
School of Engineering**

Declaration

This work has not previously been accepted in substance for any degree and is not concurrently submitted in candidature for any degree.

Signed (candidate)

Date

Statement 1

This thesis is being submitted in partial fulfillment of the requirements for the degree of PhD.

Signed (candidate)

Date

Statement 2

This thesis is the result of my own independent work/investigation, except where otherwise stated. Other sources are acknowledged by explicit references.

Signed (candidate)

Date

Statement 3

I hereby give consent for my thesis, if accepted, to be available for photocopying and for inter-library loan, and for the title and summary to be made available to outside organisations *after expiry of a bar on access previously approved by the Graduate Development Committee*.

Signed (candidate)

Date

Copyright © 2017 Charalampos Marmaras.

Copies (by any process) either in full, or of extracts, may be made only in accordance with instructions given by the Author and lodged in the Library of Cardiff University. Details may be obtained from the Librarian. This page must form part of any such copies made. Further copies (by any process) of copies made in accordance with such instructions may not be made without the permission (in writing) of the Author. The ownership of any intellectual property rights which may be described in this thesis is vested with the author, subject to any prior agreement to the contrary, and may not be made available for use by third parties without his written permission, which will prescribe the terms and conditions of any such agreement.

to my family

Abstract

The objective of this thesis was to investigate the feasibility of EV charging management for reducing the electricity cost of commercial buildings.

A predictive model was developed to assist the commercial building manager reduce its energy bills by predicting the “triad” peak dates and the building’s energy demand. Real weather data were analysed and considered to increase the accuracy of the forecast. The model was evaluated using real “triad” peak, weather and energy consumption data from a commercial building facility in Manchester.

To enable the building manager reduce the EV charging costs, a charging control algorithm was developed and its impact on the demand profile and daily electricity cost of a commercial building facility were studied. The predictive model and the charging control algorithm were integrated into a cloud-based Local Energy Management System (LEMS) for the aggregation and flexible demand management of buildings, energy storage units and EVs. The operation of the LEMS was demonstrated through simulation scenarios using real data from a commercial building facility in Manchester.

To fully understand the EV integration consequences, the behaviour of the EV drivers and its impact on the road transport and electric power system has been studied. A multi-agent simulation model was developed to simulate the charging and routing behaviour of the EV drivers. The EV drivers were simulated as autonomous agents in a complex environment consisted of an electric power and road transport network. Different behavioural profiles were considered to describe the way an EV driver deals with the everyday challenges.

Acknowledgements

First of all, I would like to express my sincerest gratitude to my PhD supervisor Dr Liana M. Cipcigan for her continuous trust and support during my PhD. I would also like to thank my second PhD supervisor Prof Nick Jenkins for his patience and motivation during these years. The advice and encouragement I received from both my supervisors was invaluable to the completion of this thesis.

I would also like to thank my colleague and friend Dr. Erotokritos (Kriton) Xydias for his expertise and advice. The collaboration with him was an unforgettable experience. Special thanks go to my brother Christos and to my dear friend Mr. Marios Michas for their help and support during the last year of my PhD studies. Having them in Cardiff helped me in many ways. My thanks are extended to all my friends for being always there for me. I deeply value their friendship and belief in me.

Most importantly, none of this would have been possible without the love and patience of my family. My parents, sister and brothers to whom this thesis is dedicated to, have been a constant source of love, concern, support and strength all these years. Their unfailing support and continuous encouragement made this accomplishment possible.

Contents

Abstract	ix
Acknowledgements	xi
Contents	xiii
List of Publications	xix
List of Figures	xxiii
List of Tables	xxix
List of Algorithms	xxxi
List of Acronyms	xxxiii
1 Introduction	1
1.1 Integration of Electric Vehicles	1
1.1.1 Electric Vehicles	1
1.1.2 Future Uptake of Electric Vehicles	2
1.1.3 Impact of EV battery charging	4

1.2	Problem Statement	5
1.3	Thesis Objectives	8
1.4	Thesis Structure	9
2	Predicting the energy demand of buildings during triad peaks in GB	11
2.1	Introduction	11
2.2	Literature Review	13
2.3	Model Description	17
2.3.1	Model Inputs	18
2.3.2	Triad Probability Assessment model	19
2.3.3	Pre-Forecast Analysis model	22
2.3.4	Electricity Demand Forecast model	25
2.4	Model Results	27
2.4.1	Triad Probability Assessment	27
2.4.2	Pre-Forecast Analysis	30
2.4.3	Electricity Demand Forecast	33
2.5	Model Validation	34
2.6	Summary	40
3	Management of EV charging at commercial buildings	41
3.1	Introduction	41
3.2	Literature Review	43
3.3	Charging Control Model	46
3.3.1	Off-Peak Strategy	47
3.3.2	Cost-Reduction Strategy	49

3.3.3	Control Algorithm	49
3.4	Charging Control Model with V2B	52
3.4.1	Off-Peak Strategy	52
3.4.2	Cost Reduction Strategy	53
3.4.3	Control Algorithm	54
3.5	Description of the simulation scenario	57
3.6	Simulation results	61
3.6.1	Impact on the demand profile	61
3.6.2	Impact on the daily electricity cost	66
3.6.3	Additional unintended consequences	67
3.6.4	Additional case studies	69
3.7	Summary	71
4	A Local Energy Management System for the building manager	73
4.1	Introduction	73
4.2	Literature Review	75
4.3	Description of the LEMS	78
4.3.1	Architecture	78
4.3.2	Peak Shaving Schedule	81
4.3.3	Triad Cost Reduction Schedule	83
4.3.4	Demand Response Schedule	83
4.3.5	Operational Workflow	84
4.4	Demonstration of the LEMS	86
4.4.1	Deployment on Cloud	86

4.4.2	Simulated Scenarios	88
4.5	Experimental Results	88
4.5.1	Scenario 1: Peak Shaving Operation	88
4.5.2	Scenario 2: Triad Cost Reduction Operation	91
4.5.3	Scenario 3: Demand Response Operation	93
4.5.4	Using LEMS to explore different simulation scenarios	96
4.6	Summary	98
5	Simulation of EV driver behaviour in road transport and electric power networks	101
5.1	Introduction	101
5.2	Literature Review	103
5.3	The EV agent's architecture	104
5.4	Modelling the environment of the EV agent	105
5.4.1	The Road Transport Network	105
5.4.2	The Electricity Grid	109
5.5	Modelling the characteristics of the EV agent	113
5.5.1	The EV agent's battery	113
5.5.2	The EV agent's energy consumption	115
5.6	Modelling the behaviour of the EV agent	118
5.6.1	The behavioural profiles of the EV agent	118
5.6.2	Interactions with the Road Transport network	120
5.6.3	Interactions with the Electricity Grid	124
5.7	Case Study	128

5.7.1	Description of the simulation scenarios	128
5.7.2	Simulation Results	128
5.8	Summary	133
6	Conclusions and Suggestions for Further Work	135
6.1	Thesis Contributions	135
6.2	Overview of Chapter 2	136
6.2.1	Summary	136
6.2.2	Conclusions	136
6.2.3	Limitations and suggestions for further work	137
6.3	Overview of Chapter 3	137
6.3.1	Summary	137
6.3.2	Conclusions	138
6.3.3	Limitations and suggestions for further work	138
6.4	Overview of Chapter 4	139
6.4.1	Summary	139
6.4.2	Conclusions	140
6.4.3	Limitations and suggestions for further work	140
6.5	Overview of Chapter 5	141
6.5.1	Summary	141
6.5.2	Conclusions	141
6.5.3	Limitations and suggestions for further work	142
6.6	Overall Research Benefit	142

A Electricity demand and weather data used in Chapter 2	145
A.1 Electricity Demand Data	145
A.2 Weather Data	147
B Matlab code used in Chapter 2	153
B.1 Matlab Code	153
C Management of EV charging at residential buildings	157
C.1 Description of the simulation scenario	157
C.2 Simulation results	161
C.2.1 Impact on the demand profile	161
C.2.2 Impact on the daily electricity cost	164
C.2.3 Additional unintended consequences	165
D Matlab code used in Chapter 4	167
D.1 Matlab Code	167
E The developed model for the battery pack of the EV agents	185
E.1 The battery pack model	185
F Implementation of the charging / discharging procedure of the EV chargers in SeSAm	193
F.1 The charging/discharging process	193
G The developed multi-agent simulation model in SeSAm	197
G.1 Screenshots from SeSAm	197
Bibliography	203

List of Publications

The following papers have been accepted for publication or published based on work done for this thesis, work done within the framework of the doctorate degree, or collaboration with other researchers.

JOURNAL PAPERS

1. C. Marmaras, A. Javed, L. M. Cipcigan and O. Rana, *Predicting the energy demand of buildings during triad peaks in GB*, Energy and Buildings, Volume 141, Pages 262–273, April 2017
2. C. Marmaras, E. Xydas and L. M. Cipcigan, *Simulation of EV driver behaviour in road transport and electric power networks*, article in press, Elsevier Journal of Transportation Research Part C: Emerging Technologies, Special Issue on Technologies and Control for Sustainable Transportation.
3. E. Xydas, C. Marmaras, and L. M. Cipcigan, *A multi-agent based scheduling algorithm for adaptive electric vehicles charging*, Applied Energy, Volume 177, Pages 354–365, September 2016.
4. E. Xydas, C. Marmaras, L. M. Cipcigan, N. Jenkins, S. Carroll, and M. Barker, *A data-driven approach for characterising the charging demand of electric vehicles: A UK case study*, Applied Energy, Volume 162, Pages 763–771, January 2016.
5. E. Xydas, M. Qadrdan, C. Marmaras, L. M. Cipcigan and N. Jenkins, *Probabilistic Wind Power Forecasting and its Application in the Scheduling of Gas-fired Generators*, Applied Energy, Volume 192, Pages 382–394, April 2017.

BOOK CHAPTERS

6. C. Marmaras, E. Xydas, L. M. Cipcigan, O. Rana, and F. Klügl, *Electric Vehicles in Road Transport and Electric Power Networks*, in *Autonomic Road Transport Support Systems*, Springer International Publishing, 2016, pp. 233–252.
7. E. Xydas, C. Marmaras, L. M. Cipcigan, and N. Jenkins, *Smart Management of PEV Charging Enhanced by PEV Load Forecasting*, in *Plug In Electric Vehicles in Smart Grids*, Springer, 2015, pp. 139–168.

CONFERENCE PAPERS

8. C. Marmaras, A. Javed, O. Rana and L. M. Cipcigan, *A cloud-based energy management system for building managers*, in the 8th ACM/SPEC on International Conference on Performance Engineering Companion (ICPE), 2017, pp. 61–66.
9. C. Marmaras, E. Xydas, L. M. Cipcigan, and O. Rana, *An integrated approach for simulating EVs in transport and electric power networks*, in 2014 International Conference on Connected Vehicles and Expo (ICCVE), 2014, pp. 185–190.
10. C. Marmaras, M. Corsaro, E. Xydas, L. M. Cipcigan, and M. A. Pastorelli, *Vehicle-to-building control approach for EV charging*, in 2014 49th International Universities Power Engineering Conference (UPEC), 2014, pp. 1–6.
11. A. Javed, O. Rana, C. Marmaras and L. M. Cipcigan, *Fog paradigm for local energy management systems*, in 3rd International Workshop on Energy-aware Simulation (ENERGY-SIM), 2017, pp. 1-10.
12. R. O. Oliyide, C. Marmaras, E. Xydas, and L. M. Cipcigan, *Estimating the true GHG emissions reduction due to electric vehicles integration*, in 2015 50th International Universities Power Engineering Conference (UPEC), 2015, pp. 1–5.
13. M. De Marco, E. Xydas, C. Marmaras, L. M. Cipcigan, M. Repetto, and M. Fantino, *Technical impacts of electric vehicles charging in an Italian distribution network*, in CIRED Workshop, 2014, pp. 1–5.

14. A. S. Hassan, A. Firrincieli, C. Marmaras, L. M. Cipcigan, and M. A. Pastorelli, *Integration of electric vehicles in a microgrid with distributed generation*, in 2014 49th International Universities Power Engineering Conference (UPEC), 2014, pp. 1–6.
15. J. Su, C. Marmaras, and E. Xydas, *Technical and environmental impact of electric vehicles in distribution networks*, in 2014 International Conference and Utility Exhibition on Green Energy for Sustainable Development (ICUE), 2014, pp. 1–9.
16. R. Tolosana-Calasan, J. A. Banares, O. Rana, C. Pham, E. Xydas, C. Marmaras, P. Papadopoulos, and L. Cipcigan, *Enforcing Quality of Service on OpenNebula-Based Shared Clouds*, in 2014 14th IEEE/ACM International Symposium on Cluster, Cloud and Grid Computing, 2014, pp. 651–659.
17. E. S. Xydas, C. Marmaras, L. M. Cipcigan, A. S. Hassan, and N. Jenkins, *Forecasting Electric Vehicle charging demand using Support Vector Machines*, in 2013 48th International Universities Power Engineering Conference (UPEC), 2013, pp. 1–6.
18. E. Xydas, C. Marmaras, A. S. Hassan, L. M. Cipcigan, and N. Jenkins, *Electric Vehicle Load Forecasting using Data Mining Methods*, in Hybrid and Electric Vehicles Conference 2013 (HEVC 2013), 2013, pp. 10.1–10.1.
19. A. S. Hassan, E. S. Xydas, C. Marmaras, L. M. Cipcigan, and N. Jenkins, *Integrating renewable energy with flexible storage systems: A case study of GB and Greece*, in 2013 48th International Universities Power Engineering Conference (UPEC), 2013, pp. 1–6.
20. A. S. Hassan, C. Marmaras, E. S. Xydas, L. M. Cipcigan, and N. Jenkins, *Integration of wind power using V2G as a flexible storage*, in IET Conference on Power in Unity: a Whole System Approach, 2013, pp. 1.11–1.11.
21. E. L. Karfopoulos, C. E. Marmaras, and N. Hatziargyriou, *Charging control model for Electric Vehicle Supplier Aggregator*, in 2012 3rd IEEE PES Innovative Smart Grid Technologies Europe (ISGT Europe), 2012, pp. 1–7.

List of Figures

1.1	Evolution of the global electric car stock from 2010 to 2015 [1]	3
1.2	Deployment scenarios for the stock of electric cars to 2030 [1]	3
2.1	The Triad Demand Predictive Model	18
2.2	The Pre-Forecast Analysis process	23
2.3	The daily probability distribution for “triad” peaks	28
2.4	The 5-days probability distribution for “triad” peaks	28
2.5	The half-hourly probability distribution for “triad” peaks in a day	30
2.6	Weather sensitivity analysis for all buildings	32
2.7	Electricity demand forecast for all buildings	34
2.8	The actual “triad” peak days of 2014/2015 compared to the calculated daily probability distribution	35
2.9	The actual “triad” peak days of 2014/2015 compared to the calculated 5-day probability distribution	35
2.10	Percentage of predicted “triad” peaks for different interval sizes	36
2.11	Number of generated “triad” warnings for different interval sizes	36
2.12	The actual “triad” peak half-hours of 2014/2015 compared to the calcu- lated half-hourly probability distribution	38

2.13	Forecasted and actual power demand for all buildings	39
2.14	Error of power demand forecast for all buildings	39
3.1	The stages of the EV coordination	47
3.2	The <i>Schedule</i> stage of the charging control model	51
3.3	The <i>Schedule</i> stage of the charging control model with V2B	56
3.4	The typical power demand of an office building	57
3.5	Probability distribution of arrival times at workplace	58
3.6	Probability distribution of departure times from workplace	59
3.7	Probability distribution of travelled distance before workplace	59
3.8	The daily electricity prices	60
3.9	The modified UK Generic Low Voltage Distribution Network	61
3.10	Impact of Uncontrolled EV charging	63
3.11	Impact of EV charging with the Off-Peak Strategy	64
3.12	Impact of EV charging with the Cost-Reduction Strategy	65
3.13	Increase of the daily electricity cost comparing to the case without EV charging	66
3.14	Minimum bus voltage with Off-Peak strategy	67
3.15	Minimum bus voltage with Cost-Reduction strategy	68
3.16	Impact of EV charging for different levels of Unresponsive EVs	70
4.1	The architecture of the LEMS	79
4.2	The workflow chart of the LEMS	85
4.3	The adopted distributed architecture	87
4.4	The aggregated demand of the building facility	90

4.5	Demand of the facility with Peak Shaving Operation	90
4.6	The power set points sent to the EVs	91
4.7	The power set points sent to the ESUs	91
4.8	The electricity prices and the predicted triad peak hours	92
4.9	Demand of the facility with Triad Cost Reduction Operation	93
4.10	The power set points sent to the EVs	93
4.11	The power set points sent to the ESUs	94
4.12	The demand response requests	94
4.13	Demand of the facility with Demand Response Operation	95
4.14	The power set points sent to the EVs	95
4.15	The power set points sent to the ESUs	96
4.16	Demand of the facility with Peak Shaving Operation	97
4.17	Demand of the facility with Triad Cost Reduction Operation	97
4.18	Demand of the facility with Demand Response Operation	98
5.1	The architecture of the modelled EV agent	105
5.2	The topology of the Road Transport Network	106
5.3	The fundamental diagrams assumed in this work	108
5.4	The topology of the modelled electricity network in SeSAm	110
5.5	Generated discharge characteristics for the battery pack	115
5.6	EV power consumption versus EV driving speed	118
5.7	The battery voltage, charge current and SoC of the EV battery, and the power demand of the EV charger	125
5.8	Impact of EV charging at Home (aggregated)	129

5.9	Distribution of Public EV charging demand to the districts	130
5.10	Traffic distribution on avenue A1_2	131
5.11	Average traffic distribution of EVs on all avenues	132
A.1	The daily electricity demand of Building 1	145
A.2	The daily electricity demand of Building 2	146
A.3	The daily electricity demand of Building 3	146
A.4	The daily electricity demand of Building 4	146
A.5	The daily electricity demand of Building 5	147
A.6	The daily electricity demand of Building 6	147
A.7	The total amount of cloud in octas	148
A.8	The cloud base distance in meters	148
A.9	The mean wind speed in knots	148
A.10	The mean wind direction in degrees	149
A.11	The daily maximum gust in knots	149
A.12	The mean air temperature in degrees Celsius	149
A.13	The rainfall in mm	150
A.14	The hourly global radiation in kJm^2	150
A.15	The relative humidity in %	150
A.16	The daily sunshine hours	151
C.1	The typical power demand of a house	157
C.2	The UK Generic Low Voltage Distribution Network	158
C.3	Probability distribution of arrival times at home	160
C.4	Probability distribution of departure times from home	160

C.5	Probability distribution of travelled distance before home	160
C.6	Impact of Uncontrolled EV charging	161
C.7	Impact of EV charging with the Off-Peak Strategy	162
C.8	Impact of EV charging with the Cost-Reduction Strategy	163
C.9	Increase of the daily electricity cost comparing to the case without EV charging	164
C.10	Minimum bus voltage with Off-Peak strategy	165
C.11	Minimum bus voltage with Cost-Reduction strategy	166
E.1	Typical Discharge Curve of a battery	186
E.2	Discharge characteristics of the 18650 Li-Ion battery cell (from [2])	188
E.3	Generated and actual discharge characteristics for the 18650 Li-Ion bat- tery cell	189
E.4	The 11S 9S 69P configuration	190
E.5	Generated discharge characteristics for the battery pack	192
G.1	The structure of the developed model in SeSAm	198
G.2	The reasoning engine of the EV agent in SeSAm	199
G.3	EV agents on the road network during simulation	199
G.4	EV agent characteristics during simulation	200
G.5	Power demand from Public Charger entities during simulation	200
G.6	Power demand from Transformer entities during simulation	201
G.7	Traffic of Avenue entities during simulation	201

List of Tables

2.1	Mean Absolute Error (MAE) for every technique	26
2.2	Correlation matrix of weather attributes with daily energy consumption	30
2.3	The actual “triad” peak dates and times of 2014/2015	34
3.1	Parameters of the normal distributions for <i>BC</i> and <i>MEC</i>	60
3.2	The technical characteristics of the network	62
4.1	EV and ESU assumptions	89
5.1	Battery pack specifications	114
5.2	Data used in the power consumption calculations	117
5.3	The characteristics of the EV chargers	124
5.4	The distribution of the times spent for each activity	128
C.1	The technical characteristics of the network	159
E.1	18650 Li-Ion battery cell specifications (from [2])	188
E.2	Parameters of the 18650 Li-Ion battery cell	189
E.3	Parameters of the battery pack	191

List of Algorithms

2.1	Algorithm of the “Electricity Demand Forecast” model	26
-----	--	----

List of Acronyms

AC Alternate Current

ANN Artificial Neural Network

ASHRAE American Society of Heating, Refrigerating, and Air-Conditioning Engineers

BEMS Building Energy Management System

BEV Battery Electric Vehicle

CC Constant Current

CHP Combined Heat and Power

CI Computational Intelligence

CPU Central Processing Unit

CV Constant Voltage

DC Direct Current

DER Distributed Energy Resources

DG Distributed Generation

DNO Distribution Network Operator

DOE Department of Energy

EV Electric Vehicle

ESU Energy Storage Unit

FL Fuzzy Logic

GA Genetic Algorithms

GB Great Britain

HEV Hybrid Electric Vehicle

HV High Voltage

HVAC Heating, Ventilation and Air-Conditioning

ICE Internal Combustion Engine

IEA International Energy Agency

ISO International Organization for Standardization

LEMS Local Energy Management System

LV Low Voltage

MAPE Mean Absolute Percentage Error

MAS Multi-Agent System

MV Medium Voltage

NIST National Institute of Standards and Technology

NTS National Travel Survey

PALM Poisson Arrival Location Model

PHEV Plug-in Hybrid Electric Vehicle

PV Photovoltaic

SoC State of Charge

SVM Support Vector Machines

TNUoS Transmission Network Use of System

TOC Time of Use

UK United Kingdom

UKERC UK Energy Research Centre

US United States

V2B Vehicle to Building

V2G Vehicle to Grid

V2m Vehicle to microgrid

Introduction

1.1 Integration of Electric Vehicles

1.1.1 Electric Vehicles

Electric Vehicles (EVs) use electric machines to drive their wheels. They derive some or all of their power from rechargeable batteries. The distance an EV can drive between recharges is known as its range. There are three different categories of EVs: battery electric, plug-in hybrid and hybrid electric vehicles.

Battery Electric Vehicles

The Battery Electric Vehicles (BEVs), also known as the all-electric or the pure-electric vehicles, are powered solely by an electric machine and have no internal combustion engine (ICE). Their battery is charged entirely by electricity from the grid. As the battery is their sole power source, BEVs tend to be equipped with powerful lithium-ion batteries with a capacity of typically 20 kWh or more than 50kWh for high performance (luxury) models. Some common examples of the BEV are: the BMW i3, the Renault Zoe, the Tesla Model S and the Nissan Leaf.

Plug-in Hybrid Electric Vehicles

Plug-in Hybrid Electric Vehicles (PHEVs) have an ICE and a small battery, typically lithium-based, that can either be charged by the ICE or directly from the grid. They are able to run on electric power alone, at urban speeds, for short distances and have an all-electric range of 5 to 40 miles. When the all-electric range reaches its range limit, the

ICE provides the necessary power. The PHEV addresses the range issues of the BEV by combining the electric machine and battery with the combustion engine. Examples include: the Toyota Prius Plug-in Hybrid and the Chevrolet Volt.

Hybrid Electric Vehicles

The Hybrid Electric Vehicles (HEVs) used to be known simply as the “hybrid” or the “full hybrid” but nowadays are often referred to as the “conventional hybrid”. They have a battery which is charged by the ICE but not from an external source of electricity. Typically, they are capable of pure electric drive at low speeds and for a very limited range. Terms like “parallel hybrid”, “series hybrid” (or “range-extended electric vehicle”), and “mixed hybrids” describe sub-categories of HEVs, involving different configurations of batteries and ICEs. Some common examples of the HEV are the early versions of the Toyota Prius, Honda Insight and Honda Civic Hybrid.

1.1.2 Future Uptake of Electric Vehicles

In 2015 the global threshold of 1 million electric cars on the road was exceeded, counting 1.26 million EVs. This is an important achievement which highlights the significant efforts deployed by governments and industry over the past ten years. This becomes even more remarkable, considering that in 2014 only half of that number existed while in 2005 EVs were still measured in hundreds.

Ambitious targets and policy support have decreased the vehicle costs, extended vehicle range and reduced consumer barriers in a number of countries. The market shares of electric cars rose above 1% in seven countries in 2015: Norway, the Netherlands, Sweden, Denmark, France, China and the United Kingdom. Market shares reached 23% in Norway and nearly 10% in the Netherlands. China’s growing electric car sales in 2015 made it the main market worldwide, before the United States, for the first time. China is also home to the strongest global deployment of e-scooters and electric buses.

EVs of all types lie at the heart of future sustainable transport systems, alongside the optimisation of urban structures to reduce trip distances and shift mobility towards public transportation. The wide global deployment of EVs across all modes is neces-

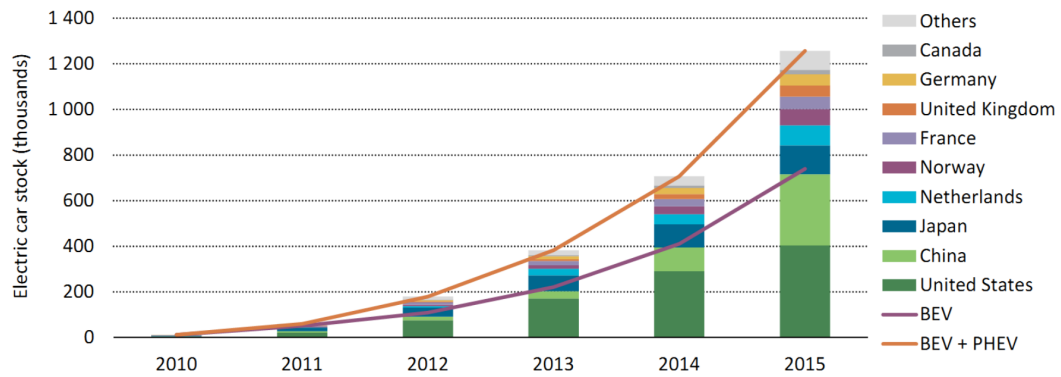
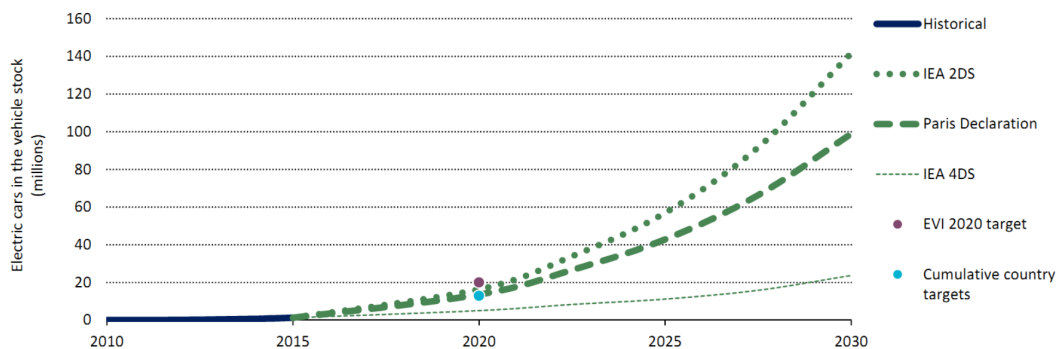


Figure 1.1: Evolution of the global electric car stock from 2010 to 2015 [1]

sary to meet sustainability targets. The EVI 20 by 20 target calls for an electric car fleet of 20 million by 2020 globally [1]. The Paris Declaration on Electro-Mobility and Climate Change and Call to Action sets a global deployment target of 100 million electric cars and 400 million electric 2- and 3-wheelers in 2030. The IEA 2DS, describing an energy system consistent with an emissions trajectory giving a 50% chance of limiting average global temperature increase to 2°C, outlines an even more ambitious deployment pathway for electric cars by 2030 (150 million). Meeting these targets implies substantial market growth to develop further the current 1.26 million electric car stock, as well as the swift deployment of electric 2-wheelers and buses beyond the Chinese market.



Note: 2DS = 2°C Scenario; 4DS = 4°C Scenario.

Figure 1.2: Deployment scenarios for the stock of electric cars to 2030 [1]

1.1.3 Impact of EV battery charging

The emergence of electric mobility is an important development for the power sector. While the adoption of EVs can provide new opportunities - such as creating additional electricity sales for utilities and a demand for charging infrastructure and related services - the charging of EVs at a large scale can also create challenges for local distribution grids and their operators, if not properly managed.

The challenge posed by the increasing use of electricity by EVs lies not so much in the volume of the associated power demand, but rather in the potential increase in peak demand, which is determined by the rate, time, and location of EV charging. Fast-charging (i.e., charging at a higher power) will have a more significant impact on the grid than slow-charging. The time of charging (i.e., when charging happens) also impacts the grid: throughout the day, electricity demand follows a load curve; when EV drivers charge their cars can either intensify peaks or level them out. Finally, the location of the charging (where charging takes place) has implications for the power infrastructure (considering the available grid capacity and infrastructure). If all the registered vehicles in United States had to charge 5-10kWh on a daily basis, this would lead to an increase of 12-23% at the electricity generation requirement [3]. In UK, an uncontrolled EV charging regime increases the British winter day peak demand by 3.2 GW (3.1%) for a low EV uptake case (7%) and the British winter day peak demand by 37GW (59.6%) for a high EV uptake case (48.5%), for the year 2030 [4, 5].

Depending on the system's peak demand, a different generation mix is used to meet the demand. As the demand increases, more expensive generator units are included in the generation mix, increasing the generation cost per kWh. If the system's peak demand exceeds the network capacity, the system will face voltage-drops, power losses increase and overloading of distribution transformers [6]. Overloaded transformers and feeder cables have to be upgraded to maintain the normal operation of the network. This network reinforcement will require large capital investments from the distribution network operators. A tool to calculate these additional costs was developed in project Green eMotion (<http://www.greenemotion-project.eu/>) by Imperial College London. It was found that the incremental annualised cost of electricity supply

per EV in UK and Ireland could be around €200/EV/year for EV penetration levels between 5% and 30%, consisting mainly from operational and capital costs at the distribution level [7].

1.2 Problem Statement

The market penetration rates of electric vehicles are still rather low [8] despite the number of public programs launched to promote their use (e.g. [9, 10]). Among the most important reasons are low battery performance and lack of charging infrastructure implying limited and uncertain driving ranges - the so-called range-anxiety [8, 11–15]. While residential charging is the foreseen primary option even though limitations can exist in large apartment buildings, commercial charging opportunities are gaining increasing attention as the major secondary option [16, 17].

The installation of EV charging points at commercial buildings requires a significant up-front cost, discouraging the building managers to make this investment. To tackle with this issue, the U.S. Department of Energy (DOE) launched the program “Workplace Charging (WPC) Challenge” in 2013 [18], “with a goal of achieving a tenfold increase in the number of U.S. employers offering workplace charging in the next five years”. In 2016, the Office for Low Emission Vehicles (OLEV) in UK initiated a voucher-based grant scheme for the installation of electric vehicle charging infrastructure. The scheme provides support towards the up-front costs of the purchase and installation of electric vehicle charge-points, for eligible businesses, charities and public sector organisations [19].

However, the charging service provision at commercial buildings creates a number of costs for the building manager. Apart from the initial installation cost that is necessary, the use of EV charging facilities impacts the demand profile of the buildings, and creates additional operational costs which need to be covered. These costs are associated with the impact of EV charging on the daily peak demand and energy requirements of the building facility.

The contribution of the building’s peak demand to the system’s peak demand is used

by National Grid to apply charges for the Use of the Transmission Network in the period between November to February (“triad season”) each year [20]. The charges, known as “triad” charges, are currently (approximately) £45/kW, meaning that a commercial facility with an average consumption of 2MW would create an additional cost of £90,000 every year to the building manager for its contribution to the system’s peak demand. However, the “triad” charges of each year are announced by National Grid after the end of the “triad season”, usually sometime in March. Recent studies indicate that the “triad” charges are going to increase in the following years, and could reach £72/kW by 2020 [21]. Consequently, there is a great deal of interest from the building managers to know beforehand the “triad” periods so they can reduce their electricity consumption and their bills [22].

The energy requirements of EV charging are reflected on the building manager’s electricity bills. In cases where a variable electricity rate is applied to the building facility, the cost of EV charging demand varies [23]. In commercial buildings, EVs are expected to charge as soon as they arrive at the building facility [24]. This uncontrolled EV charging is not a cost-effective solution for the building manager as the EV charging events could occur during the expensive hours. Additionally, the uncontrolled EV charging demand will increase the peak demand of the building and force the building managers to upgrade their private network (such as transformers and cables) [6]. On a larger scope, the commercial building sector accounts for approx. 31% of the total energy demand in UK [25], and high EV uptake levels will stress the existing infrastructure of the distribution networks, resulting in additional costs for the DNOs. Considering that in most cases the actual charging duration (time needed to charge the EV) is less than the connection duration (time that the EV is parked, connected to the charging point), EVs offer a flexibility that can benefit both the building manager and the DNOs. This flexibility could be enhanced by utilising bi-directional energy exchanges from EVs and energy storage units [26]. In this case however, the system’s complexity is increased and the building managers will have to cope with the intermittent characteristics of the different elements of the building facility (arrival times of EVs, charging duration needed, capacity of the storage units etc.) [27]. To this end, an energy management system is required in order to coordinate the EV charging and

minimise the electricity bill of the building manager.

The EV charging demand is related to the routing and charging behaviour of the EV drivers. The travelled distance affects the energy consumption of the EV and consequently the necessary charging requirements. The availability of EV charging facilities affects the route choice behaviour of the EV drivers, as they modify their trip in order to include a recharging stop [28]. As a result, the traffic of the road network will be affected. The charging behaviour of EV drivers affects the frequency and duration of their recharging demand. According to [29], the average EV charging demand in different areas has a different daily profile depended on the charging station location and rate. EV drivers with a strong range anxiety feeling are expected to charge more often compared to EV drivers that feel more confident regarding the range of their EV [13, 14]. However, an increased battery capacity and availability of charging points was found to reduce the frequency of charging at non-residential public stations [17]. Technological developments improving the driving range of EVs, as well as an increasing availability and speed of charging infrastructure, could change the routing and charging behaviour of the EV drivers, as well as the need for charging infrastructure in the future. To fully understand the EV integration consequences, the behaviour of the EV drivers and its impact on both the electricity and road transport network should be modelled.

1.3 Thesis Objectives

This thesis investigates the feasibility of EV charging management for reducing the electricity cost of commercial buildings. To this end, the following objectives were set:

1. Design a model that predicts the “triad” peaks of the grid and the energy demand of a building. The developed model generates warnings for expected “triad” peaks, allowing the building manager to reduce their electricity demand during expensive hours.
2. Develop an algorithm to schedule the EV charging in commercial buildings. The developed algorithm utilises bi-directional power exchanges and the flexibility offered by EVs in order to reduce the cost of EV charging at a commercial building facility.
3. Design a local energy management system (LEMS) that coordinates the charging of EVs and energy storage in commercial building facilities. The LEMS is developed as a generic software package to operate on the cloud, and was tested in different scenarios.
4. Develop a tool that simulates the charging and routing behaviour of EV drivers on a given electricity and road transport network. The tool is built on a multi-agent simulation platform and the EV drivers are modelled as autonomous agents having to cope with constraints from the EV battery, the electricity grid and road transport network.

1.4 Thesis Structure

This thesis is structured in the following way:

Chapter 2: A predictive model is described that aims to assist the commercial building manager to reduce its energy bills by predicting the “triad” peak dates and the building’s energy demand on those dates. The model is validated using real weather and building energy consumption data from commercial buildings at a science park.

Chapter 3: A charging control algorithm is described to enable the building manager reduce the EV charging costs of a building facility. The charging control algorithm is simulated on a realistic charging scenario and the impact on the demand profile and daily electricity cost of a commercial building are studied.

Chapter 4: A Local Energy Management System (LEMS) is described for the aggregation and flexible management of the demand from buildings, energy storage and EVs. The LEMS is developed as a software package deployed on cloud, and tested in three scenarios.

Chapter 5: A multi-agent simulation model is developed to simulate the charging and routing behaviour of the EV drivers. The EV drivers are simulated as autonomous agents in a complex environment consisted of an electric power and road transport network. Different behavioural profiles are considered to describe the way an EV driver deals with the everyday challenges.

Chapter 6: The main conclusions of this thesis are summarised. Limitations and suggestions for further work are given.

Predicting the energy demand of buildings during triad peaks in GB

2.1 Introduction

The “triad season” is the four-month period from 1st of November to the end of February, during which National Grid looks back to find the three half-hour periods when the electricity demand was highest in GB [30]. These three periods, also known as “triad” periods, must be separated by at least ten days and are used by National Grid to estimate the average peak demand of each distribution network operator (DNO) for that winter. According to its corresponding peak demand, each DNO pays then a “capacity charge” to National Grid to ensure the availability of this peak amount of electricity [20]. These capacity costs are shifted from the DNOs to the electricity suppliers, and the electricity suppliers transfer this cost to their customers (end-users) by charging extra for the electricity used during a “triad” period.

The domestic low-consumption customers have this extra charge built into an all-inclusive electricity rate so they don’t notice any difference at their electricity charges on a “triad” period. On the other hand, the high-consumption customers (usually commercial/industrial) may be charged a higher rate of £/MWh for the electricity they use during the “triad” periods. Depending on their agreement with the utility company, they might even be separately invoiced for these charges. These charges are currently (approximately) £45/kW, meaning that a high-consumption consumer with an average consumption of 2MW would have to pay £90,000 every year for their

contribution to the system's peak demand. The "triad" periods of each year are announced by National Grid after the end of the "triad season", usually sometime in March. Recent studies indicate that the "triad" charges are going to increase in the following years, and could reach £72/kW by 2020 [21]. Consequently, there is a great deal of interest from the high-consumption customers to know beforehand the "triad" periods so they can reduce their electricity consumption and their bills [22]. A typical case is that of Saint-Gobain which, in order to tackle the "triad" cost, switched off some machinery and rescheduled the factory operation for a short period of time from around 4pm-6pm, the period which is most likely to witness a "triad" peak. By doing this the company was able to save around 11% of energy costs (equating to a financial value of £165,000) [31].

Many suppliers offer warning services to their customers in order to help them reduce their "triad" charges (e.g. NPower [32]). Predicting the "triad" peaks meets a number of challenges, one of them being the so-called "negative feedback" problem according to which knowing about a "triad" could in fact prevent it [33]. The "triad" peaks are mainly caused by the small commercial buildings and domestic houses, rather than the large commercial/industrial consumers. Consequently "triad" peaks are largely dependent on weather, and they usually coincide with cold snaps [6]. Unfortunately that means that "triad" peaks are more unpredictable in mild winters. Considering the complexity associated with predicting "triads", probabilistic approaches can be utilised for estimating the "triad" peaks. There is a need for a tool that decodes these "fuzzy" correlations in a simple yet effective manner, and could be operated from the (non-expert) building manager.

However, having information about the future "triad" peaks is not enough for the building managers to reduce their bills. Information about the electricity demand of their buildings on a "triad" period is also necessary, in order to identify the buildings that contribute the most to these extra charges. Knowing the future demand of their buildings, the building managers can identify the ones which operate with unnecessary loads and reduce their electricity consumption. The weather has a significant impact on the electricity demand of a building, as heating during this period could lead

to increase in their energy consumption. In order to predict the energy consumption of a building, it is necessary to take into account the local weather.

In this chapter a predictive model is proposed that aims to assist the commercial building manager to reduce its energy bills by predicting the “triad” peak dates and the building’s energy demand on those dates. The model consists of three stages/parts. In the first part, a stochastic model was developed to predict the triad days and hours for the next year. In the second part a sensitivity analysis was performed in order to calculate the impact of weather on the electricity demand of a commercial building. In the last part, a forecasting model was developed using Artificial Neural Networks (ANN) to forecast the building’s energy demand at the most probable half hour a “triad” could occur. The model was evaluated using real weather and building energy consumption data from commercial buildings at a science park.

2.2 Literature Review

Forecasting the peak electricity demand has been studied extensively in the past by many researchers. The applied forecasting models are usually characterized by their time horizon: i) short-term forecasts (five minutes to one week ahead) for ensuring system stability, ii) medium-term forecasts (one week to six months ahead) for maintenance scheduling, and iii) long-term forecasts (six months to ten years ahead) for network planning. Other factors used to evaluate these models are their computational cost, calibration complexity and size of dataset required.

Semi-parametric regression models have been found to perform well with time-series datasets with missing data, as they use parameters (estimators based on distribution assumptions) to estimate the missing values [34, 35]. However the configuration of those parameters is difficult and their accurate calibration requires a large dataset. Non parametric regression models such as time varying splines on the other hand, are not based on distribution assumptions [36, 37]. The degree of confidence of the forecast however is depended on the quality and the size of the dataset. Time series modelling is much easier to implement, and decodes accurately the trend of the time

series [38]. Decomposition techniques are often used in such models to recognise underlying patterns and increase the forecasting accuracy. Depended on the resolution of the data however, these models can be susceptible to noise and abnormal events that differ from the trend [39–41]. Exponential smoothing techniques have been found to give very accurate results in short-term forecast applications, require very limited information and are easy to apply [42]. However, they do not perform well when there is an underlying pattern in the dataset, such as seasonal variation, making them inappropriate for medium and long term forecasts. Artificial neural networks have a proven record of accurate forecasts in various time horizons [43, 44]. Although their training is slow, the time needed for the forecast is very fast. Their configuration however is very complicated and usually parametric studies are needed to calibrate the model. This drawback is intensified in applications with a large degree of uncertainty or when a confidence interval is needed. Grey dynamic models can perform better when there is large uncertainty among the dataset as they combine quantitative and qualitative information [45]. However, if the historical information is not fully available (e.g. missing values) their performance is reduced significantly. Judgemental forecasting techniques show a fast adaptability to changes in the underlying trend at a small computational cost [46]. However, their strong dependence on qualitative information can lead to biased forecasts, and usually expert input is needed for their calibration.

While a point forecast provides an estimate of the expected value of the future demand, probabilistic forecasts contain additional valuable information. Having access to prediction intervals, such as a lower and upper boundary of the forecast distribution [45] or a prediction density [47], would inform the decision maker of the uncertainty inherent in the forecast. Quantification of this forecast uncertainty is essential for managing the risk associated with decision making. Bayesian statistics have been found to perform well without requiring a large dataset [48, 49]. However they are computationally intensive and are not suitable for dynamic or continuous forecast applications. Other probabilistic methods which are able to capture the various factors that govern the electricity demand and forecast its peak are found in [50–52].

Despite the extensive research work available in the literature on forecasting the (single) peak demand of a power system, predicting the “triad” peaks has attracted very little attention globally. One obvious reason is that the “triad” charging system is found only in UK, as other countries use other ways to calculate their transmission network charges. Another reason is that many UK electricity suppliers are already providing warning services to their customers when a “triad” peak is expected to occur. These warnings however is often one day before the actual “triad” peak, not leaving enough time to the customers to adjust their electricity requirements. To overcome this problem the customers need to use their own probabilistic models in order to forecast the “triad” peaks in the beginning of the “triad” season. However, these models are often very complex and require a great amount of data for their calculations. A non-expert customer like the building manager it is very unlikely to be able to operate these models or even have access to the required data for their calculations. There is a clear need for a “triad” prediction tool that is simple enough to be operated by the non-expert building manager but also provides satisfactory forecasts on the times of the future “triad” peaks.

However, knowledge about the future “triad” peaks is useless for the building managers unless the electricity demand of their buildings is also known in advance. Forecasting the electricity demand of a building is well studied subject in the literature. The prediction models need to consider many factors in order to accurately predict the daily, hourly or half-hourly power consumption of a building. These factors may be internal like the geometrical characteristics of the building or the occupants’ type and number, or they could be external factors like the weather. The existing approaches can be broadly classified as engineering, statistical and artificial intelligence approaches.

The engineering models use details of physical characteristics, operational profiles and cost to calculate precisely the energy for each component of the building and simulate its operation [53]. The procedure for calculating the energy consumption of a building is also standardised by major organizations such as ISO and ASHRAE. Various tools such as DesignBuilder, EnergyPlus, TREAT etc. have been developed commercially to calculate the energy efficiency and the sustainability of a building. A solid list of such

tools can be found in [54], hosted by the US Department of Energy. However, these tools require detailed information about the building and its environment as an input and cannot be used by the non-expert building manager.

Another way to predict the energy consumption of a building is to use statistical regression models that correlate the power consumption with a number of influencing variables. These models are strongly dependent on the historical datasets, and need a large dataset in order to produce accurate results. By using such a regression model, the authors of [55] showed that a single variable linear model is able to predict the energy consumption in hot and cold weather conditions. Another regression model was developed in [56] to predict the annual energy consumption by using one day, one week and three month measurements. The results displayed strong influence to the forecast horizon as the errors were found to be up to 100% for one day, 30% for one week and 6% for three months data. An auto-regressive integrated moving average model was developed in [57] to forecast load profiles for next day based on historical data records. This model was later enhanced with external inputs in order to predict the peak electricity demand for a building [58, 59].

Artificial intelligence methods have been found effective for solving complex non-linear problems. ANN has been often applied by researchers to predict the building's energy consumption in different environments. A neural network which predicted the long term energy demand using short term energy data (2-5 weeks), was presented in [60]. Another interesting technique was used in [61], where the short term electricity demand was predicted by using two phases of neural network. In phase one the weather variable was predicted using neural networks, and this output was then fed into a second neural network which predicted electricity consumption. In addition to ANN, support vector machines (SVM) are gaining popularity in predicting electricity consumption. Using SVM, the authors of [62] predicted the monthly electricity consumption for a year by using 3 years data to train the model.

Including weather data has also been found to support the prediction of a building's energy consumption [63, 64]. The monthly average temperature was used in [65] to improve the accuracy of prediction of monthly power consumption of a building.

Later, this approach was compared to the temperature frequency methods in [66]. In [67] the energy consumption for one season was predicted by considering many components like space heating, hot water etc. and by applying a specific model for each component. A feed forward neural network was used in [68] to predict the electricity consumption by relating the local weather and occupancy of the building. Another model used SVM to predict 1 year electricity consumption using weather variables [69]. The above models however used the same weather variables in every forecast without considering the difference of weather effect in different buildings.

According to [70], the energy consumption of different buildings varies according to the building's geometry, structure and energy control systems in place. These characteristics define the correlation between the building's energy consumption and the outside weather. Trying to capture this correlation, this chapter proposes a model that filters the weather data and identifies the optimal combination of weather attributes separately for every building. In addition, the proposed model is combined to a "triad" prediction model in order to forecast the building's energy demand and the "triad" peak at the same time in order to assist the building manager reduce its energy consumption and its bills. The aim of this chapter is (i) to forecast the most probable day and most probably half an hour on that day a "triad" could occur, (ii) to identify the most dominant weather attributes which would improve the demand forecast and (iii) to forecast the building's demand at the most probable "triad" day and half-hour.

2.3 Model Description

The proposed "Triad Demand Predictive Model" is presented in Figure 2.1 and consists of three sub-models, namely "Triad Probability Assessment" model, "Pre-Forecast Analysis" model and "Electricity Demand Forecast" model. Each of these sub-models performs different tasks using inputs from external sources or the other sub-models.

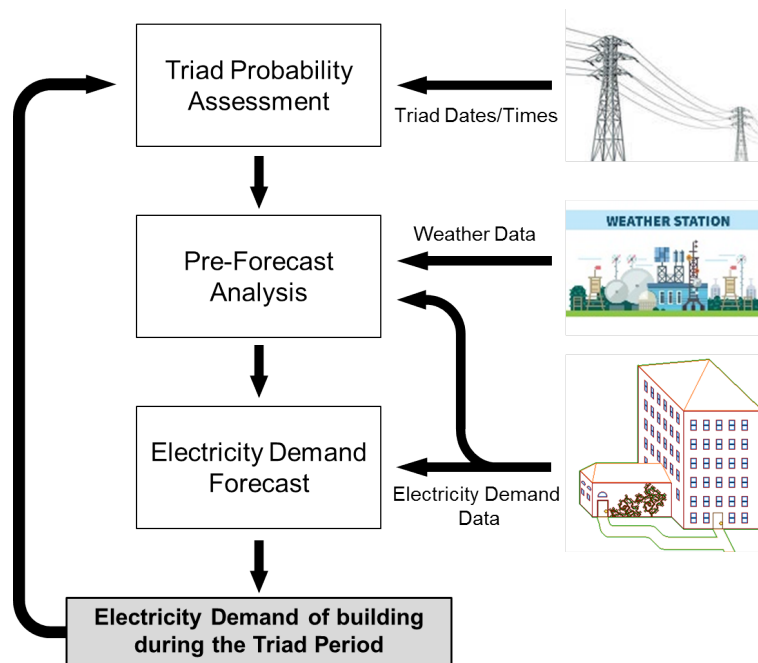


Figure 2.1: The Triad Demand Predictive Model

2.3.1 Model Inputs

The predictive model uses data from three different sources at various stages to predict the most probable half hour of the day where the triad could occur. The data is fed into the model in three stages (one for each sub-model).

For the “Triad Probability Assessment” model twenty five years of triad data were collected from National Grid (<http://www2.nationalgrid.com/uk/>) including information regarding the dates and times of the “triad” peaks of the corresponding years. These data were used in order to calculate the most probable dates and times of the triad peaks of the forthcoming year.

The second dataset was consisted of weather data. Two year weather data were obtained from the MetOffice (<http://www.metoffice.gov.uk/>) to be used as an input to the “Pre-Forecast” model. The data contained information from the local weather station from the period of 2012-2013. Hourly information about the sunny hours, air temperature, rainfall, hourly global radiation, relative humidity, mean wind direction, wind mean speed, extend of cloud cover and gust knots was available. The weather

data was used for our analysis to improve the accuracy of the predictive model.

The third data input to the model was historical energy consumption data from commercial buildings. Half-hourly power demand data from the period of 2012-2013 were available from six commercial buildings in Manchester Science Park, allowing the evaluation of the model on a realistic environment. The data were granted from Manchester Science Partnerships, as part of the EPSRC project “Ebbs and Flows of Energy Systems”. The historical power demand data were used by both the “Pre-Forecast Analysis” model and the “Electricity Demand Forecast” model.

The weather dataset and the building dataset are presented in Appendix A. In order to increase the quality of the datasets, the data were checked for missing or incorrect values (e.g. negative energy demand values). It was found that no missing or incorrect values existed in the datasets.

2.3.2 Triad Probability Assessment model

A stochastic model was developed to estimate the “triad” days of the forthcoming year. The model uses historical triad data (date and time) to calculate the probability of having a “triad” peak on certain dates during the “triad season”. The most probable dates for a “triad” peak are calculated with configurable granularity, using intervals which have duration from 1 to 20 days. Assuming that there are 120 days between 1st of November and the end of February, setting the interval to -1- would result in 120 probability values (one for each day). In case the interval is set to -2-, the model produces 60 probability values (one for each 2-day period) etc. As seen in the next sections, reducing the forecasting resolution (by increasing the interval size) increases the forecasting accuracy. This trade-off between forecast resolution and forecast accuracy has to be determined by the model’s operator according to the application, and it is out of the scope of this chapter.

The probability $P(i)$ of each interval i to include a “triad” peak is calculated using

Equation (2.1) below:

$$P(i) = \frac{\sum_{n=1}^N \left(\sum_{k=1}^3 \left(n \cdot \frac{1}{\sigma\sqrt{2\pi}} \cdot e^{-\frac{(i-T_n^{(k)})^2}{2\sigma^2}} \right) \right)}{\sum_{n=1}^N 3n} \quad (2.1)$$

where

$P(i)$ is the probability of interval- i including a triad day (if the interval is one day, $P(i)$ is the probability of that day being a triad one)

i is the interval index

n is the year index (N^{th} year is the most recent year)

N is the total number of years that triad data are available

k is the triad index for a year

σ is the standard deviation of the normal distribution (=1 in our model)

$T_n^{(k)}$ is the interval that includes the k^{th} triad day of year n

As seen from Equation (2.1), the probability $P(i)$ of each interval i is obtained by superimposing a set of 3 normal distributions for each year that triad data are available. These normal distributions have as mean value the index of the “triad” interval (the interval that includes a “triad” day in that year), and a standard deviation of 1. With this method, each “triad” date affects not only the probability of the same interval but also the probability of the neighbouring ones. Considering weekly intervals for example, if week 5 includes a “triad” date, its probability is increased but so is the probability of weeks 4, 6 and 3, 7 according to the normal distribution. This is done in order to consider the uncertainties introduced by the weather in the calculations. It is known that the “triad” dates are affected by the weather, e.g. it is more probable to have a “triad” peak when the mean temperature is low and the heating systems of the consumers are operating. By increasing the probability of the neighbouring intervals the model expresses the fuzzy relationship:

If the weather is cold \Rightarrow

We might have a “triad” peak

, and interprets it in order to be used for a probabilistic assessment:

If we had a “triad” peak in the past \Rightarrow

This period of the year has been cold \Rightarrow

This period and its neighbours might also be cold in the future \Rightarrow

We might have a “triad” peak on those periods in the future

The model is built with a learning feature which improves the probability assessment on an annual basis when new “triad” data are available. Emphasis is given on the most recent data, by including weights (n in Equation (2.1)) that increase as data are available from a more recent year. In this way the model can detect possible changes in the pattern caused by external factors that change on an annual basis (e.g. weather, technology). A linear weight relationship was assumed for these factors – however, any prior knowledge that a user may have can be used to modify these weights. Finally, the sum of the weighted normal distributions is divided by the sum of weights n in order to obtain the probability $P(i)$ as a weighted average.

The model also calculates the most probable half-hours within a day during which the “triad” peak demand is expected to occur. Equation (2.1) is used in a different way to obtain the half-hourly probability of a “triad” peak in a day. In this case the intervals have a fixed duration of 30 minutes, so only 48 intervals are assessed for one day. The model looks only at the times that the “triad” peaks occurred, and tries to identify the most probable half-hours for one. The weather is not an important factor in this case. What is most important is the daily profile of electricity demand in the system. This profile is directly related with the activities of the customers and their energy consumption patterns. By superimposing normal distributions for each “triad” half-hour, we are able to identify an “alert” band, a set of intervals where the “triad” peaks are expected to appear. The interpreted relationship in this case is:

If we had a “triad” peak at this half hour in the past \Rightarrow
 Certain electricity-demanding activities are happening at this time of day \Rightarrow
 These activities could happen at this time and its neighbours in the future \Rightarrow
 We might have a “triad” peak this time in the future

The model is able to detect possible changes on a daily basis, caused by changes in the daily patterns of the customer’s consumption. This could be the case in a few years from now, when the majority of the electricity consumers will be more proactive with regards to electricity charges, and shift their energy consumption at hours when the £/MWh is low. The increasing number of electric vehicles (EVs) will also have a significant effect on the daily patterns of a consumer [71]. According to [72–75], the charging fashion of EVs can change completely the electricity profile of a consumer. By including annual weights the model can detect these changes and update the probability assessment of the “triad” half-hours.

2.3.3 Pre-Forecast Analysis model

A “Pre-Forecast Analysis” model was developed in order to increase the performance of the “Electricity Demand Forecast” model by including weather information in the forecasting process. The objective of this model is to identify the optimal number of weather attributes to be considered by the “Electricity Demand Forecast” model to generate an accurate forecast. To this end an iterative process is followed, as presented in Figure 2.2.

Using historical local weather data and building energy consumption data, a correlation analysis was performed in order to calculate the correlation of the available weather data with the electricity demand of each building. The Pearson’s correlation matrix was calculated in order to identify the attributes which have the highest correlation with the energy consumption of each building.

Pearson’s correlation coefficient (also known as r -correlation) is a statistical metric that measures the correlation strength between two random variables X and Y [76]. It has been applied to various indices in statistics, such as data clustering and classification

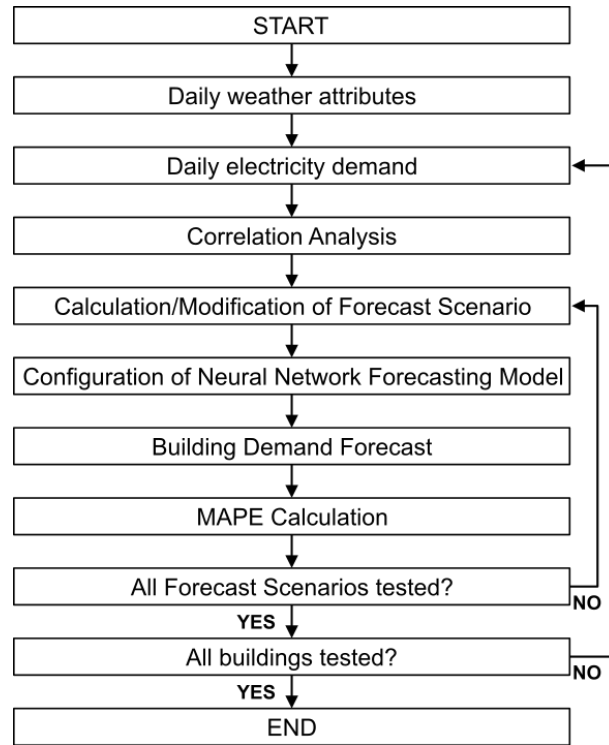


Figure 2.2: The Pre-Forecast Analysis process

[77], time series analysis [78], decision making [79], finance analysis [80], and biological research [81]. The Pearson's correlations coefficient (r) is calculated by dividing the covariance of the variables by the product of their standard deviations, as presented in Equation (2.2). The r coefficient takes values between -100% and $+100\%$. Positive values denote a positive correlation, negative values denote a negative correlation and zero values denote no correlation at all. The closer the values are to $\pm 100\%$, the stronger the correlation between the two variables. In this analysis, variable X is the power demand from a building (2-year time series), while variable Y is the weather attribute (2-year time series).

$$r = \frac{\sum_{n=1}^N (X_i - \bar{X})(Y_i - \bar{Y})}{\sqrt{\sum_{n=1}^N (X_i - \bar{X})^2} \sqrt{\sum_{n=1}^N (Y_i - \bar{Y})^2}} \cdot 100\% \quad (2.2)$$

where

N is the number of values in the time series (17520 half hours in the two years dataset)

i is the half-hour index

X_i is the power demand of the building in half-hour i

\bar{X} is the mean value of the power demand of the building

Y_i is the weather attribute value in half-hour i

\bar{Y} is the mean value of the weather attribute

Ten weather attributes were studied for each building to calculate the correlation of each weather attribute to the building's electricity demand. Since the buildings have different energy consumption profiles, the correlation coefficient was calculated separately for every building and the results are presented in a table (correlation matrix).

Having the correlation matrix, a sensitivity analysis was performed in order to identify the optimal set of attributes to be considered in the forecast. A set of 11 "Forecast Scenarios" was defined for each building, consisted of different sets of attributes to be considered in the forecast. The base attributes were assumed to be the power demand, time, day and type of day (weekday/weekend). The considered scenarios and their corresponding attributes are listed below:

1. *No weather attributes*: Considering only the power demand, time, day, type of day (weekday/weekend)
2. *y weather attribute*: Considering the power demand, time, day, type of day (weekday/weekend) and y most dominant weather attribute(s), i.e. attributes with the highest correlation factor. The index y varies from 1 to 10.

To identify the optimal forecast scenario, an ANN forecasting model was built using the WEKA toolkit [82], and the half-hourly electricity consumption on a random day was forecasted for each building. The data was divided into two datasets: the first dataset consisted of the first $n - 1$ days and was used to train the model and the second dataset consisted of the $n - th$ day in order to test the model. The default

settings of WEKA were used for the configuration of the ANN static parameters (training time, epochs, learning rate). The only dynamic parameter of the ANN in WEKA is the number of hidden layers which by default is equal to half the number of the dataset attributes. To calibrate this parameter, a parametric study was performed to identify the optimal number of hidden layers for each forecast scenario. It was found that the best results were achieved when the number of hidden layers matched the number of attributes considered during the training/testing phase. In the “No weather attributes” scenario for example, 4 hidden layers were used in the ANN model. The forecast accuracy for each scenario was calculated using the mean absolute percentage error (MAPE) index from Equation (2.3). For each building the attribute set (forecast scenario) that resulted in the least MAPE was selected as the optimal one for the electricity demand forecast.

$$MAPE = \frac{1}{n} \sum_{t=1}^n \left| \frac{A_t - F_t}{A_t} \right| \quad (2.3)$$

where

n is the number of half-hours in a day (48)

i is the half-hour index

A_i is the actual power demand of the building in half-hour i

F_i is the forecasted power demand of the building in half-hour i

2.3.4 Electricity Demand Forecast model

The third sub-model is the “Electricity Demand Forecast” model. In this model the outputs of the previous sub-models were combined in order to forecast the electricity demand of the building on a “triad” peak period considering the optimal set of weather attributes. The model performs a day-ahead power demand forecast using the optimal ANN configuration suggested by the “Pre-Forecast Analysis” model.

The ANN technique was selected after comparing five techniques, namely Linear Regression, Instance-based learning (K*), Support Vector Regression, Multi-Layer Perceptron ANN and Decision Trees. Each technique was trained and tested on the same dataset using the default parameters of WEKA toolkit. The results are presented in Table 2.1.

Table 2.1: Mean Absolute Error (MAE) for every technique

	Linear Regression	Instance-based Learning (K*)	Support Vector Regression	MLP ANN	Decision Trees
Building 1	3.52	5.42	0.06	5.95	1.33
Building 2	12.65	8.11	3.91	17.74	2.51
Building 3	11.70	7.11	15.69	7.17	16.60
Building 4	13.35	9.12	6.57	13.95	5.61
Building 5	15.08	7.62	7.09	12.51	7.35
Building 6	22.18	17.16	7.11	14.40	7.21

As observed from Table 2.1, the ANN had an overall better performance than the other techniques for our dataset. Algorithm 2.1 describes the model's operation for the considered 6 buildings.

Algorithm 2.1: Algorithm of the "Electricity Demand Forecast" model

Input Most probable triad days and half hours, optimal forecast scenario

Output Building power demand during a triad half hour

- 1: Select the most probable days triad and half hours on that day as calculated from "Triad Probability Assessment" model
- 2: **while** $i \leq 6$ **do**
- 3: Configure the ANN according to the Pre-Forecast Analysis of building- i
- 4: Build the training and the testing dataset
- 5: Train the model
- 6: Forecast the power demand of building- i at the most probable half-hour
- 7: $i = i + 1$
- 8: **end while**

Algorithm 2.1 describes the process of forecasting the power demand for the most

probable half hour of a triad day for the 6 buildings. Two inputs are required for this. The first is the periods identified as the most probable periods for a “triad” peak (output of the “Triad Probability Assessment” model). The second input is the forecast scenario of the “Pre-Forecast Analysis” model that gives the lowest MAPE for each building. Having these inputs from the previous sub-models, the “Electricity Demand Forecast” model goes in an iterative loop and performs a power demand forecast for each building. Inside this loop, the ANN parameters are set based on the forecast scenario identified in the “Pre-Forecast Analysis” model. Once the ANN is configured, the training and testing files are built according to the optimal forecast scenario. The ANN is different for each building, as it may follow a different forecast scenario. At the end of this iterative process, the power demand for each building is calculated for the most probable triad half-hour. This demand forecast gives the building manager a pre-emptive advantage to reduce its energy bills by using various control methods to decrease the consumption of its buildings.

2.4 Model Results

2.4.1 Triad Probability Assessment

The model was developed in Matlab and was trained on real “triad” data from the period 1990 - 2014. The code is presented in Appendix B. The data were obtained from National Grid and include information regarding the dates and times of the “triad” peaks of the corresponding years. As mentioned before, intervals were defined to calculate the probability of the “triad” dates. Figures 2.3 and 2.4 present the results when considering intervals of 1-day and 5-days respectively. It is assumed that the building manager can define a warning threshold to the model, and gets warnings for periods that are calculated to have a “triad” peak probability greater than a certain level. In this case this threshold is assumed at 70% of the maximum calculated probability from all intervals (the building manager will be warned for periods which are at the top 30% of the results).

Looking at Figure 2.3, the most probable “triad” intervals for 2014-2015 (the ones

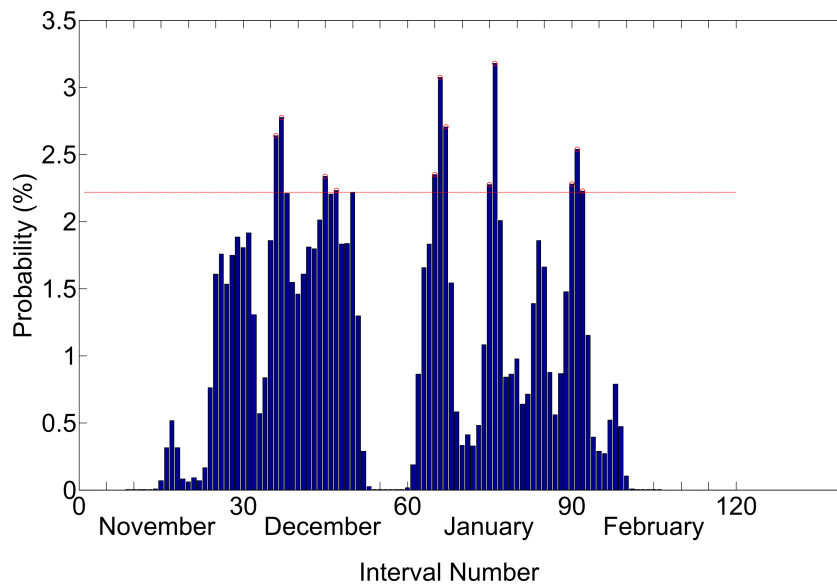


Figure 2.3: The daily probability distribution for “triad” peaks

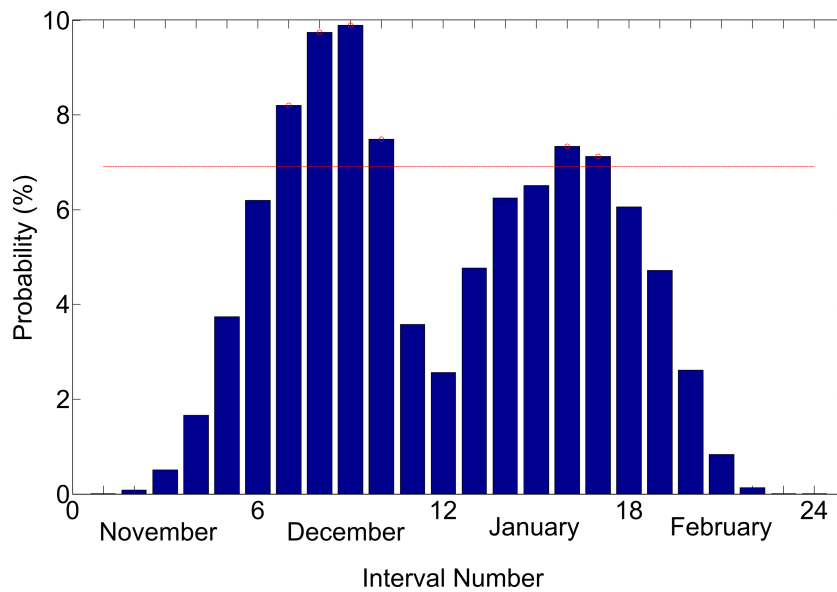


Figure 2.4: The 5-days probability distribution for “triad” peaks

above the threshold) were calculated to be the following 12 days:

$6^{th} - 7^{th}$, 15^{th} and 17^{th} of December

$5^{th} - 7^{th}$, $15^{th} - 16^{th}$ and 31^{th} of January

$1^{st} - 2^{nd}$ of February

Looking at Figure 2.4, when the interval duration is increased to 5 days, the most probable dates for a “triad” peak are following 30 days:

The first 4 intervals of December ($1^{st} - 20^{th}$ of December)

The 4^{th} and 5^{th} intervals of January ($16^{th} - 25^{th}$ of January)

As seen from the results, the increase of the intervals’ duration results in more “relaxed” probability distributions. This is expected, as explained in the previous sections, since the effect of one “triad” peak on its neighbouring dates expands at longer interval durations. This results in having longer periods above the defined threshold, and consequently a greater number of “triad” warnings.

It is important to define correctly both the interval duration and the warning threshold correctly. Assuming that a “triad” warning triggers certain demand reduction actions, the number of warnings is associated with a set of costs an example of which is the comfort of the building’s occupants. The calculation of these costs is out of the scope of this chapter. The objective is to provide a tool to the building manager to calculate the probability of “triad” peaks. The building manager must carefully consider all costs associated with demand reduction actions on the building facility, and decide the optimal number of warnings for each particular case.

The model was also used to calculate the most probable half-hours for a “triad” peak in a day. As mentioned before, the interval duration was fixed to 30 minutes and the probability of each of 48 intervals in a day was assessed. The results are shown in Figure 2.5.

Assuming the same warning threshold as before, the most probable half-hour for a “triad” peak was calculated between 17:00 - 17:30. An “alert” band between 16:30 - 18:00 is clearly demonstrated. Using the model to calculate the probability of each half-hour of a day offers a number of advantages to the building manager. By identifying the exact half-hours for a “triad” peak, the duration of the demand reduction actions are limited and consequently so is the disruption of the occupants’ comfort in the building. Reducing the need for long response periods reduces the overall risk of “missing” a triad peak, as the building managers will be able to increase the number

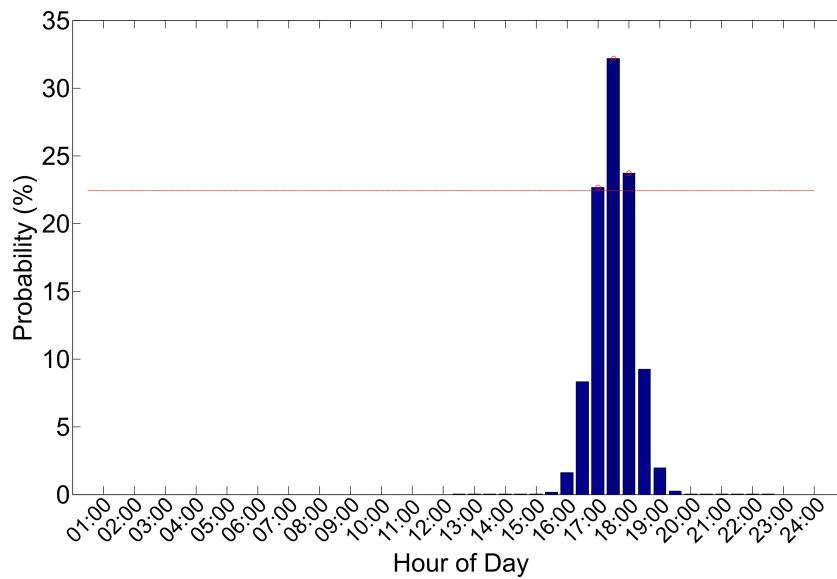


Figure 2.5: The half-hourly probability distribution for “triad” peaks in a day

of “triad” warnings they can respond to.

2.4.2 Pre-Forecast Analysis

The “Pre-Forecast Analysis” model was applied on data from the period of 2012-2013. Half-hourly energy consumption data from six commercial buildings were analysed and correlated with the corresponding local weather information. The Pearson’s correlation matrix is presented in Table 2.2.

Table 2.2: Correlation matrix of weather attributes with daily energy consumption

Building	Cloud Total	Cloud Base	Wind Mean Speed	Wind Mean Direction	Max Gust	Air Temperature	Rainfall	Global Radiation	Relative Humidity	Sunny Hours
Building 1	3.52	5.42	0.06	5.95	1.33	1.91	3.53	3.23	0.45	8.78
Building 2	12.65	8.11	3.91	17.74	2.51	36.53	2.32	30.79	6.28	22.43
Building 3	11.70	7.11	15.69	7.17	16.60	35.11	5.91	20.22	2.05	13.73
Building 4	13.35	9.12	6.57	13.95	5.61	34.14	2.02	33.05	11.80	23.33
Building 5	15.08	7.62	7.09	12.51	7.35	46.30	2.30	45.14	17.99	24.41
Building 6	22.18	17.16	7.11	14.40	7.21	59.83	2.13	67.05	31.23	40.60

As seen from Table 2.2, the correlation of energy consumption with the local weather is different for each building. The strength of these correlations can be extracted from the magnitudes of the Pearson’s correlation coefficients in this table (bigger is stronger).

The weather attribute with the highest correlation to the demand of the Building 1 was the sunny hours. For the Buildings 2-5 the attribute with the highest correlation was the outside air temperature. Lastly for Building 6 the attribute with highest correlation was that of hourly global radiation. As each building has different structural architecture, area and occupancy, it normal to respond differently to the different weather attributes.

The purpose of this “Pre-Forecast Analysis” model is to identify the optimal combination of weather attributes to include in the “Electricity Demand Forecast” model. To this end, a number of forecasting scenarios were defined and their contribution to the forecast accuracy was calculated using the MAPE index as explained in Section 2.3.3. This way, a weather sensitivity analysis was performed, testing each forecasting scenario and defining the hidden layers of the ANN to be used in the “Electricity Demand Forecast” model for each building. The results are presented in Figure 2.6.

For Building 1 the forecast MAPE without considering any weather attributes was around 7% and when the most dominant weather attribute (sunny hours) was considered in the forecasting model the MAPE increased to 8%. After running all forecast scenarios, the lowest MAPE was found when considering all the weather attributes in the forecasting model (last scenario). Based on this, the ANN to be used in the “Electricity Demand Forecast” model for Building 1 needs to consider all weather attributes and use 14 hidden layers (same as the number of the attributes considered in the last scenario).

The electricity demand forecast for Building 2 without considering any weather attributes resulted in a MAPE of 13%. This was reduced to 6.4% when the outside air temperature was added to the training and testing file. The MAPE was further reduced to 5.8% when the top two correlated weather attributes (outside air temperature and hourly global radiation) were added to the training and testing file. Unlike the forecast results of Building 1 which had the lowest MAPE when considering all weather attributes, for Building 2 the MAPE remained higher than 5.8% as the number of considered weather attributes was increased. According to this, the ANN of the “Electricity Demand Forecast” model for Building 2 needs to consider two wea-

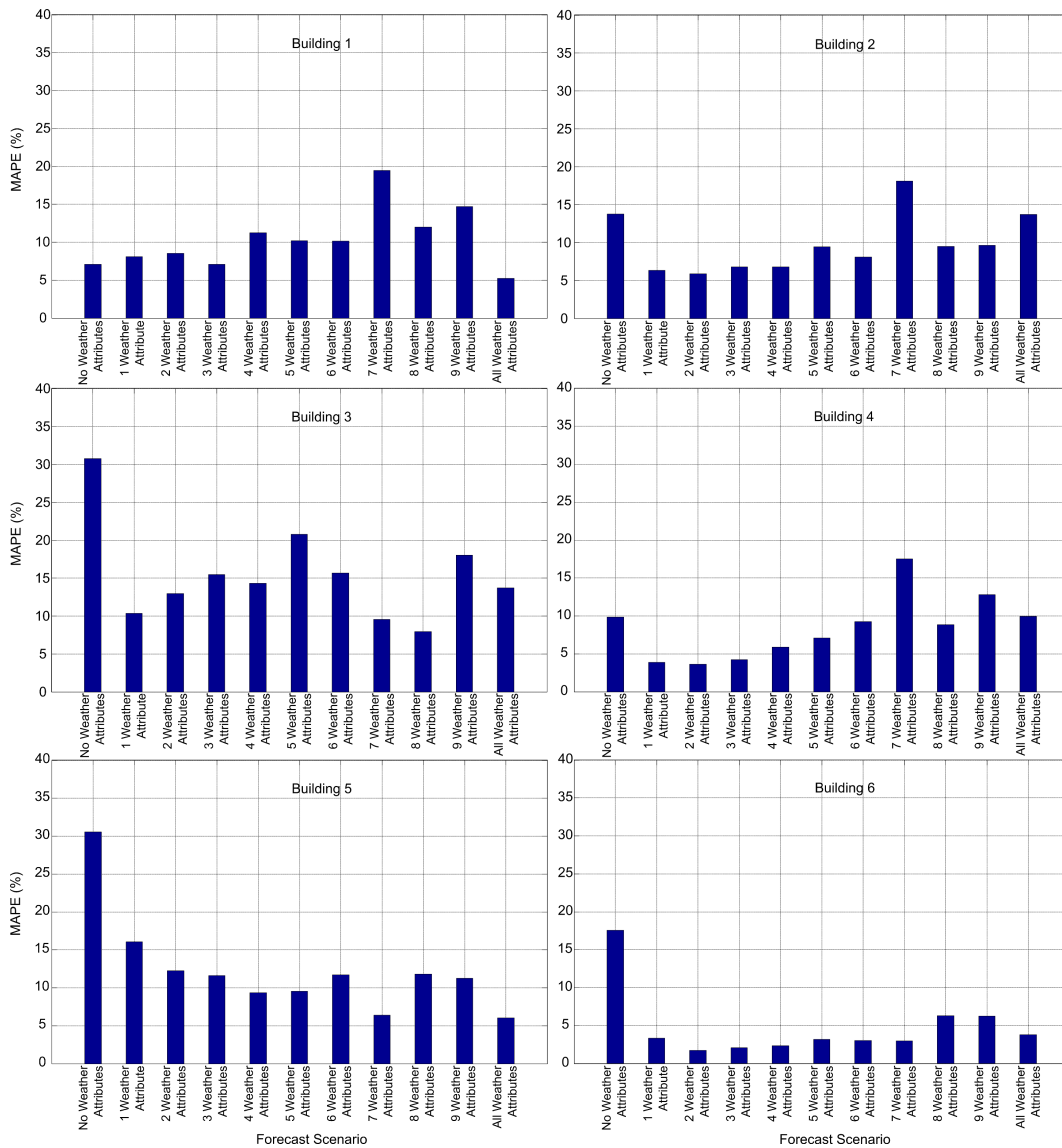


Figure 2.6: Weather sensitivity analysis for all buildings

ther attributes (outside air temperature and hourly global radiation) and use 6 hidden layers.

With Building 3, the daily forecasting model gave a MAPE of 30% when the demand was forecasted without considering any weather attributes. It was reduced substantially when weather attributes were added to the training procedure, and a minimum MAPE of around 7% was reached when considering the 8 most dominant weather attributes. Based on these findings the ANN of the “Electricity Demand Forecast” model

for Building 3 was configured to use 12 hidden layers and the top 8 weather attributes.

Building 4 had similar results to Building 2, although at a smaller magnitude. In this case, the lowest MAPE was recorded when considering the two strongest weather attributes and the ANN of the “Electricity Demand Forecast” model for Building 4 was configured to use 6 hidden layers.

The forecasting error reduction when considering weather attributes was very large for Building 5. A quite high MAPE (around 30%) was found when the forecast was done without considering any weather attributes. This number reduced to 6% when considering all the weather attributes, and 14 hidden layers were used in the ANN of the “Electricity Demand Forecast” model for this building.

The smallest forecast errors were found for Building 6. Despite the MAPE was greater than 15% in the No Weather Attributes scenario, in almost all the forecast scenarios which considered some weather attributes the MAPE were reduced to below 5%. A maximum MAPE reduction of 88% was found when considering the two most dominant weather attributes for this building, and consequently the ANN of the “Electricity Demand Forecast” model for Building 6 was configured to use 6 hidden layers.

As seen from this analysis, considering weather information when forecasting the electricity demand of a building reduces the forecasting errors. Furthermore, by choosing the correct weather attributes to be considered in the forecasting process, results in removing the irrelevant and “noisy” data and increases the forecast accuracy.

2.4.3 Electricity Demand Forecast

The power demand at 17:30 of the 6th of December 2013 (actual triad half hour and day) was forecasted separately for each building. The findings of the “Pre-Forecast Analysis” model were used in order to consider the optimal combination of weather attributes and configure the ANN for each building separately. The forecasted demand for each building is presented in Figure 2.7.

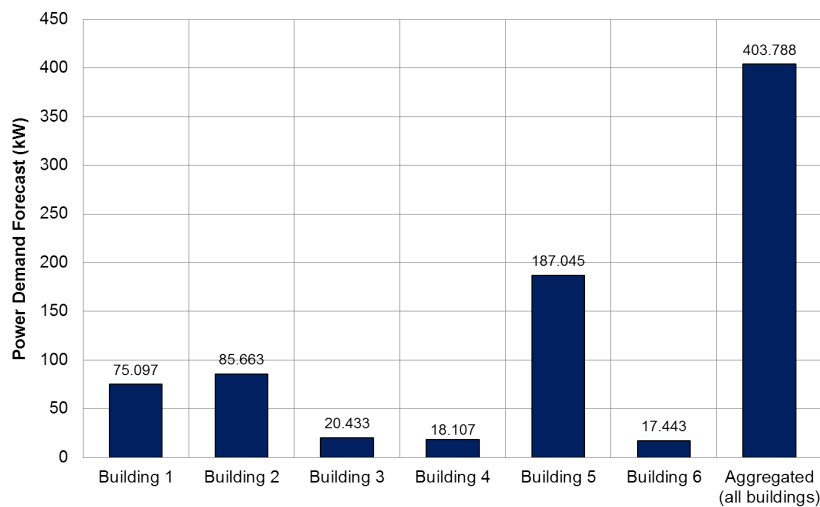


Figure 2.7: Electricity demand forecast for all buildings

2.5 Model Validation

To validate the proposed model, the results were compared with the actual triad dates and times as well as the actual electricity demand of each building on the forecasted day and half-hour. The actual “triad” dates for 2014/2015 are presented in Table 2.3:

Table 2.3: The actual “triad” peak dates and times of 2014/2015

Triad Date	Triad Half-Hour
4th of December 2014	17:00 - 17:30
19th of January 2015	17:00 - 17:30
2nd of February 2015	17:30 - 18:00

To compare the results of the “Triad Probability Assessment” model to the actual “triad” dates for 2014/2015, Figures 2.8 - 2.12 present the actual dates/times with red colour.

As seen from Figure 2.8, one “triad” peak was above the warning threshold when considering daily intervals for the calculations. The results are considered satisfactory, bearing in mind that the “triad” peak of December was only missed for two days.

Looking at Figure 2.9, when the interval duration was increased to 5 days, the “Triad Probability Assessment” model was able to predict two “triad” peaks of the same

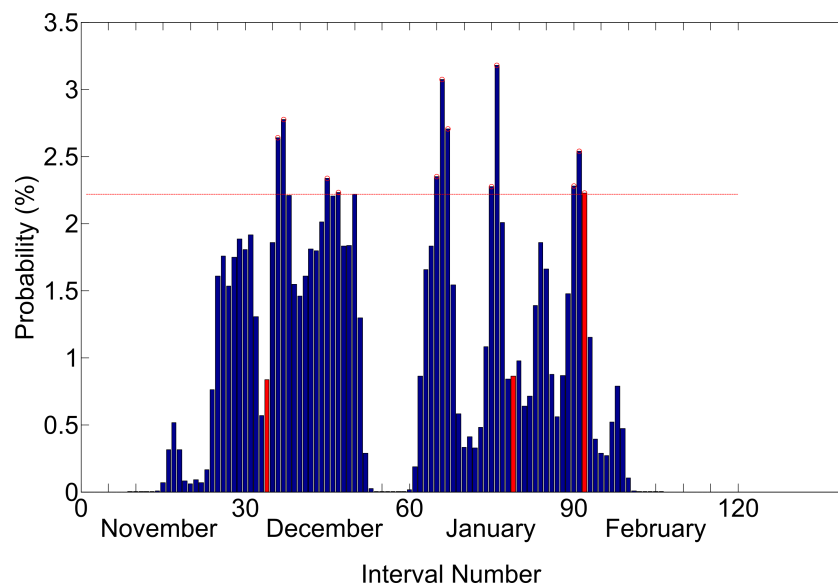


Figure 2.8: The actual “triad” peak days of 2014/2015 compared to the calculated daily probability distribution.

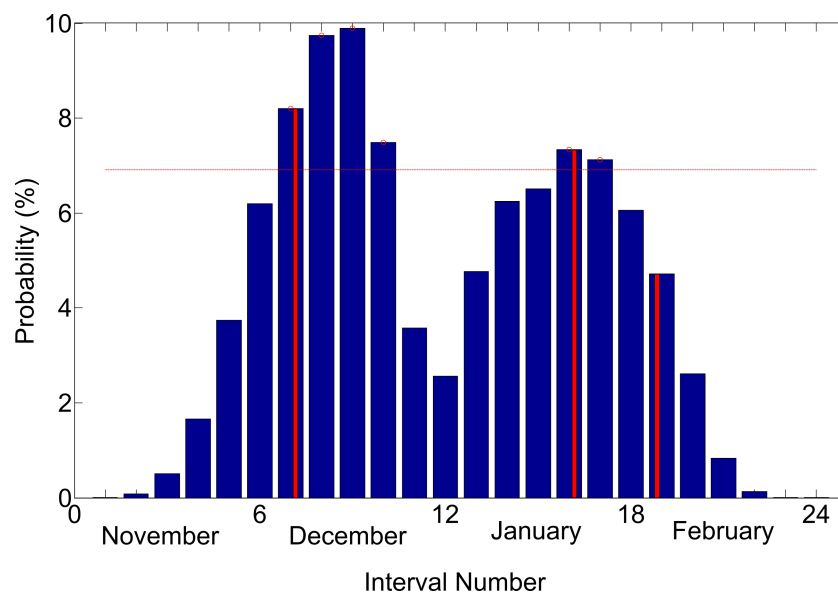


Figure 2.9: The actual “triad” peak days of 2014/2015 compared to the calculated 5-day probability distribution.

year. As explained in the previous sections however, an increase at the duration of the intervals results in a large number of “triad” warnings (30 compared to 12). This is something which should be carefully considered by the building manager.

To better understand the usefulness of increasing the interval size of the forecast, a sensitivity analysis was performed, increasing the interval size from 1 to 10 days for 5 consecutive years (2010-2015). The average number of generated warnings as well as the average percentage of predicted triad peaks are presented in Figures 2.10 and 2.11.

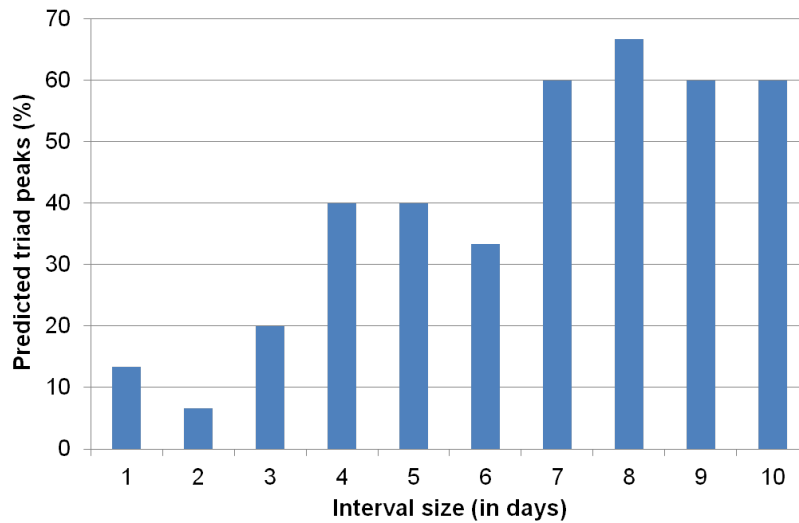


Figure 2.10: Percentage of predicted “triad” peaks for different interval sizes

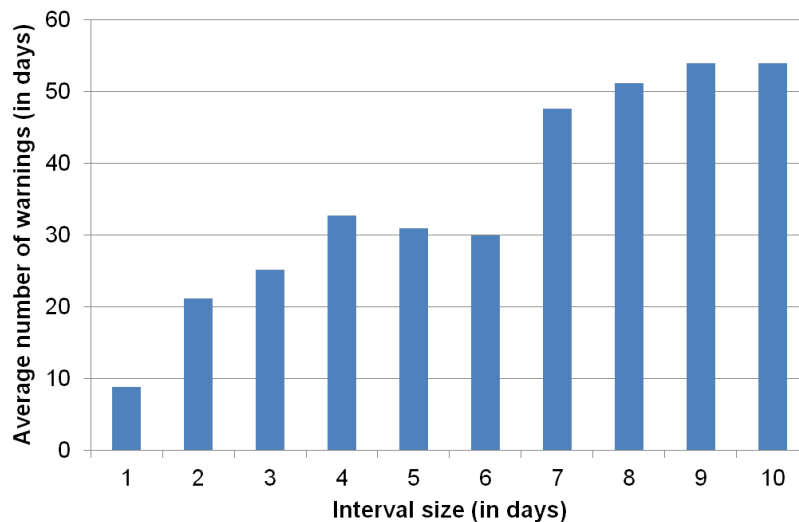


Figure 2.11: Number of generated “triad” warnings for different interval sizes

As seen from these figures, the results can be grouped into three categories. The first category includes interval sizes ≤ 3 days, where the number of generated warnings

varies from 9-25 days and less than 20% of the triad peaks (in average) are successfully predicted. The second category includes interval sizes between 4-6 days, generates on average 30 warnings and predicts successfully 30-40% of the triad peaks. The third category has interval size ≥ 7 days and is able to predict successfully 60% of the triad peaks; however the number of generated warnings varies from 48-53 days.

As not all buildings have the same usage / occupancy patterns, the building managers can select the interval size according to the type of the building facility (e.g. residential / industrial). In a residential building facility for example, the building manager may not be willing to respond to a large number of triad warnings as reducing the demand of the building in the evening would affect the comfort of the occupants. In this case, the building manager would prefer to use this tool with a small interval size. On the other hand, the building manager of an industrial facility might be keen to rearrange electricity demanding operations and avoid the “triad” peak hours between 16:00 - 19:00, even on a frequent basis. Considering that the cost savings would be significant, the building manager of an industrial facility could accept a higher number of triad warnings and use this tool with a large interval size, as this would increase the chance of avoiding the peak.

It is important to say that the increase of the interval size does not make the model more accurate; it simply “relaxes” the probability distributions and generates more warnings for the building manager. However, as seen from Figure 2.10, this increases the likelihood of including the actual “triad” peaks in the warnings.

Figure 2.12 presents the actual “triad” peak half-hours of 2014/2015 compared to the calculated half-hourly probability distribution. As seen from Table II, two “triad” peaks occurred between 17:00 and 17:30, while the third one occurred between 17:30 and 18:00. The “Triad Probability Assessment” model calculated the period between 16:30 and 18:00 to be the most probable for a “triad” peak which was correct for all three “triad” peaks. The performance of the model here is excellent as warnings were issued for all “triad” half-hours. Having an accurate prediction of the exact “triad” half-hours, the building managers are able to avoid the “triad” peaks and reduce their bills. Furthermore, the fact that the “alert” zone is only 1.5 hours long reduces any

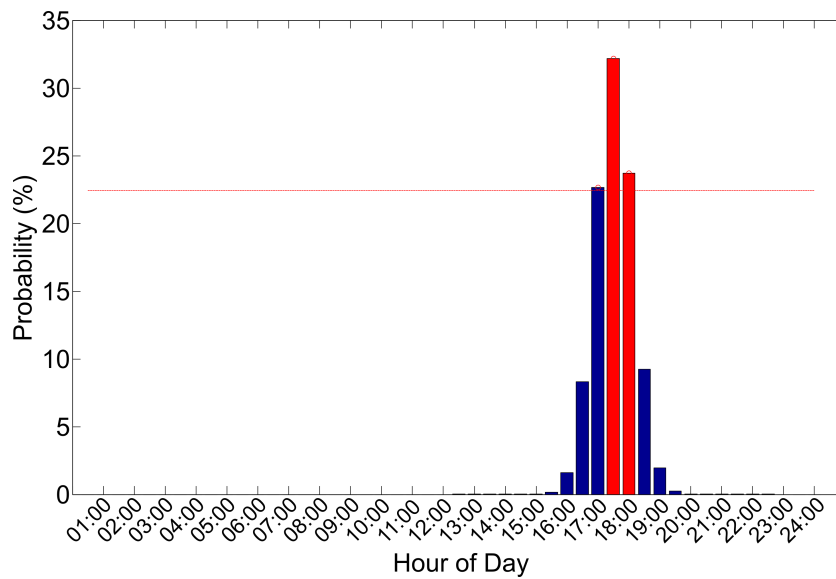


Figure 2.12: The actual “triad” peak half-hours of 2014/2015 compared to the calculated half-hourly probability distribution.

other costs generated when reducing a building’s demand (e.g. the cost of the occupants’ discomfort).

To validate the “Pre-Forecast Analysis” and the “Electricity Demand Forecast” models, the forecasted power demand for each building was compared to the actual one. Figure 2.13 presents the forecasted and actual power demand for all buildings, while Figure 2.14 presents the forecasting percentage errors in each case.

As seen from Figures 2.13-2.14, the maximum error was found to be -13.56% for Building 5. Three forecasts had errors less than 3% which are considered very accurate, while the accuracy of the other three was found above 89%.

As mentioned before, this model aims to assist the building manager to estimate the triad days/hours and forecast the electricity demand of the facility. From this point of view, what is also valuable to the building manager is the aggregated electricity demand of the facility (all buildings combined). As seen from Figure 2.14, the error when aggregating the forecasts from each building is only -2.422%. Because the individual errors are positive and negative (the demand was overestimated in some buildings and underestimated in some others), their aggregation results in an overall smaller

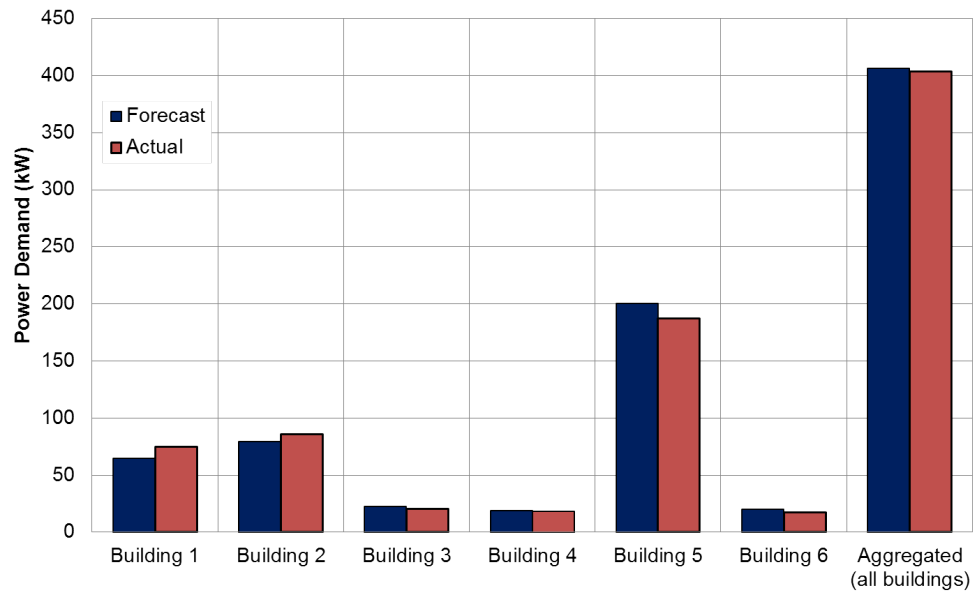


Figure 2.13: Forecasted and actual power demand for all buildings

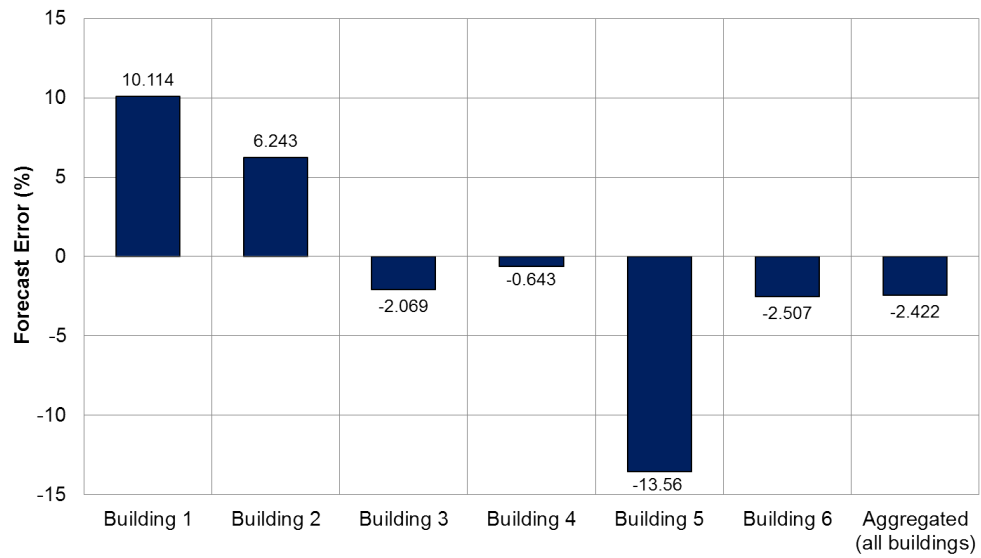


Figure 2.14: Error of power demand forecast for all buildings

error. Furthermore, having both negative and positive errors proves that the forecast errors are not systematic and the proposed forecasting model is unbiased.

2.6 Summary

A Triad Demand Predictive model was developed to forecast the power demand of commercial buildings during the “triad” periods. The model calculates the probability of having a “triad” on a daily and half-hourly basis and predicts the power demand of the building at the periods when a “triad” peak is more likely to occur. A Pre-Forecast stage was considered where the performance of the forecasting model was improved by considering weather attributes in the forecasting procedure.

The *Triad Probability Assessment* model was validated against the UK “triad” dates and times of 2014/2015. For an interval size of 5-days, the model predicted successfully the dates of two out of three “triad” peaks of 2014/2015. It was showed that by increasing the interval size, the model generates more warnings for the building manager, and this increases the likelihood of including a “triad” peak. The times of all three “triad” peaks of 2014/2015 were predicted successfully. It was also showed that the “triad” peaks tend to occur in a relatively narrow zone during a day (between 16:30 and 18:30).

The *Electricity Demand Forecast* model was validated with real weather and electricity demand data from six commercial buildings in Manchester. It was showed that the weather information plays a significant role in the accuracy of the building energy demand forecast. The *Pre-Forecast* stage proved that the choice of weather attributes is very important to the forecasting accuracy, and in some cases, using less weather data is more valuable and can lead to more accurate predictions. The *Electricity Demand Forecast* model was tailored to each of the six building according to the results of the Pre-Forecast stage, resulting to an overall 2.4% forecast error for the building facility.

However, reducing the electricity demand of a building is not a trivial activity. Many other costs are associated to such actions (e.g. the cost of disrupting the comfort of the occupants) and should be considered by the building managers before forcing a demand reduction in a building. The occupants must be aware and willing to participate in such a scheme. Contractual agreements might also need to be in place to compensate the occupants, leaving room for new business models. Social studies and questionnaires could also help in this direction.

Management of EV charging at commercial buildings

3.1 Introduction

It is widely recognized that the electrification of the road transport sector combined with low carbon electricity generation can significantly improve the conditions in cities with respect to air pollution and noise. Despite the fact that considerable technological and economic barriers still exist (mainly related to the storage technologies), a mass deployment of electric and plug-in hybrid electric vehicles is expected in the forthcoming years. This is indicated by several prospective studies and projects, for instance Valentine-Urbschat & Bernhart (2009), National Academy of Sciences USA (2009) and The Royal Academy of Engineering UK (2010), IEA (2011) etc. The rapid development of EV charging infrastructure as well as forceful incentives from government will enable the mass integration of EVs into power systems.

During the initial phase of EV uptake, EVs will be regarded as mere additional loads like any other conventional load, and will be billed at normal retail prices. There are several studies [73–75, 83–85] indicating that uncontrolled charging of EVs might increase the system peak demand resulting in feeder voltage drops and/or equipment overloads, in case of already stressed networks. Furthermore, since load is highly correlated with market prices, it is expected that the increase in domestic consumption, due to EV charging, will trigger an increase in the market prices. This becomes more intense when medium or high EV penetration level is considered, as it is analysed

in [86, 87]. In addition, the EV uptake affects the daily routines of their owners as they have to consider charging their vehicles on a daily basis. This creates a need for charging stations both at private and public places so that the EV owners can charge at home, in parking lots or even on the streets. Trying to accommodate this need for charging, the building managers install charging stations at their premises and provide local charging facilities to the occupants/visitors of their buildings. However, this charging service provision creates a number of costs for the building manager. Apart from the initial installation cost that is necessary, the EV charging stations have operational and maintenance costs which the building managers need to cover. Furthermore, EV charging increases the electricity demand of the building and affects the demand profile creating additional costs for the building manager. To reduce these costs, the building manager must coordinate the charging of the EVs and minimise its impact.

EV charging coordination requires a new market entity namely a Charging Station Manager. The Charging Station Manager is responsible for managing the demand from the charging stations of large EV fleets according to its strategy [72, 86]. The aim of the Charging Station Manager is to serve the EV demand in a beneficial way for all parties involved. Under such a business concept, both the Charging Station Manager and EV owners can share benefits depending on bilateral contracts [72]. Moreover, the Charging Station Manager can be incentivized by the distribution network operation (DNO) in order to offer additional load management services for the improvement of the network performance. Several management concepts for efficient EV charging have been presented in the literature [87–94]. Different objectives [90] can be considered when defining an EV charging strategy, namely technical objectives regarding the physical assets and constraints of the energy system [90, 92, 94], economical objectives associated with the energy market-related stakeholders (consumers, producers and retailers) [87, 88, 93] and techno-economic objectives where technical and economic aspects are part of the total energy price to be paid by the end-user [89, 91].

In this chapter, a charging control algorithm was developed for the building manager to reduce the EV charging costs of a building facility. A control model is presented that

enables the Charging Station Manager to schedule the EV charging and discharging events following two strategies. The first strategy aims to minimise the impact of EV charging on the demand profile of a building facility and reduce its peak demand by discharging the EVs during the peak hours. The second strategy aims to minimize the total electricity cost of the building facility by charging and discharging the EVs at the cheap and expensive hours respectively. The control model was evaluated on a workplace charging scenario at the UK's generic distribution LV network. The impact on the demand profile and daily electricity cost was studied for a realistic EV fleet.

3.2 Literature Review

Several approaches for the management of EV charging have been presented in the literature the past few years. The existing EV charging control strategies can be classified into two categories, namely centralised and decentralised.

The centralised control strategy uses a central controller (an EV aggregator) which coordinates all the EVs. According to [95], the implementation of a centralized control strategy allows real time insight at all points of the network and a better utilisation of the network capacity. However, it requires significant communication infrastructure across the network and communication links between the central controller and each individual EV for the acquisition of local information. In addition, a real-time operation requires significant computational resources in order to process large amounts of data and solve the scheduling problem of EV charging. Therefore, the centralised control strategies are costly to implement and susceptible to single-point failures (e.g. if the EV aggregator fails, the entire EV management system will stop working) [96]. Implementation examples of this control strategy are found to use linear programming [97], model predictive control [98], dynamic programming [93, 99] and particle swarm optimisation [100]. Linear programming is a method to achieve the best outcome (such as maximum profit or lowest cost) in a mathematical model whose requirements are represented by linear relationships [97]. Although it lets to perform an extensive analysis of "what-if" scenarios with a small computational cost (since only linear calcu-

lations are included in the process), it assumes that a linear relationship between the variables which in some cases is not realistic (e.g. relationship between network losses and demand) [101]. Model predictive control techniques have been found to outperform linear programming methods, converging faster to the optimal solution even on linear problems [98]. However, they are very sensitive to uncertainties, and that often leads to suboptimal solutions or even non-convergence for large problems with variables of probabilistic nature [102]. On the other hand, dynamic programming allows a more realistic representation of the system since it allows the optimization parameters to change during the optimization process. The computational requirements however are significant, and the time needed for solving a large optimization problem could make this method impractical for a near-real time operation [93]. Particle swarm optimization methods have been found to perform well with problems considering uncertainties, as they have intrinsic parameters with “memory” which are used to return to a previous better solution of the optimization problem. The correct parametrisation however requires large amounts of data, and the convergence is slow [103].

On the other hand, decentralised control strategies require information exchanges among neighbouring units through a local communication network. This eliminates the need for powerful data processing units and reduces the size of the required communication infrastructure, making this control approach a cost-effective solution. In addition, the computational requirements are significantly lower when comparing to centralised approaches for large numbers of EVs [95]. Examples of decentralised control strategies can be found in [104–107]. Following this strategy, researchers have often implemented a multi-agent system to control the charging of the EVs, according to which every EV is seen as an autonomous agent with individual objectives and constraints. Papers [86, 108–110] present relevant approaches. Simulating the rationale of an EV driver, game theoretic approaches are also implemented following a decentralised control architecture, where the scheduling problem is formulated as a cooperative or non-cooperative game and the participants try to reach the Nash equilibrium (the state where each EV driver chooses the best possible charging schedule, taking into account the decisions of the other EV drivers) [111, 112].

In addition to the flexibility they offer during their charging periods, EVs have the potential to be used as a flexible storage giving energy back to the grid or to a building. The acronyms V2G for “Vehicle-to-Grid” or V2B for “Vehicle-to-Building” are often used. This technology was introduced for the first time by Kempton et al. in 1997 [113], and it implies bi-directional power components that let the batteries share part of their energy and let it flow towards the grid or the building. The energy storage capacity of an EV fleet in the V2G concept can be used for ancillary services like reserve and frequency regulation. V2B concept uses energy exchange between the EVs and a building, affecting the local demand and/or reducing the building’s energy cost. In both cases, control, metering and communication technologies will be required within a proper regulated and standardized framework [114].

The utilisation of the EV batteries in a V2G concept is found in a number of papers in the literature. Focusing on mitigating the variation of renewable energy generation, the authors of [115] propose a hierarchical framework which regulates the V2G power and minimises the total operational cost (TOC). Similar approaches can be found in [116, 117]. The V2G potential in the ancillary service market was evaluated in [118], and the results showed that a 40.3% optimal gain factor (defined in [118] as “the average power discharge to the grid by each vehicle”) is obtainable. The economic value of V2G in a real time power flow control algorithm was also studied in [119] for a large scale scenario of EV uptake. The participation of EV charging / discharging in the ancillary services market is investigated in [120], where V2G is used for primary frequency regulation through a droop-control mechanism that follows a $\Delta f / \Delta P$ curve in order to define the V2G output according to the system’s frequency. A frequency droop-based control is also used in [121], where a distributed regulation dispatch algorithm is developed aiming to meet the regulation dispatch signals sent to the EV aggregator by the system operator. Other approaches of EV participation in the ancillary services market through V2G can be found in [122–128]. A game theoretic approach is also implemented in [129], while the authors of [130] developed an economic benchmark model for the EV charging strategies and showed that V2G provides additional revenues to the EV owners. Despite the promising results from the various V2G models, the authors of [131] highlight a number of concerns that arise, especially regarding

the necessary power electronics hardware, and suggest some research directions for the near future, in order to possibly make V2G a practical reality.

Apart from the grid-side benefits of V2G, the bi-directional power exchanges of EVs are also beneficial in small-scale applications like the parking lots of buildings. Using the EVs in a microgrid that includes a number of buildings and distributed energy resources (DER) is found in a few papers in the literature. Such an example is found in [114] and [132], where the authors perform an economic analysis for an office building in California, and use EVs with Vehicle-to-microgrid (V2m) capabilities in order to optimize their storage usage in combination with other DER. Similar work can be found in [133–135]. Prediction models are also incorporated to the scheduling algorithms in [136, 137] to forecast the demand profile of local DER and EV charging respectively. A model predictive control based algorithm is presented in [138] that co-schedules the HVAC operation, EV charging demand and battery storage to reduce the total building energy consumption and the peak energy demand, while maintaining the temperature within the comfort zone for building occupants and meeting the deadlines for EV charging. The authors of [139] present a multi-agent based model for the energy management of the building with EVs, and compare three different charging strategies with respect to their impact on building comfort. A game theoretic approach is presented in [140], where a non-cooperative game is played by the EVs to flatten the demand profile of a building.

According to the best of the author’s knowledge however, the existing models do not consider the electricity cost of the building manager as the main objective of the charging control. This chapter proposes a charging control model that reduces impact of EV charging on the demand profile and the electricity cost of the building, according to the building manager’s objectives.

3.3 Charging Control Model

The proposed charging control model for the Charging Station Manager follows two different centralised control strategies namely “Off-Peak Strategy” and “Cost-Reduction

Strategy". A two-stage coordination approach is followed as presented in Figure 3.1. In order to increase the sensitivity of the control model, and offer a dynamic coordination of the EV charging, both stages of the coordination cycle are repeated on a 15 minutes basis (timestep). This timestep duration was considered small enough to ensure a dynamic response to unexpected changes in the system, but also big enough to avoid the computational delays that are introduced for large numbers of EVs.



Figure 3.1: The stages of the EV coordination

During the *Schedule* stage the Charging Station Manager coordinates the charging of every EV that is connected to a charging point. It calculates the most preferable future timesteps for the EV charging according to its strategy, considering constraints both from the infrastructure side (nominal power of charger, network limits) and the vehicle side (battery capacity, departure time). During the *Dispatch* stage the Charging Station Manager sends the charging set point to all EVs that are scheduled to charge during that timestep.

3.3.1 Off-Peak Strategy

The goal of the Off-Peak strategy is to minimize the impact of EV charging on the demand profile of the building. To this end, the off-peak hours of the building' daily power demand are preferred for the EV charging. The future power demand of the building is assumed known, and the scheduled charging set points for an EV are obtained from solving the minimization problem of Equation (3.1). In order to achieve the optimal solution for the whole EV fleet it is crucial to solve this minimization problem sequentially for all the connected EVs. That is because the charging schedule of each EV affects the future power demand of the charging facility ($P_S(t)$ from Equation (3.1)), and consequently the charging schedules of the EVs that have not yet scheduled their charging. The use of the Charging Station Manager is highlighted at this point, as it aggregates the information from all the EVs and coordinates their charging. Variable

t_0 is the arrival timestep of an EV, while CP is the connection period of an EV (number of timesteps between arrival and departure). Variable CP together with the timestep duration (15min) defines the resolution and size of the power vectors for each EV (e.g. for an EV that arrives at 10:00 and leaves at 14:00, the CP is 16 and all the power vectors will have 16 values).

$$\min \sum_{t=t_0}^{t_0+CP} (P_{EV}(t) + P_S(t)) \quad (3.1)$$

subject to:

$$\sum_{t=t_0}^{t_0+CP} (T \cdot P_{EV}(t)) = \frac{(SoC_{max} - SoC_{in}) \cdot BC}{C_{eff}}$$

$$P_{EV}(t) \leq P_n$$

$$P_{EV}(t) \leq P_L(t) - P_S(t)$$

, where

$P_{EV}(t)$ is the scheduled charging set point for timestep t

T is the duration of the timestep in hours

$P_S(t)$ is the building's demand without EV charging at timestep t

$P_L(t)$ is the network limit, the maximum energy that can be supplied from the grid at timestep t (covering both the building demand and the EV charging)

P_n is the nominal power of the EV charger

BC is the battery capacity

C_{eff} is the charger efficiency

SoC_{in} is the initial SoC level

SoC_{max} is the maximum SoC that can be reached until the departure of the EV

Such a charging strategy is directly beneficial for the electricity grid as it prevents the stressing of the network. Depending on the contractual agreements between the energy provider and the building manager, this charging control strategy could be also beneficial for the latter, especially if the number of EVs is high.

3.3.2 Cost-Reduction Strategy

The goal of the Cost Reduction strategy is to reduce the daily energy cost of the building. The EVs are charged during the cheapest hours of their presence in the parking lot. Following the electricity price curve, the EVs are charging when the kWh is cheaper. The scheduled charging set points for an EV are obtained from solving the minimization problem of Equation (3.2).

$$\min \sum_{t=t_0}^{t_0+CP} (P_{EV}(t) \cdot p(t)) \quad (3.2)$$

subject to:

$$\sum_{t=t_0}^{t_0+CP} (T \cdot P_{EV}(t)) = \frac{(SoC_{max} - SoC_{in}) \cdot BC}{C_{eff}}$$

$$P_{EV}(t) \leq P_n$$

$$P_{EV}(t) \leq P_L(t) - P_S(t)$$

, where $p(t)$ is the electricity price for timestep t .

Such a charging strategy emphasises on minimizing the charging cost for the building manager. Unlike the Off-Peak strategy, the optimality of the solution is not affected by the dependencies between the charging schedules of the EVs because the charging schedule of one EV is not able to affect the electricity prices. There are however indirect dependencies due to the overall network constraint ($P_L(t)$) which prevents the EVs from charging when the scheduled demand exceeds this limit.

3.3.3 Control Algorithm

In every operating timestep t the Charging Station Manager performs the following steps:

Step 1. Create a list l_t with all the EVs that are connected to their charging point.

- Step 2. Sort the list l_t according to their disconnection time. EVs that depart first are placed on the top of the list. The EVs that depart on the same time are classified according to their SoC (emptiest first)
- Step 3. Calculate the energy requirements for the EV which is first on list l_t
- Step 4. Identify the most preferred charging timesteps according to the strategy
- Step 5. Calculate the future power set points of the EV charger with respect to the EV charger's nominal power and the network's limits
- Step 6. Update the scheduled demand of the facility (necessary to maintain optimality)
- Step 7. Remove EV from list l_t
- Step 8. If there are unscheduled EVs, return to Step 3 otherwise continue to the *Dispatch* stage

The *Schedule* stage of the charging control model for both strategies during one timestep is described using Figure 3.2. In the *Dispatch* Stage, the scheduled power set points in timestep t are forwarded to the EV chargers in order to charge the EVs.

The abbreviations used in Figure 3.2 are explained in the following list:

l_t is a list with all the connected EVs at timestep t

D_{EV} is the departure timestep of the EV, as specified from the EV owner

SoC_t is the SoC of the EV at timestep t

(\uparrow) indicates the ascending order of the sorting

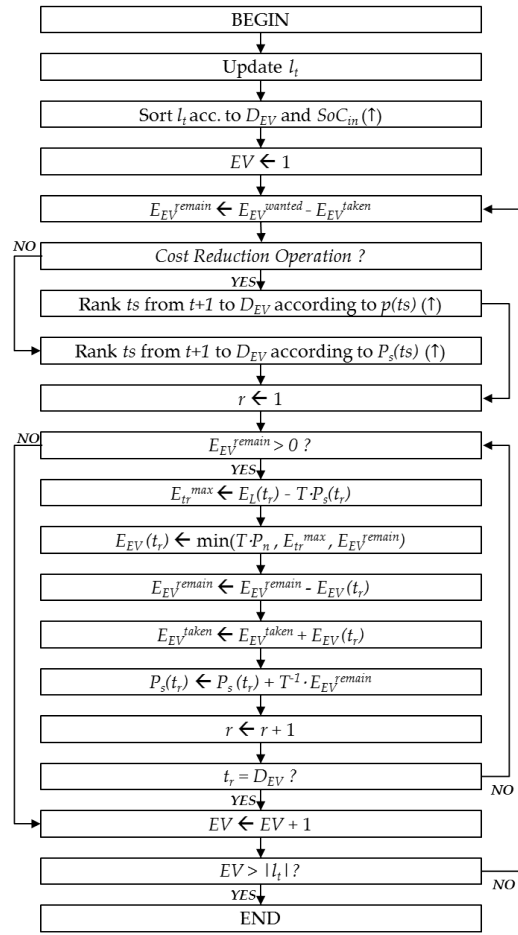
EV is a counter variable for the connected EVs

E_{EV}^{remain} is the remaining energy to be supplied to EV

E_{EV}^{wanted} is the total energy requirements of the EV

E_{EV}^{taken} is the scheduled energy to be supplied to EV

ts a counter variable for the timesteps of the day

Figure 3.2: The *Schedule* stage of the charging control model

$p(ts)$ is the electricity price in $/MWh$ at timestep ts

$P_s(ts)$ is the total scheduled power demand at timestep ts in kW

r indicates the ranking value (1 is the highest)

t_r is the timestep with ranking value r

E_L is the network limit, the maximum energy that can be supplied from the grid at timestep ts (covering both the building demand and the charging of all the EVs)

T is the duration of the timestep in hours

$E_{t_r}^{max}$ is the maximum energy that the EV can take from the grid at timestep ts

P_n is the nominal power of the EV charger

E_{EV} is the energy that the EV is scheduled to take at timestep tr

3.4 Charging Control Model with V2B

The charging control model was modified in order to include V2B operational capabilities when bi-directional power exchanges are available to the Charging Station Manager. Under the V2B operational mode, the Charging Station Manager coordinates the EVs to charge and discharge according to the same Off-Peak and Cost Reduction strategies. As presented before, these strategies are mainly different in the way the scheduling process is performed, while the dispatch stage is the same. The Charging Station Manager follows the two stage coordination approach in every timestep, and schedules the charging and discharging events of every EV that is connected to a charger. It is assumed that a contractual agreement exists between the EV owner and the building manager that regulates the maximum depth of discharge for each EV. This depth of discharge level ($V2B$) defines the amount of energy that the EV owner agree to extract from their EV and provide to the building manager ($V2B^{agreed}$). The design of contractual agreements to reward the participants, as well as business models evaluating the viability of a reward system are not studied in this thesis; it is assumed that both parties are benefited and willing to participate in a V2B scheme. Each EV owner decides the discharge capacity to offer, according to its needs and use of EV.

3.4.1 Off-Peak Strategy

The *Off-Peak Strategy* has the same objective as before. The off-peak hours of the building's daily power demand are preferred for charging the EVs. Utilizing the discharging functionality of the EVs, the Charging Station Manager discharges the EVs during the peak demand hours in order to reduce the overall peak demand of the building and flatten the demand profile of the building facility. Such a charging strategy offers great benefits to the electricity grid as it reduces the stressing of the network. Apart from the contractual agreements between the energy provider and the building manager, additional agreements between the building manager and the EV owners could be beneficial to both parties. The EVs could be rewarded for their participation to such a scheme, while the building manager would have a flattened demand profile

for his building facilities and be able to postpone possible unnecessary upgrades of the installed infrastructure.

3.4.2 Cost Reduction Strategy

The Cost Reduction Strategy is the same as before, only this time the EVs are discharging at the expensive hours to further reduce the overall cost for the building manager. In case the EV owners pay for their charging on a fixed rate, this strategy could be applied in order to reduce the electricity cost for the building manager. In this case however, financial or other incentives should be given to the EV owners as a reward for their participation to the scheme.

The optimization problems of Equation (3.1) and Equation (3.2) were modified and transformed into one generalised minimization problem, applicable to both strategies. A ranking function is used to identify the most preferable timesteps for charging / discharging. The charging / discharging power set points are obtained after solving Equation (3.3).

$$\min \sum_{t=t_0}^{t_0+CP} (P_D(t) \cdot r_1(t) + P_C(t) \cdot r_2(t)) \quad (3.3)$$

subject to:

$$\sum_{t=t_0}^{t_0+CP} (T \cdot P_C(t)) = \frac{(SoC_{max} - SoC_{in}) \cdot BC}{C_{eff}}$$

$$\sum_{t=t_0}^{t_0+CP} (T \cdot P_D(t)) = \frac{V2B \cdot BC}{C_{eff}}$$

$$P_C(t) \leq P_n$$

$$P_C(t) \leq P_L(t) - P_S(t)$$

$$P_D(t) \leq P_n$$

$$P_D(t) \leq P_S(t)$$

, where:

$P_C(t)$ is the scheduled charging set point for timestep t

$P_D(t)$ is the scheduled discharging set point for timestep t

$r_1(t)$ is the output of the charge ranking function for timestep t

$r_2(t)$ is the output of the discharge ranking function for timestep t

T is the duration of the timestep in hours

$P_S(t)$ is the building's demand without EV charging at timestep t

$P_L(t)$ is the network limit, the maximum energy that can be supplied from the grid at timestep t (covering both the building demand and the EV charging)

P_n is the nominal power of the EV charger

$V2B$ is the agreed depth of discharge level (in % of BC)

BC is the battery capacity

C_{eff} is the charger efficiency

SoC_{in} is the initial SoC level

SoC_{max} is the maximum SoC that can be reached until the departure of the EV

3.4.3 Control Algorithm

The steps that the EV aggregator executes in every timestep t are listed below:

Step 1. Create a list l_t with all the EVs that are connected to their charging point

Step 2. Sort the list l_t according to their disconnection time. EVs that depart first are placed on the top of the list. The EVs that depart on the same time are classified according to their SoC (emptiest first)

Step 3. Calculate the remaining discharge capacity for the EV which is first on list l_t

Step 4. Identify the most preferred discharging timesteps according to the strategy

Step 5. Calculate the future power set points of the EV charger with respect to the EV charger's nominal power and the network's limits

- Step 6. Update the scheduled demand of the facility (necessary to maintain optimality)
- Step 7. Flag the discharging timesteps in order to prevent charging and discharging at the same time
- Step 8. Calculate the energy requirements for the EV which is first on list l_t
- Step 9. Identify the most preferred charging timesteps according to the strategy
- Step 10. Calculate the future power set points of the EV charger with respect to the EV charger's nominal power and the network's limits
- Step 11. Update the scheduled demand of the facility (necessary to maintain optimality)
- Step 12. Remove EV from list l_t
- Step 13. If there are unscheduled EVs, return to Step 3 otherwise continue to the Dispatch stage

The *Schedule* stage of the charging control model for both strategies during one timestep is described using Figure 3.3. In the *Dispatch* Stage, the scheduled power set points in timestep t are forwarded to the EV chargers in order to charge the EVs.

The abbreviations used in Figure 3.3 are explained in the following list:

l_t is a list with all the connected EVs at timestep t

D_{EV} is the departure timestep of the EV, as specified from the EV owner

SoC_t is the SoC of the EV at timestep t

(\uparrow) indicates the ascending order of the sorting

(\downarrow) indicates the descending order of the sorting

EV is a counter variable for the connected EVs

$V2B_{EV}^{remain}$ is the remaining energy to be extracted from EV

$V2B_{EV}^{agreed}$ is the total agreed energy to be extracted from EV



E_L is the network limit, the maximum energy that can be supplied from the grid at timestep ts (covering both the building demand and the charging of all the EVs)

T is the duration of the timestep in hours

E_{tr}^{max} is the maximum energy that the EV can take from the grid at timestep ts

P_n is the nominal power of the EV charger

E_{EV} is the energy that the EV is scheduled to take/give at timestep tr

$discharge$ is a Boolean variable to prevent charging and discharging at the same time

3.5 Description of the simulation scenario

The developed EV charging coordination algorithm was evaluated on a workplace charging scenario and the impact of the EV charging / discharging on the demand profile and electricity cost of a building facility was assessed. In the studied scenario the EVs were coordinated to charge/discharge during office hours in the parking lot of an office building.

A typical UK office building was considered to evaluate the performance of the proposed coordination algorithm in the workplace charging Scenario. The considered office building has a peak demand of 24kW and a typical load profile curve from the UK Energy Research Centre (UKERC) (see Figure 3.4).

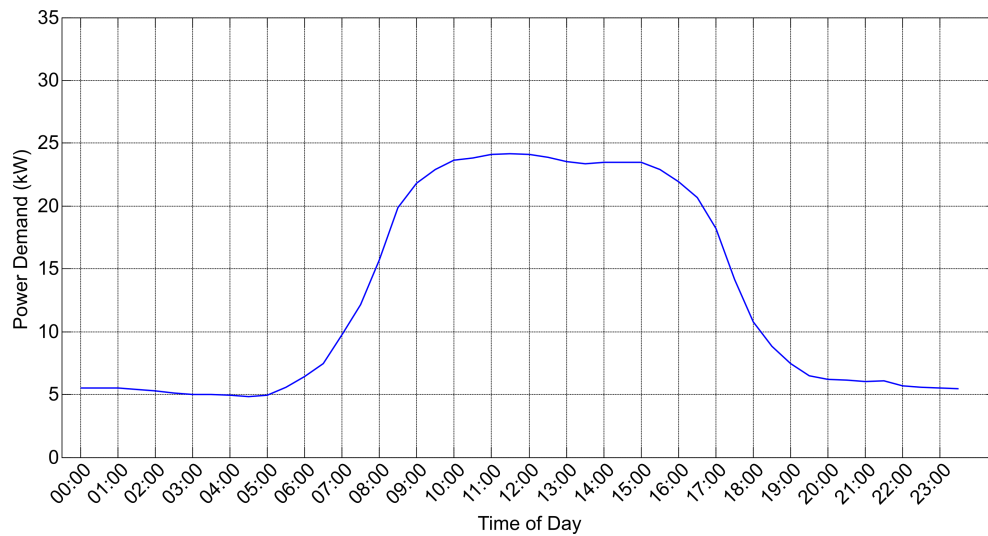


Figure 3.4: The typical power demand of an office building

According to [141] and [142], 25 employees are assumed to work in this building. Considering that an average 67% of the employees go to their work by car [143], approximately 16 vehicles arrive every day in the building (or in the area near the building). Assuming a 20% EV uptake (estimated for 2025 in [144]), 3 EVs were considered for each office building in the network.

The behaviour of the EV drivers has been statistically modelled using the data provided by the NTS regarding the region of Wales (<https://www.gov.uk>), in order to calculate arrival / departure times and energy requirements for every EV. Raw files and extended reports were available from the UK Data Service, providing information about the arrival and departure times to/from work along with the travelled distance from 2002 up to 2010. A total of 962 people and 4,099 dairy days have been analysed, and the model was evaluated on these data. After the data from NTS were analysed, the arrival and departure time distributions of Figures 3.5-3.6 as well as the travelled distance distribution of Figure 3.7 was calculated.

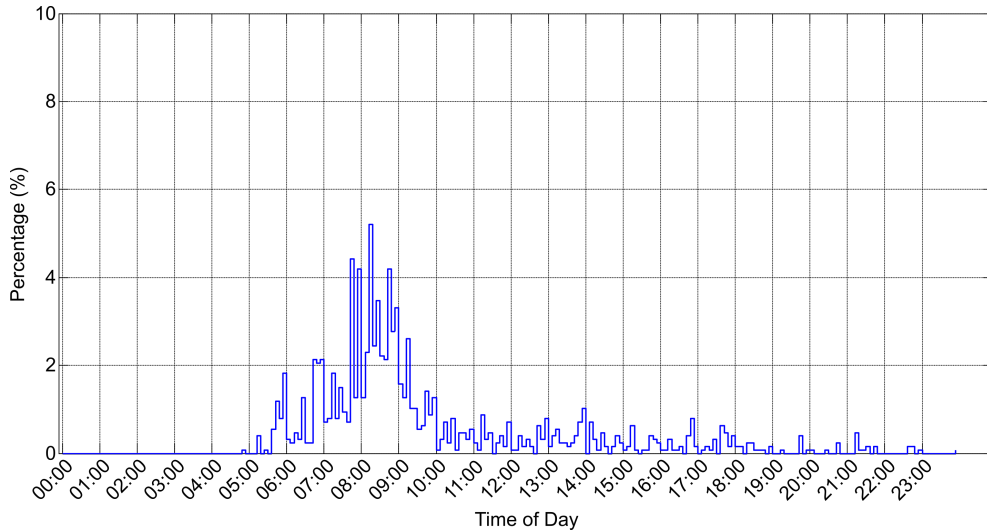


Figure 3.5: Probability distribution of arrival times at workplace

The distribution of Figure 3.7 was used to calculate the EV's energy requirements when arriving at home. It is used to identify the initial state of charge (SoC_{in}) of an EV when arriving at the parking lot, based on the battery capacity (BC) and the

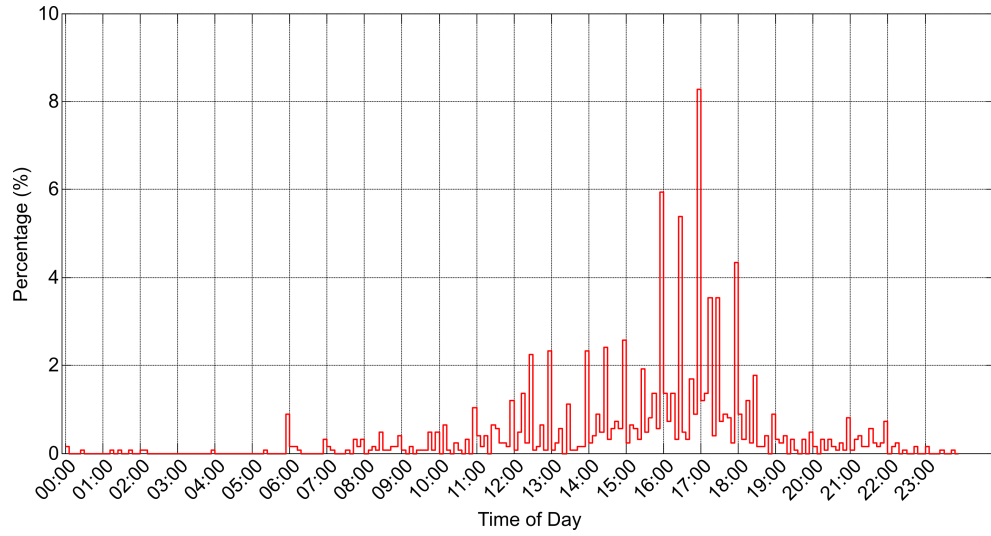


Figure 3.6: Probability distribution of departure times from workplace

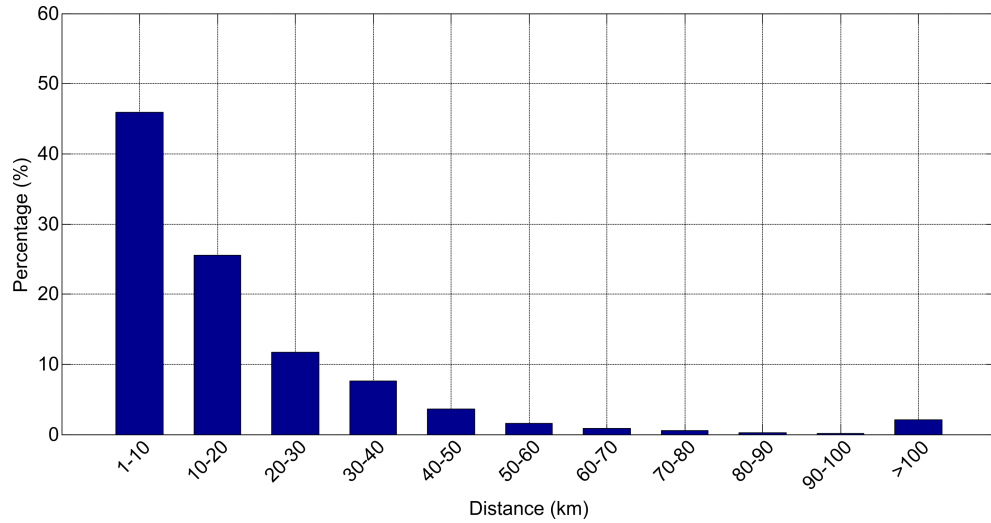


Figure 3.7: Probability distribution of travelled distance before workplace

mean energy consumption per km (MEC) of its battery:

$$SoC_{in} = 100 - \frac{MEC \cdot distance \cdot 100}{BC} \quad (3.4)$$

Information regarding the battery capacity and the energy consumption of an EV are usually published by the EV manufacturers in the vehicle's datasheet. Looking at the UK market [144], typical values for the battery capacity are around 28kWh and

for the mean energy consumption around 0.16kWh/km. In this model, the normal distributions of Table 3.1 have been considered for both battery capacity and energy consumption for each EV.

Table 3.1: Parameters of the normal distributions for BC and MEC

	Battery Capacity (kWh)	Energy Consumption (kWh/km)
Mean	28	0.16
sigma	2	0.02

The charging stations were assumed to have a charging rate of 7kW. For the Charging Control Model with V2B two scenarios were considered for the agreed depth of discharge of the EVs ($V2B_{agreed}$), with values of 5% and 15% respectively. The daily electricity prices were obtained from (<http://www.n2ex.com/>) for a typical winter weekday. The electricity price curve is presented in Figure 3.8:

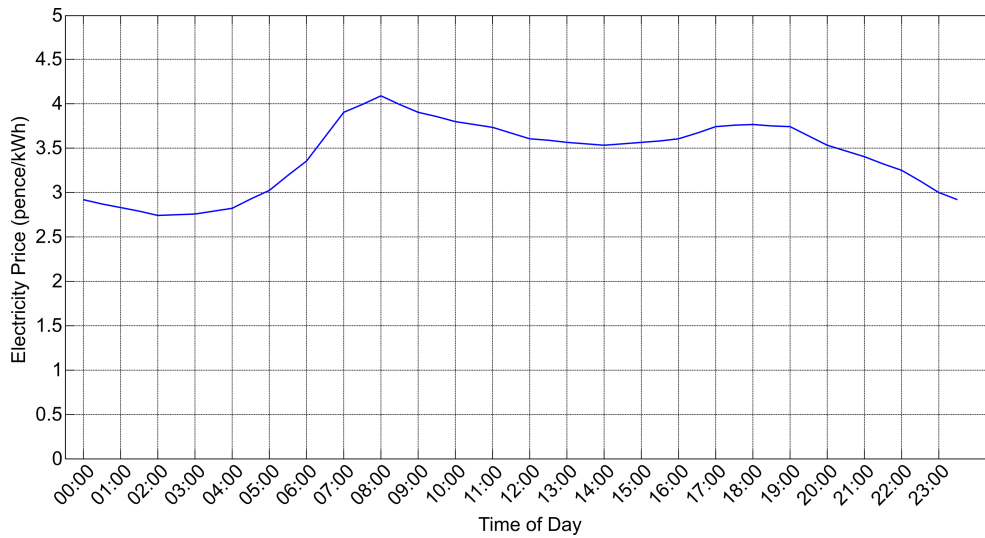


Figure 3.8: The daily electricity prices

The Charging Station Manager was assumed to be located at the LV substation, responsible for a number of office buildings. The structure of the UK Generic Low Voltage Distribution Network [145] was considered and modified for a realistic workplace charging scenario. An 11kV “commercial” feeder was implemented to study the impact on the electricity grid. The updated network structure for this scenario is presented in Figure 3.9, while its technical characteristics are summarized in Table 3.2.

As seen from Figure 3.9, the LV substation supplies electric energy to 16 office buildings and consequently coordinates the charging / discharging of 48 EVs.

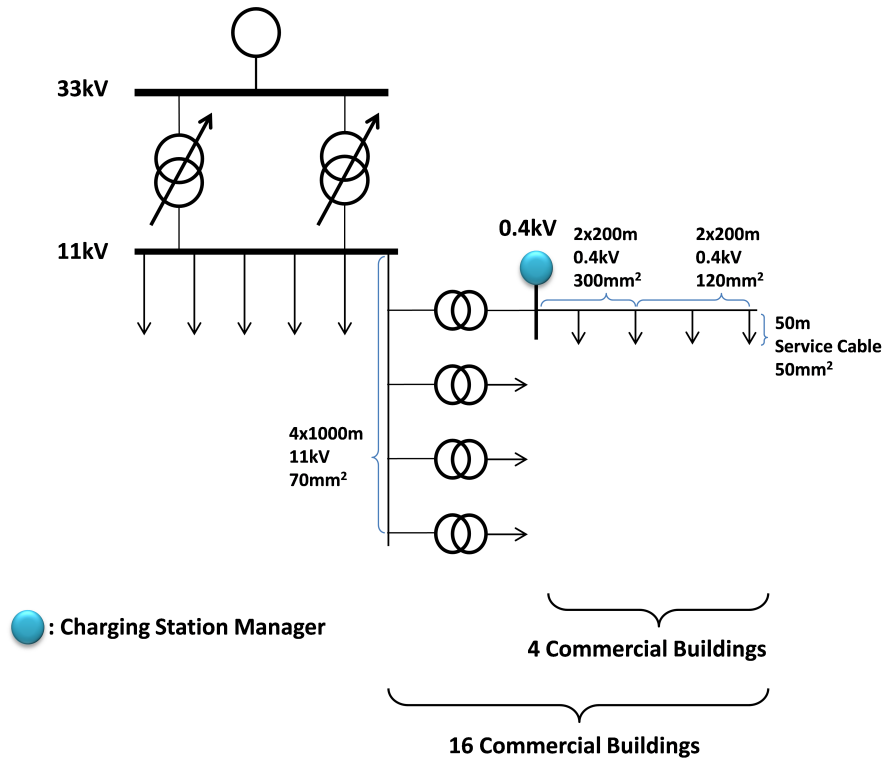


Figure 3.9: The modified UK Generic Low Voltage Distribution Network

3.6 Simulation results

3.6.1 Impact on the demand profile

Considering 48 EVs in a group of 16 commercial customers, the impact of their charging at a 7kW charger in an uncontrolled fashion is presented in Figure 3.10. As seen from Figure 3.10, the EV charging leads to an increase of the peak demand during the arrival hours of the EVs (around 08:00 - 09:00).

As explained in the previous sections, a Charging Station Manager was assumed to be installed at the 0.4kV bus to manage the EV charging. The impact of EV charging when the Charging Station Manager operates under the Off-Peak strategy is presented

Table 3.2: The technical characteristics of the network

Object Description	Technical Characteristics
33/11kV Transformer	15MVA X/R ratio = 15 18% impedance on 15MVA base
11kV Bus	5 Outgoing 11kV “domestic” feeders 3km each 1 Outgoing 11kV “commercial” feeder 4km
11kV 185mm ² “domestic” feeder segment	3-core PICAS, Cu 0.164 + j0.08 Ω/km
11kV 95mm ² “domestic” feeder segment	3-core PICAS, Cu 0.32 + j0.087 Ω/km
11kV 70mm ² “commercial” feeder segment	3-core XLPE, Al 0.568 + j0.1 Ω/km
11/0.4kV Transformer	500kVA X/R ratio = 15 5% impedance
0.4kV “commercial” Bus	1 Outgoing 0.4kV “commercial” feeder 400m
0.4kV 300mm ² “commercial” feeder segment	XLPE, Cu 0.0802 + j0.072 Ω/km
0.4kV 120mm ² “commercial” feeder segment	XLPE, Cu 0.197 + j0.072 Ω/km
0.4kV 50mm ² “commercial” service cable	XLPE, Cu 0.494 + j0.076 Ω/km

in Figure 3.11. The Off-Peak strategy of the Charging Station Manager places the EV charging events at the off-peak hours of the demand curve, and reduces the impact of EV charging on the network. When the EVs offer discharging services, the Charging Station Manager operates under the V2B operation, discharging the EVs at the

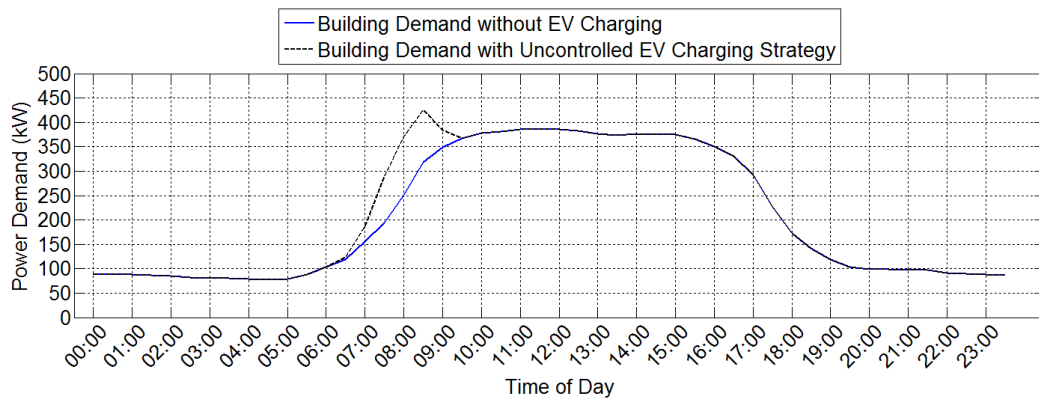


Figure 3.10: Impact of Uncontrolled EV charging

peak hours. Considering a 5% discharging allowance, the Charging Station Manager reduces the peak demand by 4.8%. When the V2B allowance is increased to 15%, the EVs discharge for longer periods resulting in further demand reduction (up to 9.7%). The increased depth of discharge results in longer charging durations from the EVs, in order to leave the workplace fully charged. This phenomenon is illustrated by looking at the distribution of the charging hours from the EVs. Longer charging durations are needed from the EVs to be able to provide this additional discharging capacity. Considering that not all EV drivers leave the same time from the workplace (also seen in Figure 3.6), the model tries to reduce the delay for every EV owner. To this end, the model prioritises EVs leaving early over EVs leaving late and charges them according to their departure time (Step 2 of the Schedule Algorithm); EVs leaving early will be charged sooner than EVs that leave later.

Figure 3.12 presents the impact of EV charging when the Charging Station Manager operates under the Cost Reduction strategy. In this strategy the cheapest hours are preferred for the charging events and the most expensive hours are preferred for discharging the EVs. As proposed in [72], a maximum limit of 500kW was set to the Charging Station Manager, in order to avoid a peak in the demand and protect the MV/LV transformer of the 0.4kV bus. This upper limit at 500kW caps the EV charging demand, and results in prolonged charging events. When bi-directional power exchanges are available, the Charging Station Manager coordinated the EVs to discharge during the (expensive) morning hours. As seen from Figure 3.12, this strategy

is very sensitive to price changes, and all EV charging events coincide between 13:00 - 15:00. This is due to the inelastic price curve. A dynamic price mechanism could solve this problem; however this is not the focus of this chapter.

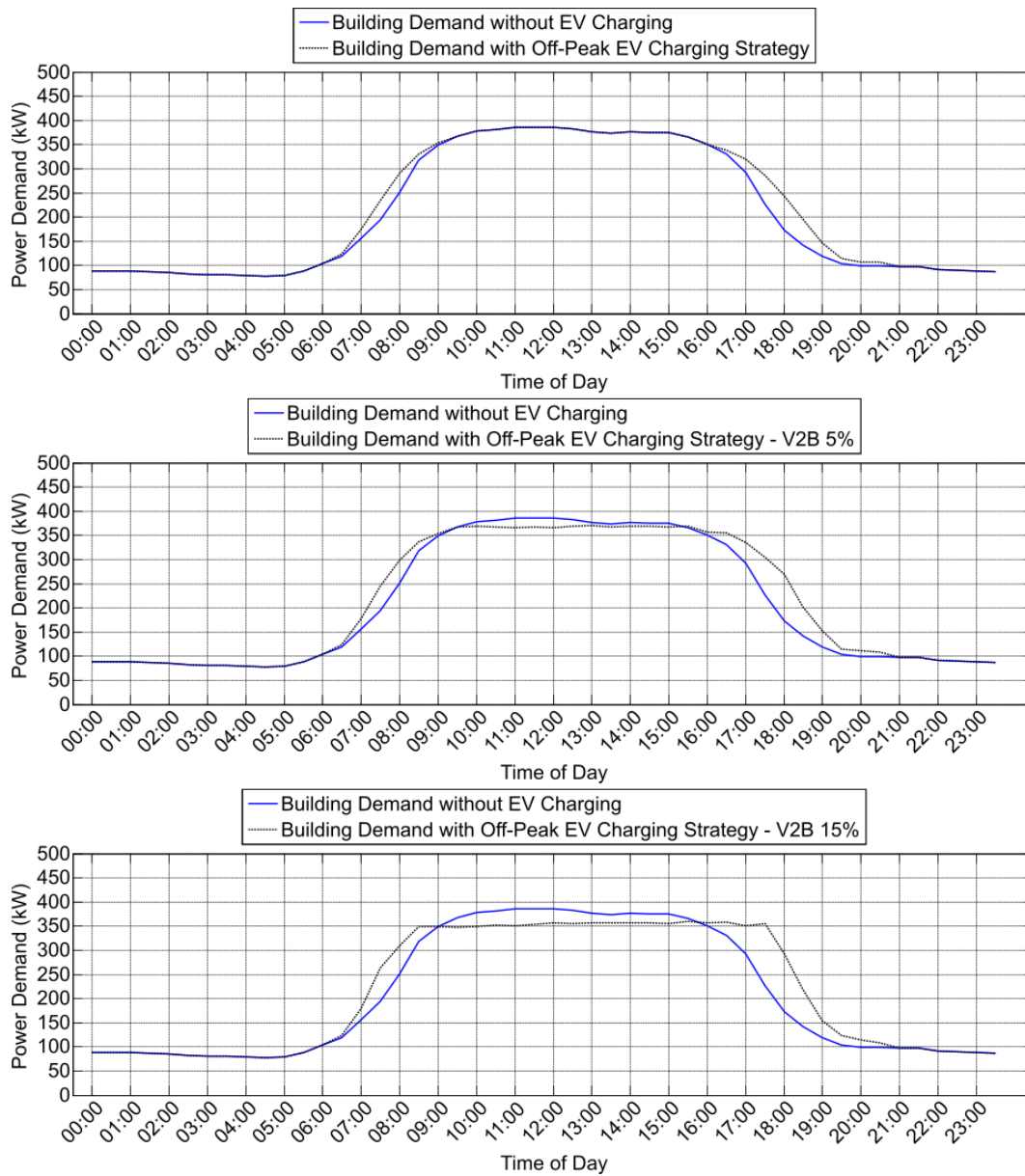


Figure 3.11: Impact of EV charging with the Off-Peak Strategy

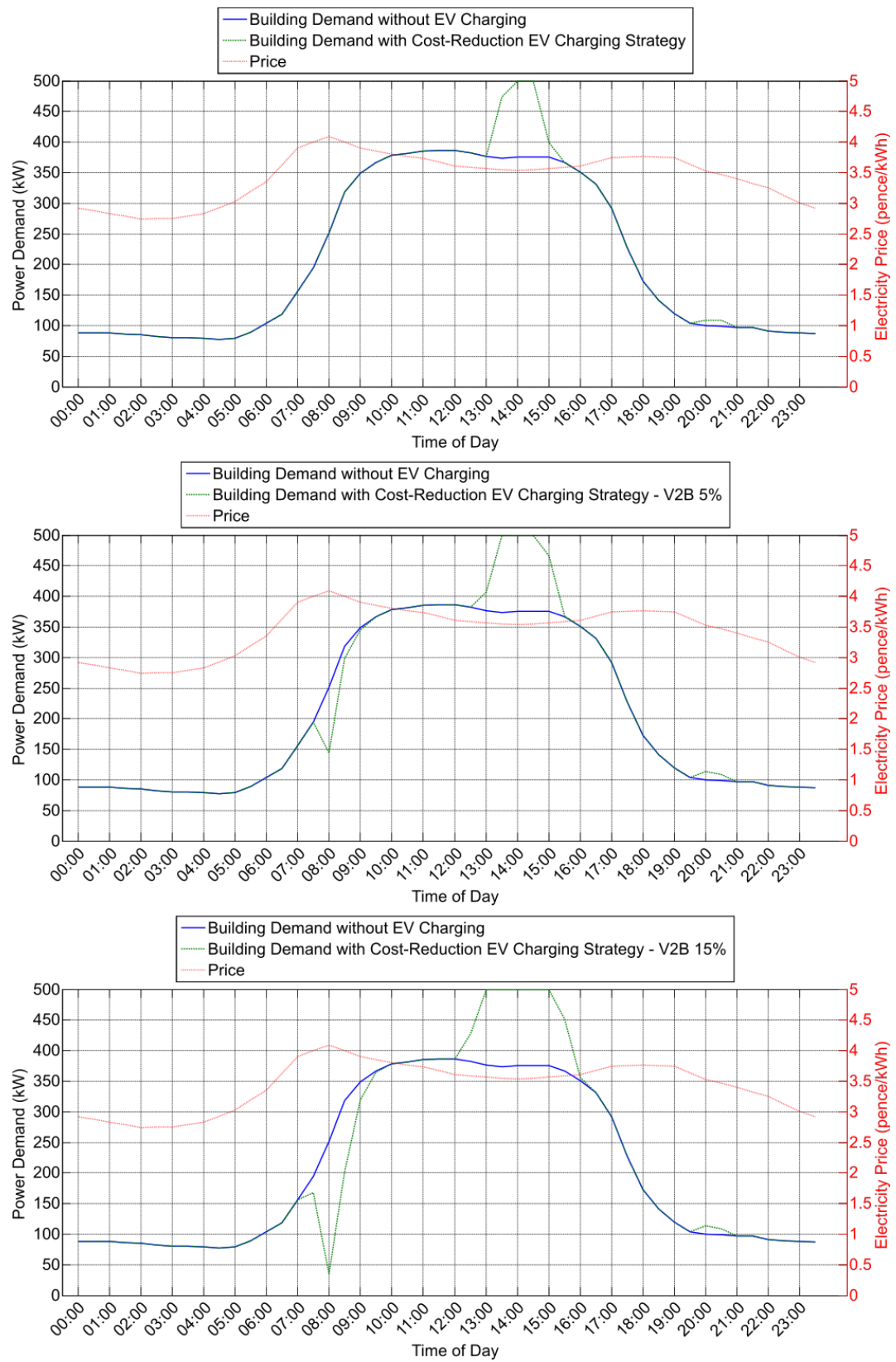


Figure 3.12: Impact of EV charging with the Cost-Reduction Strategy

3.6.2 Impact on the daily electricity cost

The different charging control strategies were also compared according to the daily electricity cost that is needed to supply the aggregated demand (as presented in Figures 3.11-3.12). Figure 3.13 presents the resulting daily cost difference between each charging strategy and the base case (without EVs at all).

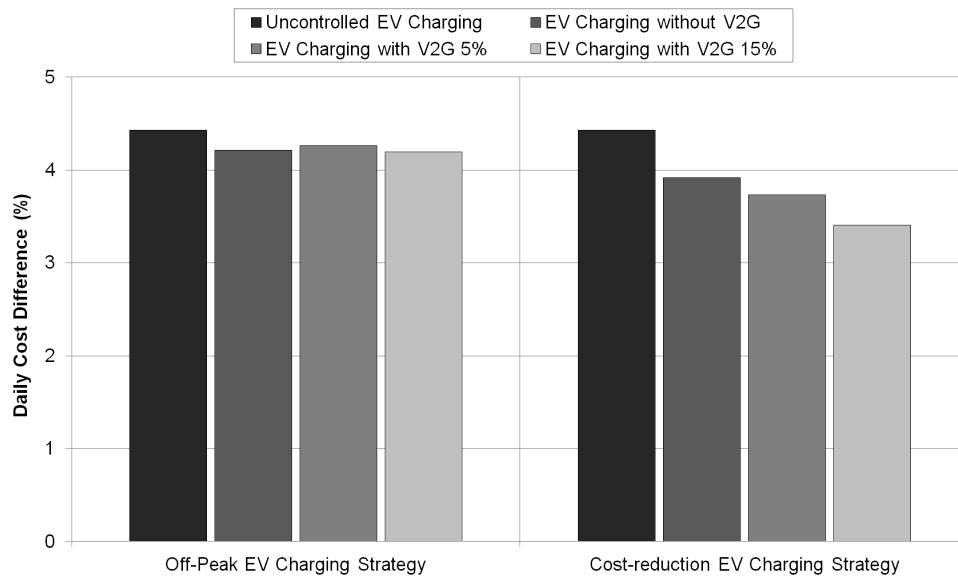


Figure 3.13: Increase of the daily electricity cost comparing to the case without EV charging.

As expected, the Uncontrolled charging scenario results in the greatest cost increase as the charging events coincide with the expensive peak hours of the demand curve. Looking at the rest of the scenarios, the overall daily cost is increased as the EV charging increases the building's demand. Due to the relatively small differences of the demand profile in all the charging strategies, the daily cost difference between the different strategies is not significant. Offering V2B services, the Charging Station Manager is able to reduce the electricity cost increase for the building manager especially in the Cost Reduction strategy. This reduction however is not massive, being only 3.4% comparing to the 4.3% of the Uncontrolled charging scenario. Looking on an annual basis however, a 1% reduction in the electricity costs is important to the build-

ing managers especially if their electricity costs are high. Furthermore, considering more EVs (offering V2B services) in the parking lot of the building would result in a greater electricity cost reduction, as more EVs would be available to discharge during the expensive hours.

3.6.3 Additional unintended consequences

As presented in the previous section, the operating strategy of the Charging Station Manager affects the building's demand profile and consequently the electricity cost of the building manager. However, reducing the electricity cost of the building manager has additional unintended consequences to the network.

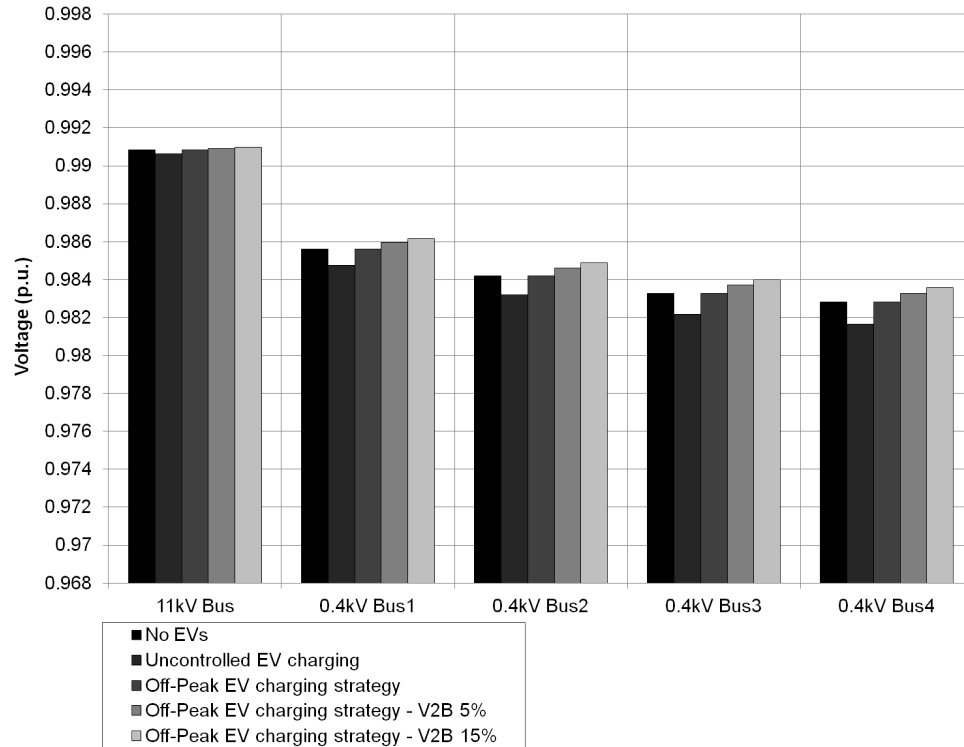


Figure 3.14: Minimum bus voltage with Off-Peak strategy

Considering the network structure of Figure 3.9, the bus voltages along the MV feeder are affected by the building's demand profile as formed by the charging strategy of the Charging Station Manager. The minimum voltage is found on the times when the demand is at its peak value. Charging the EVs in an uncontrolled fashion creates

a peak in the demand profile of the building as presented in Figure 3.10. This peak causes a voltage drop along the commercial MV feeder. Figures 3.14-3.15 present the minimum bus voltage that was observed in a day for both charging strategies.

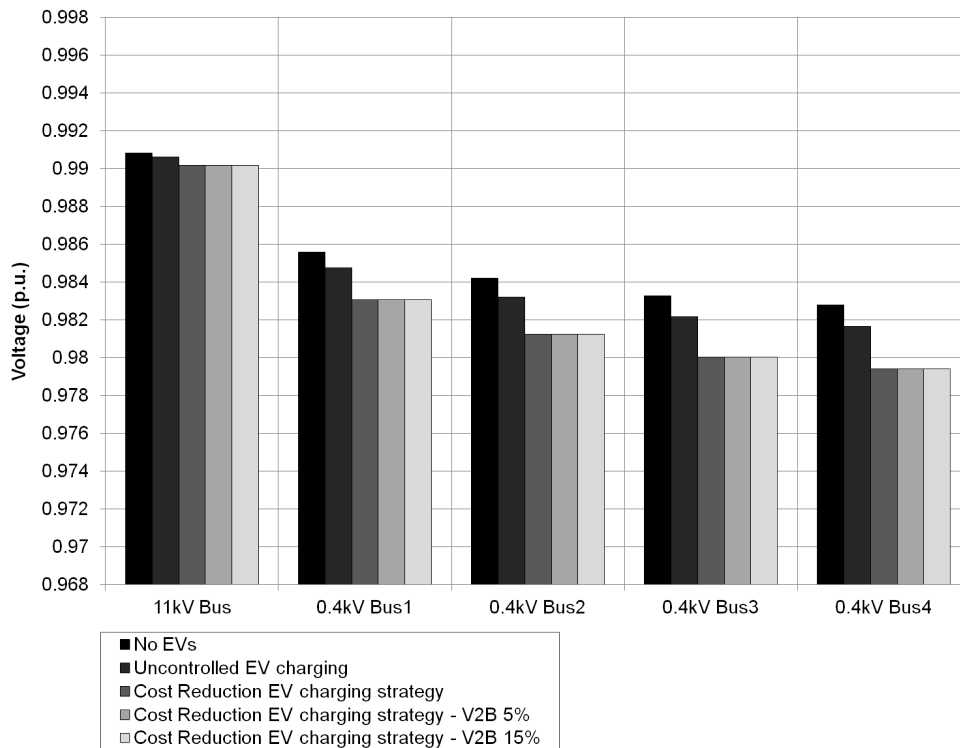


Figure 3.15: Minimum bus voltage with Cost-Reduction strategy

When the Charging Station Manager operates under the Off-Peak strategy (without V2B) the EV charging demand is not creating a new peak at the demand profile of the building and thus the minimum bus voltage is the same with the case without any EV charging. When the EVs offer discharging capacity, the Charging Station Manager reduces the peak demand of the building and the minimum voltage of the buses along the MV feeder are increased. The voltage increase is not significant, however considering a case with high levels of EV penetration, the reduction of the impact of EV charging on the bus voltage could be very valuable to the network (especially to areas with long MV lines).

When the Charging Station Manager operates under the Cost Reduction strategy, the EVs charge during the cheap hours and create a peak at the demand profile of the

building. This peak is capped by the 500kW limit of the Charging Station Manager. The number of EVs considered in the scenario results in a peak that is larger from this cap in all cases of the Cost Reduction charging strategy. Consequently the voltage drop is the same for all cases of this strategy, regardless of the availability or level of the discharging capacity. The value of the demand cap is highlighted here, as otherwise the EV charging would result in great stress for the network and further voltage drops.

3.6.4 Additional case studies

One of the key assumptions in this model is that all EV drivers participate in the control scheme; however this might not always be the case. To understand the model's sensitivity to this assumption, additional scenarios were studied for different numbers of unresponsive EV drivers (EV drivers who don't respond to the control signals of the Charging Station Manager). Figure 3.16 presents the impact of EV charging for different levels of unresponsive EV drivers.

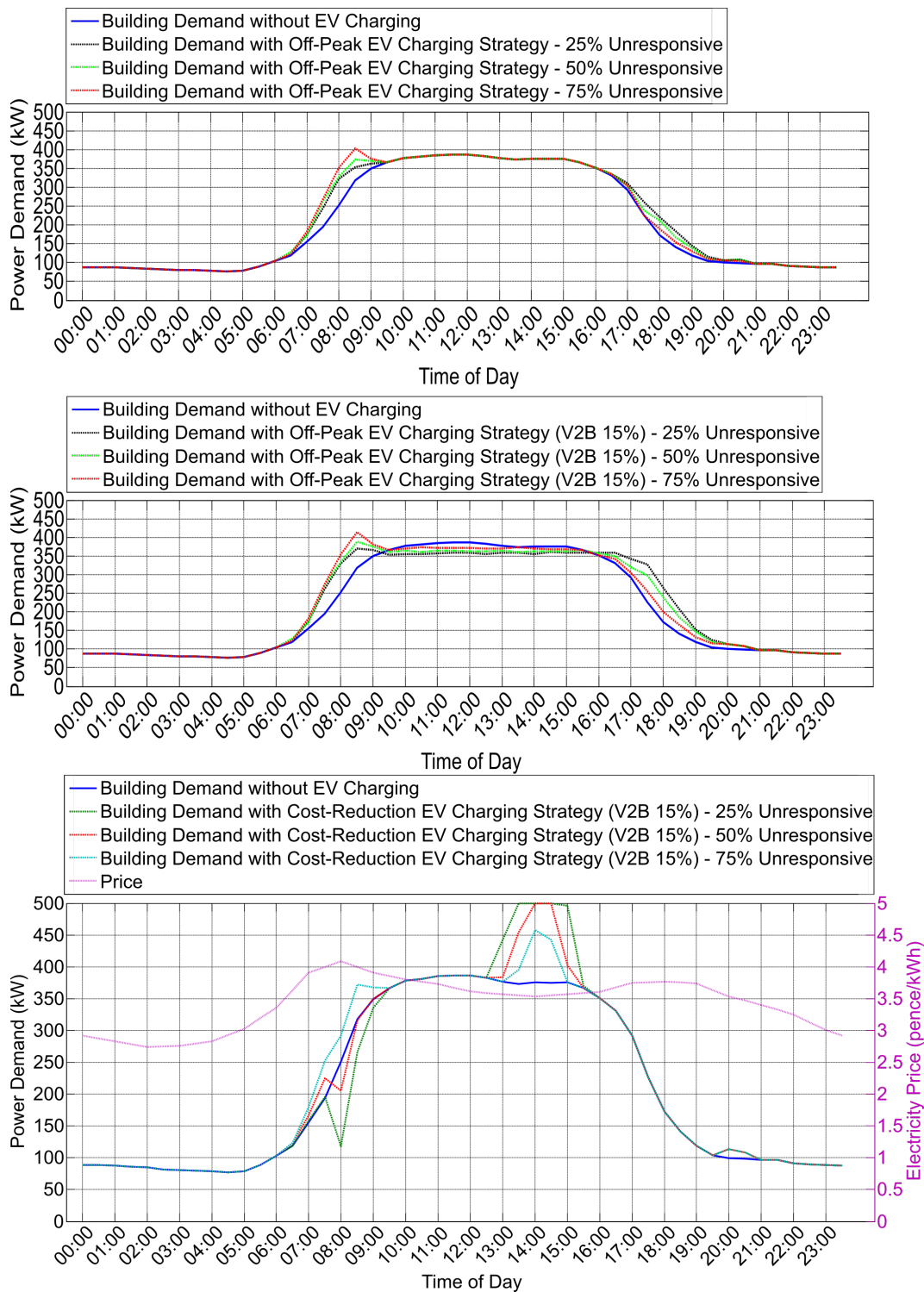


Figure 3.16: Impact of EV charging for different levels of Unresponsive EVs

As seen from the results, high levels of unresponsive EV drivers lead in a result which

is not optimal. When the Charging Station Manager operates under the Off-Peak charging strategy the unresponsive EV drivers cause a new peak in the demand profile of the building, and when the Charging Station Manager operates under the Cost-Reduction charging strategy the unresponsive EV drivers charge during the expensive hours increasing the electricity cost for the building manager. The problem of having unresponsive EV drivers in the EV fleet has been studied in [146], where we propose the use of a forecasting model to predict the EV demand from the unresponsive EV drivers so that the charging schedules of the responsive EV drivers can be adapted and lead to an optimal result; this work however is not part of this thesis.

The model was also used in a residential charging scenario and the complete results are presented in Appendix C.

3.7 Summary

In this chapter a control model was presented that enables the Charging Station Manager to schedule the EV charging and discharging events following two different strategies. The Off-Peak strategy aims to minimise the impact of EV charging on the demand profile of the building and, when V2B is available, reduce its peak demand by discharging the EVs during the peak hours. Operating under this control strategy, the Charging Station Manager reduces the overall impact of EV charging to the grid and enables an efficient network operation, in terms of line overloads, energy losses and voltage drops. The Cost Reduction strategy aims to minimize the total electricity cost of the building facility by charging and discharging the EVs at the cheap and expensive hours respectively. Both strategies ensure compliance with equipment nominal ratings and network technical constraints. The proposed control model was evaluated using a realistic EV fleet modelled based on real statistical data from the NTS. To study the impact on the grid, the UK generic distribution network was modelled in MATPOWER. The impact on the demand profile, daily electricity cost and bus voltage was studied for a workplace charging scenario.

The results showed that the Off-Peak strategy combined with a 15% V2B provision

reduces the aggregated peak demand of the building by 9.7%. In this case however the EVs need to charge for longer periods and due to the bell shaped demand profile of a commercial building and the long peak period, this could lead to insufficient charging of some EVs. The distribution network is also benefited from this charging strategy. Studying UK generic distribution network, it was found that the fleet of 48 EVs was able to increase the minimum voltage of the 0.4kV bus by 0.2%.

Considering that the building managers are often charged for their electricity according to the “triad” system [30], the Cost Reduction strategy of the Charging Station Manager is useful in this case, as it could lead to significant cost savings. It was found that the Cost Reduction strategy combined with a 15% V2B provision reduces the daily electricity cost of the building by 1%. However, a demand cap is necessary to be applied in order to protect the existing infrastructure from excessive stress and overloading due to the simultaneous charging events during cheap hours.

A Local Energy Management System for the building manager

4.1 Introduction

The International Energy Agency (IEA) estimates that buildings represent globally the 32% of the total final energy consumption (energy that is supplied to consumers for all final energy uses, such as heating, cooling, and lighting), and around 40% of primary energy consumption in most IEA countries [147]. The United Nations Environment Program estimates that residential and commercial buildings consume approximately 60% of the world's electricity, in addition to using 40% of global energy, 25% of global water, and 40% of global resources. Because of the high energy consumption, buildings are also one of the major contributors to greenhouse gas production [148–150], but also offer the greatest potential for achieving significant greenhouse gas emission reductions, with numbers projected to increase [149], [151]. For these reasons the energy efficiency of buildings receives a lot of attention globally [152]. Looking at a smaller scale, the energy efficient buildings lead to significant cost savings for the building manager, increasing the utility of the paid energy unit.

According to the US National Institute of Standards and Technology (NIST), buildings are an integral part of a Cyber-Physical system (defined as “a co-engineered interacting network of physical and computational components”) [153]. Being part of this “smart” ecosystem, the buildings need to integrate with the future smart grids and transform their simplistic consumption-only profile to a complex one that includes

local distributed energy resources (DER) and/or storage. Depending on the available assets, the building managers must change from typical consumers to “prosumers”, being able to both produce and consume energy in their building premises. Remarkable work has been done in the past years to this direction. Pacific Northwest National Laboratory, with support from the U.S. Department of Energy (DOE), developed VOLTTRON - an open-source common platform offering in-depth understanding of complex systems that integrate new challenges, such as renewable energy generation, energy storage, and EVs [154]. However, the integration of highly variable factors, such as renewable energy, demands control methodologies that are adaptable and dynamic [155]. NIST has been investing in building integration with the smart grid since 2011 developing tools like the Virtual Cybernetic Building Testbed and Net Zero Energy Residential Test Facility [156]. They have recognized the need for new standards to enable homes and buildings to interact with the grid, with buildings becoming both energy renewable generators and consumers.

Energy management in buildings is realised through building energy management systems (BEMSs) which control the heating, ventilation and air conditioning (HVAC) and lighting systems. Nowadays BEMSs are fundamental components of modern buildings, performing tasks that seem contradictory e.g. reducing energy consumption while maintaining occupants’ comfort [152]. However, the buildings are not static components of the smart ecosystem; on the contrary they evolve and interact with their surroundings. Going through years of exploitation, the thermal characteristics of the buildings deteriorate, their usage patterns change and their indoor spaces get rearranged. In time, both the inner and outer micro-climates adjust to changes in surrounding buildings, overshadowing patterns, and local climates, not to mention building retrofitting [157, 158]. Due to these ever-changing and uncertain indoor and outdoor characteristics, the performance of typical BEMS often falls short of expectations, lacking the necessary data processing, evaluating, and control methodologies. Being part of a smart ecosystem, a building must not be seen as a singularity but as an element of a miniature (local) energy system that interacts with the other elements of the system in a coordinated fashion. A typical BEMS that tries to optimise the building’s energy efficiency will always fail (in the general context), if other elements of

the system are not considered. On the other hand, considering the building in a local energy system with other buildings, distributed energy resources, energy storage and EVs, the energy management and coordination becomes more difficult.

Advanced algorithms are necessary to cope with the intermittent characteristics of the different elements of the system, and handle the large amounts of data. Predictive models should also be incorporated in the coordination mechanism in order to deal with the associated uncertainties and increase the control efficiency. From the building manager's perspective, these algorithms must be able to facilitate different control strategies according to the overall coordination objective and enhance the awareness of the system.

In this chapter a complete Local Energy Management System (LEMS) was presented, developed to control EVs and Energy Storage Units (ESUs) at commercial building premises. The LEMS uses the Triad Prediction Tool and Electricity Forecast Tool of Chapter 2 as well as the EV charging control algorithm of Chapter 3 and enables the building manager to reduce its electricity costs and increase its benefits from EVs and ESUs at the building premises. The objectives of the LEMS are i) to flatten the demand profile of the building facility and reduce its peak, ii) to reduce the demand of the building facility during triad peaks in order to reduce the Transmission Network Use of System (TNUoS) charges of the building manager and iii) to enable the participation of the building manager in the grid balancing services market through demand side management and response.

4.2 Literature Review

Considerable work is found in the literature on intelligent BEMSs that utilise sophisticated algorithms to maximise the energy savings while maintaining the occupants' comfort. Computational Intelligence (CI) techniques including fuzzy set theory (fuzzy logic - FL), evolutionary computing (genetic algorithms - GA) and artificial neural networks (ANN) have been used to boost the performance of BEMSs in various applications.

Fuzzy logic (FL) was developed to deal with the uncertainties that are present in real world problems. The difference between classical and fuzzy logic is that classical logic requires objects to have either 0% or 100% membership to a certain characteristic, whereas fuzzy logic allows to have any degree of membership between 0% and 100% [159]. Fuzzy logic based systems mimic the human thinking and execution ability that helps to deal with uncertainty and vagueness [160]. Therefore, fuzzy systems are capable of approximating any type of problem, even with the existence of inexact information [161]. However, generating the rules for a fuzzy system is a challenging task. Expert knowledge and best practices are required to create the initial rule base, which may not always be available [162]. Genetic algorithms are an adaptive heuristic search technique based on the process of natural selection [163, 164]. They generate sets of possible solutions and through an iterative modification process (called “evolution”) they reach to the global optimum. Depending on the number of possible solutions and local optimums however, the convergence rate is low [162]. GAs are mostly applied when a problem does not require an absolute solution. In some studies, GAs were also combined with artificial neural networks. ANNs were used for modelling purposes due to their ability to model complex non-linear system, whereas GAs were used to find a global optimum (e.g. in [165]). ANN is one of the widely used techniques to make predictions without having any knowledge of the system. They have a proven record of accurate forecasts in various time horizons, operating as a black box (looking only at the relationship between the inputs and the outputs) [43, 44]. They are classified as data driven method and as such, they heavily rely on the quality of the training data. The model is built by using historical data and when data outside the training set are present then the previous model may no longer be valid, which limits the use of ANNs in datasets with uncertainties [162]. Furthermore, the calibration of the neural network is challenging and in most cases a trial and error approach is followed [166].

The use of ANNs to control BEMSs has been examined in [167, 168], offering self-learning abilities and improving the control system for the thermal comfort and energy savings in public buildings. Ferreira et al. [167] demonstrated an ANN deployment for balancing the desired thermal comfort level and energy savings at the University of Algarve with energy savings of more than 50%. Energy consumption has been the

focus of research interests as well, and various models have been developed to understand and predict the energy requirements of a building. For example, the authors of [169] have used classification techniques on the daily electricity consumption in buildings from Birmingham, demonstrating a 99% accurate prediction. Yuce and Rezgui [170] have used an ANN-GA approach to generate semantic rules and improve the energy consumption forecast, demonstrating a 25% energy reduction while satisfying occupants' comfort. ANNs have been also used for the electricity demand forecast of a large office building [171], capturing 97% of variability in hourly electricity demand (based on weather and electric power consumption alone). Other CI techniques such as fuzzy c-means clustering, support vector machines, and GAs have been used for describing the energy consumption behaviour in [172, 173]. A review of the existing systems for building energy and comfort management can be found in [174].

Recently, much work has been devoted in finding ways to operate the buildings in a "smart" way considering them as part of a local energy system (microgrid). Considering energy storage, EVs, PV panels or other distributed generators (DGs), various control models have been developed to optimise the overall operation of buildings in a microgrid. In [175], the authors use the general mixed integer programming method to schedule the operation of a PV panel, energy storage and CHP unit in order to minimise the total electricity cost of the building. Similar work can be found in [176], while in [177] the authors perform a cost-benefit analysis to calculate the optimal size of battery storage in a microgrid with buildings. The authors of [135] and [178] have used EVs in order to consume locally the generated power from PVs and reduce the grid impact of the building's energy demand.

Considering a grid-connected operation of a microgrid with buildings, demand response capabilities have also been incorporated to its energy management systems. A review of possible control architectures for such a microgrid can be found in [179]. In [180] the authors present an algorithm that enables the participation to a demand response scheme through utilising home appliances and EVs. In this direction, multi agent systems (MAS) theory has also been applied in [100, 181]. Based on MAS theory, the authors of [182] developed a negotiation agent to facilitate bi-directional energy

trading between the microgrid and the grid. A bidding strategy was developed in [183], which enabled the participation of a microgrid with buildings in the day-ahead energy market.

However, the existing control models and energy management systems can only serve one purpose, and do not provide flexibility when it comes to their objective. Consequently, this limits their efficiency and performance in a real application. The building managers require an energy management system which offers flexibility and demonstrates adequate performance regardless of the operational target.

4.3 Description of the LEMS

In this chapter a complete Local Energy Management System (LEMS) is proposed in order to assist the building manager reduce its electricity costs and increase its benefits from EVs and ESUs at the building premises. The objectives of the LEMS are i) to flatten the demand profile of the building facility and reduce its peak, ii) to reduce the demand of the building facility during triad peaks in order to reduce the Transmission Network Use of System (TNUoS) charges of the building manager and iii) to enable the participation of the building manager in the grid balancing services market through demand side management and response.

4.3.1 Architecture

The proposed LEMS architecture is presented in Figure 4.1. The *Triad Prediction Tool* and the *Electricity Demand Forecast Tool* described in Chapter 2 were implemented to work with the LEMS. The *Triad Prediction Tool* calculates the probability of having a triad peak and provides warnings for the dates and times that a triad peak is expected to occur. The *Electricity Demand Forecast Tool* forecasts the electricity demand of the building for that period using a neural network (NN). To generate the triad warnings, the *Triad Prediction Tool* uses historical triad data available from the System Operator. To forecast the electricity demand of the building, the *Electricity Demand Forecast Tool*

uses historical data regarding the demand of the building and the local weather. The Pre-Forecast Analysis stage described in Chapter 2 was used to identify the optimal number of weather attributes and the optimal NN configuration to be considered by the *Electricity Demand Forecast Tool*.

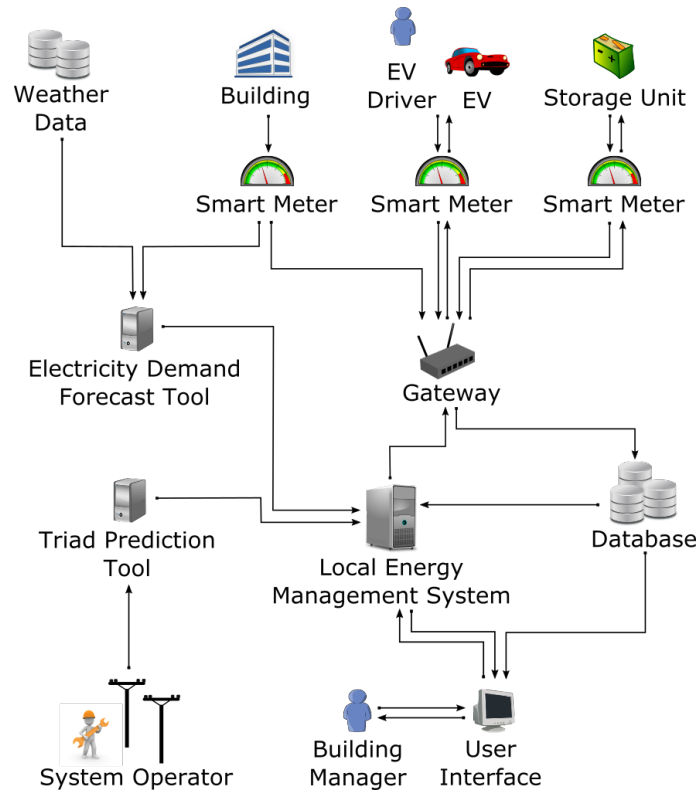


Figure 4.1: The architecture of the LEMS

The LEMS operates in timesteps during which the system is considered static (changes are only discovered at the end of the timestep). Obviously, a very short timestep (e.g. 1 sec) provides the best representation of the system and enables the near real-time dynamic operation of the LEMS. However, such level of detail in representation makes the system susceptible to synchronization problems and affects the LEMS operation as the latency of the communication infrastructure is comparable to the timestep duration and the time needed to complete the calculations. In addition, the cost of trying to minimise these latencies is often high and additional communication equipment would be necessary [184], making this not a practical solution. On the other hand, long timestep durations (e.g. 1 hour) lead to the opposite result, and make the system

inelastic to changes. Depending on the application, significant changes to the status of the system would be ignored if they lasted less than one timestep (e.g. an EV needs to charge for less than one timestep). Considering that the settlement period in the electricity market (period during which the electricity suppliers buy energy to meet their customer's demand) is 30min [185], a timestep higher than 30 min would not be practical for demand response applications. The timestep duration applied in this work was considered 15 minutes. According to [186], this timestep duration is a acceptable trade-off between a dynamic and a reliable operation that allows the frequent capture of the system's condition and reduces the risk of communication lags.

Smart Meters are necessary to monitor the demand of the buildings and the status of the EV charging stations and ESUs. Information regarding the battery capacity, state of charge (SoC), expected disconnection times, charging / discharging power rate, charging / discharging schedule and available discharge capacity is requested from the EV charging stations upon the connection of every EV. Information regarding the available capacity, state of charge (SoC), charging / discharging power rate and charging / discharging schedule is requested from every ESU. This information is stored in a Database, and is accessed from the LEMS on a regular basis (every 15 min).

According to the available information, the LEMS calculates the charging / discharging schedules for the EVs and ESUs and communicates them through a Gateway. As seen in Figure 4.1, the Gateway enables bi-directional exchange of information, gathering the data from the Smart Meters and pushing them to the Database, while at the same time allows the LEMS to push charging and discharging power set points to the EVs and ESUs.

The building manager can supervise the operation of the LEMS through a User Interface. The interface allows the building manager to access the data stored in the Database and produce visualisations of the previous and/or scheduled operation of the system. Additionally, the building manager can directly intervene to the operation of the LEMS in case of a fault or an abnormal event.

The LEMS maximises its utility to the building manager by adjusting its operational target (objective) according to the system status and condition. Three scheduling al-

gorithms for the management of the EVs and the ESUs were designed, namely *Peak Shaving Schedule*, *Triad Cost Reduction Schedule* and *Demand Response Schedule*. Each algorithm serves one objective and the LEMS shifts from one scheduling strategy to another depending on the objective that maximises the utility for the building manager. The Matlab code of the LEMS is included in Appendix D.

4.3.2 Peak Shaving Schedule

The Peak Shaving Schedule aims at flattening the aggregated demand profile of the building facility (similar to the *Off-Peak Strategy* described in Chapter 3). This is achieved by filling the valleys and shaving the peaks of the demand profile using the controllable loads (EVs, ESUs) of the building facility. The LEMS calculates the charging / discharging schedules of the EVs and ESUs, and sends them the corresponding power set points at the beginning of every timestep.

A ranking function is used in every timestep to identify the most preferable timesteps for charging / discharging. The outputs of this function are two sets of weights ($r_1(t)$ and $r_2(t)$) indicating the preference order for charging and discharging respectively according to the aggregated scheduled demand of the building facility. Lower weights are given to the most preferred timesteps (the most preferred timestep has a weight of 1 etc.) and vice versa. To schedule the charging / discharging of the EVs, the LEMS calculates the charging / discharging power set points by solving Equation (4.1) upon the connection of an EV. Similar to the *Off-Peak Strategy* of Chapter 3, it was assumed that the EV drivers agree to provide a certain discharging capacity ($V2B$) to the LEMS and submit their estimated departure time upon arrival.

$$\min \sum_{t=t_0}^{t_0+CP} (P_D(t) \cdot r_1(t) + P_C(t) \cdot r_2(t)) \quad (4.1)$$

subject to:

$$\sum_{t=t_0}^{t_0+CP} (T \cdot P_C(t)) = \frac{(SoC_{max} - SoC_{in}) \cdot BC}{C_{eff}}$$

$$\sum_{t=t_0}^{t_0+CP} (T \cdot P_D(t)) = \frac{V2B \cdot BC}{C_{eff}}$$

$$P_C(t) \leq P_n$$

$$P_C(t) \leq P_L(t) - P_S(t)$$

$$P_D(t) \leq P_n$$

$$P_D(t) \leq P_S(t)$$

, where:

t_0 is the arrival timestep of the EV

CP is the connection period of an EV (number of timesteps between arrival and departure)

$P_C(t)$ is the scheduled charging set point for timestep t

$P_D(t)$ is the scheduled discharging set point for timestep t

$r_1(t)$ is the output of the discharge ranking function for timestep t

$r_2(t)$ is the output of the discharge ranking function for timestep t

T is the duration of the timestep in hours

$P_S(t)$ is the scheduled power demand of the building at timestep t

$P_L(t)$ is the network limit, the maximum energy that can be supplied from the grid at timestep t (covering both the building demand and the EV charging)

P_n is the nominal power of the EV charger

$V2B$ is the agreed depth of discharge level (in % of BC)

BC is the battery capacity

C_{eff} is the charger efficiency

SoC_{in} is the initial SoC level

SoC_{max} is the maximum SoC that can be reached until the departure of the EV

Unlike EVs, the ESUs are not mobile therefore they are always connected to their charging equipment. The calculation of the charging / discharging power set points is repeated every timestep (for the remaining timesteps of the day), after calculating the

set points of the connected EVs. This way the demand / generation profile of the ESUs is adjusted to the arrival / departure times of the EVs. To extend the battery life, the LEMS is only allowed to operate the ESU within a “safety” zone between 20% and 80% of the nominal storage capacity. To calculate the charging / discharging schedule of the ESUs, the LEMS uses Equation (4.1) in a slightly different way. $V2B$ now expresses the “safety” band of the ESU capacity, while SoC_{out} (since there is no disconnection) expresses the maximum SoC that the ESU can reach.

4.3.3 Triad Cost Reduction Schedule

The *Triad Cost Reduction Schedule* aims at reducing the electricity cost of the building manager during triad peaks. This is achieved by shifting demand from the expensive triad timesteps to the cheap off-peak timesteps. The LEMS adjusts the charging / discharging schedules of the EVs and ESUs to an electricity price curve, and places the charging and discharging events during cheap and expensive timesteps respectively. This operation is triggered from the warnings of the *Triad Prediction Tool*. The charging / discharging power set points are calculated using Equation (4.1), only this time the ranking function changes the way it generates the weights and gives discharging preference to the triad timesteps. Once a triad warning is received, the LEMS recalculates the charging / discharging schedules of every controllable asset that is available (connected EVs, ESUs).

4.3.4 Demand Response Schedule

The *Demand Response Schedule* aims at enabling the building manager to participate in the ancillary services market and provide demand response actions to the grid. It was assumed that the System Operator sends requests to the building manager to either reduce or increase its aggregated demand in the next timestep (15 min). Triggered by the arrival of such a request, the LEMS overrides the charging / discharging schedules of the available controllable assets. In case the request is to increase the demand, the LEMS forces the ESUs and the connected EVs to charge at the maximum power rate

possible (respecting at the same time the nominal charger rates, the battery capacity and the SoC “safety” zones). In case the received request is to decrease the demand, the LEMS forces the available ESUs and EVs to discharge, reducing the overall demand of the building facility.

4.3.5 Operational Workflow

The LEMS operates in two workflow cycles, namely the *Normal* and the *On-Demand* operation workflow. The operation is illustrated in Figure 4.2.

During *Normal* operation workflow, the LEMS forecasts the electricity demand of the building using the *Electricity Demand Forecast Tool*. On the first timestep of the day, the *Electricity Demand Forecast Tool* forecasts the demand of the building facility for every timestep of the day. The forecasted demand is updated on every timestep using the actual demand of the last timestep. In case there are no demand response requests from the System Operator or triad warnings from the *Triad Prediction Tool*, the LEMS uses the *Peak Shaving* sub-workflow to manage the charging / discharging of the EVs and ESUs. The calculated power set points of the next timestep are forwarded to the chargers of the EVs and the ESUs through the Gateway. The cycle is repeated in every timestep, considering the new arrivals of EVs.

In case a demand response request is received, the *On-Demand* operation workflow is activated and the LEMS executes the *Demand Response* sub-workflow. Depending on the availability of the EVs and ESUs, the LEMS calculates the demand response capacity at that timestep (the maximum increase / reduction of demand it can offer). In case the demand response request is to increase the demand, the LEMS cancels any scheduled discharging events and forces every available asset to charge at maximum power. Constraints for nominal charger rates, battery capacity and SoC “safety” zones are applied and considered. In case the demand response request is to reduce the demand, the LEMS overrides the existing charging schedules and discharges the ESUs and the connected EVs. The calculated power set points are sent to the EVs and ESUs through the Gateway. It is important to note that the *Demand Response* sub-workflow

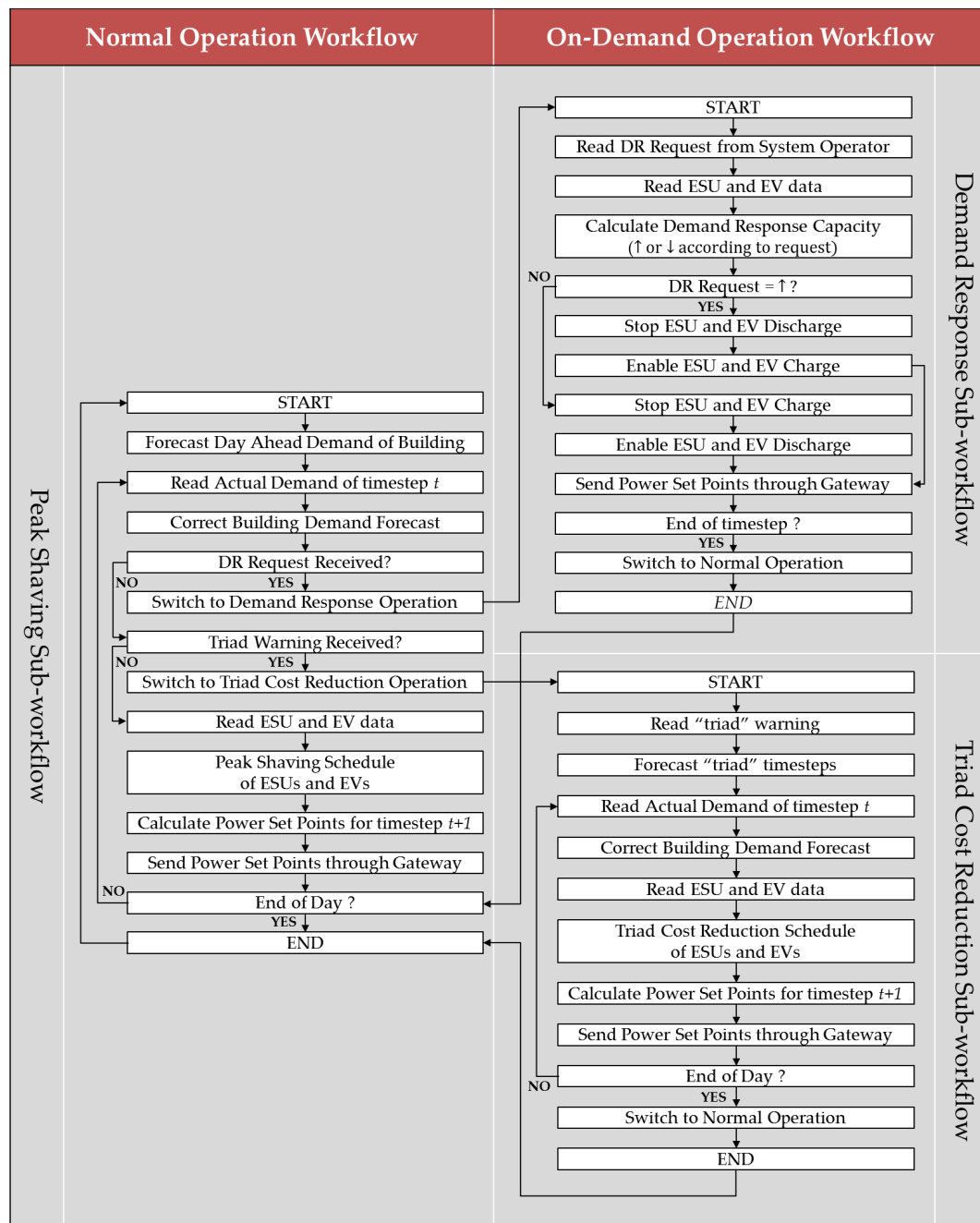


Figure 4.2: The workflow chart of the LEMS

lasts only one timestep (the one with a demand response request), and on the next timestep the LEMS switches back to *Normal* operation workflow.

In case a triad warning is received for a certain day, the LEMS switches to the *On-Demand* operation workflow and executes the *Triad Cost Reduction* sub-workflow. In

contrast to the *Demand Response* sub-workflow, the *Triad Cost Reduction* sub-workflow lasts for the whole day for which the triad warning is issued. As soon as this sub-workflow is activated, the LEMS cancels the existing charging / discharging schedules and forecasts the timesteps where the triad peaks are most probable to occur using the *Triad Prediction Tool*. These timesteps are the ones where the demand should be reduced to decrease the triad charges for the building manager. The ESUs and every connected EV, as well as every other EV that arrives during that day, are scheduled to discharge at those timesteps. The charging events are scheduled according to the daily electricity prices of the building manager, always avoiding the triad timesteps. At the end of the day, the LEMS switches back to *Normal* operation workflow.

The LEMS generates schedules for the period during which the EVs are connected to their charging points. In case an EV driver needs to leave earlier than the submitted departure time, the charging cycle might not be completed and the EV battery will not be fully charged. This is considered acceptable, otherwise having the EV fully charged at all times would cancel the purpose of the control system (which is to utilise the flexibility offered by the EVs). To incentivise the participation of EV owners in such a scheme, it is assumed that contractual agreements exist between the EV owners and the building manager which rewards the EV owners according to the level up to which their EV battery is discharged. EV owners that offer greater discharge capacity are rewarded more than those who offer less discharge capacity. This reward system would also prevent the participants of “gaming” the LEMS operation (e.g. EV owners try to avoid the discharging hours), simply because the reward is calculated according to the discharge level.

4.4 Demonstration of the LEMS

4.4.1 Deployment on Cloud

The proposed system was deployed on cloud to enable future scalability and reduce the computational time. The distributed engine of CometCloud [187] was adopted, using a master-worker architecture as seen in Figure 4.3. By combining local and re-

remote computational resources, CometCloud realizes a virtual cloud with resizeable computational capabilities and enables scale-up, scale-down and scale-out to address a dynamic workload.

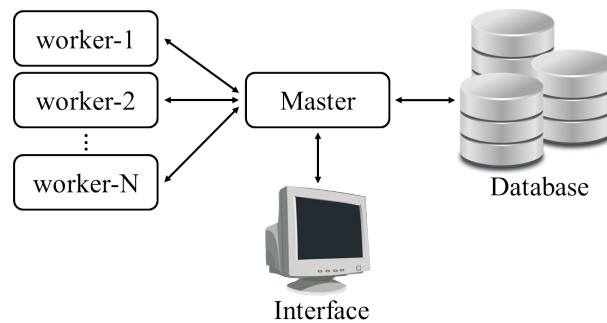


Figure 4.3: The adopted distributed architecture

A *Master* processing unit is responsible to distribute the necessary forecasting and scheduling processes (defined as “tasks”) to remote *worker* processing units. The *worker* units execute the assigned tasks and return the results to the *Master* unit. The necessary number of *worker* units to complete a task is variable and defined by the *Master* unit according to the workload. A local *Interface* was designed to communicate with the *Master* processing unit and enable the user to give instructions regarding the LEMS operation. Reading and writing operations on the *Database* can only be performed from the *Master* unit for security and reliability reasons.

For each LEMS operation workflow the procedure is carried out in the following manner: When a request comes from the user through the *Interface*, the *Master* reads the database and fetches the configuration required for that specific request. Then the *Master* creates a job task with all the necessary data required to process the task and uses a unique identifier for that task. Once the task is created it is posted to be picked up by an idle *worker*. The *worker* carries out the operation and will push the result back to *Master*. The *Master* aggregates the results from all the *workers* and generates a signal to whether charge or discharge either the ESUs or the EVs.

4.4.2 Simulated Scenarios

Three scenarios were studied to test the performance of the proposed system, namely “Peak Shaving Operation”, “Triad Cost Reduction Operation” and “Demand Response Operation”. As indicated from their name, each scenario aims at simulating the operation of the LEMS in different operation cycles. In the “Peak Shaving Operation” scenario the LEMS operates in *Normal* mode, aiming to reduce the peak demand of the building facility. In the “Triad Cost Reduction” scenario it is assumed that the *Triad Prediction Tool* sends a triad warning to the LEMS, indicating the probability of having a triad in the following day. This scenario studies the performance of the LEMS trying to reduce the triad electricity cost for the building manager. Finally, the “Demand Response” scenario studies the performance of the LEMS in a demand response occasion, where two demand response requests are received from the System Operator.

A fleet of 10 EVs was considered in all three scenarios, assuming normal distributions for their arrival / departure times, initial SoC and battery capacity. Table 4.1 presents the mean and standard deviation values of these distributions. It was also assumed that the EV drivers were willing to discharge up to 15% of their vehicle’s battery. The building facility was assumed to have 2 ESUs with characteristics presented in Table 4.1.

The six commercial buildings of Chapter 2 were considered as the “building facility” in the simulation scenarios. Their demand on a random winter day was aggregated and presented in Figure 4.4.

4.5 Experimental Results

4.5.1 Scenario 1: Peak Shaving Operation

Figure 4.5 presents the aggregated demand of the building facility when the LEMS operates under Normal operation (Peak Shaving). The EVs and the ESUs are scheduled to charge during the off-peak hours, and discharged during the peak hours. A 6.9%

Table 4.1: EV and ESU assumptions

	Parameter	Value	
EVs	Arrival Times	Mean: 08:00	StdDev: 0.75h
	Departure Times	Mean: 19:00	StdDev: 1h
	Battery Capacity	Mean: 27kWh	StdDev: 3kWh
	SoC upon connection	Mean: 84%	StdDev: 4%
	V2B	15%	
	Nominal charging/discharging power	3kW	
	Charger Efficiency	0.95	
ESUs	Initial SoC	75%	25%
	Battery Capacity	10kWh	20kWh
	Max SoC	80%	
	Min SoC	20%	
	Nominal charging/discharging power	7kW	
	Charger Efficiency	0.95	

peak reduction was achieved comparing to the initial demand of the facility (without EVs and ESUs).

As explained in Section 4.3, the LEMS sends power set points to the EVs and the ESUs according to the calculated charging/discharging schedule. These power set points are messages with the exact power rate at which each EV/ESU must charge/discharge at each timestep. A message of 2.7kW sent to EV-1 for example means that in this timestep EV-1 must charge at 2.7kW from its charger. Similarly, a message of -1.6kW sent to ESU-1 means that in this timestep ESU-1 must discharge at a rate of 1.6kW. The messages (power set points) that LEMS sent to the EVs and ESUs in this scenario are presented in Figures 4.6 and 4.7 respectively.

In those figures, each bar is a message to a particular EV/ESU. The bar height indicates the power rate magnitude, while its sign indicates a charging (positive) or a discharging (negative) set point. Different bar colours indicate the different receiver (EV/ESU), so for example in Figure 4.7 the light bars are messages to ESU-1 while the

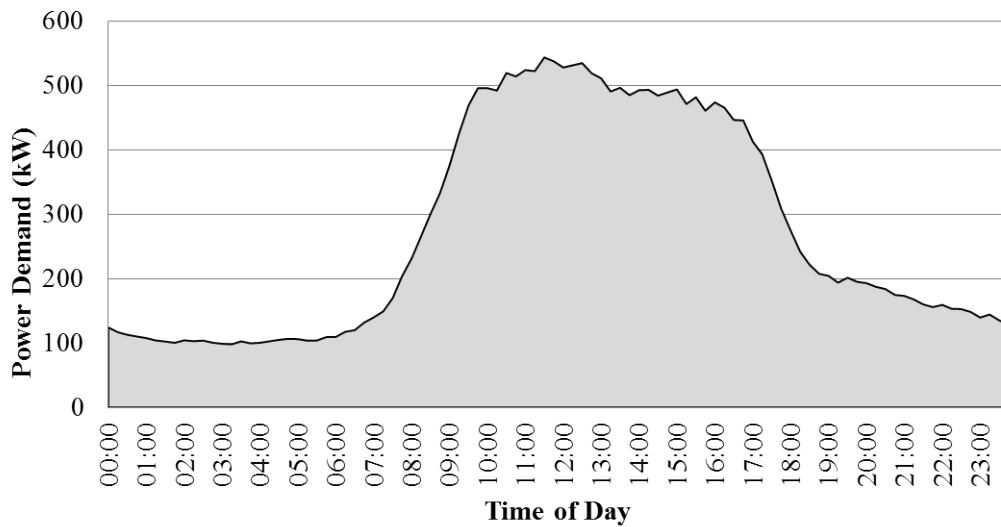


Figure 4.4: The aggregated demand of the building facility

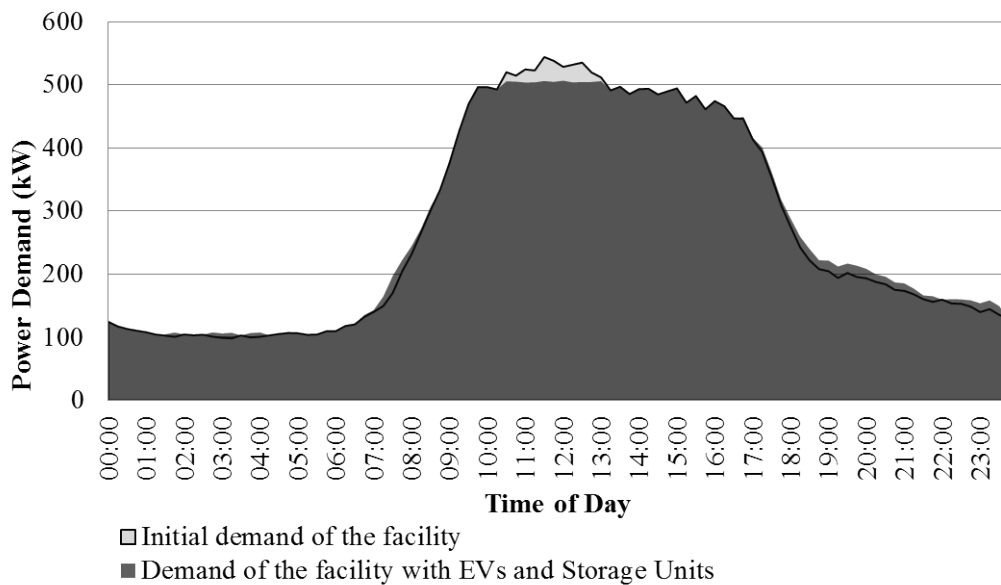


Figure 4.5: Demand of the facility with Peak Shaving Operation

dark bars are messages to ESU-2. This distinction is difficult in Figure 4.6 as there are 10 different EVs (and consequently 10 different colours); however looking at the graph we can immediately identify the charging and discharging periods during the day.

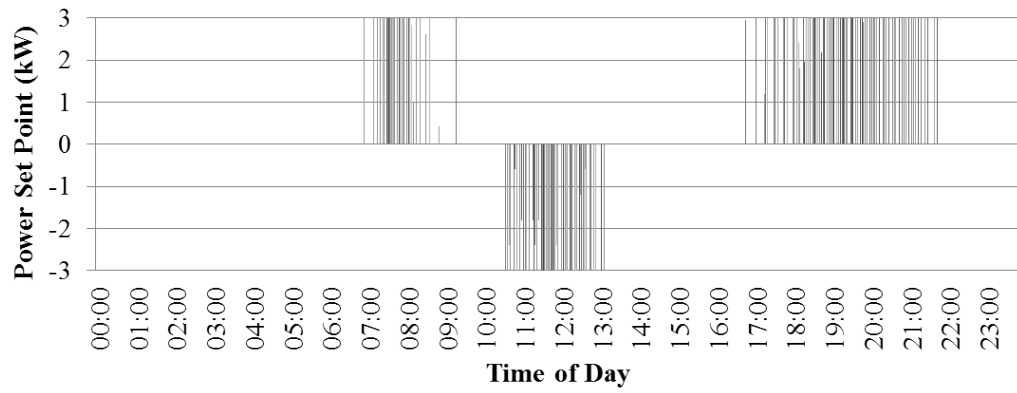


Figure 4.6: The power set points sent to the EVs

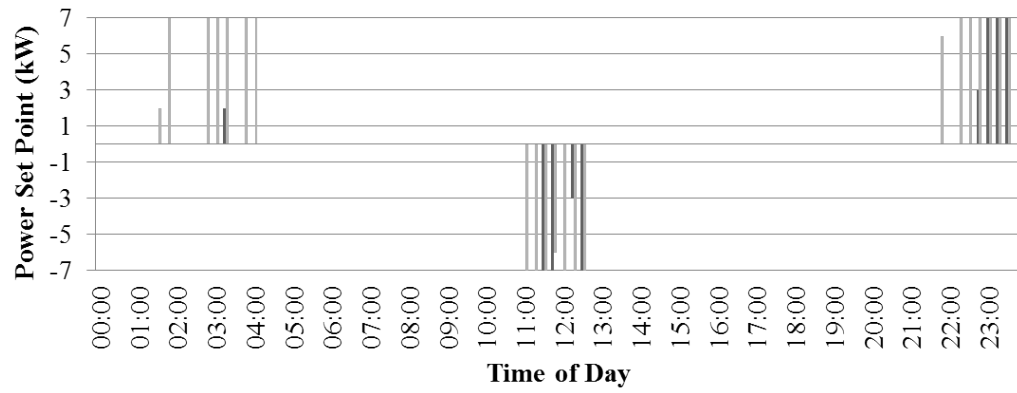


Figure 4.7: The power set points sent to the ESUs

4.5.2 Scenario 2: Triad Cost Reduction Operation

In this scenario it is assumed that the LEMS receives a triad warning from the *Triad Prediction Tool* and the *Triad Cost Reduction Operation* is activated. Figure 4.8 presents the triad peak hours (as predicted from the *Triad Prediction Tool*) and the electricity prices for that day.

This information was used by the LEMS in order to schedule the charging / discharging of the EVs and ESUs and reduce the overall electricity cost for the building manager. The resulting aggregated demand of the building facility is presented in Figure 4.9. The controllable assets were scheduled to charge during the cheap hours (according to Figure 4.8) and discharge during the expected triad peak hours. Due to the simultaneous charging of the EVs and ESUs at the cheap hours, the peak demand was

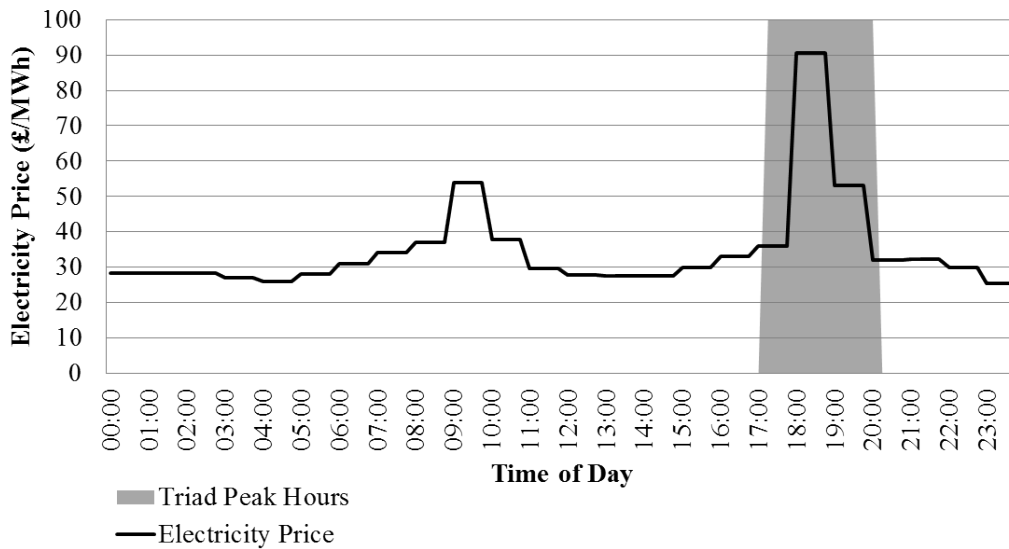


Figure 4.8: The electricity prices and the predicted triad peak hours

increased however this increase is very small ($<1\%$). In case more EVs are charging at the facility this peak is expected to increase and possibly stress the existing equipment. Additional measures should be taken then, like the demand cap mentioned in Chapter 3. The discharging of the EVs/ESUs resulted in a 7.5% reduction of the electricity requirements during the triad peak hours (17:00 – 20:00). This number is expected to rise when more EVs are available, increasing the cost savings of the building manager.

The power set points sent to the EVs and ESUs are presented in Figures 4.10 and 4.11 respectively. The discharging events are concentrated in the period between 17:30 and 19:30 as indicated by the triad warning. After the discharging period, the LEMS tried to charge the EVs in order for them to leave the facility fully charged. However, because the discharging period was very close to their departure times, there was not enough time for them to fully recharge. It was found that 6 out of 10 EVs left the facility with a battery SoC less than 100% (2 of those actually left the facility during the discharging period). This happens because this is a commercial building facility and the average departure times of EVs coincide with the discharging period. This is a risk that all EV drivers are aware of, and highlights the utility of a maximum discharge capacity agreement (V2B level) being the worst case scenario for the EV driver. Obviously this is not the case for the ESUs, as their charging/discharging schedules are not

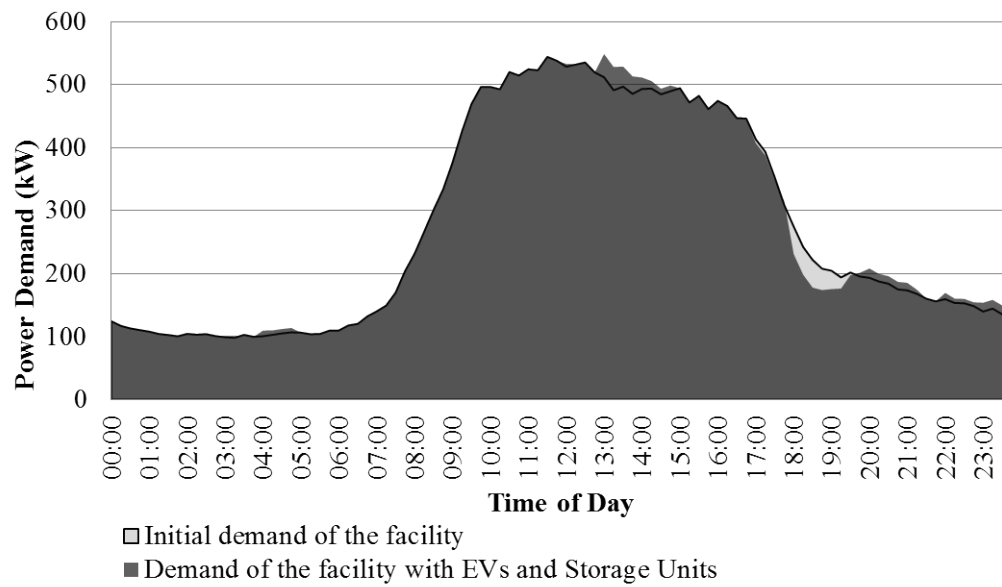


Figure 4.9: Demand of the facility with Triad Cost Reduction Operation

subject to time limitations.

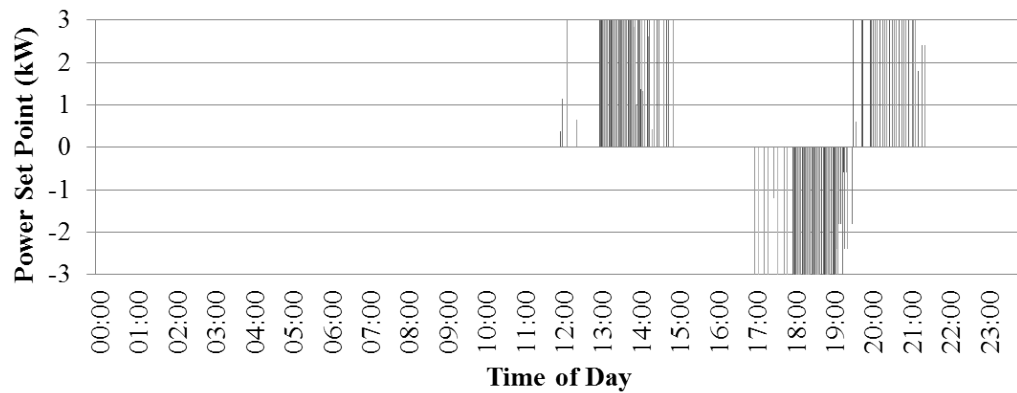


Figure 4.10: The power set points sent to the EVs

4.5.3 Scenario 3: Demand Response Operation

In this scenario it was assumed that the LEMS receives two requests for demand response as presented in Figure 4.12 by negative and positive bars. A request was received at 08:00, asking the LEMS to reduce the demand of the building facility. A second request was received at 14:00, asking the LEMS to increase the demand of the

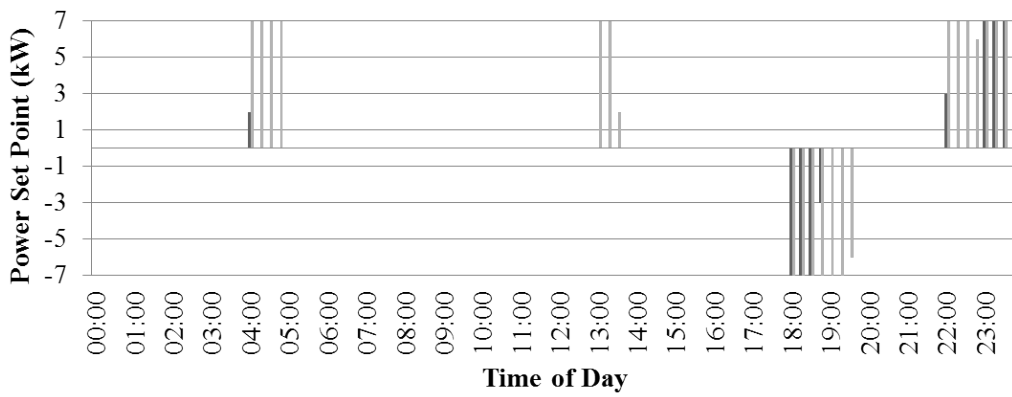


Figure 4.11: The power set points sent to the ESUs

facility.

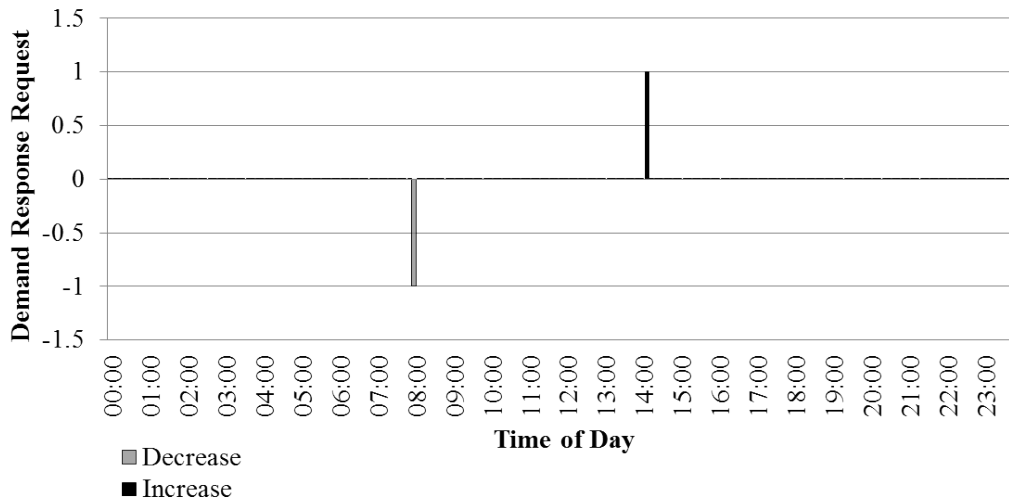


Figure 4.12: The demand response requests

Figure 4.13 presents the aggregated demand of the facility. As explained in Section 4.3, the *Demand Response Operation* is not a “full-day” cycle like the *Peak Shaving* and the *Triad Cost Reduction* cycles. The LEMS activates this operation only for one timestep to satisfy the demand response request, and returns to the *Normal Operation* (Peak Shaving) at the end of it. As seen in Figure 4.13, the LEMS successfully reduced the aggregated demand of the facility at 08:00 by discharging the connected EVs and ESUs. A 17.7% demand reduction was achieved comparing to the case without any EVs/ESUs. After this, it returned to *Normal Operation* until the second demand response

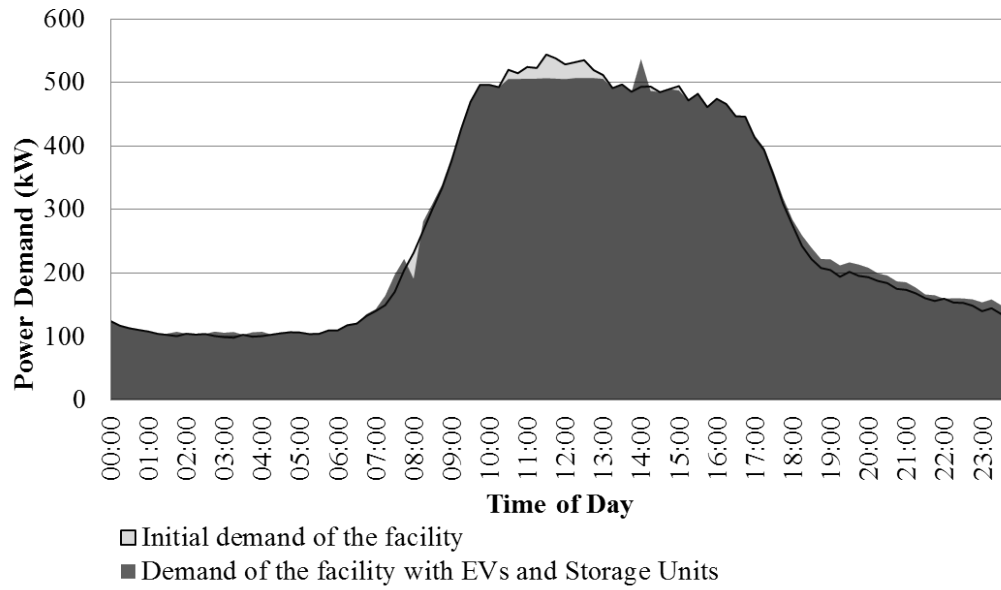


Figure 4.13: Demand of the facility with Demand Response Operation

request was received at 14:00. Upon receipt of the “demand increase” request, the LEMS overrode the charging / discharging schedules of the EVs/ESUs and charged every available unit increasing the demand by 8.9%.

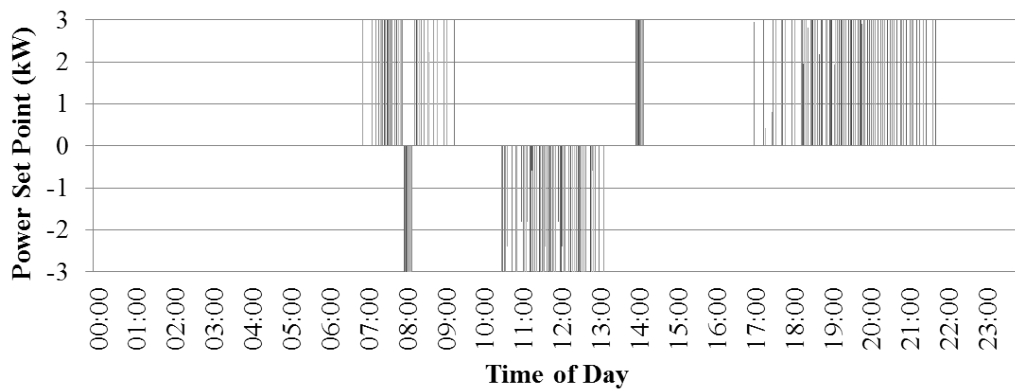


Figure 4.14: The power set points sent to the EVs

The LEMS’ response to the requests is also seen in Figures 4.14 and 4.15 where the power set points sent to EVs and ESUs are presented. Discharge set points were sent to both EVs and ESUs at 08:00 in order to decrease the overall demand of the facility. Similarly, charge set points were sent to the EVs/ESUs at 14:00 in order to increase the

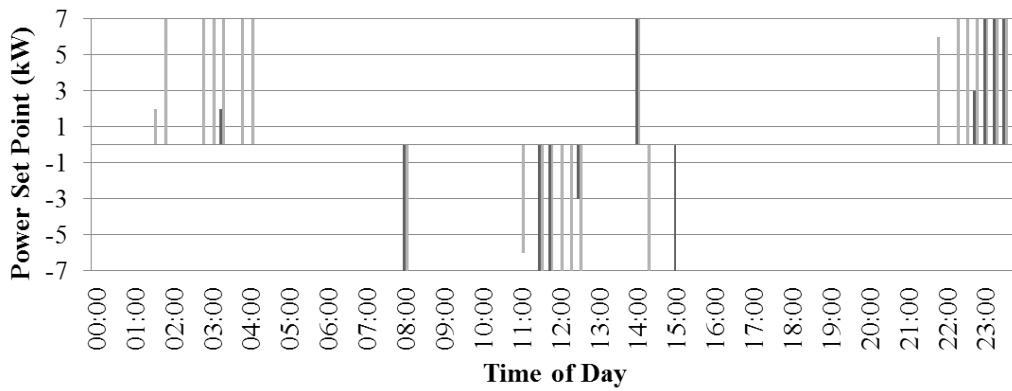


Figure 4.15: The power set points sent to the ESUs

aggregated demand of the facility. To maximise the demand change (increase or decrease), the set points in both cases are of high magnitude requesting discharge/charge at the nominal power rates of the chargers. Since the LEMS returns to the *Normal Operation* right after the *Demand Response Operation*, Figures 4.14 and 4.15 can be compared to Figures 4.6 and 4.7. Especially for EVs the demand response set points were the opposite of the scheduled ones, something realised if we look at the period between 07:00 and 09:00 (clearly a charging period).

4.5.4 Using LEMS to explore different simulation scenarios

Apart from its real time operation, the LEMS can be also used for simulation purposes in order to explore different use cases (what-if scenarios). By modifying the input parameters (Table 4.1), the building manager can see the impact of EVs and ESUs on the demand profile of the building and/or calculate the demand response capacity to offer to DNOs. One of the key variables in this case is the charging / discharging rate (nominal power of the chargers). Figures 4.16-4.18 present the simulation results considering EV and ESU chargers of 3kW and 7kW rate for all three operating modes of the LEMS.

As seen from Figure 4.16, changing the rate of the chargers does not have a significant effect on the demand profile of the building facility under the Peak Shaving Operation. On the other hand, under the Triad Cost Reduction Operation (Figure 4.17), an

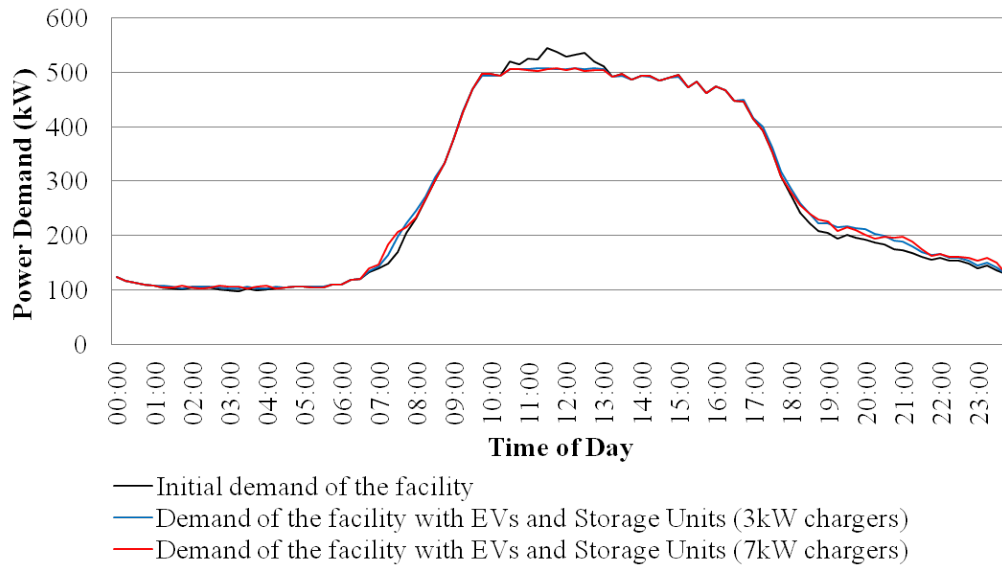


Figure 4.16: Demand of the facility with Peak Shaving Operation

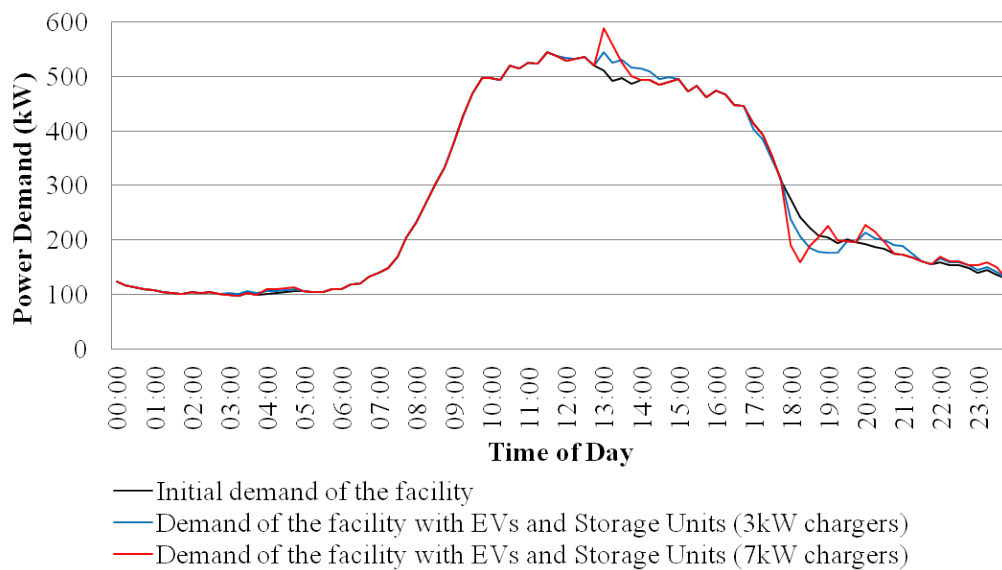


Figure 4.17: Demand of the facility with Triad Cost Reduction Operation

increase on the charging rate is immediately reflected on the demand profile of the building facility. During the hours when the electricity rate is cheap the connected EVs and ESUs are scheduled to charge, and during the triad peak hours the connected EVs and ESUs are scheduled to discharge. Increasing the rate of the chargers results in

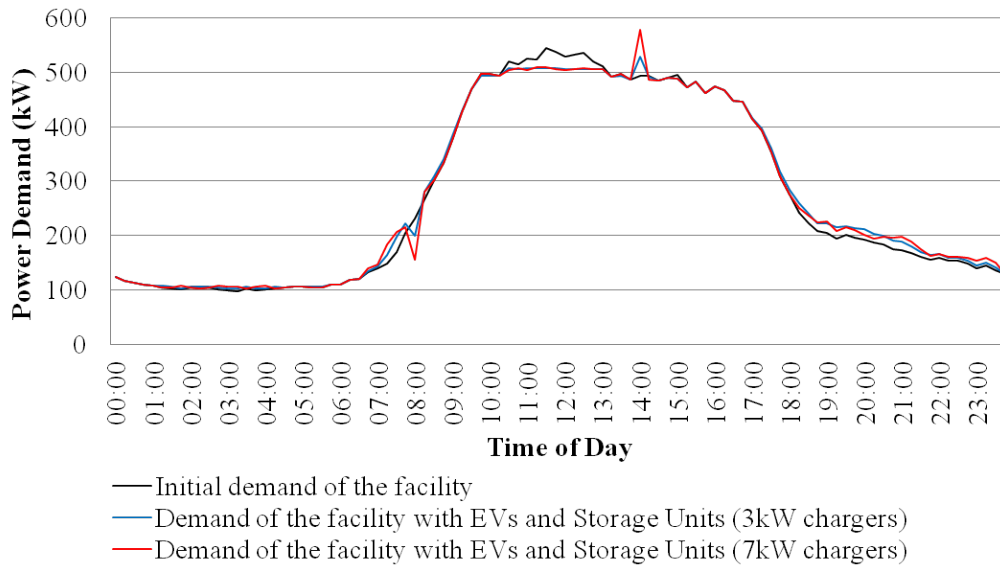


Figure 4.18: Demand of the facility with Demand Response Operation

steeper demand changes, as the LEMS tries to maximise its cost savings by increasing the demand during the cheap hours and reducing the demand during the triad peak hours. Similar results were found for the Demand Response Operation of the LEMS (Figure 4.18). Increasing the charger rate allows the LEMS to offer greater demand response capacity to DNOs, which could lead to greater rewards for the building manager. Scenarios like this can be useful for planning purposes, as the building managers can simulate the LEMS operation under different use cases and calculate the results for different applications/objectives.

4.6 Summary

In this chapter a complete Local Energy Management System (LEMS) was presented, developed to control EVs and ESUs at the building premises and reduce the electricity costs of the building manager. The LEMS controls the charging and discharging of ESUs and EVs in order to i) flatten the demand profile of the building facility and reduce its peak, ii) reduce the demand of the building facility during triad peaks and consequently the triad charges of the building manager, and iii) enable the participa-

tion of the building manager in the grid balancing services market through demand side management and response. The LEMS operates under a *Normal* or *Emergency* mode according to the operational objective. Three scheduling algorithms were developed, namely *Peak Shaving*, *Triad Cost Reduction* and *Demand Response* in order to schedule the charging / discharging of the EVs and ESUs. The *Triad Prediction Tool* and the *Electricity Demand Forecast Tool* of Chapter 2 were used in order to predict the future triad peaks of the system and forecast the building demand at those times. The V2B charging control algorithm of Chapter 3 is also used as part of the LEMS scheduling algorithm.

The LEMS was deployed on cloud using the CometCloud architecture, and its operation was demonstrated in three simulation scenarios namely “Peak Shaving Operation”, “Triad Cost Reduction Operation” and “Demand Response Operation”. In the “Peak Shaving Operation” scenario the EVs and the ESUs were scheduled to charge during the off-peak hours, and discharged during the peak hours of the building’s electricity demand. According to the results, a 6.9% peak reduction was achieved comparing to the initial demand of the facility (without EVs and ESUs). In the “Triad Cost Reduction Operation” scenario the controllable assets were scheduled to charge during the cheap hours and discharge during the expected triad peak hours. It was found that the LEMS resulted in a 7.5% reduction of the electricity requirements during the triad peak hours (17:00 - 20:00), reducing the triad costs for the building manager. In the “Demand Response Operation” scenario, the LEMS was assumed to receive requests for reducing and increasing the demand of the building facility at 08:00 and 14:00 respectively. According to the results, the LEMS was able to override the existing charging/discharging schedules of the EVs and ESUs, and reduce the overall demand by 17.7% as a response to the demand reduction request. In addition, an overall 8.9% demand increase was achieved at 14:00, as a response to the demand increase request.

Simulation of EV driver behaviour in road transport and electric power networks

5.1 Introduction

Environmental and energy security reasons are setting Electric Vehicles (EVs) as a major part in the future road transport networks [144]. Integration of EVs will affect the road transport networks due to their particular characteristics, such as the frequency and the time needed for recharging the EV battery. Apart from becoming a major part in road transport networks, EVs are expected to influence significantly the electric power networks [188]. Considering a typical battery capacity of 30kW, the energy needs for recharging an EV is nearly double the average daily needs of a house. EV charging will affect significantly the customer load profiles unless smart grid control techniques are applied. Several studies indicate that uncontrolled charging of EVs will increase the peak demand of the power system, resulting in feeder voltage excursion and overload of the transformers and cables, especially in already stressed networks [6, 73–75]. The integration of EVs will affect both electricity and transport systems, and consequently, research is needed on finding possible ways to make a smooth transition to the electrification of the road transport. To fully understand the EV integration consequences, the behaviour of the EV drivers and its impact on these two systems should be studied.

Because of the limitations in the current battery technology, the EVs offer relatively low driving range. With no major changes in the following years, the EVs will need regular recharging periods depending on the average daily trip distances. EVs are expected to recharge mainly at night, when the EV owners return home from their work [6, 75]. However, this will not exclude recharging events during the day. Charging in public or street locations requires at least a parking space per charging point. Due to the finite number of parking spaces in a city, especially in the city centre, the number of EVs that are charging at the same time is limited. This will affect the road transport networks particularly the daily travel patterns and the congestion parameters [189]. Authorities should take into consideration this behavioural change and implement proper mechanisms and parking schemes for the EV deployment.

The complexity of the dependencies between road transport and the electric power system is therefore likely to increase with higher EV market penetration. Coordination is essential to preserve a stable distribution network operation and avoid unnecessary investments in infrastructure. Due to limits in power capacity within an electricity network, it might not be possible to serve all EVs that want to recharge their batteries. In order to protect the electric power network, and maintain a robust operation, the condition of the various components (e.g. transformers, feeders) needs to be monitored. Future scenarios utilize advanced EV charging management mechanisms that use the available storage in the EV batteries and the flexibility of the charging demand to provide ancillary services to the grid operators [72, 116, 123, 190].

This chapter proposes an integrated simulation-based approach, introducing the EV as an intelligent unit living in both road transport and electric power systems. The main components of both systems have been considered, and the EV driver behaviour was modelled using a multi-agent simulation platform. The proposed simulation-based approach serves as enabling technology in order to understand the EV driver behaviour and its impact on both the road transport and electric power system.

5.2 Literature Review

The route choice behaviour of the drivers and the characteristics of the road transport network are strongly correlated. The route choice behaviour of drivers is affected by various factors like traffic information, weather and route attributes. According to Arentze et al. [191], the road accessibility characteristics have a substantial impact on route preferences. Raveau et al. [192] defined an angular cost variable to reflect the directness of the chosen route, and used it to improve the explanation of route choices. On the other hand, the route choice behaviour of the drivers affects the road transport network [67, 193]. Multi-agent models are often used to model the behaviour of drivers on road networks [194–196]. Traffic simulation tools like SUMO, OMNet++ and Veins are generally used by researchers in order to quantify the impact of the route choice behaviour.

EV drivers however, need to consider additional factors when deciding their route. Factors like energy consumption, charging station availability, charging duration are introduced in the route choice decision. Nicholas et al. [28] investigated the charging behaviour of EV drivers by simulating EVs travelling and charging at public chargers. They showed that more than 5% of the trips would require recharging at a public charger for different driving range and charging assumptions. The location of the charging stations is directly related to the impact of driving behaviour in urban road transport networks. In [197] a general corridor model is used to propose the optimal location of EV charging stations, while the authors of [198] propose a multi-period optimization model to expand the charging network. Similar studies for an urban environment can be found in [199, 200]. A spatial-temporal demand coverage location approach is used in [201] to address the location problem of electric taxi charging stations. Some traffic simulator platforms offer EV support and give to the user the ability to run traffic simulations with all or partially electrified vehicle fleets. Such a simulation can be found in [202], where EVs are simulated in highway networks with on-line charging. Another example is found in [203], where a spatial-temporal model is build based on a poisson-arrival-location-model (PALM) for EVs charging at public chargers on the highway. These models however ignore the impact of EV charging on the electricity

grid.

The charging behaviour of the EV drivers not only at public but also at the home chargers affects the electricity grid. The charging fashion in particular has been the centre of interest, as it defines the magnitude of this impact [74], [73]. To take this impact into account, integrated models have been developed, which combine a traffic simulator with power flow studies or another electricity grid simulation model. MATSim was used in [204], as part of an integrated approach to model EVs in transport and electric power systems. A vehicle technology assessment model was also used to simulate the EV's energy consumption and driving cycle, while a power system simulator was used to calculate the impact of EV charging on the electricity grid. However, the EV driver's behavioural profile is not modelled in detail and the EV charging procedure is assumed to be controlled by a third-party entity.

A few probabilistic approaches are found, which generate a number of driving and charging demand profiles for the EVs [205, 206]. These probabilistic models however can only be used as an input to another simulation tool in order to capture the impact of EV behaviour on both transport and electric power networks. In addition, the existing studies assume one behavioural profile for the EV drivers, ignoring the development of the EV integration and the increase of the decision support infrastructure. In this chapter, an integrated approach is presented to model EVs in a complex road transport and electricity network. Two behavioural profiles were considered for the EV drivers in order to describe the driving and charging behavioural change for different stages of EV adoption. The impact of each behavioural profile on the road transport and electricity network is demonstrated through a case study.

5.3 The EV agent's architecture

An *EV agent* was created using SeSAm [207], simulating the behaviour of a "rational" EV driver (an EV driver that tries to get to its destination through the shortest path, and utilises available information to reduce its travelling and charging time). The EV agent interacts with the other agents, makes calculations and takes decisions regarding

potential future actions. It lives in a complex environment consisted of a Road Transport network, an Electricity Grid and other EV agents. Its decisions and behaviour adapts to the behaviour of the other EV agents of the environment, and is affected from the status of the other simulated objects in the system. The EV agent's architecture is presented in Figure 5.1.

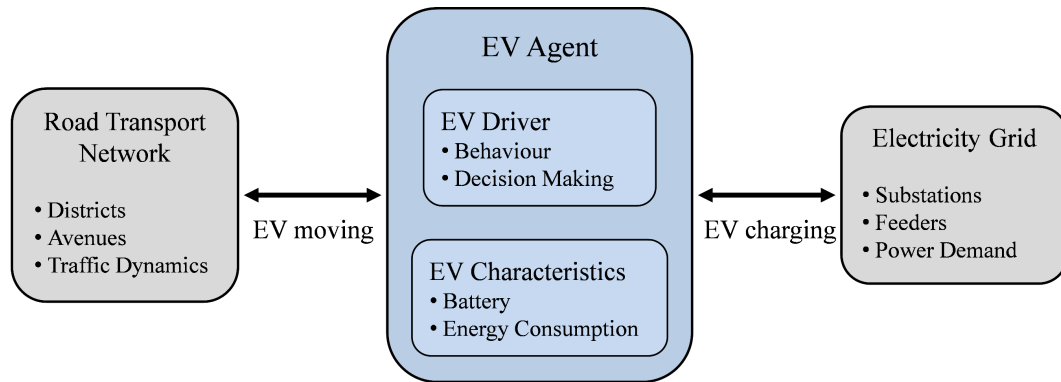


Figure 5.1: The architecture of the modelled EV agent

The EV agent combines the driver and the vehicle in one entity. It operates according to the EV driver's decisions and strategy but is constrained by the vehicle's intrinsic characteristics like battery capacity. Its moving and charging actions entangle the EV agent with the Road Transport Network and the Electricity Grid respectively. The simulation of many EV agents and their environment is important in studying and understanding their interactions in a realistic EV context. The following sections describe the developed modelling framework.

5.4 Modelling the environment of the EV agent

5.4.1 The Road Transport Network

The modelled road transport network represents a geographical region with a few communities. It is the geographical area where all the EV agents live, move and interact with each other. Each community was modelled as a *district* resource entity, considered as one node of a road transport network. Apart from the nodes, the con-

sidered road transport network contains links (which connect the nodes) to represent the roads connecting one community (district) to another. Each link was modelled as an *avenue* resource entity. The topology is presented in Figure 5.2.

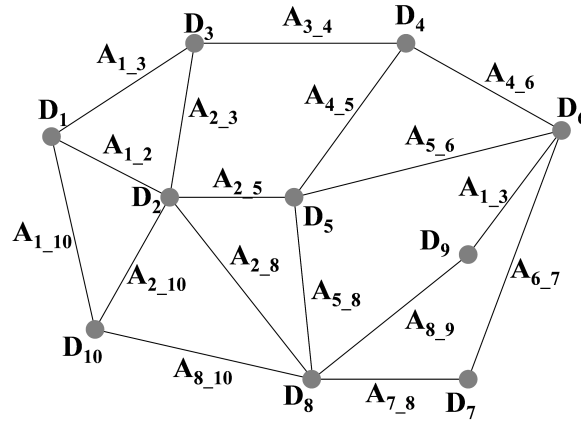


Figure 5.2: The topology of the Road Transport Network

A district (D_X) is an area with both residential and commercial buildings, and thus it can be used either as a home district (where an EV agent's home is) or as a work / shopping district (where an EV agent does various activities) for the EV agents. It was assumed that the home district is different from the work/shopping district of an EV agent. The avenue entities (A_X) represent the roads of the transport network, therefore they have traffic. The traffic on the roads was modelled following a macroscopic approach on a per-minute granularity. Three variables were used to describe the traffic on an avenue:

1. Density (k)
2. Flow Rate (q)
3. Mean Speed (u)

Density $k(t)$ reflects the number of vehicles per kilometre of road and is expressed in vehicles per kilometre (veh/km). At a specific time t , the density k of a road segment with length ΔX is calculated from Equation (5.1) where $n(t)$ is the number of vehicles

at time t on that road segment.

$$k(t) = \frac{n(t)}{\Delta X} \quad (5.1)$$

The flow rate $q(t)$ can be compared to the flux of a stream. It represents the number of vehicles that passes through a certain section per time unit and is expressed in vehicles per hour (veh/h). The maximum possible flow rate of a road is called its *capacity*. For a time interval ΔT , the flow rate is calculated from Equation (5.2) where m represents the number of vehicles that passes the specific location during ΔT .

$$q(t) = \frac{m}{\Delta T} \quad (5.2)$$

The mean speed $u(t)$ is defined as the quotient of flow rate and density and expresses the average speed of all the vehicles on a road. The three variables are linked through the *fundamental relation of traffic flow theory* as shown in Equation (5.3) [208].

$$q(t) = k(t) \cdot u(t) \quad (5.3)$$

Assuming a stationary (flow rates do not change along a road and over time) and homogeneously composed traffic (all vehicles are the same), the three variables are described graphically by the *fundamental diagrams*. These diagrams are usually the result of curve fitting on actual measurements and present the equilibrium traffic states. Three traffic states require special attention:

Free flowing traffic: When the vehicles are not impeded by other traffic they travel at the maximum speed u_f . This speed is dependent among other factors on the design speed of the road, the speed restrictions at a particular time and the weather. At the free flow state, the flow rate and density are close to zero.

Capacity traffic: The capacity of a road is equal to the maximum flow rate q_c . The maximum flow rate has an associated capacity density k_c and a mean speed u_c (smaller than u_f).

Saturated traffic: On saturated roads the flow rate and speed are zero. The vehicles are queuing and there is a maximum density of k_j (jam density).

The fundamental diagrams that describe the traffic on the avenue entities are presented in Figure 5.3.

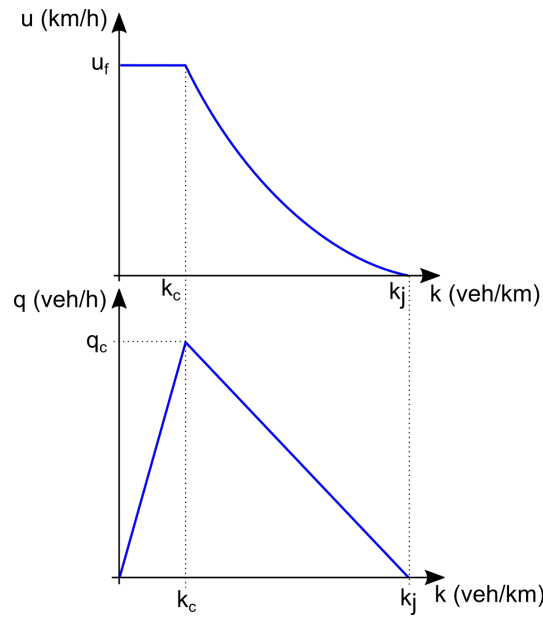


Figure 5.3: The fundamental diagrams assumed in this work

A triangular $k-q$ relationship was assumed, as stated in [208]. The density $k(t)$ of each avenue is calculated from Equation (5.1) using the number of EV agents travelling on the avenue at time t and the avenue length. For densities smaller than the capacity density the mean speed equals the free flow speed and the flow rate is calculated from Equation (5.3). In case the density is higher than the capacity density (but smaller than the jam density), the mean speed is calculated from Equation (5.3) and the flow rate is calculated from Equation (5.4):

$$q(t) = \frac{q_c}{k_c - k_j} \cdot (k(t) - k_j) \quad (5.4)$$

The fundamental diagrams are statistical diagrams obtained from real data, and represent the relationship between the macroscopic characteristics of the traffic on a road (density, flow and mean speed). The triangular diagrams are the most commonly

used diagrams in macroscopic traffic flow modelling when no abrupt density changes are considered (e.g. a traffic accident) [208]. In this work, the road network used is not based on a real road network, therefore no real data were available regarding the traffic of the roads. If data from a real road network were available, the fundamental diagrams could be extracted directly from the statistical data for a more accurate representation of the traffic.

Another way to model the traffic flow on a road network is by following a microscopic approach. In this approach traffic is not modelled using aggregate variables such as density, flow rate or mean speed. Microscopic traffic models describe the interactions between individual drivers, vehicles and the infrastructure [208]. Since it is impossible to predict the behaviour of each driver with absolute certainty, stochastic models such as Markov Decision Process (MDP) based models are commonly used to model the behaviour of drivers [194]. In contrast to macroscopic models this method makes it easier to specify different types of vehicles and drivers. However, the required computing power and the large number of parameters sometimes impede the use of these models.

5.4.2 The Electricity Grid

The considered electricity network follows the structure of the UK generic distribution network [145], and is consisted of 6 types of elements. Each type was modelled as a resource entity. These are:

1. HV Substations
2. MV Feeders
3. MV Substations
4. Non-EV loads
5. Home Chargers
6. Public Chargers

The detailed characteristics of those elements were not modelled. Such an abstraction level was considered acceptable in this study since the elements' purpose is to operate as aggregating points of electricity demand (entities 1-4) and points of EV connection to the AC network (entities 5-6). Nevertheless, efficiency factors were considered to represent the energy losses from each element. More specifically:

The *HV Substations* are the highest level of electricity demand aggregation in the model. They represent the 132kV/33kV transformers connecting the transmission network to the distribution network. The HV Substations supply electricity to the districts through the MV Feeders and the MV Substations. The *MV Feeders* represent the 33kV lines connecting the HV Substations to the MV Substations. The *MV Substations* represent the 33kV/11kV transformers and aggregate the electricity demand coming from all the Non-EV loads (residential, commercial etc.) and the EV chargers in a district. The considered network structure and components are shown in Figure 5.4.







Structure	SeSAM Object	Voltage Level
		132kV Transmission Network
	HV Substations	
	MV Feeders	33kV Distribution Network
	MV Substations	
	Non-EV Loads	11kV Distribution Network
	EV chargers	

Figure 5.4: The topology of the modelled electricity network in SeSAM

Based on this topology, the power demand aggregation is described by Equations (5.5)-(5.6).

$$P_{33kV}^{HV}(t) = \sum_1^{N_{MV}} P_{33kV}^{MV}(t) \quad (5.5)$$

$$P_{11kV}(t) = \sum_1^{N_{EV}} P^{AC}(t) + \sum_1^{N_L} P(t) \quad (5.6)$$

, where

$P_{33kV}^{HV}(t)$ is the power demand at the secondary winding of the HV Substation

$P_{33kV}^{MV}(t)$ is the power demand at the primary winding of the MV Substation

N_{MV} is the number of MV Substations connected to the HV Substation

$P_{11kV}(t)$ the power demand at the secondary winding of the MV Substation

$P^{AC}(t)$ is the power demand of an EV charger

$P(t)$ is the power demand of a non-EV load

N_{EV} is the number of EV chargers connected to the MV Substation

N_L is the number of non-EV loads connected to the MV Substation

Assuming an efficiency factor n_{FD} for the losses from the MV Feeders, Equation (5.5) becomes as follows:

$$P_{33kV}^{HV}(t) = n_{FD} \cdot \sum_1^{N_{MV}} P_{33kV}^{MV}(t) \quad (5.7)$$

Considering also the power losses from the voltage transformation, Equations (5.8)-(5.9) are obtained.

$$P_{132kV}(t) = n_{HV} \cdot P_{33kV}^{HV}(t) \quad (5.8)$$

$$P_{33kV}^{MV}(t) = n_{MV} \cdot P_{11kV}(t) \quad (5.9)$$

, where

$P_{132kV}(t)$ is the power demand at the primary winding of the HV Substation

n_{HV} is the efficiency factor of the HV Substation

n_{MV} is the efficiency factor of the MV Substation

The required energy to charge the EV batteries is supplied from the electricity grid through the charging stations (EV chargers). Two types of chargers were considered in this work: the *Home Chargers* and the *Public Chargers*. A Home Charger represents a private charging station which is installed at the EV owner's house; it is therefore unique for every EV and every EV owner was assumed to have one Home Charger. Depending on the number of EV owners living in the geographical area, each district in the model can have more than one Home Chargers. The Public Chargers are chargers distributed throughout the districts and offer a recharging point to every EV. They were modelled with one charging connector allowing the charging of one EV at a time. Each Public Charger was designed with a queuing feature, so when more than one EV agent wants to use a Public Charger at the same time, a queue is created and each EV agent has to wait for the previous one to finish charging.

An efficiency factor was also considered in order to express the losses from the power conversion in the EV charger. An AC/DC converter is necessary to provide the DC power the battery needs. The maximum DC voltage that can be produced when connected to an AC network of 230V is calculated from Equation (5.10) for 1-phase and from Equation (5.11) for 3-phase connection.

$$V_{max}^{DC}(t) = \frac{2}{\pi} \cdot \sqrt{2} \cdot V_{rms}^{AC} = \frac{2}{\pi} \cdot \sqrt{2} \cdot 230V = 207.7V \quad (5.10)$$

$$V_{max}^{DC}(t) = \frac{3}{\pi} \cdot \sqrt{2} \cdot \sqrt{3} \cdot V_{rms}^{AC} = \frac{3}{\pi} \cdot \sqrt{2} \cdot 230V = 537.99V \quad (5.11)$$

Depending on the charging voltage of the EV battery, a DC/DC boost converter might be necessary to adjust the voltage output of the charger. Considering separate efficiency factors for each conversion stage, the overall efficiency factor n_{EV} of the EV

charger is given from Equation (5.12).

$$n_{EV} = n_{AC/DC} \cdot n_{DC/DC} \quad (5.12)$$

Based on this factor, the grid side power demand of the charger $P^{AC}(t)$ is calculated from the DC side (battery side) demand $P^{DC}(t)$ using Equation (5.13).

$$P^{AC}(t) = n_{EV} \cdot P^{DC}(t) \quad (5.13)$$

5.5 Modelling the characteristics of the EV agent

5.5.1 The EV agent's battery

A fundamental element of an EV is the battery. The EV battery operates in two modes: the charging mode and the discharging mode. In charging mode the battery stores energy drawn from a charging station (point of connection to the electricity grid) and thus acts as an electricity load. In discharging mode the battery acts as an electricity source and releases its stored energy to power the electric motor of the vehicle.

Different ways to model the behaviour and the characteristics of a battery exist in the literature. Depending on the required level of accuracy, these models can be very complex. Equivalent circuit models and electrochemical models are often combined with analytical or machine learning approaches in order to realistically simulate the states of a battery. The advantages and limitations of such approaches can be found in [209, 210]. However, the increased accuracy of those models comes with a computational cost which is not suitable for all applications. In this work a much simpler approach was followed, based on a modification of the Shepherd battery model. In [211], Shepherd developed a generic equation to describe the electrochemical behaviour of a battery directly in terms of terminal voltage, open circuit voltage, internal resistance, discharge current and state-of-charge.

The modified Shepherd model of [212] was used in this work to model the behaviour of a Li-ion EV battery on a 1-minute granularity. A 18650 Li-Ion battery cell with the characteristics of [2] was modelled with respect to its terminal voltage, discharge/charge current and state of charge. The model was used to simulate the behaviour of a battery pack similar to the one of a Tesla Roadster vehicle (<https://www.teslamotors.com>). According to [213], such a battery pack is consisted of 6,831 Li-Ion battery cells type-18650 following an 11S 9S 69P configuration. In this configuration 69 Li-Ion battery cells connected in parallel form 1 group, 9 groups connected in series form 1 module and 11 modules connected in series form the battery pack.

Assuming that the battery pack is consisted of the 18650 Li-Ion battery cells with the characteristics of [2], the battery pack specifications were calculated. For these calculations a battery cell management system was assumed to be in place to balance the battery cell utilisation, enabling the battery pack to behave like a single cell. The results are presented in Table 5.1. The modified Shepherd model was used to calculate the discharge characteristics of the battery pack for discharge rates of 0.2C, 0.5C, 1C and 2C (30.36A, 75.9A, 151.8A and 303.6A respectively). The characteristics are presented in Figure 5.5.

Table 5.1: Battery pack specifications

Maximum Capacity	151.8Ah
Nominal Capacity	144.9Ah
Nominal Voltage	366.3V
Internal Impedance	0.05739Ω
Standard Charge Conditions	Constant Current and Constant Voltage (CC/CV) Charge Current = 75.9A (0.5C) End-up Voltage = 415.8V End Current = 1.518A
Standard Discharge Conditions	Constant Current (CC) Charge Current = 75.9A (0.5C) End Voltage = 297V

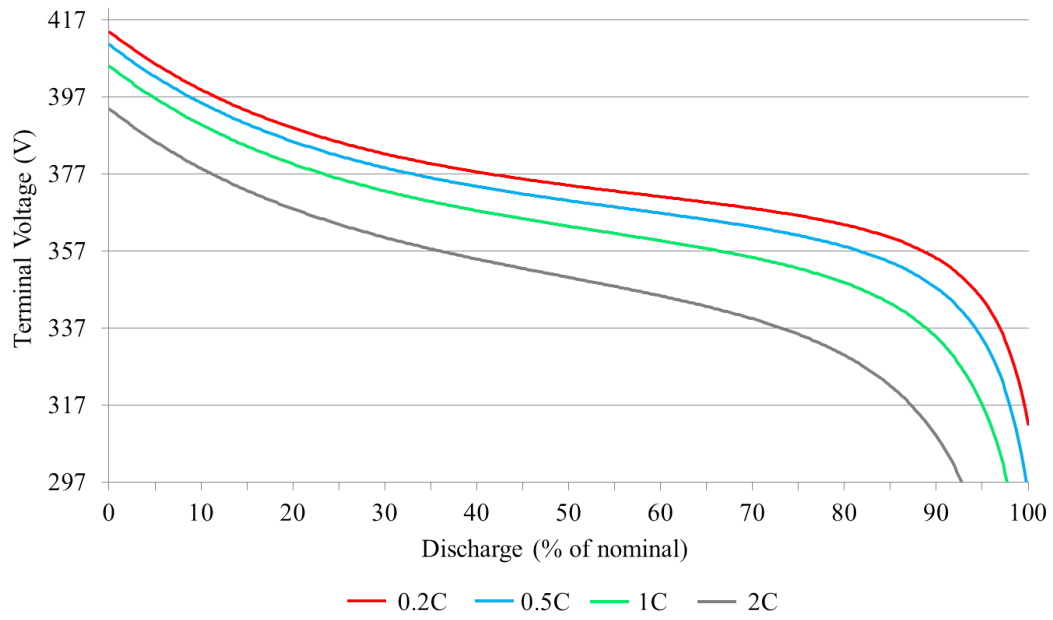


Figure 5.5: Generated discharge characteristics for the battery pack

More details on the developed battery model can be found in Appendix E.

5.5.2 The EV agent's energy consumption

When the EV agent is moving there is energy consumption from the EV battery. The power consumption of the EV agent was calculated following the approach described in [214]. According to this approach, the energy usage of an electric vehicle is distributed into 4 categories:

1. Aerodynamic Losses
2. Tire Losses
3. Drivetrain Losses
4. Ancillary Losses

The *aerodynamic losses* depend directly on the driving speed. The force of air friction

F_A on a moving object is a vector pointing to the opposite direction of movement and it has a magnitude calculated from Equation (5.14).

$$F_A = \frac{1}{2} \cdot C_d \cdot p \cdot A \cdot V^2 \quad (5.14)$$

, where

F_A is the air fiction (N)

C_d is the drag coefficient

p is the air density ($1.225kg/m^3$)

A is the frontal area of the moving object (m^2)

V is the object speed (relative to air) (m/s)

Assuming that the EV agent is moving at a constant speed V , the power requirements P_A are described with Equation (5.15).

$$P_A = F_A \cdot V \quad (5.15)$$

The *drivetrain losses* include those that the driver doesn't typically control: the efficiency of the motor controller, the motor itself, the gearbox and generally all losses in converting the DC power from the battery pack into useful torque at the wheels of the car. This is proportional to the speed due to the spinning losses in the gearbox and motor and also proportional to the power output due to the conversion losses in the various subsystems. Compared to the aerodynamics, drivetrain losses are more difficult to calculate using simple equations as the performance of each subsystem has to be individually modelled. In this work, the vehicle's speed is assumed to have a 3rd order polynomial relationship to the required drivetrain power P_{dr} , as mentioned in [214]. Equation (5.16) describes this relationship:

$$P_{dr} = \alpha \cdot V^3 + \beta \cdot V^2 + \gamma \cdot V + P_{stop} \quad (5.16)$$

, where α, β and γ are the drivetrain coefficients and P_{stop} is the drivetrain power when the EV is not moving.

Tire losses are mainly determined by the weight of the vehicle and the rolling drag of its tires. The power required to overcome the rolling resistance is a function of the vehicle's weight w and rolling resistance coefficient C_{rr} and is proportional to the driving speed V . This power P_T is described by Equation (5.17).

$$P_T = w \cdot C_{rr} \cdot V \quad (5.17)$$

All other electrical loads in the vehicle are considered as *ancillary losses* P_{anc} . These include losses from audio systems, electric windows, heating ventilation and air conditioning systems (HVAC), battery cooling and management systems as well as interior and exterior lightning. According to [214], these losses are assumed to be independent to the vehicle's speed, and were considered constant in this study.

Since the simulated EV carries a battery similar to the one in Tesla Roadster, the power consumption calculations were performed using data for the same model, and were obtained from [215]. The data used in these calculations are presented in Table 5.2. For vehicle speeds up to 150km/h , the power consumption is presented in Figure 5.6.

Table 5.2: Data used in the power consumption calculations

C_d	0.31
A	2.097m^2
α	0.00096
β	0.193
γ	18.21
P_{stop}	0.375kW
w	13096.35N
C_{rr}	0.0089
P_{anc}	2kW

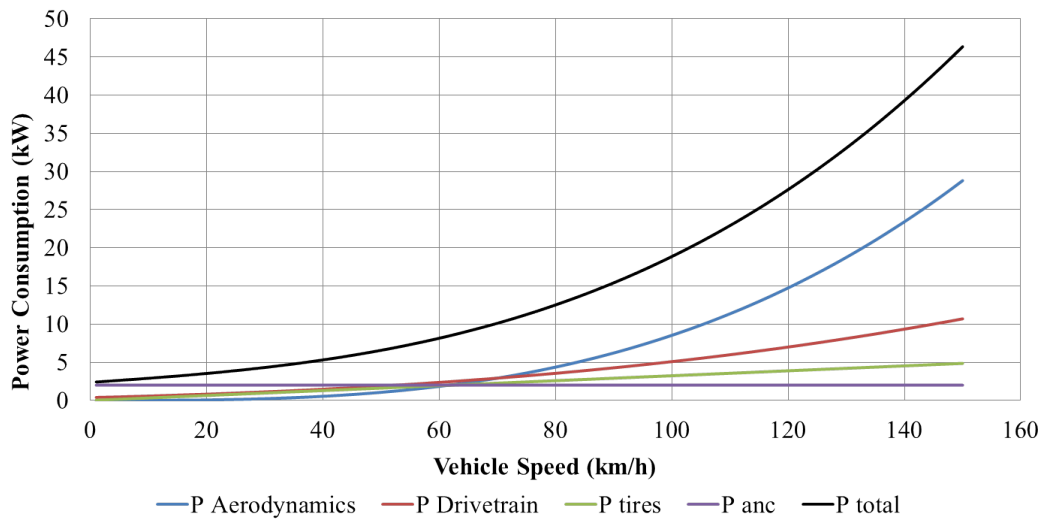


Figure 5.6: EV power consumption versus EV driving speed

5.6 Modelling the behaviour of the EV agent

5.6.1 The behavioural profiles of the EV agent

The EV agent is an agent designed to simulate the behaviour of the EV owner/driver while driving and charging the EV. In real life, an EV driver drives the EV to various destinations and makes sure that the EV has sufficient energy to make the necessary trips. To simulate this behaviour the EV agent was designed to “think” like a human EV driver and take logical decisions according to the available information. Living in a complex environment (road transport and electricity grid), the EV agent operates in an intelligent way in order to achieve its goals. The goals of the EV agent are summarised below [216]:

1. Find a route to my destination(s)
2. Recharge my EV battery when the SoC is low
3. Start the next day with a full battery

These goals describe the basic challenges an EV owner faces during the everyday use of its EV. The way that the EV owner achieves those goals affects its environment, both

the road transport and the electricity grid.

Many factors affect the EV driver's behaviour. External factors like traffic data availability affect the route of the EV driver (e.g. information about a car accident could help the EV driver avoid traffic) [17, 216]. The "range anxiety" feeling increases the frequency an EV driver recharges its vehicle and affects the distance an EV driver "thinks" the EV can make [17]. The available charging infrastructure and the overall EV integration framework affects the EV driver charging awareness as well as its willingness to respond to economic incentives regarding their charging times and fashion [217]. To model these factors two behavioural profiles were considered for the EV agent in this work: the *Unaware* and the *Aware* profile.

The *Unaware EV agent* represents an EV driver with limited intelligence regarding its routing and charging decisions. It tries to achieve its goals with minimum interactions with its environment, looking for the simplest solution to its routing / charging challenges. The "range anxiety" feeling is strong and the Unaware EV agent seeks to frequently recharge its EV - even when it is not absolutely necessary. This kind of behaviour is most likely to be found during the early stages of EV adoption, where the charging infrastructure and EV driver awareness is limited [218].

The *Aware EV agent* represents an EV driver with increased intelligence. Looking for the best possible solution to its routing and charging challenges, this EV agent interacts with its environment and affects the decisions of other Aware EV agents. The Aware EV agent is more confident about the vehicle's range (the "range anxiety" feeling is low) and thus the Aware EV agent recharges its EV only when it is necessary [17]. This type of EV driver is most likely to exist during the mature stages of EV adoption, where sophisticated charging / communication infrastructure is in place to assist in the decision making process of the EV owner, and new business entities are emerged to provide economic incentives according to the charging fashion of the EV owners [218, 219].

Each behavioural profile was modelled separately and forms the EV agent's reasoning engine. The reasoning engine is consisted of activities (behavioural states) and transitions (links between activities). Each activity defines a sequence of actions that are

executed and can trigger different procedures in the same entity and/or other entities. Time-dependent variables were defined to dynamically capture the state of the EV agent (e.g. terminal voltage of its battery) influenced by the interactions from the EV agent's environment. Independent variables were also used for the static characteristics of the EV agent (the parameters not affected by other agents or the environment). Such a parameter is the *SoC Threshold*, a parameter used to describe the "range anxiety" feeling, which defines the SoC level at which an EV agent expresses its need for recharging. All interactions among the EV agents follow request-response logic, thus each request must precede the corresponding response. Following this rule, all EV agents were modelled with an *idle* state in which they wait to receive an answer from another EV agent. This is critical for the EV agent coordination, as during this state, other EV agents perform various actions that need to be executed prior to this EV agent's next action e.g. one EV agent uses the result of another EV agent's calculation.

5.6.2 Interactions with the Road Transport network

The EV agent interacts with the road transport network of the developed model. It moves along the avenues to get to the district it wants. It affects the traffic of the avenue it is on, but also its moving speed is affected by the avenue's traffic as seen in the previous sections. To simulate the routing rationale of an EV driver, a routing algorithm was developed for the EV agents. The routing algorithm is the procedure followed by the EV agent in order to calculate the route from the current location to its destination. This procedure is different according to the behavioural profile of the EV agent.

The Unaware EV agent wants the simplest solution. That is to reach its destination district from the shortest path. The Unaware EV agent was designed to use an exhaustive breadth-first search algorithm [220] to calculate all the possible routes (unique sequence of avenues) to reach the defined destination district. For each possible route, it calculates the total trip distance by aggregating the lengths of all avenues in the route.

It then selects the route with the minimum trip distance according to Equation (5.18).

$$\min D_{Route_i}^{S \rightarrow D} \quad (5.18)$$

, where

S is the starting district of the trip

D is the destination district of the trip

N is the number of possible unique routes from S to D

$i = 1..N$

$Route_i = \{ a_1..a_k \mid K \text{ avenues connecting } S \text{ to } D \}$

$$D_{Route_i}^{S \rightarrow D} = \sum_{k=1}^K d_{a_k}$$

d_a is the length of avenue a of $Route_i$

The Aware EV agent on the other hand wants the best solution. That is to reach its destination district in the minimum time. Using the same search algorithm as the Unaware EV agent, the Aware EV agent calculates all the possible routes to the defined destination district. The difference is that the Aware EV agent uses live traffic data to identify the quickest path to its destination. The Aware EV agent estimates the total travelling time for each possible route to the destination district according to the current mean travelling speed on each avenue. It then selects the route with the minimum trip duration according to Equation (5.19). An alternative way to calculate the quickest path is by using the Dijkstra's algorithm [221] which is proven to be very efficient specifically for large graphs [222]; this however was not necessary in this work, as the considered road network is small.

$$\min T_{Route_i}^{S \rightarrow D} \quad (5.19)$$

, where

S is the starting district of the trip

D is the destination district of the trip

N is the number of possible unique routes from S to D

$i = 1..N$

$Route_i = \{ a_1..a_k \mid K \text{ avenues connecting } S \text{ to } D \}$

$$T_{Route_i}^{S \rightarrow D} = \sum_{k=1}^K \frac{d_{a_k}}{u_{a_k}}$$

d_a is the length of avenue a of $Route_i$

u_a is the current mean speed on avenue a of $Route_i$

In case the SoC of the EV agent's battery is lower than the pre-defined *SoC Threshold*, the EV agent seeks to recharge. If this need is expressed during a trip, the EV agent tries to modify its route in order to include a recharging stop at a Public Charger. Trying to simulate a realistic EV driver behaviour, different methodologies to calculate this recharging stop were developed for each behavioural profile of the EV agent.

The Unaware EV agent follows again a "simplest solution" strategy to this problem. It seeks for the closest Public Charger. It acquires the location of all Public Chargers in the region and calculates the shortest path route from its current location to the location of each Public Charger. The Unaware EV agent then selects the Public Charger which requires the least travelling distance from its current location. As soon as a Public Charger is selected, the Unaware EV agent recalculates its route to include a recharging stop. When the Unaware EV agent reaches the Public Charger, it enters the queue and charges its battery until its SoC reaches 100%.

The Aware EV agent on the other hand follows a much more sophisticated approach. It seeks for a recharging stop that minimises the total time needed to reach its initial destination district. In contrast to the Unaware EV agent, the Aware EV agent considers the live traffic of the avenues and the waiting time (queue) at the Public Chargers when calculating the recharging stop. It selects the Public Charger that minimises Equation (5.20).

$$\min(T_{Route_i}^{A \rightarrow PC} + T_{wait}^{PC} + T_{charge}^{PC} + T_{Route_j}^{PC \rightarrow D}) \quad (5.20)$$

, where

A is the current district of the Aware EV agent

PC is the district of the Public Charger

D is the destination district of the Aware EV agent

N is the number of possible unique routes from A to PC

$i = 1..N$

$Route_i = \{ a_1..a_k \mid K \text{ avenues connecting } A \text{ to } PC \}$

$$T_{Route_i}^{A \rightarrow PC} = \sum_{k=1}^K \frac{d_{a_k}}{u_{a_k}}$$

d_{a_k} is the length of avenue a of $Route_i$

u_{a_k} is the current mean speed on avenue a of $Route_i$

M is the number of possible unique routes from PC to D

$j = 1..M$

$Route_j = \{ a_1..a_w \mid W \text{ avenues connecting } PC \text{ to } D \}$

$$T_{Route_j}^{PC \rightarrow D} = \sum_{w=1}^W \frac{d_{a_w}}{u_{a_w}}$$

d_{a_w} is the length of avenue a of $Route_j$

u_{a_w} is the current mean speed on avenue a of $Route_j$

T_{wait}^{PC} is the waiting time at PC (before charging)

T_{charge}^{PC} is the charging time at PC

The Aware EV agent uses the live traffic data to estimate the travelling times ($T_{Route_i}^{A \rightarrow PC}$ and $T_{Route_j}^{PC \rightarrow D}$) for each Public Charger. In contrast to the Unaware EV agent, the Aware EV agents charge only for the necessary time in order to reach their destination. To this end the Aware EV agent estimates the energy requirements to get to its destination district and simulates the recharging cycle at that Public Charger. The energy requirements for each possible route are calculated using the live traffic data. To calculate the recharging time needed to cover these energy requirements, a “Virtual Battery Model” was developed for the Aware EV agent. The “Virtual Battery Model”

is used by the Aware EV agent to simulate (in zero time) the whole recharging cycle of each recharging option and calculate the necessary recharging time at a particular Public Charger. When the appropriate Public Charger is selected, its queue is updated accordingly with the estimated recharging time of the Aware EV agent. To calculate the waiting time at a Public Charger, the Aware EV agent aggregates the estimated recharging times of the Aware EV agents waiting at the Public Charger's queue.

5.6.3 Interactions with the Electricity Grid

The EV agent interacts with the electricity grid through the charging at the EV chargers. All EV chargers were modelled to operate on a constant current - constant voltage (CC-CV) charging cycle. Considering the EV chargers with the characteristics presented in Table 5.3, a full charging cycle of the EV agent's battery is presented in Figure 5.7.

Table 5.3: The characteristics of the EV chargers

Type	Home Charger	Public Charger
P_{nom}^{AC}	7.4kW	22kW
$n_{AC/DC}$	0.97	0.97
$n_{AC/DC}$	0.97	0.97
i_{cc} (calculated)	16.745 A	49.783 A

Depending on the nominal power rate and the efficiency factor of each charger, the charge current of the CC phase was calculated. Figure 5.7 presents the EV battery voltage, current and SoC, as well as the charger's power demand from the AC grid.

More details on the implementation of the charging / discharging process for the EV battery can be found in Appendix F.

The duration of charging is different for the two EV agent profiles. The Unaware EV agent charges its battery at a Public Charger until it is fully charged while the Aware EV agent charges its battery only for the time necessary to complete its trip. Longer charging durations affect the electricity grid, as the required energy for one

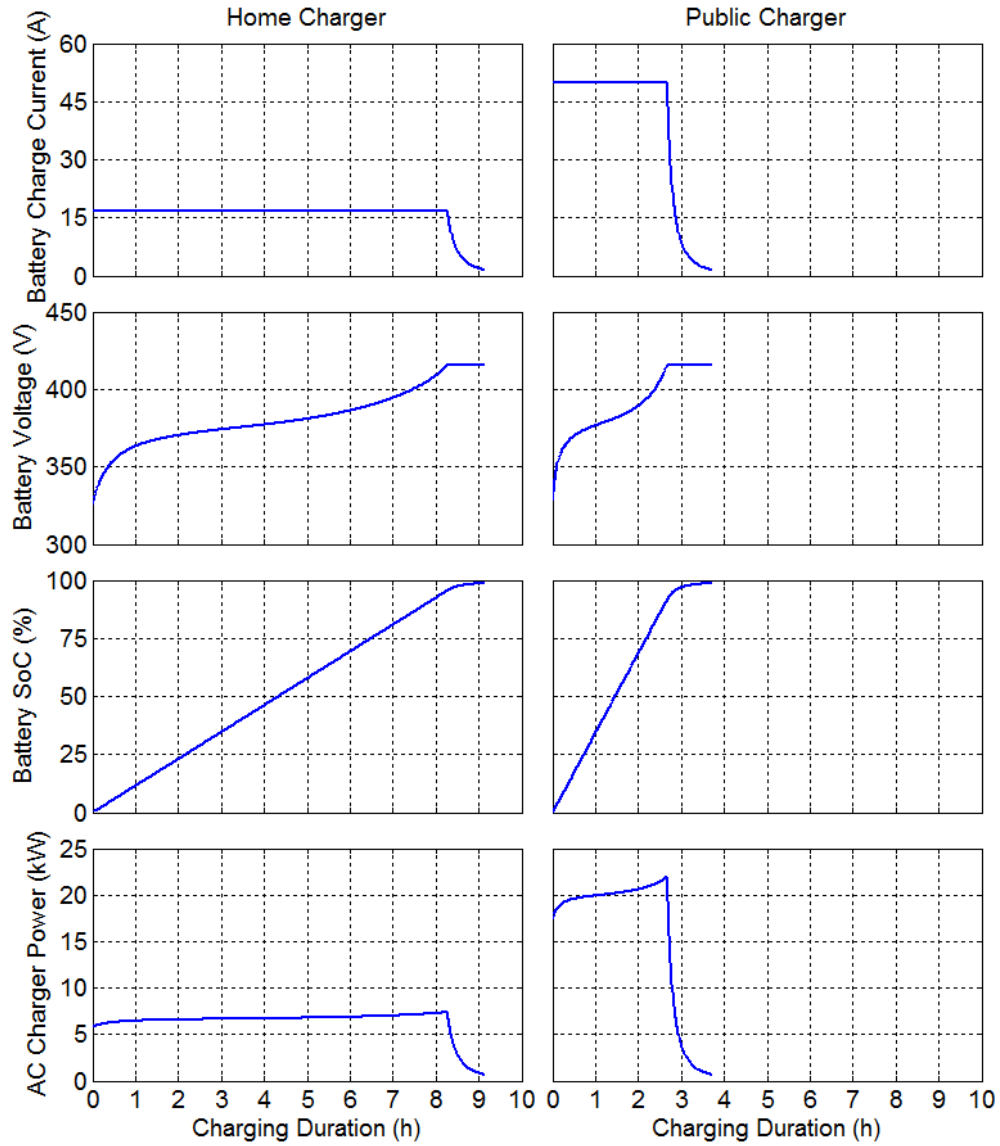


Figure 5.7: The battery voltage, charge current and SoC of the EV battery, and the power demand of the EV charger.

charging event is higher. In addition, the “range anxiety” feeling (expressed by the *SoC Threshold* variable), has an effect on the electricity grid as it defines the charging frequency for an EV agent. When the “range anxiety” feeling is strong (*SoC Threshold* is high), the EV agent charges its vehicle multiple times in a day.

In the developed model, the EV agents charge at home every night. Trying to simulate

the charging behaviour of unconcerned and concerned EV owners, the Unaware EV agent and the Aware EV agent were modelled to follow different charging regimes at home.

The Unaware EV agents follow an uncontrolled charging regime. As soon as they return home from their daily trips, they begin charging regardless the network's condition. Their charging stops when the EV battery is fully charged.

The Aware EV agents follow a different approach for their home charging. Their goal is to minimise the impact of their charging at a local level (district level). They coordinate with the other Aware EV agents that live in the same district, and charge during the off-peak hours of the MV Substation of that district. To identify the off-peak hours, the expected day-ahead demand of a district was assumed known to the district's Aware EV agents. Upon its arrival at home, each Aware EV agent calculates the optimal start time (start minute since the simulation runs minute-wise) for its charging. The optimal start time t_s is the one which results in the minimum standard deviation of the expected day-ahead demand of the MV Substation. The Aware EV agent was modelled to follow a charging strategy that minimises the standard deviation of the district's demand profile according to the following function:

$$\min \sqrt{\frac{\sum_{t=t_c}^{t_c+N} (X_t - \bar{X})^2}{N}} \quad (5.21)$$

, where

$N = 1440$ day-ahead minutes

t_c is the current minute

$$\bar{X} = \frac{\sum_{t=t_c}^{t_c+N} X_t}{N}$$

$$X_t = \begin{cases} P_{ch}(t - t_s) + P_{DA}(t) & , \text{if } t_s < t \leq t_s + cd \\ P_{DA}(t) & , \text{otherwise} \end{cases}$$

cd is the necessary charging duration (in minutes)

t_s is the start time of charging

$P_{ch}(t)$ is the charging demand at minute t

$P_{DA}(t)$ is the day-ahead demand of the district's MV Substation

In order to calculate the charging demand, the Aware EV agent uses the “Virtual Battery Model” to simulate the charging procedure at its Home Charger. When the optimal start time is calculated, the Aware EV agent updates the expected day-ahead demand of the MV Substation accordingly. Equation (5.22) was used to update the day-ahead demand.

$$X_{DA-new}(t) = \begin{cases} P_{ch}(t - t_s) + P_{DA-old}(t) & , \text{if } t_s < t \leq t_s + cd \\ P_{DA-old}(t) & , \text{otherwise} \end{cases} \quad (5.22)$$

The next Aware EV agent that arrives at home in the same district uses the updated day-ahead demand to calculate the optimal time to charge its battery. After all Aware EV agents return home, the result is a coordinated charging with the minimum impact on the electricity grid.

However, the participation of the EV drivers to such a charging coordination scheme might result in a charging plan which is not in line with the individual constraints and wishes of the EV drivers. A form of incentive has to be in place in order to reward the EV drivers for their participation in such a scheme. This reward can be realised through a dynamic pricing scheme according to which, the EV drivers are benefited from cheaper electricity rates when offering a flexible charging profile [146, 223]. In this work it is assumed that such a rewarding mechanism is in place, and all Aware EV agents are willing to participate in the coordinated charging scheme.

5.7 Case Study

5.7.1 Description of the simulation scenarios

The developed model was used in order to study the impact of the EV agents' behavioural profiles in two different scenarios (one for Unaware behaviour and one for Aware behaviour). In these scenarios, 10000 electricity consumers were considered for the whole network (geographical area). The consumers were evenly distributed in each district and were assumed to have different daily electricity demand profiles obtained from the UK Energy Research Centre (<http://www.ukerc.ac.uk/>). An EV uptake of 10% was assumed, and a fleet of 1000 EVs (EV agents) was created.

An activity-based travel pattern was assumed for all EV agents in our model. The travel pattern assumes a sequence of 4 activities in a day. Starting from Home the sequence of the activities is Work-Lunch-Work-Shopping. After completing their activities, the EV agents return Home for the night. A random number generator was used to define the location (district) of each activity, with the assumption that these districts must be different from Home. The times each EV agent spent for each activity were assumed to be random numbers following a normal distribution (different for each destination). The distributions are presented in Table 5.4.

Table 5.4: The distribution of the times spent for each activity

Activity	Mean Value (μ)	Standard Deviation (σ)
Work	4 hours	0.3 hour
Lunch	0.5 hour	0.25 hour
Work	3 hours	0.3 hour
Shopping	0.5 hour	0.25 hour

5.7.2 Simulation Results

The impact of the different behaviour of the EV agents on their environment and their battery characteristics was studied. Every dynamic variable of the model is monitored

during the simulation. A sample of the simulation results was selected and is presented in this section. Screenshots from the SeSAM GUI can be found in Appendix G.

As mentioned in the previous sections, the Home charging fashion is different for Unaware and Aware EV agents. The Unaware EV agents start charging immediately when they arrive at Home, while the Aware EV agents calculate the optimal start time for charging according to Equation (5.21). The impact of EV charging at Home on the demand profile of the HV Substation is presented in Figure 5.8 for both EV behavioural profiles. To emphasise the impact of Home charging demand and increase the EV charging requirements, it was assumed that the EV agents don't charge from Public Chargers during the day.

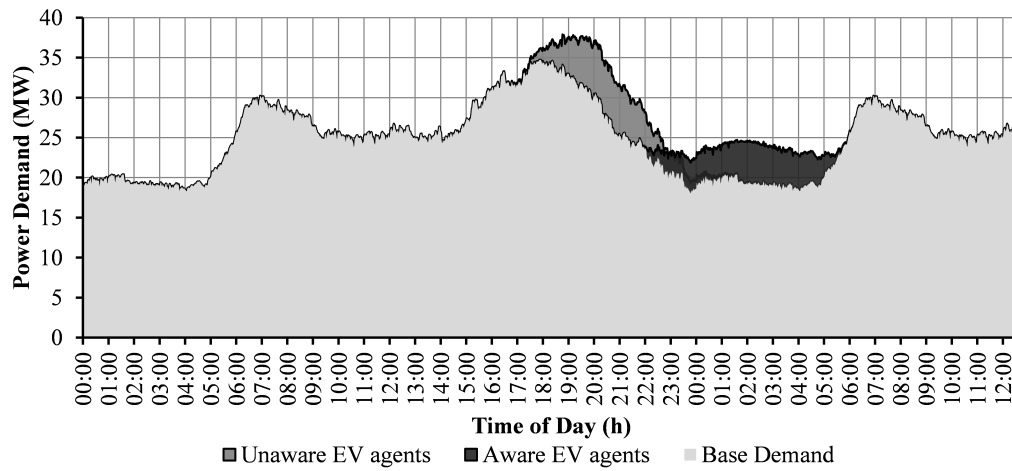


Figure 5.8: Impact of EV charging at Home (aggregated)

As seen from Figure 5.8, the Unaware EV agents start charging when they return home (around 17:30-18:00) and their charging demand coincides with the evening peak of the residential demand. Consequently, a 9.11% increase of the peak demand is created, and the electricity network is stressed. On the other hand, the Aware EV agents place their charging during the off-peak hours (between 22:00 and 06:00) resulting in a valley-fill effect on the demand profile of the HV Substation. This “grid-sensitive” behaviour of the Aware EV agents not only avoids the increase of the peak demand, but also reduces the stress of the electricity network and postpones any unnecessary upgrades of the existing infrastructure.

As described before, the EV agents have a large battery pack ($53kWh$). Assuming a full battery in the morning and a realistic SoC Threshold of 30%, the EV agents would not normally need a recharging stop during the day (especially when the trips are only five). In order to study the behaviour of the EV agents when a recharging stop at a Public Charger is required, it was assumed that the need for a recharging stop is triggered at a much higher SoC level, at 70%. Although this value is unrealistic, it serves well the demonstrating purposes of this case study. To this end, 100 Public Chargers were distributed equally to the 10 Districts offering recharging services to the EV agents.

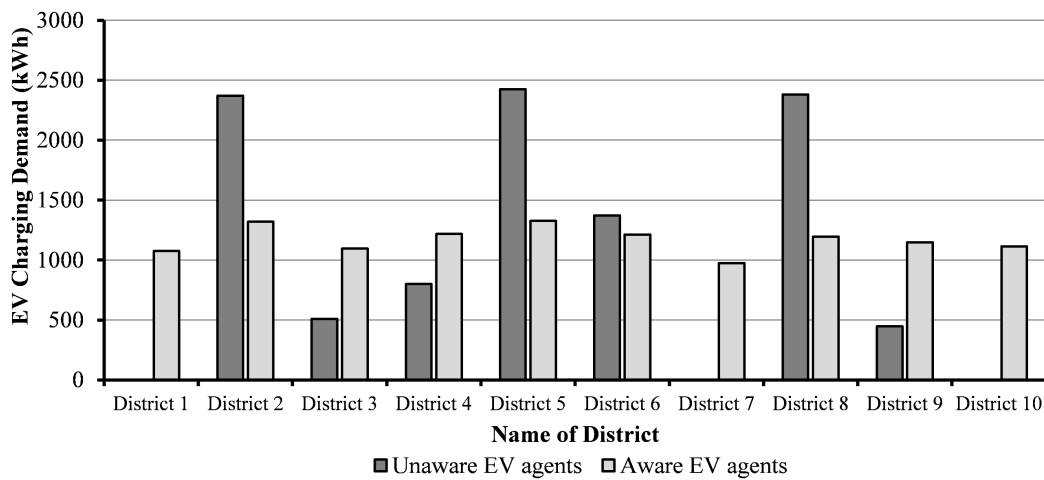


Figure 5.9: Distribution of Public EV charging demand to the districts

Figure 5.9 presents the aggregated charging demand from the Public Chargers of each District. The Unaware EV agents look for the closest Public Charger when they need a recharging stop, while the Aware EV agents try to minimise the total duration of the recharging stop by considering the waiting times at a Public Charger. Due to this behaviour, the Unaware EV agents prefer the central nodes of the transport network (Districts 2, 5 and 8) for their public charging. This causes an uneven utilisation of the Public Chargers (only the ones at central districts are used), as well as a significant impact on the local electricity grid. Queues are also created to the popular Public Chargers, delaying the charging procedure for the EV agents. On the other hand the Aware EV agents use the information regarding the availability of Public Chargers, and charge at Public Chargers in all Districts. This way they avoid the queues and

reduce their recharging times. Moreover, the Aware EV agent behaviour increases the utilisation of the public charging facilities and offers an even distribution of the charging demand to all Districts, reducing the stress of the electricity grid.

The uneven distribution of the charging demand affects the electricity grid. The high charging demand stresses the distribution network infrastructure and causes increased line losses and deep voltage drops. As the distribution network has certain limits and load capacity, an upgrade might be necessary in order to facilitate this additional demand. In addition, the charging demand is directly related to the number of charging requests in the district. Increased number of charging requests in a district means that more EVs arrive to that district seeking to recharge, affecting the traffic on the roads of each district (not modelled in this work). The utilization rate of the public chargers is also affected by the distribution of charging requests. Considering third-party companies that own and manage these public chargers, the utilization rate has a significant effect on their income. The capital and operational costs of the public chargers are seen as investments by these companies, and an underused public charger reduces the efficiency of this investment. These companies need to understand the EV owners' behaviour and calculate the expected utilisation ratio of each public charger when planning its location to make sure that their investment will not be inefficient.

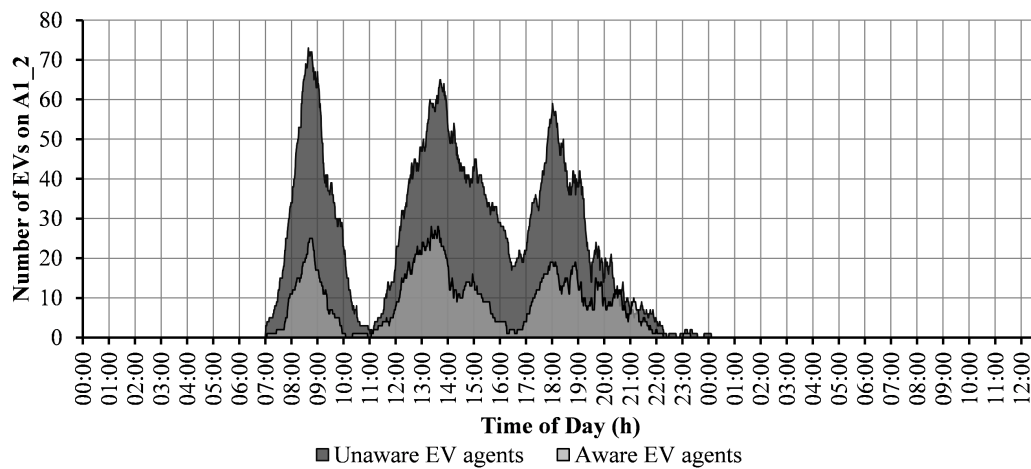


Figure 5.10: Traffic distribution on avenue A1_2

The EV agents affect the road transport network according to their behavioural profile

and their recharging requirements. Figure 5.10 presents the average number of EVs on a random road (avenue A1_2) of the transport network. Three traffic “peaks” are created from the EV agents. The first peak occurs during the morning hours, when all the EV agents go to their work. The second peak is in the early afternoon, when the EV agents go to lunch, following their pre-defined activity cycle. Due to the stochastic approach that was followed for the duration of each activity, the width of this peak is considerably wider than the first peak as not all the EV agents go for lunch at the exact same time. The same goes for the third peak in the evening hours, when the EV agents leave their work to go shopping and return home.

The Unaware EV agents choose the shortest route to their destination judging by the driving distance. The Aware EV agents on the other hand, consider the real time traffic information and choose the fastest route to their destination, avoiding the busy roads. Due to this behaviour, the traffic of avenue A1_2 was reduced as seen in Figure 5.10. Of course, this is not the case with all the avenues in the transport network. The average traffic density in a day of all the avenues in the transport network is presented in Figure 5.11.

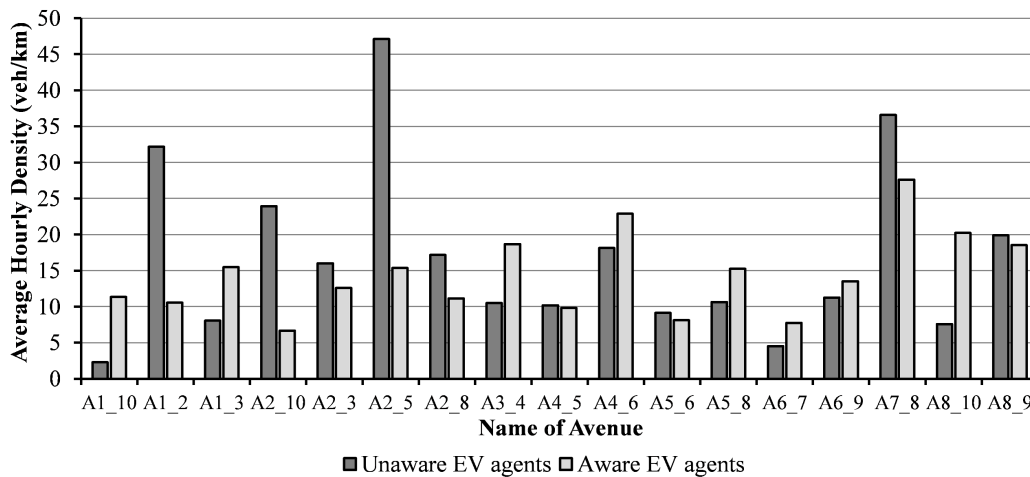


Figure 5.11: Average traffic distribution of EVs on all avenues

The Unaware routing behaviour increased the traffic of popular avenues, and led to an uneven distribution of traffic throughout the network. The Unaware EV agents face delays in their return to home and the energy consumption of their vehicles is

increased. Their recharging requirements combined to their charging behaviour increases even more the traffic of the avenues which lead to the central districts. Due to a high SoC Threshold, the need for a recharging stop is frequent. Considering that the Unaware EV agents choose the closest Public Charger, many EVs arrive at the central districts seeking for an available Public Charger increasing the traffic of the surrounding avenues.

On the other hand, the Aware EV agents try to minimise the total duration of their trips. By using the avenues with reduced traffic, they distribute the traffic to all the transport networks. This reduces the risk of a traffic jam and enables a smooth and continuous flow of traffic. Their Aware charging behaviour and confidence on the EV range, allows the Aware EV agents to have less frequent recharging stops and when they do these are at available Public Stations at less popular districts. This helps in the disaggregation of traffic from the central districts of the network.

5.8 Summary

A multi-agent system based simulator was developed for the integration of transport and electricity networks capable of reproducing the behaviour of an intelligent entity (electric vehicle) co-existing in both systems. The main components of both networks were modelled in a multi-agent simulation platform to simulate the environment of the EV. The main EV characteristics were also modelled in detail, allowing a more in-depth approach to the EV's interdependencies with its environment. One of the main aims of this simulator is to enable a variety of possible scenarios to understand the EV context, bringing together two distinctly different but highly inter-related infrastructures. To this end, two realistic behavioural profiles (Unaware/Aware) were considered to describe the way an EV driver deals with the everyday challenges.

Considering a fleet of 1000 EV agents, two scenarios were considered to understand the impact of different EV driver behaviour to the road transport and the electricity grid. The scenarios represent the different stages of EV integration, starting with Unaware EV drivers when the public acceptance of EVs is limited, and developing to

Aware EV owners as the electrification of road transport is promoted in an overall context. Following a realistic activity-based trip pattern, the EV agents move and stay at random destinations for durations that were stochastically defined.

It was found that the EV agents' behavioural profile has direct and indirect impact on both the road transport network and the electricity grid, affecting the traffic of the roads, the stress of the distribution network and the utilization of the charging infrastructure. According to the results, the Unaware EV agents increased the traffic of popular avenues, and led to an uneven distribution of traffic throughout the network. On the other hand, the Aware EV agents used the avenues with reduced traffic, and distributed the traffic throughout the transport network.

When charging at home, the uncontrolled charging of the Unaware EV agents caused a 9.11% increase of the peak demand of the modelled distribution network. On the other hand, the Aware EV agents place their charging during the off-peak hours (between 22:00 and 06:00) resulting in a valley-fill effect on the daily demand profile of the district. When charging at Public Chargers, it was found that the Unaware EV agents prefer the central nodes of the transport network. This causes an uneven utilisation of the Public Chargers, as well as a stress at the local electricity grid. On the other hand, the Aware EV agents were able to offer an even distribution of the charging demand to all Districts, reducing the stress of the electricity grid and increasing the utilisation of the Public Chargers.

Observing EV behaviour under different situations with multi-agent simulations will help understand the impact of future EV integration on both systems and to better understand how a variety of differing roles within both networks could co-exist. Therefore, authorities will have knowledge of possible irregularities or needs for adjustments / re-configuration in order to allow and support the EV adoption in the future. The awareness of the EV drivers should be supported (and incentivised) by the authorities as it reduces the impact of EVs on road transport and electricity networks and ensures a smooth electrification of road transport.

Conclusions and Suggestions for Further Work

6.1 Thesis Contributions

This thesis investigated the feasibility of EV charging management for reducing the electricity cost of commercial buildings. The contributions of this thesis are:

1. The development of a model that predicts the “triad” peaks of the grid and the energy demand of a building. The tool supports the building manager in reducing the high electricity costs of the building during triad peak hours.
2. The development of a local energy management system (LEMS), combining a triad prediction tool, an electricity demand forecast tool and a charging control algorithm in a cloud-based program. The management system enables the building manager to reduce their overall electricity cost, and participate in grid balancing services.
3. The development of a multi-agent simulation tool that simulates the routing and charging behaviour of the EV driver in a realistic environment. The tool enables studying the impact of EV driver behaviour on a road transport and electric power network.

6.2 Overview of Chapter 2: Predicting the energy demand of buildings during triad peaks in GB

6.2.1 Summary

In this chapter a model was developed to forecast the power demand of commercial buildings during the “triad” periods. The model includes three stages. In the first stage, a stochastic model was developed to calculate the probability of having a “triad” on a daily and half-hourly basis and warn the building manager accordingly. In the second stage, real weather data were analysed and included in the model to increase its forecasting accuracy. In the third stage, an ANN forecasting model was developed to predict the power demand of the building at the periods when a “triad” peak is more likely to occur.

The stochastic model was trained on real “triad” peak data from 1990 onwards, and validated against the actual UK “triad” dates and times of 2014/2015. The ANN forecasting model was trained on real electricity demand data from six commercial buildings in Manchester for one year. Real local weather data for the same period were analysed. The electricity demand of each building on an actual “triad” peak date and time was predicted successfully.

6.2.2 Conclusions

It was found that modifying the granularity of the calculations affects the number of “triad” warnings that are generated, and consequently the likelihood of predicting a “triad” peak. A sensitivity analysis showed that higher interval sizes result in higher numbers of “triad” warnings. Depending on the application, the building managers can select the appropriate interval size and respond to the corresponding “triad” warnings.

The times of all three “triad” peaks of 2014/2015 were predicted successfully. It was showed that the “triad” peaks tend to occur in a relatively narrow zone during a day

(between 16:30 and 18:30). The building managers can use this information and adjust their demand profiles in order to reduce their costs.

The aggregated power demand of the building facility during an actual “triad” peak was predicted with 97.6% accuracy. It was showed that the weather information plays a significant role in the accuracy of the building energy demand forecast. It was demonstrated that the choice of weather attributes is very important to the forecasting accuracy, and in some cases, using less weather data is more valuable and can lead to more accurate predictions.

6.2.3 Limitations and suggestions for further work

Although the results are very promising, more data are needed before the conclusions are generalised. Diverse data from other geographical areas should be considered to capture the effect of local weather on forecasting the electricity demand of a building. Other types of buildings should also be analysed (e.g. industrial) prior the application of the proposed model to a non-commercial facility.

6.3 Overview of Chapter 3: Management of EV charging at commercial buildings

6.3.1 Summary

In this chapter a charging control algorithm was developed for the Charging Station Manager to schedule the EV charging and discharging (V2B) events in a commercial building. Two strategies were implemented, namely Off-Peak Strategy and Cost-Reduction Strategy. The Off-Peak strategy aims to minimise the impact of EV charging on the demand profile of the building and reduce its peak demand. The Cost Reduction strategy aims to minimize the total electricity cost of the building facility by adjusting the EV charging demand to the electricity prices.

A realistic EV fleet was modelled based on real statistical data from the NTS, in order to evaluate the control model. To study the impact on the grid, the UK generic distribution network was modelled in Matlab. The impact on the demand profile, daily electricity cost and bus voltage was studied for a workplace charging scenario.

6.3.2 Conclusions

It was found that the Off-Peak strategy combined with a 15% V2B provision reduces the aggregated peak demand of the building by 9.7%. In this case however the EVs need to charge for longer periods and due to the bell shaped demand profile of a commercial building and the long peak period, this could lead to insufficient charging of some EVs. The distribution network is also benefited from this charging strategy. Studying UK generic distribution network, it was found that the fleet of 48 EVs was able to increase the minimum voltage of the 0.4kV bus by 0.2%.

Considering that the building managers pay additional charges on triad peaks (as explained in Chapter 2), the Cost Reduction strategy of the Charging Station Manager is useful in this case, as it could lead to significant cost savings. It was found that the Cost Reduction strategy combined with a 15% V2B provision reduces the daily electricity cost of the building by 1%. However, a demand cap is necessary to be applied in order to protect the existing infrastructure from excessive stress and overloading due to the simultaneous charging events during cheap hours.

A sensitivity analysis showed that the ratio between responsive/unresponsive EV drivers affects significantly the results. High percentages of unresponsive EV drivers will lead to a non-optimal result, creating a new peak on the building's demand profile or charging at the expensive hours increasing the electricity cost for the building manager.

6.3.3 Limitations and suggestions for further work

Apart from avoiding discharging the EV batteries when their SoC is lower than 20%, no other measures are considered by the Charging Station Manager to prolong their

State-of-Health. A detailed modelling of the EV batteries would enable capturing the effect of charging / discharging cycles on the EV battery's life.

In addition every EV driver is assumed to participate in this control scheme, allowing the Charging Station Manager to manage the charging / discharging of their EV battery. This relationship should be agreed and regulated through a contractual agreement, for both parties to enjoy economic incentives and benefits. Such a business model is not considered in this work.

6.4 Overview of Chapter 4: A Local Energy Management System for the building manager

6.4.1 Summary

In this chapter a complete Local Energy Management System (LEMS) was presented, developed to control EVs and Storage Units at the building premises and reduce the electricity costs of the building manager.

Three scheduling algorithms were developed, namely Peak Shaving, Triad Cost Reduction and Demand Response. The model of Chapter 2 was used in order to predict the future triad peaks of the system and forecast the building demand at those times. The charging control algorithm of Chapter 3 was also used as part of the LEMS scheduling algorithm.

The LEMS was implemented as a software package deployed on cloud, and its operation was demonstrated in different simulation scenarios. In the first scenario (Peak Shaving Operation) the EVs and the Storage Units were scheduled to charge during the off-peak hours, and discharged during the peak hours of the building's electricity demand. In the second scenario (Triad Cost Reduction Operation) the controllable assets were scheduled to charge during the cheap hours and discharge during the expected triad peak hours. In the third scenario (Demand Response Operation) the LEMS was assumed to receive demand response requests from the network operator.

The use of the LEMS for exploring different use cases (what-if scenarios) was also demonstrated by studying different charger rate scenarios.

6.4.2 Conclusions

In the Peak Shaving Operation scenario the LEMS successfully coordinated the charging / discharging of the EVs and Storage Units. According to the results, a 6.9% peak reduction was achieved comparing to the initial demand of the facility (without EVs and Storage Units).

In the Triad Cost Reduction Operation scenario the LEMS successfully coordinated the charging / discharging of the EVs and Storage Units to reduce the electricity cost of the building facility. It was found that the LEMS resulted in a 7.5% reduction of the electricity requirements during the triad peak hours (17:00 - 20:00), reducing the triad costs for the building manager.

In the Demand Response Operation scenario, the LEMS was able to override the existing charging/discharging schedules of the EVs and Storage Units, and reduce the overall demand by 17.7% as a response to the demand reduction request. In addition, an overall 8.9% demand increase was achieved as a response to the demand increase request.

6.4.3 Limitations and suggestions for further work

Similarly to Chapter 3, the LEMS operation is not based on a detailed battery model. Consequently the impact of the charging / discharging cycles on the battery State-of-Health is not modelled.

The integration of the developed LEMS with the building's HVAC systems would allow further flexibility on the demand profile of the building facility. In this case however, the impact on the occupants' comfort should be considered.

6.5 Overview of Chapter 5: Simulation of EV driver behaviour in road transport and electric power networks

6.5.1 Summary

This chapter describes an integrated simulation-based approach, modelling the EV as an intelligent unit living in both road transport and electric power systems. The main components of both systems have been considered, and the EV driver behaviour was modelled using a multi-agent simulation platform.

Considering a fleet of 1000 EV agents, two behavioural profiles were studied (Unaware/Aware) to model EV driver behaviour. The EV agents were modelled to follow a realistic activity-based trip pattern, and the impact of EV driver behaviour was simulated on a road transport and electricity grid.

6.5.2 Conclusions

It was found that the EV agents' behavioural profile has direct and indirect impact on both the road transport network and the electricity grid, affecting the traffic of the roads, the stress of the distribution network and the utilization of the charging infrastructure.

According to the results, the Unaware EV agents increased the traffic of popular avenues, and led to an uneven distribution of traffic throughout the network. On the other hand, the Aware EV agents used the avenues with reduced traffic, and distributed the traffic throughout the transport network.

When charging at home, the uncontrolled charging of the Unaware EV agents caused a 9.11% increase of the peak demand of the modelled distribution network. On the other hand, the Aware EV agents place their charging during the off-peak hours (between 22:00 and 06:00) resulting in a valley-fill effect on the daily demand profile of the district.

When charging at Public Chargers, it was found that the Unaware EV agents prefer the central nodes of the transport network. This causes an uneven utilisation of the Public Chargers, as well as a stress at the local electricity grid. On the other hand, the Aware EV agents were able to offer an even distribution of the charging demand to all Districts, reducing the stress of the electricity grid and increasing the utilisation of the Public Chargers.

6.5.3 Limitations and suggestions for further work

Due to the lack of data, it was not possible to apply the developed model on a real road / electricity network. Therefore, the results cannot be directly compared to an real scenario. However, the work in this chapter is published in a journal paper, a conference paper and a book chapter and was reviewed by experts from both the power system and the transportation research field. Researchers are encouraged to use this model on a real case study, since it was developed in such a way that supports external file inputs in order to customise the structure and parameters of the simulated road network and electricity grid.

6.6 Overall Research Benefit

A number of actors could benefit from this thesis:

The *Building Managers* may benefit from this research and use it to reduce their electricity bills. The developed tools can be used by the building managers to manage the charging / discharging of EVs and energy storage in order to reduce their impact on the electricity demand and cost of a commercial building. Insights of possible business potential with the DNOs are also offered to the building managers from their participation in the ancillary services market, which may lead to profitable contractual agreements for both sides.

The *Distribution Network Operators and Energy Suppliers* may also benefit from this research as it promotes the energy consumption awareness of the customers. The deve-

veloped tools support the flexible demand side management of EVs and energy storage and enable the participation of building managers in the ancillary services market. This prolongs the life of the existing distribution networks and postpones their costly infrastructure upgrades.

The *Operators* of charging stations may also benefit from this research with regards to the analysis of the behaviour of an EV driver. The developed simulation tool could be used to understand the possible charging and routing behaviour of EV drivers and calculate the expected utility from public charging stations in a geographical area. The operators of charging stations could use this tool to identify the locations that are expected to have large recharging requirements and plan the installation of new charging stations accordingly.

The *Society and the Environment* may generally benefit from this research. The increased awareness of electricity customers and the flexibility of the demand could help the Smart Grid development in GB and other countries. Therefore, the integration of renewable energy sources could be supported and greenhouse gas emissions reductions may be achieved.

Appendix A

Electricity demand and weather data used in Chapter 2

This appendix presents the data which were used in Chapter 2. The data include the daily electricity demand of the six commercial buildings as well as the weather information from a weather station in Manchester for the period of 12/2012 – 12/2013.

A.1 Electricity Demand Data

Figures A.1 - A.6 present the daily electricity demand of the six commercial buildings.

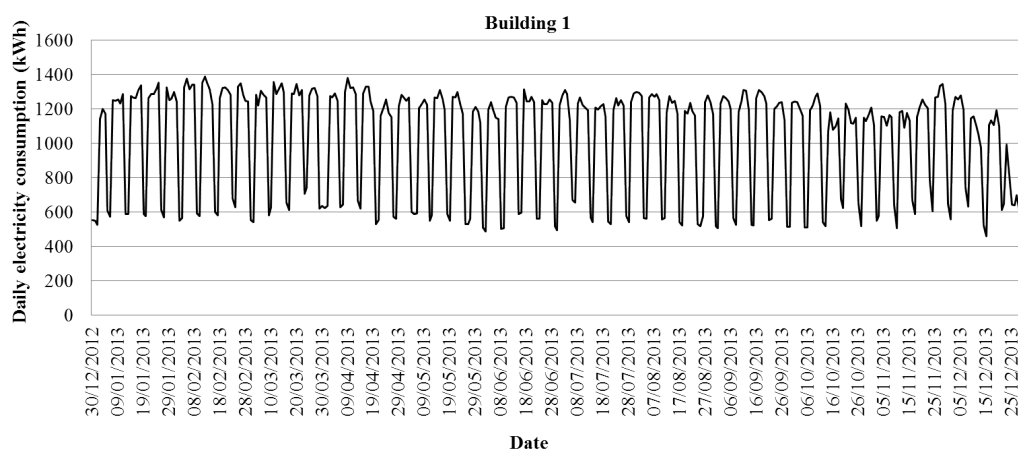


Figure A.1: The daily electricity demand of Building 1

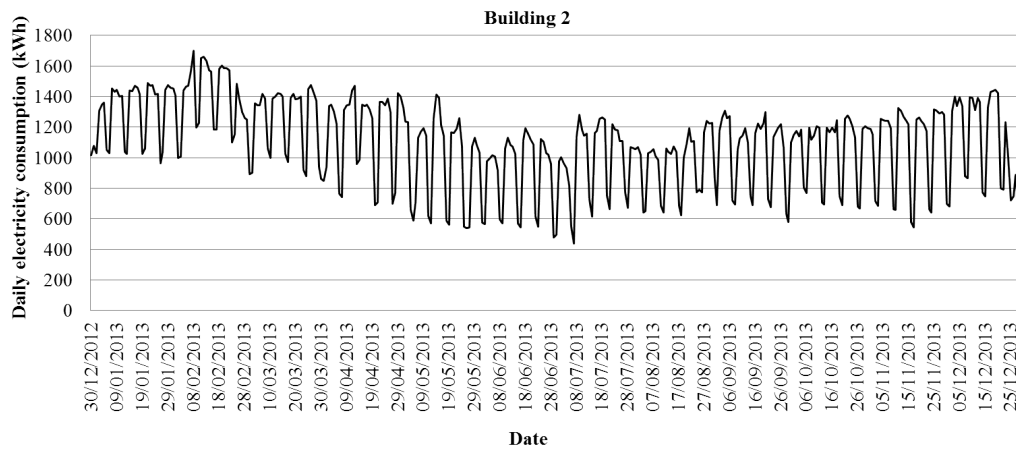


Figure A.2: The daily electricity demand of Building 2

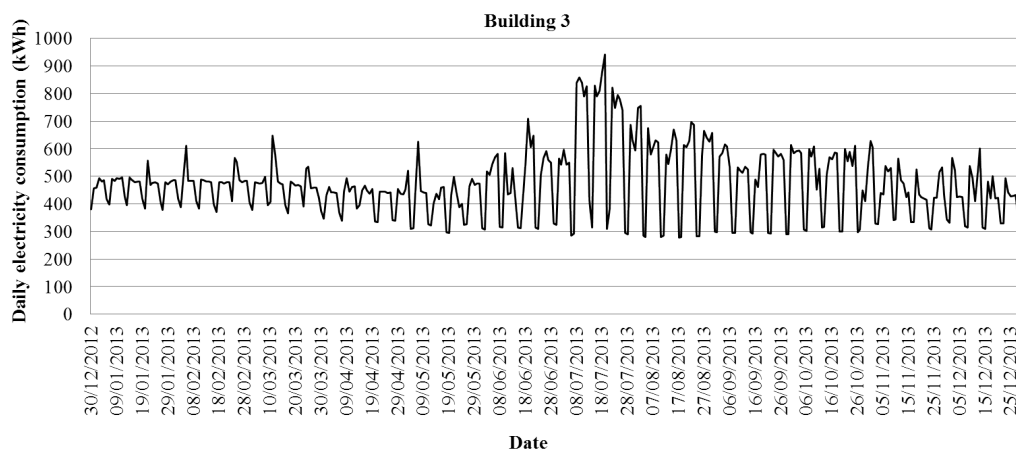


Figure A.3: The daily electricity demand of Building 3

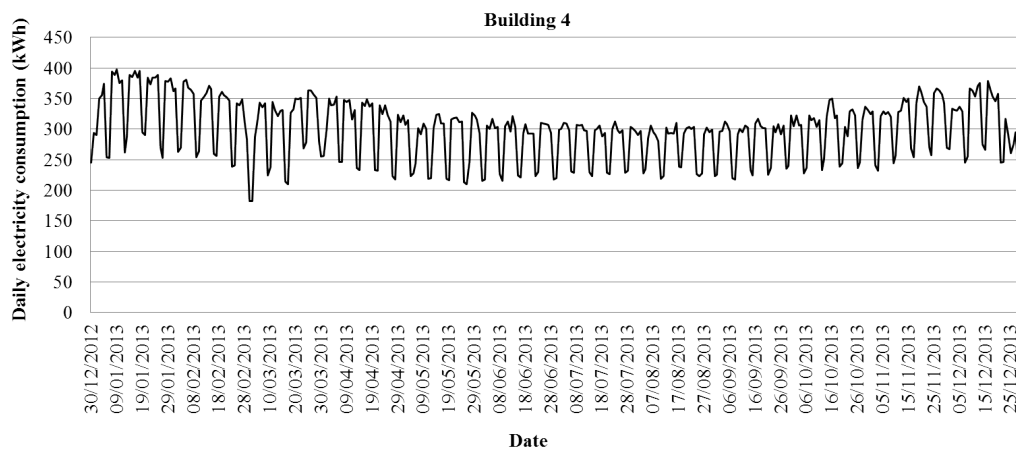


Figure A.4: The daily electricity demand of Building 4

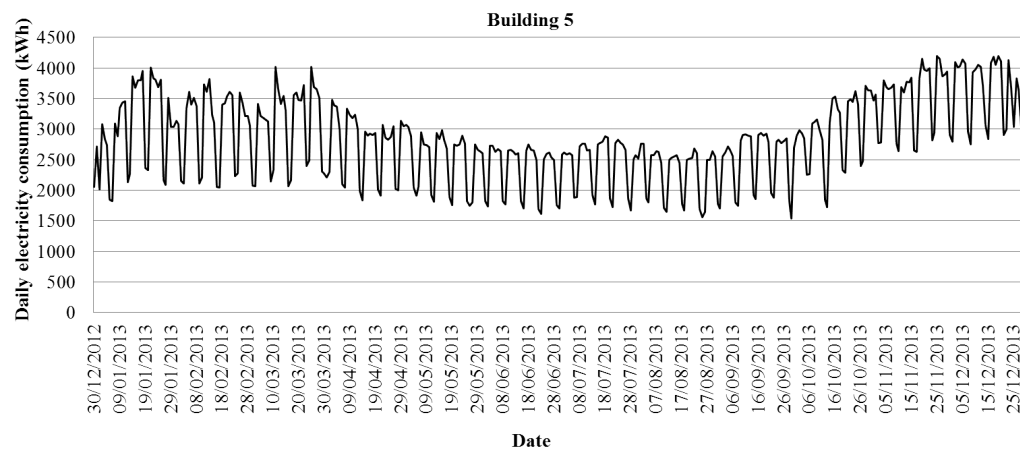


Figure A.5: The daily electricity demand of Building 5

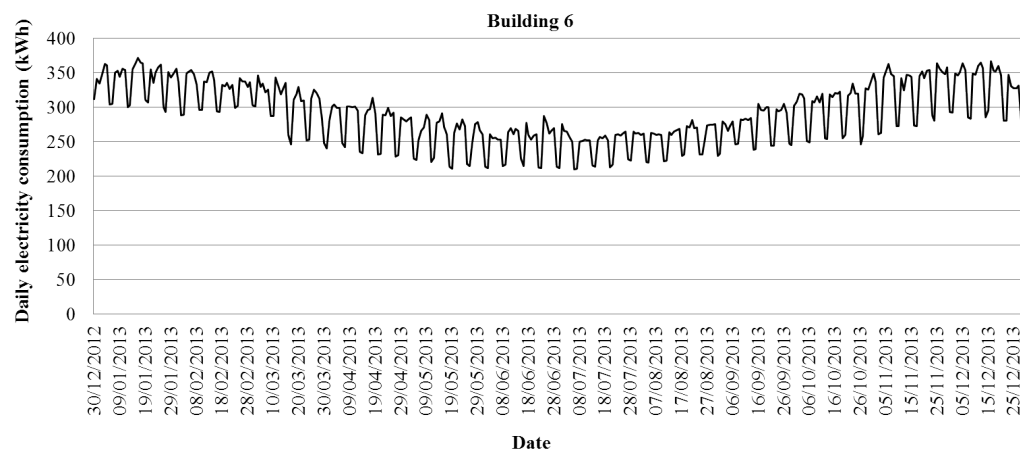


Figure A.6: The daily electricity demand of Building 6

A.2 Weather Data

Figures A.7 - A.16 present the weather data as obtained from the MetOffice.

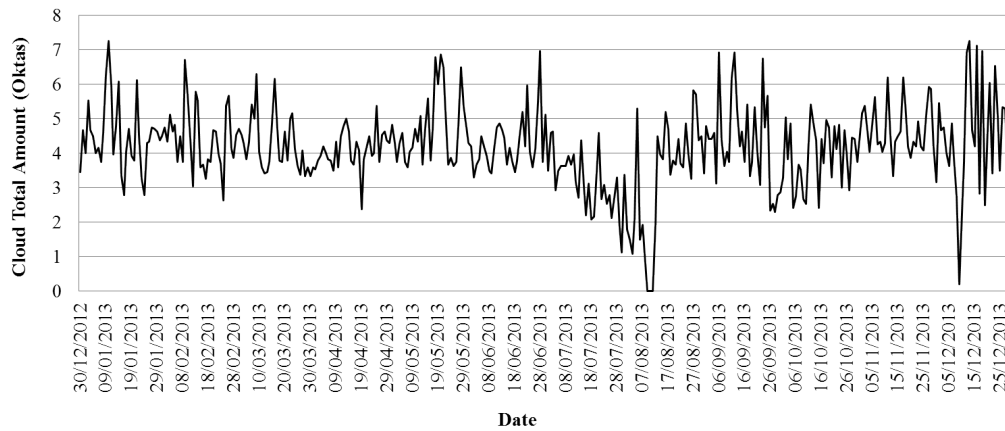


Figure A.7: The total amount of cloud in oktas

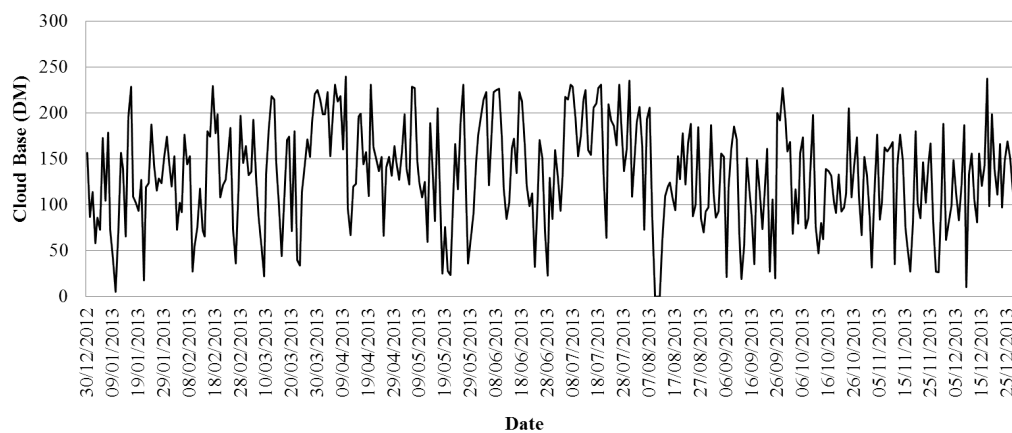


Figure A.8: The cloud base distance in meters

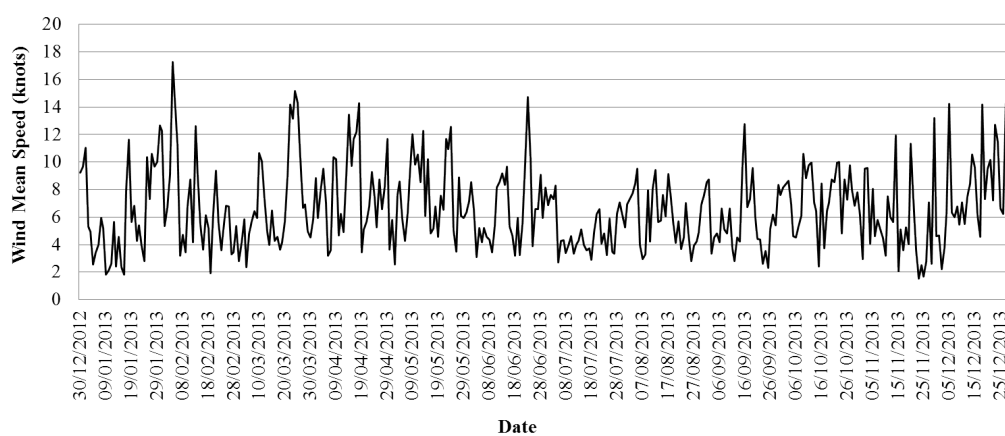


Figure A.9: The mean wind speed in knots

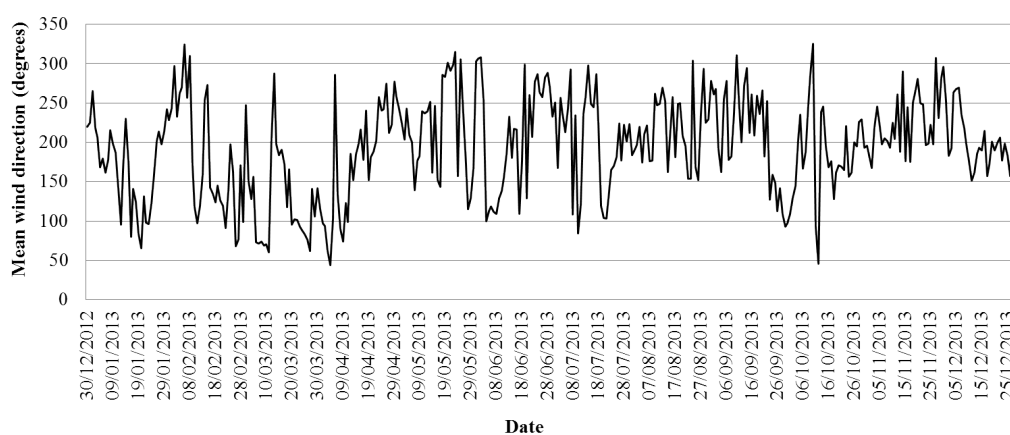


Figure A.10: The mean wind direction in degrees

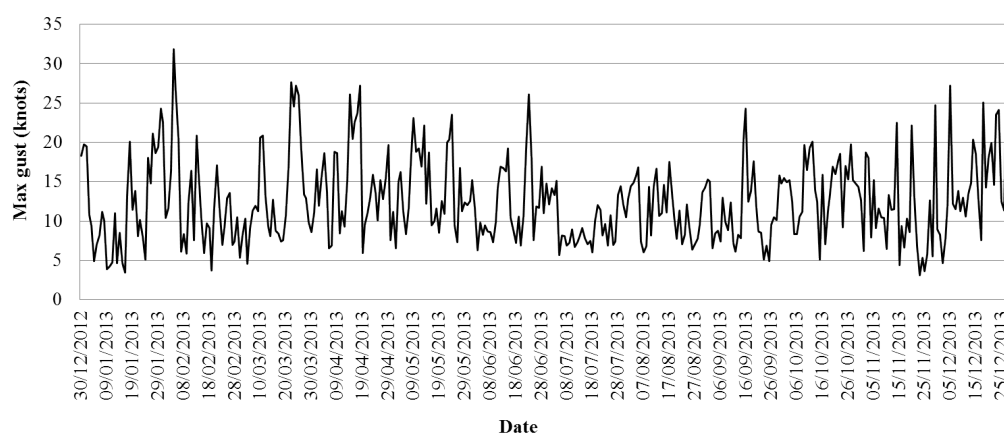


Figure A.11: The daily maximum gust in knots

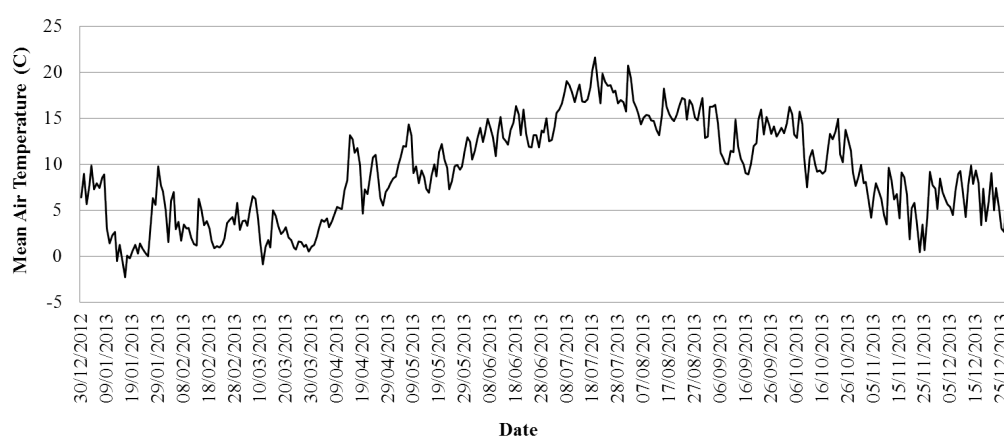


Figure A.12: The mean air temperature in degrees Celsius

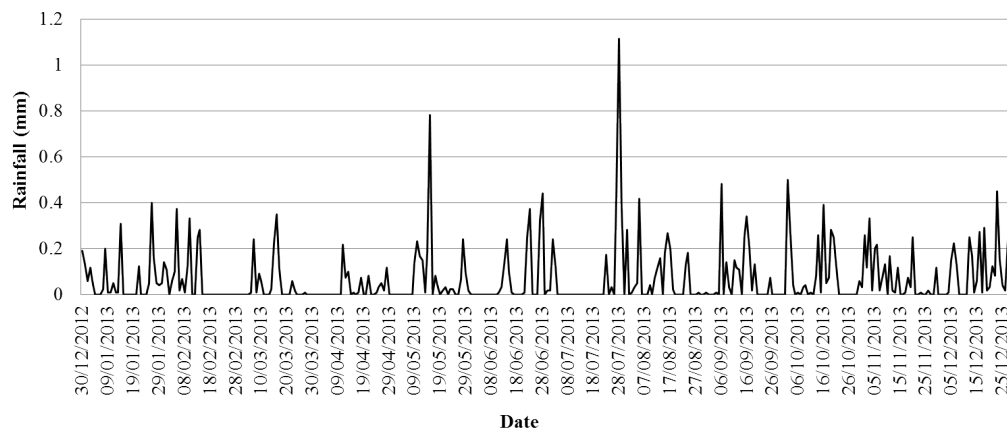


Figure A.13: The rainfall in mm

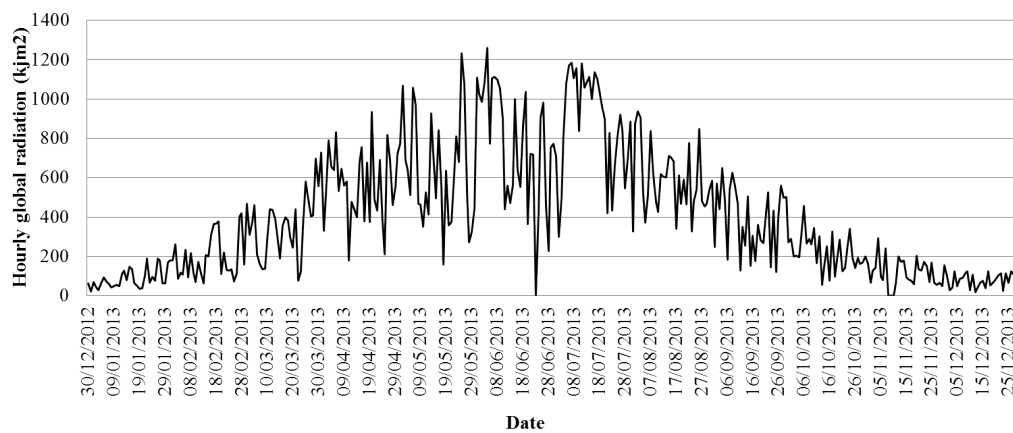


Figure A.14: The hourly global radiation in kJm2

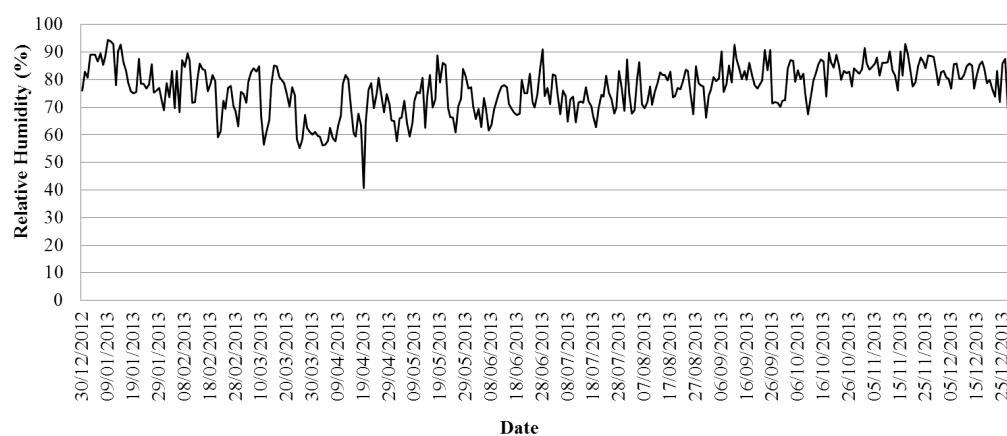


Figure A.15: The relative humidity in %

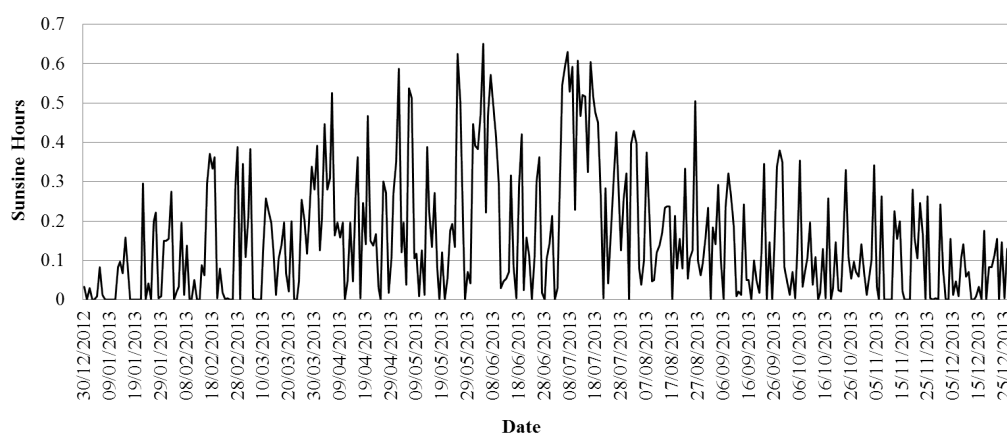


Figure A.16: The daily sunshine hours

Appendix B

Matlab code used in Chapter 2

This appendix presents the code that was developed in Matlab to calculate the triad probability.

B.1 Matlab Code

```

1 clear all;
2 close all;
3 clc;
4 %% USER INPUTS
5 load triad_data.mat %triad data in day-month-year format
6 %define duration of a period in days (less than 30)
7 step=1;
8 %define the probability threshold (percent of maximum)
9 redate_limit_perc=70;
10 redtime_limit_perc=70;
11 dev=1;
12 %% Preprocessing
13 all_dates=triads(:,[1 2 4 5 7 8]);%remove the years
14 for j=1:size(all_dates,1)%fix the months
15     for i=2:2:6
16         if all_dates(j,i)==1
17             all_dates(j,i)=3;
18         elseif all_dates(j,i)==2
19             all_dates(j,i)=4;
20         elseif all_dates(j,i)==11
21             all_dates(j,i)=1;
22         else
23             all_dates(j,i)=2;
24         end;
25     end;
26 end;
27 all_dates2=all_dates;
28 for i=1:(size(all_dates,1))%fix the days into periods
29     for j=1:2:5
30         flag=0;
31         for p=1:floor(((30/step)-1))
32             if all_dates(i,j)<=p*step
33                 all_dates2(i,j)=p;
34                 flag=1;

```



```

35         break;
36     end;
37 end;
38 if flag==0
39     all_dates2(i,j)=p+1;
40 end;
41 end;
42 end;
43 period_hits=[];
44 for i=1:(size(all_dates,1)) %fix the periods into consecutive periods
45     for j=1:2:5
46         period_hits=[period_hits
47             ((floor(((30/step)))*(all_dates2(i,j+1)-1))+all_dates2(i,j))];
48     end;
49 end;
50 %% Calculations
51 redate=[];
52 pdate=[];
53 w=0;
54 for i=1:size(period_hits,1)-6%calculate the normal distributions
55     p1=pdf('Normal',1:(4*floor(30/step)),period_hits(i,1),dev);
56     pdate=[pdate i*p1'];
57     w=w+i;
58 end;
59 probability_date=sum(pdate,2)/w;%average probability
60 redate_limit=redate_limit_perc*max(probability_date)/100;
61 figure(1);
62 bar(100*probability_date);
63 hold on
64 set(gca,'FontSize',32);
65 set(gca,'XTick',0:1:25);
66 plot([1 (4*floor(30/step))],100*[redate_limit redate_limit],'r--');
67 for i=1:(4*floor(30/step))
68     if probability_date(i,1)>redate_limit%pick the values over the threshold
69         hold on
70         plot(i, 100*probability_date(i,1), 'ro');
71         redate=[redate
72             i];
73         text(i,probability_date(i,1),strcat('(' ,num2str(i) ,')'), 'VerticalAlignment','bottom','HorizontalAlignment','center');
74     end;
75 end;
76 xlabel('Interval Number');
77 ylabel('Probability (%)');
78 set(gcf, 'Position', get(0,'Screensize'));
79 saveas(gcf,'interval1.emf');
80 hold off
81 reddy=step*(mod(redate-1,floor(30/step)));%convert back to normal dates
82 redmonth1=ceil(reddy/floor(30/step));%convert back to normal months
83 for i=1:size(redmonth1,1)
84     if redmonth1(i,1)==1
85         redmonth{i,1}='November';
86     elseif redmonth1(i,1)==2
87         redmonth{i,1}='December';
88     elseif redmonth1(i,1)==3
89         redmonth{i,1}='January';
90     else
91         redmonth{i,1}='February';
92     end;
93 end;

```



```

94 redtime=[];
95 ptime=[];
96 w=0;
97 for i=1:size(times,1)-6%calculate the normal distributions
98     p1=pdf('Normal',1:48,times(i,1),dev);
99     ptime=[ptime i*p1'];
100     w=w+i;
101 end;
102 probability_time=sum(ptime,2)/w;%average probability
103 redtime_limit=redtime_limit_perc*max(probability_time)/100;
104 figure(2);
105 bar(100*probability_time);
106 hold on
107 set(gca,'FontSize',32);
108 set(gca,'XTick',0:2:48);
109 plot([1 48],100*[redtime_limit redtime_limit],'r--');
110 for i=1:48
111     if probability_time(i,1)>redtime_limit %pick the values over the threshold
112         hold on
113         plot(i, 100*probability_time(i,1), 'ro');
114         redtime=[redtime
115             i];
116         text(i,probability_time(i,1),strcat('(' ,num2str(i),')'),'VerticalAlignment','bottom','HorizontalAlignment','
            center');
117     end;
118 end;
119 xlabel('Half Hour of Day');
120 ylabel('Probability (%)');
121 set(gcf, 'Position', get(0,'Screensize'));
122 saveas(gcf,'halfhour3.emf');
123 hold off
124 clear i p1 flag j p
125 %% Display Results
126 fprintf('Most probable periods are:\n\n');
127 for i=1:size(redmonth,1)
128     if reddy(i,1)==0
129         fprintf('Days 1 - %d of %s\n',step,redmonth{i,1});
130     elseif mod(reddate(i,1)-1,floor(30/step))==floor(30/step)-1
131         fprintf('Days %d - end of %s\n',redday(i,1),redmonth{i,1});
132     else
133         fprintf('Days %d - %d of %s\n',redday(i,1)+1,redday(i,1)+step,redmonth{i,1});
134     end;
135 end;
136 fprintf('\nMost probable half-hours are:\n\n');
137 for i=1:size(redtime,1)
138     if mod(redtime(i,1),2)==0
139         fprintf('Half-Hour %d:30 - %d:00\n',redtime(i,1)/2-1,redtime(i,1)/2);
140     else
141         fprintf('Half-Hour %d:00 - %d:30\n',floor(redtime(i,1)/2),floor(redtime(i,1)/2));
142     end;
143 end;
144 clear all_dates all_dates2 i reddate_limit redtime_limit redmonth reddy redtime step w;

```


Management of EV charging at residential buildings

The EV charging management strategies of the Charging Station Manager proposed in Chapter 3 were studied in a residential scenario. This section presents the residential scenario and its simulation results.

C.1 Description of the simulation scenario

The typical daily power demand of a house in UK was obtained from the UK Energy Research Centre and is presented in Figure C.1.

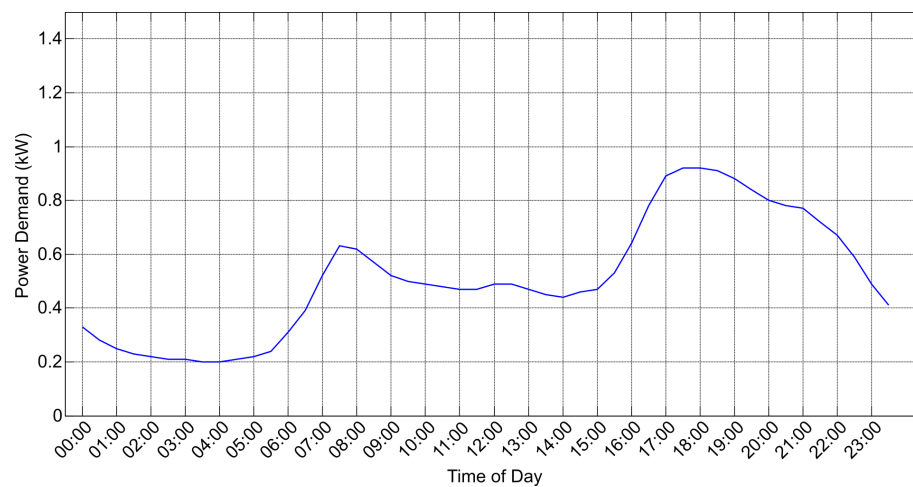


Figure C.1: The typical power demand of a house

Following the structure of the UK Generic Low Voltage Distribution Network, a LV

substation fulfils the electricity requirements of 384 domestic consumers. Figure C.2 presents the network structure and the location of the Charging Station Manager. The technical characteristics of the network are summarised in Table C.1.

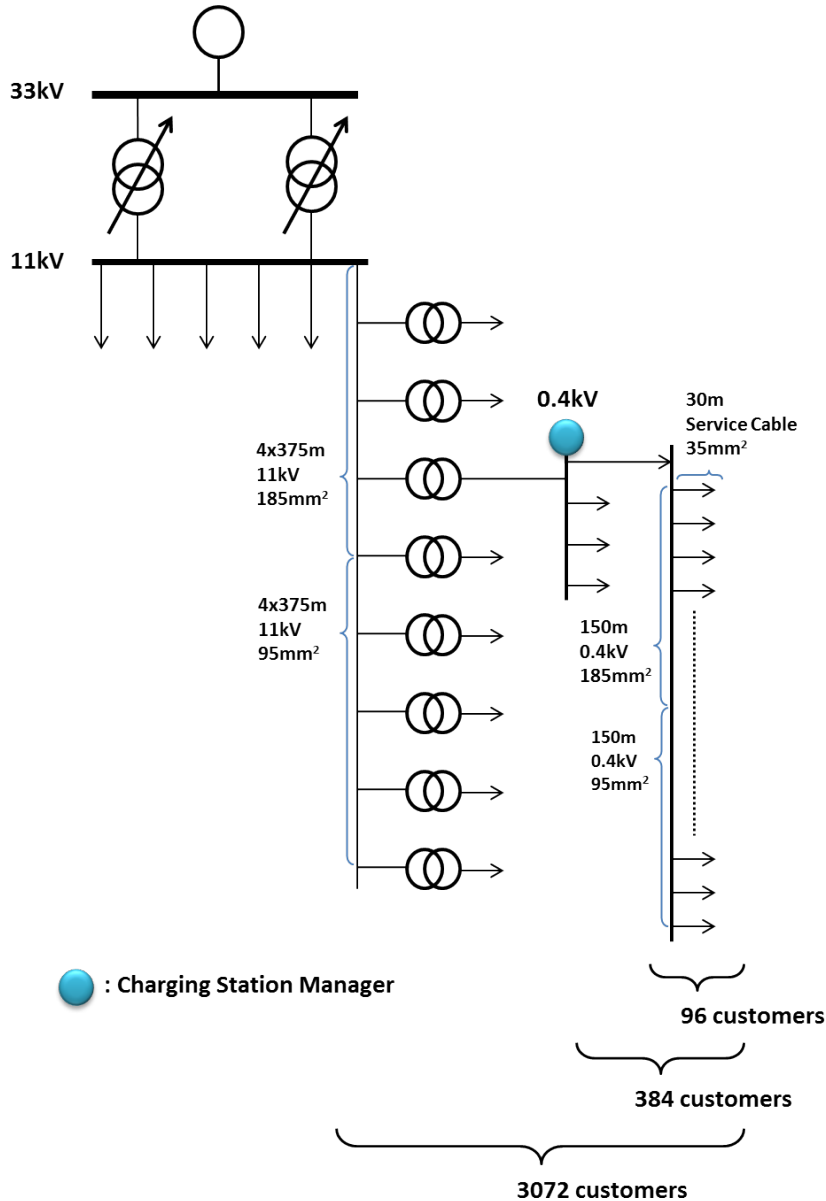


Figure C.2: The UK Generic Low Voltage Distribution Network

Assuming a 20% EV uptake, a total number of 76 EVs was considered. The EVs were randomly distributed among the 384 customers. It was assumed that the EVs are primarily used to commute between the driver's home and work. After analysing the

Table C.1: The technical characteristics of the network

Object Description	Technical Characteristics
33/11kV Transformer	15MVA X/R ratio = 15 18% impedance on 15MVA base
11kV Bus	6 Outgoing 11kV “domestic” feeders 3km each
11kV 185mm ² “domestic” feeder segment	3-core PICAS, Cu 0.164 + j0.08 Ω/km
11kV 95mm ² “domestic” feeder segment	3-core PICAS, Cu 0.32 + j0.087 Ω/km
11/0.4kV Transformer	500kVA X/R ratio = 15 5% impedance
0.4kV “domestic” Bus	4 Outgoing 0.4kV “domestic” feeders 300m each
0.4kV 185mm ² “domestic” feeder segment	XLPE, Al 0.164 + j0.074 Ω/km
0.4kV 95mm ² “domestic” feeder segment	XLPE, Al 0.32 + j0.075 Ω/km
0.4kV 35mm ² “domestic” service cable	XLPE, Al 0.851 + j0.041 Ω/km

data from NTS, the arrival and departure time distributions as well as the travelled distance distribution were calculated (Figures C.3 - C.5). The distribution of Figure C.5 was used to calculate the energy requirements of EVs when arriving at home using Equation (3.4) of Chapter 3.

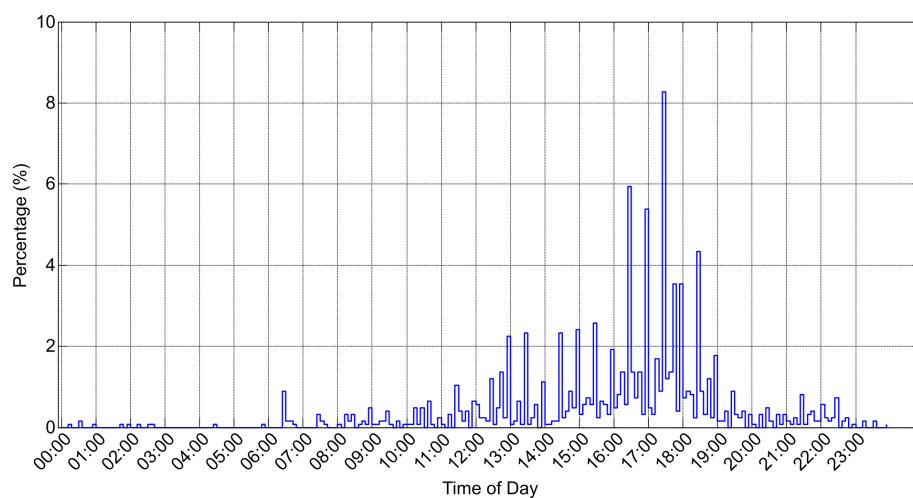


Figure C.3: Probability distribution of arrival times at home

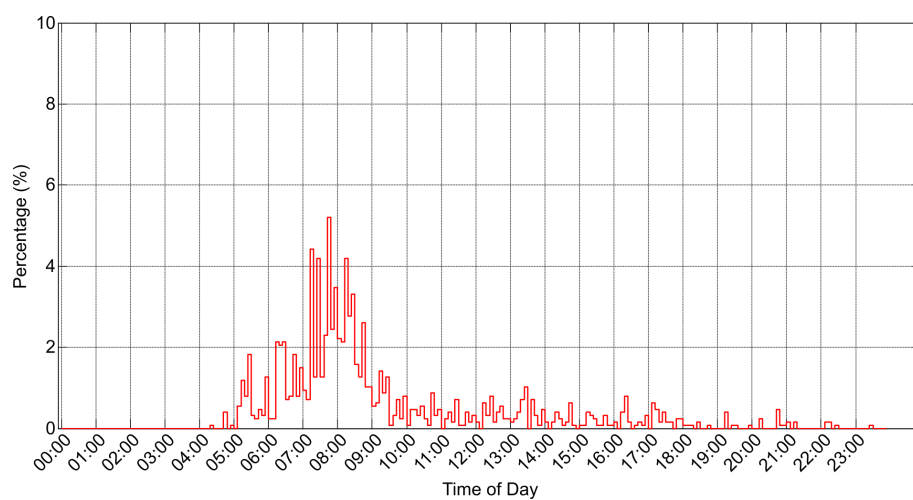


Figure C.4: Probability distribution of departure times from home

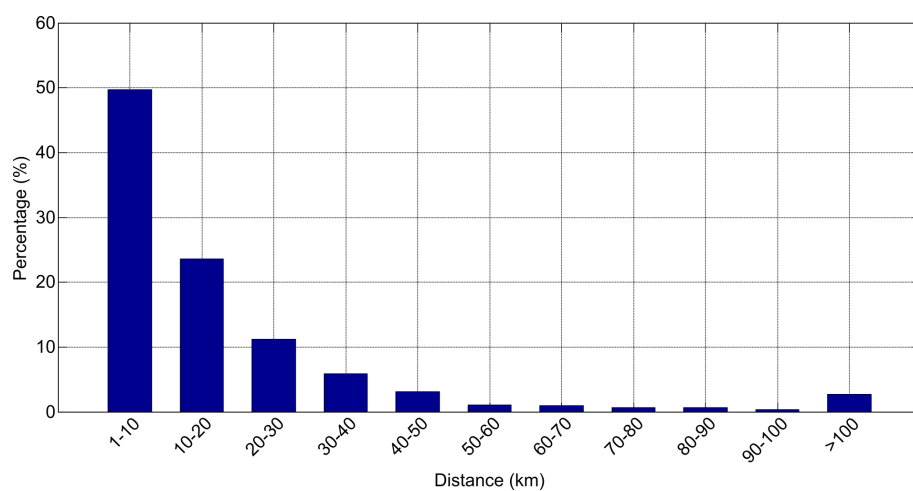


Figure C.5: Probability distribution of travelled distance before home

C.2 Simulation results

C.2.1 Impact on the demand profile

Considering 76 EVs in a group of 384 residential customers, the impact of their charging at a 3kW charger in an uncontrolled fashion is presented in Figure C.6.

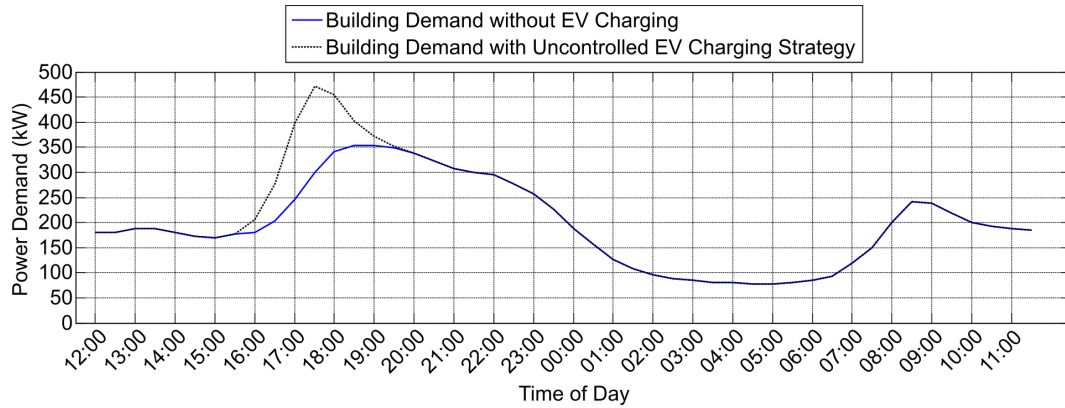


Figure C.6: Impact of Uncontrolled EV charging

As seen from Figure C.6, the EV charging leads to an increase of the peak demand during the arrival hours of the EVs at home (around 18:00). As explained in the previous section, a Charging Station Manager was assumed to be installed at the 0.4kV bus to manage the EV charging. The impact of EV charging when the Charging Station Manager operates under the Off-Peak strategy is presented in Figure C.7. The Off-Peak strategy of the Charging Station Manager places the EV charging events at the off-peak hours of the demand curve, and reduces the impact of EV charging on the network. When the EVs offer discharging services, the Charging Station Manager operates under the V2B operation, discharging the EVs at the peak hours. Considering a 5% discharging allowance, the Charging Station Manager reduces the peak demand by 12.8%. When the V2B allowance is increased to 15%, the EVs discharge for longer periods resulting in further demand reduction (up to 24.8%). The increased depth of discharge results in greater charging requirements during the night.

Figure C.8 presents the impact of EV charging when the Charging Station Manager operates under the Cost Reduction strategy. In this strategy the cheapest hours are

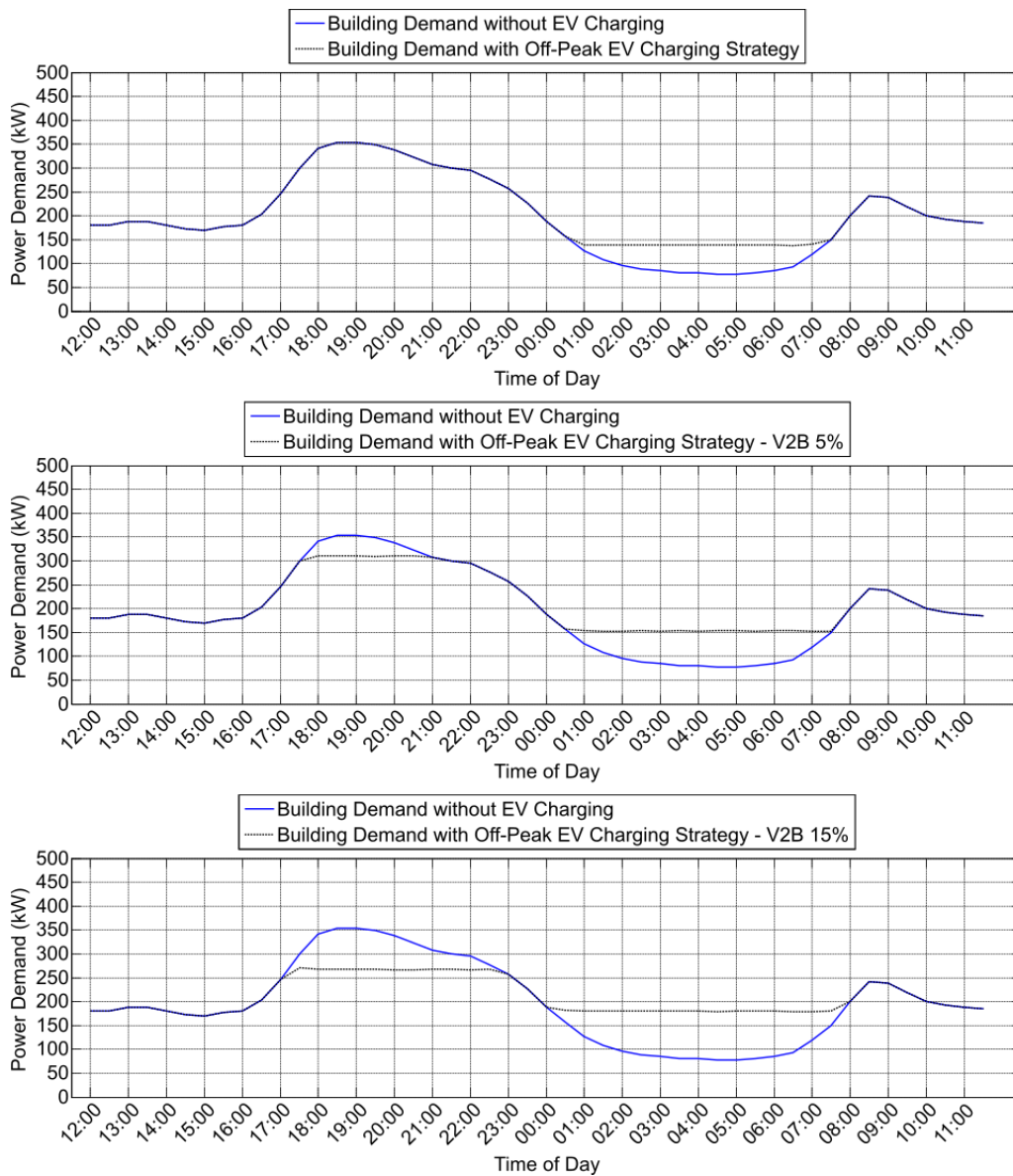


Figure C.7: Impact of EV charging with the Off-Peak Strategy

preferred for the charging events and the most expensive hours are preferred for discharging the EVs. In this case the EV charging events are concentrated between 01:00 and 03:00 resulting in the creation of a third peak in the demand profile. When bi-directional power exchanges are available, the Charging Station Manager coordinated the EVs to discharge during the (expensive) morning hours. Particularly for a 15% V2B level, the discharging of the EVs supplies almost in total the energy requirements of the buildings, resulting in a zero net demand requirements from the grid.

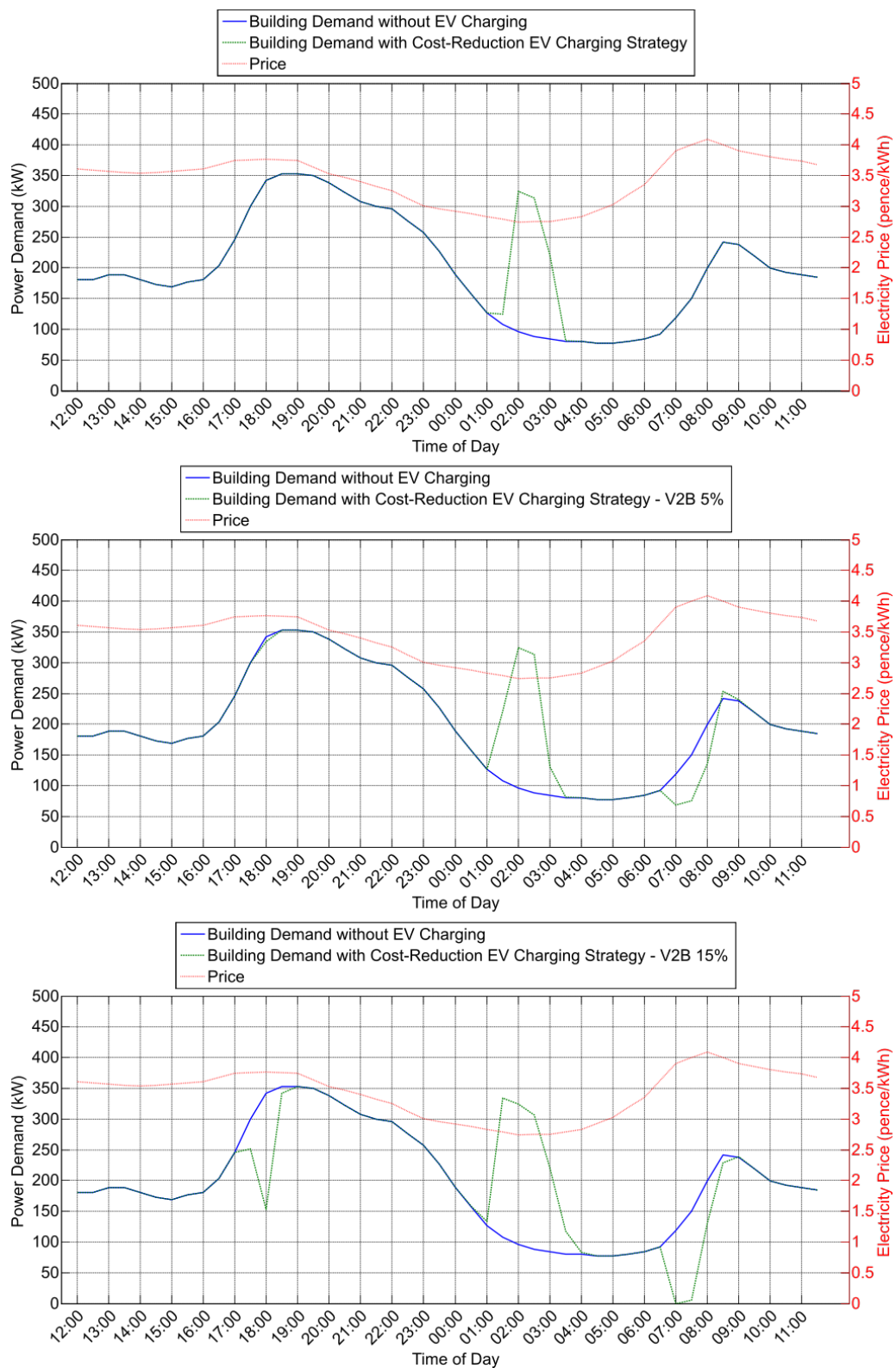


Figure C.8: Impact of EV charging with the Cost-Reduction Strategy

C.2.2 Impact on the daily electricity cost

The different charging control strategies were also compared according to the daily electricity cost that is needed to supply the aggregated demand (as presented in Figures C.7 - C.8). Figure C.9 presents the resulting daily cost difference between each charging strategy and the base case (without EVs at all).

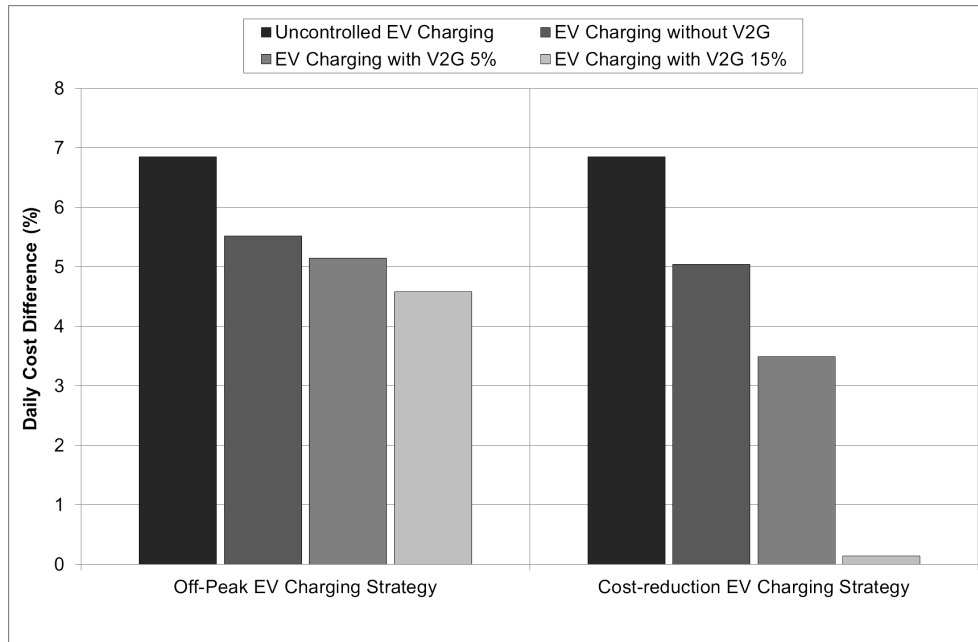


Figure C.9: Increase of the daily electricity cost comparing to the case without EV charging.

As expected, the Uncontrolled charging scenario results in the greatest cost increase as the charging events coincide with the expensive peak hours of the demand curve. Looking at the rest of the scenarios, the overall daily cost is increased as the EV charging increases the building's demand. Offering V2B services, the Charging Station Manager is able to reduce the electricity cost increase for the building manager especially in the Cost Reduction strategy. Especially for a 15% V2B allowance, the Cost Reduction strategy results in almost the same electricity cost as the case without EV charging (the EVs in this case charge almost for free).

C.2.3 Additional unintended consequences

As presented in the previous section, the operating strategy of the Charging Station Manager affects the building's demand profile and consequently the electricity cost of the building manager. However, reducing the electricity cost of the building manager has additional unintended consequences to the network.

Considering the network structure of Figure C.2, the bus voltages along the MV feeder are affected by the building's demand profile as formed by the charging strategy of the Charging Station Manager. The minimum voltage is found on the times when the demand is at its peak value. Charging the EVs in an uncontrolled fashion creates a peak in the demand profile of the building as presented in Figure C.6. This peak causes a voltage drop along the residential MV feeder. Figures C.10 - C.11 present the minimum bus voltage that was observed in a day for both charging strategies.

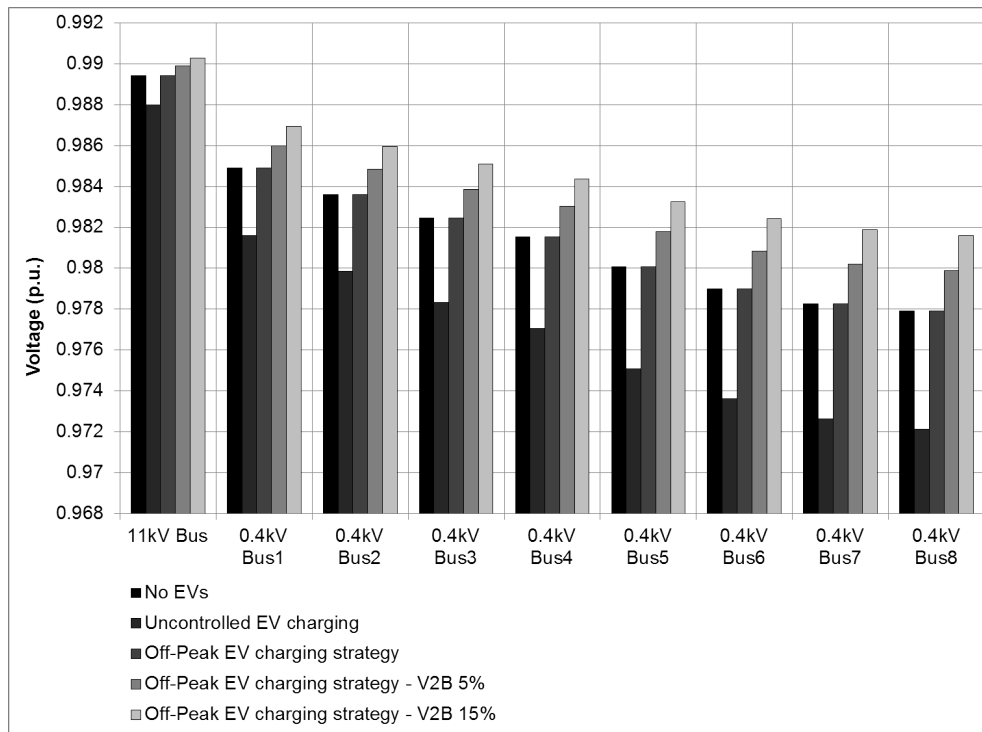


Figure C.10: Minimum bus voltage with Off-Peak strategy

When the Charging Station Manager operates under the Off-Peak strategy (without V2B) the EV charging demand is not creating a new peak at the demand profile of the

building and thus the minimum bus voltage is the same with the case without any EV charging. When the EVs offer discharging capacity, the Charging Station Manager reduces the peak demand of the building and the minimum voltage of the 0.4kV buses along the MV feeder are increased. The voltage increase is not significant, however considering a case with high levels of EV penetration, the reduction of the impact of EV charging on the bus voltage could be very valuable to the network (especially to areas with long MV lines).

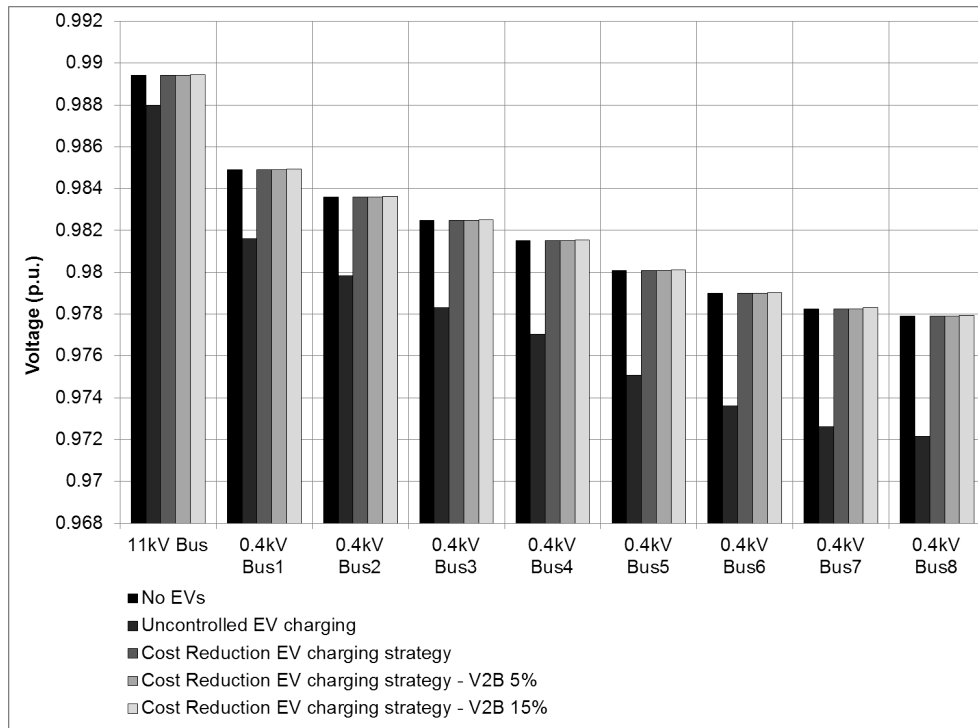


Figure C.11: Minimum bus voltage with Cost-Reduction strategy

When the Charging Station Manager operates under the Cost Reduction strategy, the EVs charge during the cheap hours and create a (third) peak at the demand profile of the building. The number of EVs considered in the scenario results in a peak that is less than the peak demand without EV charging in all cases of the Cost Reduction charging strategy. Consequently the voltage drop is the same for all cases of this strategy, regardless of the availability or level of the discharging capacity.

Appendix D

Matlab code used in Chapter 4

This appendix presents the code that was developed in Matlab for the LEMS operation. The LEMS uses a main program to operate on a timestep-basis. The main program calls secondary functions developed for different procedures in the LEMS operation.

D.1 Matlab Code

Main Program of LEMS

```

1  clear all;
2  clc;
3  global total chargers sched_load ev_set maslow_set maslow maslow_set_sched building_dmd1 building_dmd2 timestep t
   ev_set_sched type dr_up dr_down triad_prob sched_price
4  timestep=0.25;
5  wait=0.1; %in seconds
6  t=0;
7  total=[];
8  ev_set=[];
9  soc_all=[];
10 maslow_set=[];
11 while t<96
12     t=t+1;
13     read_input;
14     building_dmd2=building_dmd1;
15     if t==1
16         ev_set_sched=zeros(1,size(chargers,1));
17         maslow_set_sched=zeros(24/timestep,size(maslow,1));
18     end;
19     if type(t,1)==10;
20         cost_reduction_schedule;
21     elseif type(t,1)==0
22         peak_shaving_schedule;
23     else
24         demand_response_schedule;
25     end;
26     ev_set=[ev_set
27            ev_set_sched(1,:)];
28     if size(ev_set_sched,1)<=2

```



```

29     ev_set_sched=[ev_set_sched(2:end,:);
30         zeros(1,size(chargers,1))];
31     else
32         ev_set_sched=ev_set_sched(2:end,:);
33     end;
34     maslow_set=[maslow_set
35         maslow_set_sched(1,:)];
36     % if size(maslow_set_sched,1)<=2
37     %     maslow_set_sched=[maslow_set_sched(2:end,:);
38     %         zeros(1,size(maslow,1))];
39     % else
40     %     maslow_set_sched=maslow_set_sched(2:end,:);
41     % end;
42     maslow_set_sched=[maslow_set_sched(2:end,:);
43         zeros(1,size(maslow,1))];
44     display(t);
45     pause(wait);
46     system_simulator;
47     total=[total
48         building_dmd1 building_dmd2];
49     help11=[chargers(:,6)
50         maslow(:,1)];
51     soc_all=[soc_all help11];
52     clear help11;
53 end;

```

Secondary Function: *read_input*

```

1 function read_input
2 global chargers type maslow building_dmd1 t sched_load timestep dr_up dr_down triad_prob sched_price
3 load EV_chargers.mat;
4 load building.mat;
5 load type.mat;
6 load prices.mat;
7 load triad_probability.mat;
8 load maslow_units.mat;
9 if t==1
10     sched_load=build;
11     building_dmd1=build(1,1);
12     sched_price=price;
13     triad_prob=prob;
14 elseif t<(24/timestep)
15     sched_load=[sched_load(2:24/timestep,1)
16         build(mod(t-1,24/timestep),1)];
17     sched_price=[sched_price(2:24/timestep,1)
18         price(mod(t-1,24/timestep),1)];
19     triad_prob=[triad_prob(2:24/timestep,1)
20         prob(mod(t-1,24/timestep),1)];
21     building_dmd1=build(mod(t,24/timestep),1);
22 elseif mod(t,24/timestep)==0
23     sched_load=[sched_load(2:24/timestep,1)
24         build(24/timestep,1)];
25     sched_price=[sched_price(2:24/timestep,1)
26         price(24/timestep,1)];
27     triad_prob=[triad_prob(2:24/timestep,1)
28         prob(24/timestep,1)];
29     building_dmd1=build(24/timestep,1);
30 else
31     sched_load=[sched_load(2:24/timestep,1)

```



```

32     build(mod(t,24/ timestep),1);
33     sched_price=[sched_price(2:24/ timestep,1)
34     price(mod(t,24/ timestep),1)];
35     triad_prob=[triad_prob(2:24/ timestep,1)
36     prob(mod(t,24/ timestep),1)];
37     building_dmd1=build(mod(t,24/ timestep),1);
38 end;
39 dr_up=0;
40 dr_down=0;
41 for j=1:size(chargers,1)
42     if chargers(j,2)<=t && chargers(j,3)>t
43         help=[chargers(j,9) (100-chargers(j,6))*chargers(j,7)/(timestep*100)];
44         dr_up=dr_up+min(help);
45         help=[chargers(j,9) (chargers(j,6)*chargers(j,7))/(timestep*100)];
46         dr_down=dr_down+min(help);
47     end;
48 end;
49 for j=1:size(maslow,1)
50     help=[maslow(j,3) (100-maslow(j,1))*maslow(j,2)/(timestep*100)];
51     dr_up=dr_up+min(help);
52     help=[maslow(j,3) maslow(j,1)*maslow(j,2)/(timestep*100)];
53     dr_down=dr_down+min(help);
54 end;
55 end

```

Secondary Function: *cost_reduction_schedule*

```

1 function cost_reduction_schedule
2 global chargers timestep t sched_load ev_set_scheduled type triad_prob sched_price maslow_set_scheduled maslow
3 if type(t-1,1)~=10
4     load building.mat;
5     sched_load=zeros(24/ timestep,1);
6     for i=1:(24/ timestep)
7         if mod(t+i-1,24/ timestep)==0
8             sched_load(i,1)=build(24/ timestep,1);
9         else
10            sched_load(i,1)=build(mod(t+i-1,24/ timestep),1);
11        end;
12        if triad_prob(i,1)==1
13            sched_price(i,1)=100*sched_price(i,1);
14        end;
15    end;
16    t2=(floor(t/(24/ timestep))+1)*24/ timestep;
17    maslow_set_scheduled=zeros(t2-t, size(maslow,1));
18    for m=1:size(maslow,1)
19        bc=maslow(m,2);
20        rate=maslow(m,3);
21        soc1=maslow(m,1);
22        soc_min=maslow(m,4);
23        soc_max=maslow(m,5);
24        soc=soc1;
25        rnkk=zeros(t2-t,1);
26        help=sched_price(1:(t2-t),1);
27        help1=sort(help,'descend');
28        for i=1:(t2-t)
29            for jj=1:(t2-t)
30                if help(i,1)==help1(jj,1)
31                    rnkk(i,1)=jj;
32                    help1(jj,1)=inf;

```



```

33         break;
34     end;
35 end;
36 end;
37 clear help help1 jj i
38 Eoutmax=(soc_max-soc_min)*bc/100;
39 Eout=0;
40 cnt=1;
41 while Eout<Eoutmax && cnt<=(t2-t)
42     for w=1:(t2-t)
43         if rnkk(w,1)==cnt
44             Ewanted=Eoutmax-Eout;
45             help=[rate*timestep Ewanted ((soc-soc_min)*bc/100)];
46             Egiven=min(help);
47             soc=soc-(100*Egiven/bc);
48             Eout=Eout+Egiven;
49             sched_load(w,1)=sched_load(w,1)-(Egiven/timestep);
50             maslow_set_sched(w,m)=Egiven/timestep;
51             cnt=cnt+1;
52             break;
53         end;
54     end;
55 end;
56 rnkk=zeros(t2-t,1);
57 help=sched_price(1:(t2-t),1);
58 help1=sort(help);
59 for i=1:(t2-t)
60     for jj=1:(t2-t)
61         if help(i,1)==help1(jj,1)
62             rnkk(i,1)=jj;
63             help1(jj,1)=inf;
64             break;
65         end;
66     end;
67 end;
68 clear help help1 jj i
69 cnt=1;
70 while soc<soc_max && cnt<=(t2-t)
71     limit=zeros(t2-t,1);
72     limit(:,1)=(soc_max-soc1)*bc/100;
73     for tt=1:(t2-t)
74         for ttt=tt:(t2-t)
75             limit(ttt,1)=limit(ttt,1)-maslow_set_sched(tt,m)*timestep;
76         end;
77     end;
78     for w=1:(t2-t)
79         if rnkk(w,1)==cnt
80             if maslow_set_sched(w,m)<0
81                 cnt=cnt+1;
82                 break;
83             else
84                 Ewanted=(soc_max-soc)*bc/100;
85                 limitt=limit(w:end,1);
86                 Battery_limit=min(limitt);
87                 help=[rate*timestep Ewanted Battery_limit];
88                 Egiven=min(help);
89                 soc=soc+(100*Egiven/bc);
90                 sched_load(w,1)=sched_load(w,1)+(Egiven/timestep);
91                 maslow_set_sched(w,m)=Egiven/timestep;
92                 cnt=cnt+1;

```



```

93         break;
94     end;
95 end;
96 end;
97 end;
98 end;
99 for j=1:size(chargers,1)
100     if chargers(j,2)<=t && chargers(j,3)>t
101         id=chargers(j,1);
102         t1=chargers(j,2);
103         t2=chargers(j,3);
104         soc1=chargers(j,4);
105         soc2=chargers(j,5);
106         soc=chargers(j,6);
107         bc=chargers(j,7);
108         v2g=chargers(j,8);
109         rate=chargers(j,9);
110         E_in=bc*((soc2-soc+v2g)/100);
111         E_out=bc*(v2g/100);
112         ev_set_sched(1:(t2-t)+1,id)=0;
113         if v2g>0.00000001
114             rnk=zeros(t2-t,1);
115             help=sched_price(1:(t2-t),1);
116             help1=sort(help,'descend');
117             for i=1:(t2-t)
118                 for jj=1:(t2-t)
119                     if help(i,1)==help1(jj,1)
120                         rnk(i,1)=jj;
121                         help1(jj,1)=inf;
122                         break;
123                     end;
124                 end;
125             end;
126             clear help help1 jj i
127             cnt=1;
128             Ev2g=0;
129             while Ev2g<E_out && cnt<=(t2-t)
130                 for w=1:(t2-t)
131                     if rnk(w,1)==cnt
132                         Ewanted=E_out-Ev2g;
133                         help=[rate*timestep Ewanted (soc*bc/100)];
134                         Egiven=min(help);
135                         soc=soc-(100*Egiven/bc);
136                         Ev2g=Ev2g+Egiven;
137                         sched_load(w,1)=sched_load(w,1)-(Egiven/timestep);
138                         ev_set_sched(w,id)=-Egiven/timestep;
139                         cnt=cnt+1;
140                         break;
141                     end;
142                 end;
143             end;
144             rnk=zeros(t2-t,1);
145             help=sched_price(1:(t2-t),1);
146             help1=sort(help);
147             for i=1:(t2-t)
148                 for jj=1:(t2-t)
149                     if help(i,1)==help1(jj,1)
150                         rnk(i,1)=jj;
151                         help1(jj,1)=inf;
152                         break;

```



```

153         end;
154     end;
155 end;
156 clear help help1 jj i
157 cnt=1;
158 while soc<soc2 && cnt<=(t2-t)
159     limit=zeros(t2-t,1);
160     limit(:,1)=bc-soc1*bc/100;
161     for tt=1:(t2-t)
162         for ttt=tt:(t2-t)
163             limit(ttt,1)=limit(ttt,1)-ev_set_sched(tt,id)*timestep;
164         end;
165     end;
166     for w=1:(t2-t)
167         if rnk(w,1)==cnt
168             if ev_set_sched(w+1,id)<0
169                 cnt=cnt+1;
170                 break;
171             else
172                 Ewanted=(soc2-soc)*bc/100;
173                 limitt=limit(w:end,1);
174                 Battery_limit=min(limitt);
175                 help=[rate*timestep Ewanted Battery_limit];
176                 Egiven=min(help);
177                 soc=soc+(100*Egiven/bc);
178                 sched_load(w,1)=sched_load(w,1)+(Egiven/timestep);
179                 ev_set_sched(w,id)=Egiven/timestep;
180                 cnt=cnt+1;
181                 break;
182             end;
183         end;
184     end;
185 end;
186 else
187     rnk=zeros(t2-t,1);
188     help=sched_price(1:(t2-t),1);
189     help1=sort(help);
190     for i=1:(t2-t)
191         for jj=1:(t2-t)
192             if help(i,1)==help1(jj,1)
193                 rnk(i,1)=jj;
194                 help1(jj,1)=inf;
195                 break;
196             end;
197         end;
198     end;
199     clear help help1 jj i
200     cnt=1;
201     while soc<soc2 && cnt<=(t2-t)
202         for w=1:(t2-t)
203             if rnk(w,1)==cnt
204                 Ewanted=(soc2-soc)*bc/100;
205                 help=[rate*timestep Ewanted];
206                 Egiven=min(help);
207                 soc=soc+(100*Egiven/bc);
208                 sched_load(w,1)=sched_load(w,1)+(Egiven/timestep);
209                 ev_set_sched(w,id)=Egiven/timestep;
210                 cnt=cnt+1;
211                 break;
212             end;

```



```

213         end;
214     end;
215 end;
216 end;
217 end;
218 else
219     t2old=(floor((t-1)/(24/timestep))+1)*24/timestep;
220     for b=1:size(maslow,1)
221         for tt=1:(t2old-t)
222             sched_load(tt,1)=sched_load(tt,1)-maslow_set_sched(tt,b);
223         end;
224     end;
225     t2=(floor(t/(24/timestep))+1)*24/timestep;
226     maslow_set_sched=zeros(t2-t,size(maslow,1));
227     for m=1:size(maslow,1)
228         bc=maslow(m,2);
229         rate=maslow(m,3);
230         soc1=maslow(m,1);
231         soc_min=maslow(m,4);
232         soc_max=maslow(m,5);
233         soc=soc1;
234         rnkk=zeros(t2-t,1);
235         help=sched_price(1:(t2-t),1);
236         help1=sort(help,'descend');
237         for i=1:(t2-t)
238             for jj=1:(t2-t)
239                 if help(i,1)==help1(jj,1)
240                     rnkk(i,1)=jj;
241                     help1(jj,1)=inf;
242                     break;
243                 end;
244             end;
245         end;
246         clear help help1 jj i
247         Eoutmax=(soc_max-soc_min)*bc/100;
248         Eout=0;
249         cnt=1;
250         while Eout<Eoutmax && cnt<=(t2-t)
251             for w=1:(t2-t)
252                 if rnkk(w,1)==cnt
253                     if sched_price(w,1)<mean(sched_price) || maslow_set_sched(w,m)>0
254                         cnt=cnt+1;
255                         break;
256                     else
257                         Ewanted=Eoutmax-Eout;
258                         help=[rate*timestep Ewanted ((soc-soc_min)*bc/100)];
259                         Egiven=min(help);
260                         soc=soc-(100*Egiven/bc);
261                         Eout=Eout+Egiven;
262                         sched_load(w,1)=sched_load(w,1)-(Egiven/timestep);
263                         maslow_set_sched(w,m)=-Egiven/timestep;
264                         cnt=cnt+1;
265                         break;
266                     end;
267                 end;
268             end;
269         end;
270         rnkk=zeros(t2-t,1);
271         help=sched_price(1:(t2-t),1);
272         %help=sched_load(1:(t2-t),1);

```



```

273     help1=sort(help);
274     for i=1:(t2-t)
275         for jj=1:(t2-t)
276             if help(i,1)==help1(jj,1)
277                 rnkk(i,1)=jj;
278                 help1(jj,1)=inf;
279                 break;
280             end;
281         end;
282     end;
283     clear help help1 jj i
284     cnt=1;
285     while soc<soc_max && cnt<=(t2-t)
286         limit=zeros(t2-t,1);
287         limit(:,1)=(soc_max-soc1)*bc/100;
288         for tt=1:(t2-t)
289             for ttt=tt:(t2-t)
290                 limit(ttt,1)=limit(ttt,1)-maslow_set_sched(tt,m)*timestep;
291             end;
292         end;
293         for w=1:(t2-t)
294             if rnkk(w,1)==cnt
295                 if maslow_set_sched(w,m)<0
296                     cnt=cnt+1;
297                     break;
298                 else
299                     Ewanted=(soc_max-soc)*bc/100;
300                     limitt=limit(w:end,1);
301                     Battery_limit=min(limitt);
302                     help=[rate*timestep Ewanted Battery_limit];
303                     Egiven=min(help);
304                     soc=soc+(100*Egiven/bc);
305                     sched_load(w,1)=sched_load(w,1)+(Egiven/timestep);
306                     maslow_set_sched(w,m)=Egiven/timestep;
307                     cnt=cnt+1;
308                     break;
309                 end;
310             end;
311         end;
312     end;
313 end;
314 for j=1:size(chargers,1)
315     if chargers(j,2)==t
316         id=chargers(j,1);
317         t1=chargers(j,2);
318         t2=chargers(j,3);
319         soc1=chargers(j,4);
320         soc2=chargers(j,5);
321         soc=chargers(j,6);
322         bc=chargers(j,7);
323         v2g=chargers(j,8);
324         rate=chargers(j,9);
325         E_in=bc*((soc2-soc1+v2g)/100);
326         E_out=bc*(v2g/100);
327         if v2g>0.00000001
328             ev_set_sched(1:(t2-t),id)=0;
329             rnkk=zeros(t2-t,1);
330             help=sched_price(1:(t2-t),1);
331             help1=sort(help,'descend');
332             for i=1:(t2-t)

```



```

333         for jj=1:(t2-t)
334             if help(i,1)==help1(jj,1)
335                 rnk(i,1)=jj;
336                 help1(jj,1)=inf;
337                 break;
338             end;
339         end;
340     end;
341     clear help help1 jj i
342     cnt=1;
343     Ev2g=0;
344     while Ev2g<E_out && cnt<=(t2-t)
345         for w=1:(t2-t)
346             if rnk(w,1)==cnt
347                 Ewanted=E_out-Ev2g;
348                 help=[rate*timestep Ewanted (soc*bc/100)];
349                 Egiven=min(help);
350                 soc=soc-(100*Egiven/bc);
351                 Ev2g=Ev2g+Egiven;
352                 sched_load(w,1)=sched_load(w,1)-(Egiven/timestep);
353                 ev_set_sched(w,id)=-Egiven/timestep;
354                 cnt=cnt+1;
355                 break;
356             end;
357         end;
358     end;
359     rnk=zeros(t2-t,1);
360     help=sched_price(1:(t2-t),1);
361     help1=sort(help);
362     for i=1:(t2-t)
363         for jj=1:(t2-t)
364             if help(i,1)==help1(jj,1)
365                 rnk(i,1)=jj;
366                 help1(jj,1)=inf;
367                 break;
368             end;
369         end;
370     end;
371     clear help help1 jj i
372     cnt=1;
373     while soc<soc2 && cnt<=(t2-t)
374         limit=zeros(t2-t,1);
375         limit(:,1)=bc-soc1*bc/100;
376         for tt=1:(t2-t)
377             for ttt=tt:(t2-t)
378                 limit(ttt,1)=limit(ttt,1)-ev_set_sched(tt,id)*timestep;
379             end;
380         end;
381         for w=1:(t2-t)
382             if rnk(w,1)==cnt
383                 if ev_set_sched(w,id)<0
384                     cnt=cnt+1;
385                     break;
386                 else
387                     Ewanted=(soc2-soc)*bc/100;
388                     limitt=limit(w:end,1);
389                     Battery_limit=min(limitt);
390                     help=[rate*timestep Ewanted Battery_limit];
391                     Egiven=min(help);
392                     soc=soc+(100*Egiven/bc);

```



```

393         sched_load(w,1)=sched_load(w,1)+(Egiven/timestep);
394         ev_set_sched(w,id)=Egiven/timestep;
395         cnt=cnt+1;
396         break;
397     end;
398 end;
399 end;
400 end;
401 else
402     rnk=zeros(t2-t,1);
403     help=sched_price(1:(t2-t),1);
404     help1=sort(help);
405     for i=1:(t2-t)
406         for jj=1:(t2-t)
407             if help(i,1)==help1(jj,1)
408                 rnk(i,1)=jj;
409                 help1(jj,1)=inf;
410                 break;
411             end;
412         end;
413     end;
414     clear help help1 jj i
415     cnt=1;
416     while soc<soc2 && cnt<=(t2-t)
417         for w=1:(t2-t)
418             if rnk(w,1)==cnt
419                 Ewanted=(soc2-soc)*bc/100;
420                 help=[rate*timestep Ewanted];
421                 Egiven=min(help);
422                 soc=soc+(100*Egiven/bc);
423                 sched_load(w,1)=sched_load(w,1)+(Egiven/timestep);
424                 ev_set_sched(w,id)=Egiven/timestep;
425                 cnt=cnt+1;
426                 break;
427             end;
428         end;
429     end;
430 end;
431 end;
432 end;
433 end;
434 end

```

Secondary Function: *peak_shaving_schedule*

```

1 function peak_shaving_schedule
2 global chargers timestep t sched_load ev_set_sched maslow maslow_set_sched
3 t2old=(floor((t-1)/(24/timestep))+1)*24/timestep;
4 for b=1:size(maslow,1)
5     for tt=1:(t2old-t)
6         sched_load(tt,1)=sched_load(tt,1)-maslow_set_sched(tt,b);
7     end;
8 end;
9 t2=(floor(t/(24/timestep))+1)*24/timestep;
10 maslow_set_sched=zeros(t2-t,size(maslow,1));
11 for m=1:size(maslow,1)
12     bc=maslow(m,2);
13     rate=maslow(m,3);
14     soc1=maslow(m,1);

```



```

15 soc_min=maslow(m,4);
16 soc_max=maslow(m,5);
17 soc=soc1;
18 rnkk=zeros(t2-t,1);
19 help=sched_load(1:(t2-t),1);
20 help1=sort(help,'descend');
21 for i=1:(t2-t)
22     for jj=1:(t2-t)
23         if help(i,1)==help1(jj,1)
24             rnkk(i,1)=jj;
25             help1(jj,1)=inf;
26             break;
27         end;
28     end;
29 end;
30 clear help help1 jj i
31 Eoutmax=(soc_max-soc_min)*bc/100;
32 Eout=0;
33 cnt=1;
34 while Eout<Eoutmax && cnt<=(t2-t)
35     for w=1:(t2-t)
36         if rnkk(w,1)==cnt
37             if sched_load(w,1)<mean(sched_load) || maslow_set_sched(w,m)>0
38                 cnt=cnt+1;
39                 break;
40             else
41                 Ewanted=Eoutmax-Eout;
42                 help=[rate*timestep Ewanted ((soc-soc_min)*bc/100)];
43                 Egiven=min(help);
44                 soc=soc-(100*Egiven/bc);
45                 Eout=Eout+Egiven;
46                 sched_load(w,1)=sched_load(w,1)-(Egiven/timestep);
47                 maslow_set_sched(w,m)=Egiven/timestep;
48                 cnt=cnt+1;
49                 break;
50             end;
51         end;
52     end;
53 end;
54 rnkk=zeros(t2-t,1);
55 help=sched_load(1:(t2-t),1);
56 help1=sort(help);
57 for i=1:(t2-t)
58     for jj=1:(t2-t)
59         if help(i,1)==help1(jj,1)
60             rnkk(i,1)=jj;
61             help1(jj,1)=inf;
62             break;
63         end;
64     end;
65 end;
66 clear help help1 jj i
67 cnt=1;
68 while soc<soc_max && cnt<=(t2-t)
69     limit=zeros(t2-t,1);
70     limit(:,1)=(soc_max-soc1)*bc/100;
71     for tt=1:(t2-t)
72         for ttt=tt:(t2-t)
73             limit(ttt,1)=limit(ttt,1)-maslow_set_sched(tt,m)*timestep;
74         end;

```



```

75     end;
76     for w=1:(t2-t)
77         if rnkk(w,1)==cnt
78             if maslow_set_sched(w,m)<0
79                 cnt=cnt+1;
80                 break;
81             else
82                 Ewanted=(soc_max-soc)*bc/100;
83                 limitt=limit(w:end,1);
84                 Battery_limit=min(limitt);
85                 help=[rate*timestep Ewanted Battery_limit];
86                 Egiven=min(help);
87                 soc=soc+(100*Egiven/bc);
88                 sched_load(w,1)=sched_load(w,1)+(Egiven/timestep);
89                 maslow_set_sched(w,m)=Egiven/timestep;
90                 cnt=cnt+1;
91                 break;
92             end;
93         end;
94     end;
95 end;
96
97 for j=1:size(chargers,1)
98     if chargers(j,2)==t
99         id=chargers(j,1);
100        t1=chargers(j,2);
101        t2=chargers(j,3);
102        soc1=chargers(j,4);
103        soc2=chargers(j,5);
104        soc=chargers(j,6);
105        bc=chargers(j,7);
106        v2g=chargers(j,8);
107        rate=chargers(j,9);
108        E_in=bc*((soc2-soc1+v2g)/100);
109        E_out=bc*(v2g/100);
110        if v2g>0.00000001
111            ev_set_sched(1:(t2-t),id)=0;
112            rnk=zeros(t2-t,1);
113            help=sched_load(1:(t2-t),1);
114            help1=sort(help,'descend');
115            for i=1:(t2-t)
116                for jj=1:(t2-t)
117                    if help(i,1)==help1(jj,1)
118                        rnk(i,1)=jj;
119                        help1(jj,1)=inf;
120                        break;
121                    end;
122                end;
123            end;
124            clear help help1 jj i
125            cnt=1;
126            Ev2g=0;
127            while Ev2g<E_out && cnt<=(t2-t)
128                for w=1:(t2-t)
129                    if rnk(w,1)==cnt
130                        Ewanted=E_out-Ev2g;
131                        help=[rate*timestep Ewanted (soc*bc/100)];
132                        Egiven=min(help);
133                        soc=soc-(100*Egiven/bc);
134                        Ev2g=Ev2g+Egiven;

```



```

135         sched_load(w,1)=sched_load(w,1)-(Egiven/timestep);
136         ev_set_sched(w,id)=-Egiven/timestep;
137         cnt=cnt+1;
138         break;
139     end;
140 end;
141 end;
142 rnk=zeros(t2-t,1);
143 help=sched_load(1:(t2-t),1);
144 help1=sort(help);
145 for i=1:(t2-t)
146     for jj=1:(t2-t)
147         if help(i,1)==help1(jj,1)
148             rnk(i,1)=jj;
149             help1(jj,1)=inf;
150             break;
151         end;
152     end;
153 end;
154 clear help help1 jj i
155 cnt=1;
156 while soc<soc2 && cnt<=(t2-t)
157     limit=zeros(t2-t,1);
158     limit(:,1)=bc-soc1*bc/100;
159     for tt=1:(t2-t)
160         for ttt=tt:(t2-t)
161             limit(ttt,1)=limit(ttt,1)-ev_set_sched(tt,id)*timestep;
162         end;
163     end;
164     for w=1:(t2-t)
165         if rnk(w,1)==cnt
166             if ev_set_sched(w,id)<0
167                 cnt=cnt+1;
168                 break;
169             else
170                 Ewanted=(soc2-soc)*bc/100;
171                 limitt=limit(w:end,1);
172                 Battery_limit=min(limitt);
173                 help=[rate*timestep Ewanted Battery_limit];
174                 Egiven=min(help);
175                 soc=soc+(100*Egiven/bc);
176                 sched_load(w,1)=sched_load(w,1)+(Egiven/timestep);
177                 ev_set_sched(w,id)=Egiven/timestep;
178                 cnt=cnt+1;
179                 break;
180             end;
181         end;
182     end;
183 end;
184 else
185     rnk=zeros(t2-t,1);
186     help=sched_load(1:(t2-t),1);
187     help1=sort(help);
188     for i=1:(t2-t)
189         for jj=1:(t2-t)
190             if help(i,1)==help1(jj,1)
191                 rnk(i,1)=jj;
192                 help1(jj,1)=inf;
193                 break;
194             end;

```



```

195         end;
196     end;
197     clear help help1 jj i
198     cnt=1;
199     while soc<soc2 && cnt<=(t2-t)
200         for w=1:(t2-t)
201             if rnk(w,1)==cnt
202                 Ewanted=(soc2-soc)*bc/100;
203                 help=[rate*timestep Ewanted];
204                 Egiven=min(help);
205                 soc=soc+(100*Egiven/bc);
206                 sched_load(w,1)=sched_load(w,1)+(Egiven/timestep);
207                 ev_set_sched(w,id)=Egiven/timestep;
208                 cnt=cnt+1;
209                 break;
210             end;
211         end;
212     end;
213 end;
214 end;
215 end;
216 end

```

Secondary Function: *demand_response_schedule*

```

1 function demand_response_schedule
2 global chargers timestep t sched_load ev_set_sched dr_up dr_down type maslow maslow_set_sched
3 load building.mat;
4 sched_load=zeros(24/timestep,1);
5 for i=1:(24/timestep)
6     if mod(t+i-1,24/timestep)==0
7         sched_load(i,1)=build(24/timestep,1);
8     else
9         sched_load(i,1)=build(mod(t+i-1,24/timestep),1);
10    end;
11 end;
12 t2=(floor(t/(24/timestep))+1)*24/timestep;
13 maslow_set_sched=zeros(t2-t,size(maslow,1));
14 for m=1:size(maslow,1)
15     soc1=maslow(m,1);
16     bc=maslow(m,2);
17     rate=maslow(m,3);
18     soc_min=maslow(m,4);
19     soc_max=maslow(m,5);
20     if type(t,1)==1
21         help=[rate (100-soc1)*bc/(timestep*100)];
22         maslow_set_sched(1,m)=min(help);
23     else
24         help=[rate soc1*bc/(timestep*100)];
25         maslow_set_sched(1,m)=-min(help);
26     end;
27     soc=soc1+(100*maslow_set_sched(1,m)*timestep/bc);
28     sched_load(1,1)=sched_load(1,1)+maslow_set_sched(1,m);
29     rnk=zeros(t2-t-1,1);
30     help=sched_load(2:(t2-t),1);
31     help1=sort(help,'descend');
32     for i=1:(t2-t-1)
33         for jj=1:(t2-t-1)
34             if help(i,1)==help1(jj,1)

```



```

35         rnkk(i,1)=jj;
36         help1(jj,1)=inf;
37         break;
38     end;
39 end;
40 end;
41 clear help help1 jj i
42 if soc>soc_max
43     Eoutmax=(soc-soc_min)*bc/100;
44 elseif soc<soc_min
45     Eoutmax=(soc_max-soc)*bc/100;
46 else
47     Eoutmax=(soc_max-soc_min)*bc/100;
48 end;
49 Eout=0;
50 cnt=1;
51 while Eout<Eoutmax && cnt<=(t2-t-1)
52     for w=1:(t2-t-1)
53         if rnkk(w,1)==cnt
54             if sched_load(w+1,1)<mean(sched_load) || soc<soc_min
55                 cnt=cnt+1;
56                 break;
57             else
58                 Ewanted=Eoutmax-Eout;
59                 help=[rate*timestep Ewanted ((soc-soc_min)*bc/100)];
60                 Egiven=min(help);
61                 soc=soc-(100*Egiven/bc);
62                 Eout=Eout+Egiven;
63                 sched_load(w+1,1)=sched_load(w+1,1)-(Egiven/timestep);
64                 maslow_set_sched(w+1,m)=-Egiven/timestep;
65                 cnt=cnt+1;
66                 break;
67             end;
68         end;
69     end;
70 end;
71 rnkk=zeros(t2-t-1,1);
72 help=sched_load(2:(t2-t),1);
73 help1=sort(help);
74 for i=1:(t2-t-1)
75     for jj=1:(t2-t-1)
76         if help(i,1)==help1(jj,1)
77             rnkk(i,1)=jj;
78             help1(jj,1)=inf;
79             break;
80         end;
81     end;
82 end;
83 clear help help1 jj i
84 cnt=1;
85 while soc<soc_max && cnt<=(t2-t)
86     limit=zeros(t2-t,1);
87     limit(:,1)=(soc_max-soc1)*bc/100;
88     for tt=1:(t2-t)
89         for ttt=tt:(t2-t)
90             limit(ttt,1)=limit(ttt,1)-maslow_set_sched(tt,m)*timestep;
91         end;
92     end;
93     for w=1:(t2-t-1)
94         if rnkk(w,1)==cnt

```



```

95         if maslow_set_sched(w,m)<0
96             cnt=cnt+1;
97             break;
98         else
99             Ewanted=(soc_max-soc)*bc/100;
100             limitt=limit((w+1):end,1);
101             Battery_limit=min(limitt);
102             help=[rate*timestep Ewanted Battery_limit];
103             Egiven=min(help);
104             soc=soc+(100*Egiven/bc);
105             sched_load(w+1,1)=sched_load(w+1,1)+(Egiven/timestep);
106             maslow_set_sched(w+1,m)=Egiven/timestep;
107             cnt=cnt+1;
108             break;
109         end;
110     end;
111 end;
112 end;
113 end;
114 for j=1:size(chargers,1)
115     if chargers(j,2)<=t && chargers(j,3)>t
116         id=chargers(j,1);
117         t1=chargers(j,2);
118         t2=chargers(j,3);
119         soc1=chargers(j,4);
120         soc2=chargers(j,5);
121         soc=chargers(j,6);
122         bc=chargers(j,7);
123         v2g=chargers(j,8);
124         rate=chargers(j,9);
125         E_in=bc*((soc2-soc+v2g)/100);
126         E_out=bc*(v2g/100);
127         ev_set_sched(1:(t2-t),id)=0;
128         if type(t,1)==1
129             help=[rate (100-soc)*bc/(timestep*100)];
130             ev_set_sched(1,id)=min(help);
131         else
132             help=[rate soc*bc/(timestep*100)];
133             ev_set_sched(1,id)=-min(help);
134         end;
135         soc=soc+(100*ev_set_sched(1,id)*timestep/bc);
136         sched_load(1,1)=sched_load(1,1)+ev_set_sched(1,id);
137         if v2g>0.00000001
138             rnk=zeros(t2-t-1,1);
139             help=sched_load(2:(t2-t),1);
140             help1=sort(help,'descend');
141             for i=1:(t2-t-1)
142                 for jj=1:(t2-t-1)
143                     if help(i,1)==help1(jj,1)
144                         rnk(i,1)=jj;
145                         help1(jj,1)=inf;
146                         break;
147                     end;
148                 end;
149             end;
150             clear help help1 jj i
151             cnt=1;
152             Ev2g=0;
153             while Ev2g<E_out && cnt<=(t2-t-1)
154                 for w=1:(t2-t-1)

```



```

155         if rnk(w,1)==cnt
156             Ewanted=E_out-Ev2g;
157             help=[rate*timestep Ewanted (soc*bc/100)];
158             Egiven=min(help);
159             soc=soc-(100*Egiven/bc);
160             Ev2g=Ev2g+Egiven;
161             sched_load(w+1,1)=sched_load(w+1,1)-(Egiven/timestep);
162             ev_set_sched(w+1,id)=-Egiven/timestep;
163             cnt=cnt+1;
164             break;
165         end;
166     end;
167 end;
168 rnk=zeros(t2-t-1,1);
169 help=sched_load(2:(t2-t),1);
170 help1=sort(help);
171 for i=1:(t2-t-1)
172     for jj=1:(t2-t-1)
173         if help(i,1)==help1(jj,1)
174             rnk(i,1)=jj;
175             help1(jj,1)=inf;
176             break;
177         end;
178     end;
179 end;
180 clear help help1 jj i
181 cnt=1;
182 while soc<soc2 && cnt<=(t2-t-1)
183     limit=zeros(t2-t,1);
184     limit(:,1)=bc-soc1*bc/100;
185     for tt=1:(t2-t)
186         for ttt=tt:(t2-t)
187             limit(ttt,1)=limit(ttt,1)-ev_set_sched(tt,id)*timestep;
188         end;
189     end;
190     for w=1:(t2-t-1)
191         if rnk(w,1)==cnt
192             if ev_set_sched(w+1,id)<0
193                 cnt=cnt+1;
194                 break;
195             else
196                 Ewanted=(soc2-soc)*bc/100;
197                 limitt=limit((w+1):end,1);
198                 Battery_limit=min(limitt);
199                 help=[rate*timestep Ewanted Battery_limit];
200                 Egiven=min(help);
201                 soc=soc+(100*Egiven/bc);
202                 sched_load(w+1,1)=sched_load(w+1,1)+(Egiven/timestep);
203                 ev_set_sched(w+1,id)=Egiven/timestep;
204                 cnt=cnt+1;
205                 break;
206             end;
207         end;
208     end;
209 end;
210 else
211     rnk=zeros(t2-t-1,1);
212     help=sched_load(2:(t2-t),1);
213     help1=sort(help);
214     for i=1:(t2-t-1)

```



```

215         for jj=1:(t2-t-1)
216             if help(i,1)==help1(jj,1)
217                 rnk(i,1)=jj;
218                 help1(jj,1)=inf;
219                 break;
220             end;
221         end;
222     end;
223     clear help help1 jj i
224     cnt=1;
225     while soc<soc2 && cnt<=(t2-t-1)
226         for w=1:(t2-t-1)
227             if rnk(w,1)==cnt
228                 Ewanted=(soc2-soc)*bc/100;
229                 help=[rate*timestep Ewanted];
230                 Egiven=min(help);
231                 soc=soc+(100*Egiven/bc);
232                 sched_load(w+1,1)=sched_load(w+1,1)+(Egiven/timestep);
233                 ev_set_sched(w+1,id)=Egiven/timestep;
234                 cnt=cnt+1;
235                 break;
236             end;
237         end;
238     end;
239 end;
240 end;
241 end;
242 end

```

Secondary Function: *system_simulator*

```

1 function system_simulator
2 global chargers building_dmd2 ev_set timestep t maslow_set maslow
3 for i=1:size(chargers,1)
4     chargers(i,6)=chargers(i,6)+100*ev_set(t,i)*timestep/chargers(i,7);
5     if ev_set(t,i)<0
6         chargers(i,8)=chargers(i,8)+100*ev_set(t,i)*timestep/chargers(i,7);
7     end;
8 end;
9 save EV_chargers.mat chargers;
10 for i=1:size(maslow,1)
11     maslow(i,1)=maslow(i,1)+100*maslow_set(t,i)*timestep/maslow(i,2);
12 end;
13 save maslow_units.mat maslow;
14 building_dmd2=building_dmd2+sum(ev_set(t,:))+sum(maslow_set(t,:));
15 end

```


Appendix E

The developed model for the battery pack of the EV agents

The developed model for the battery pack of the EV agents in SeSAM is described in this section.

E.1 The battery pack model

According to [212], the terminal voltage (V_t) of a Li-ion battery is given by Equations (E.1) and (E.1) for the Discharging and Charging procedure respectively.

Discharging Procedure

$$V_t = E_0 + R \cdot i_t - K \cdot \frac{Q_{max}}{Q_{max} - q_d} \cdot (q_d - i_t^*) + A \cdot e^{-B \cdot q_d} \quad (E.1)$$

Charging Procedure

$$V_t = E_0 + R \cdot i_t - K \cdot \frac{Q_{max}}{Q_{max} - q_d} \cdot q_d + K \cdot \frac{Q_{max}}{q_d} \cdot i_t^* + A \cdot e^{-B \cdot q_d} \quad (E.2)$$

, where:

V_t = terminal voltage of the battery (V)

E_0 = battery voltage constant (V)

R = battery internal impedance (Ω)

i_t = battery current at minute t ($i_t > 0$ for charge and $i_t < 0$ for discharge)

i_t^* = filtered battery current at minute t ($i_t^* = 0$ on the beginning of a current step change and $i_t^* = i_t$ for every consecutive minute)

K = polarization constant

Q_{max} = battery capacity (Ah)

q_d = discharge capacity (Ah)

A = exponential zone amplitude

B = exponential inverse time constant

Parameters A , B , K and E_0 were extracted from the typical discharge characteristic of the battery under study following the procedure mentioned in [212]. An example discharge curve is presented in Figure E.1.

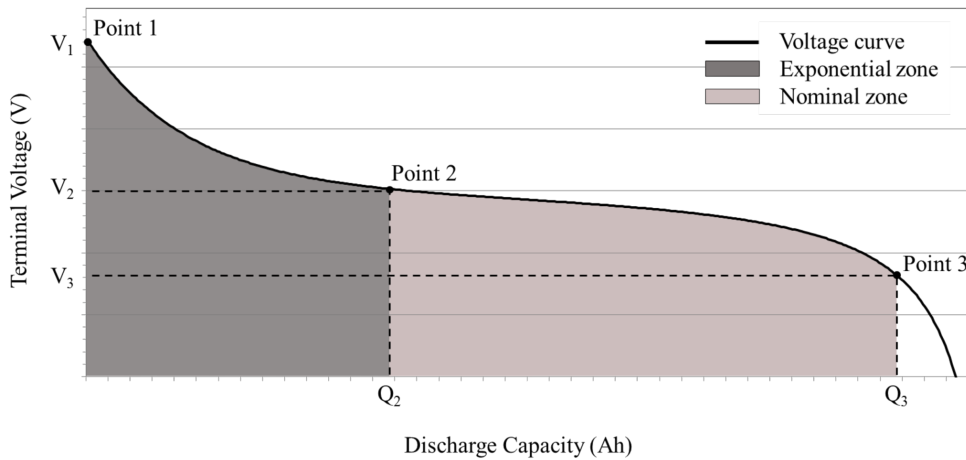


Figure E.1: Typical Discharge Curve of a battery

As seen in Figure E.1 two zones were defined in the typical discharge characteristic of a battery, namely the exponential zone and the nominal zone. To extract the parameters, three points were required from the discharge characteristic: the beginning and end of the exponential zone, and the end of the nominal zone. Having these points, Equation (E.1) was used to create Equations (E.3), (E.4) and (E.5).

In the beginning of the exponential zone (V_1, q_{d1}), the discharge capacity and the filtered current is zero ($q_{d1} = 0, i_t^* = 0$). That leads us to Equation (E.3):

$$V_1 = E_0 + R \cdot i_t + A \quad (\text{E.3})$$

At the end of exponential zone (V_2, q_{d2}) the factor B is approximated to $3/q_{d2}$ according to [212] and $i_t^* = i_t$. Thus, Equation (E.1) becomes as follows:

$$V_2 = E_0 + R \cdot i_t - K \cdot \frac{Q_{max}}{Q_{max} - q_{d2}} \cdot (q_{d2} - i_t) + A \cdot e^{-3} \quad (\text{E.4})$$

At the end of the nominal zone (V_3, q_{d3}) the terminal voltage of the battery is given by Equation (E.5).

$$V_3 = E_0 + R \cdot i_t - K \cdot \frac{Q_{max}}{Q_{max} - q_{d3}} \cdot (q_{d3} - i_t) + A \cdot e^{-\frac{3}{q_{d2}} \cdot q_{d3}} \quad (\text{E.5})$$

After solving the system of Equations (??) - (??), parameters A , K and E_0 are obtained.

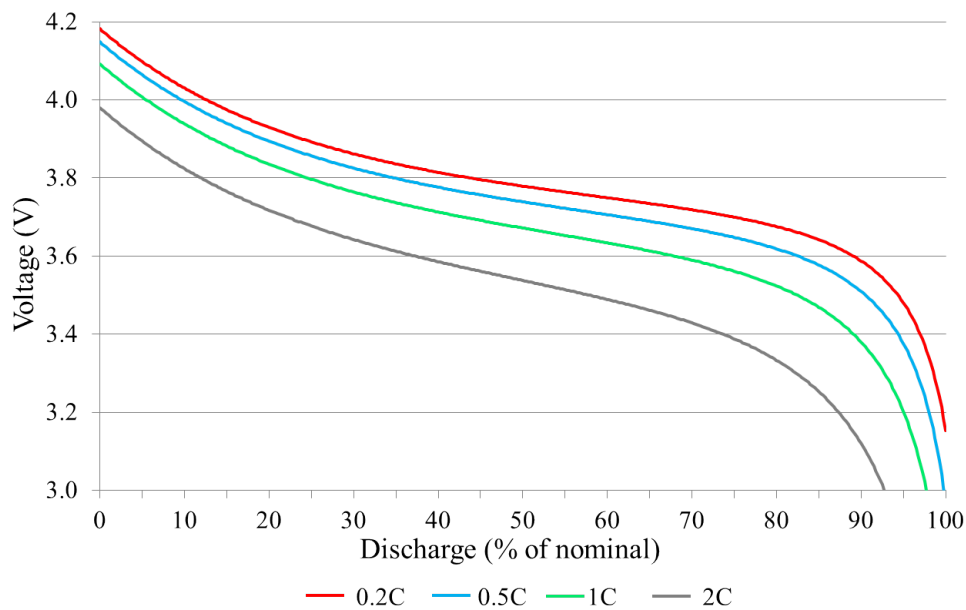
The particular battery model is based on the following assumptions / limitations:

1. The internal resistance is supposed constant during the charge and discharge cycles and independent to the amplitude of it.
2. The model's parameters are extracted from the manufacturer discharge characteristic and assumed to be the same for charging.
3. The model's accuracy is subject to the precision of the points extracted from the discharge characteristic.
4. The temperature does not affect the model's behaviour.
5. The self-discharge of the battery is neglected.
6. The battery has no memory effect.

The model was validated on an 18650 Li-Ion battery cell with the following specifications:

Table E.1: 18650 Li-Ion battery cell specifications (from [2])

Maximum Capacity	2200mAh (0.2C discharge)
Nominal Capacity	2100mAh (0.2C discharge)
Nominal Voltage	3.7V
Internal Impedance	40m Ω
Standard Charge Conditions	Constant Current and Constant Voltage (CC/CV) Charge Current = 1100mA (0.5C) End-up Voltage = 4.2V End Current = 22mA
Standard Discharge Conditions	Constant Current (CC) Charge Current = 1100mA (0.5C) End-up Voltage = 3.0 V

**Figure E.2: Discharge characteristics of the 18650 Li-Ion battery cell (from [2])**

The parameters of Equation (E.1) were extracted from the 0.5C discharge characteristic. Table E.2 presents the three points of interest and the extracted parameters. These parameters were used to reproduce the discharge characteristic of the Li-ion cell for

discharge rates of 0.2C, 0.5C, 1C and 2C (0.44A, 1.1A, 2.2A and 4.4A respectively). The results are presented in Figure E.3.

Table E.2: Parameters of the 18650 Li-Ion battery cell

Point 1	V	4.16V
	q	0 Ah
Point 2	V	3.67V
	q	1.47Ah
Point 3	V	3.4V
	q	1.9775Ah
A	0.426130069	
B	2.040816327	
K	0.010985596	
E_0	3.777869931	

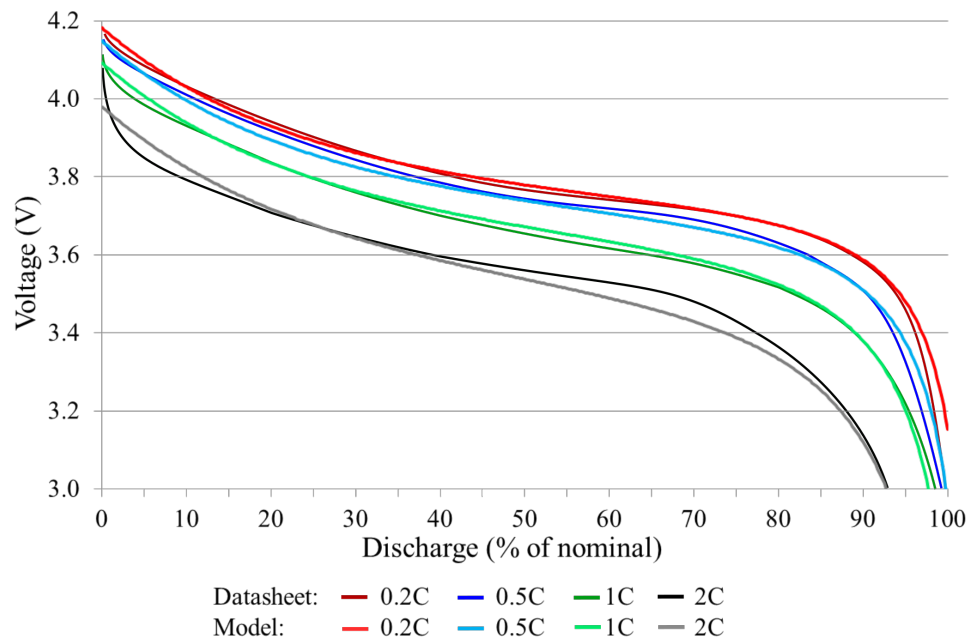


Figure E.3: Generated and actual discharge characteristics for the 18650 Li-Ion battery cell.

As seen in Figure E.3 the generated discharge characteristics correspond to the ac-

tual ones, especially for discharge rates lower than 1C. In EV applications it is highly unlikely to come across higher discharge rates, and thus this model was considered accurate enough for the purposes of this study.

The above model was used to model the behaviour of a battery pack similar to the one of a Tesla Roadster vehicle (<https://www.teslamotors.com>). According to [213], such a battery pack is consisted of 6,831 18650 Li-Ion battery cells following an 11S 9S 69P configuration (see Figure E.4).

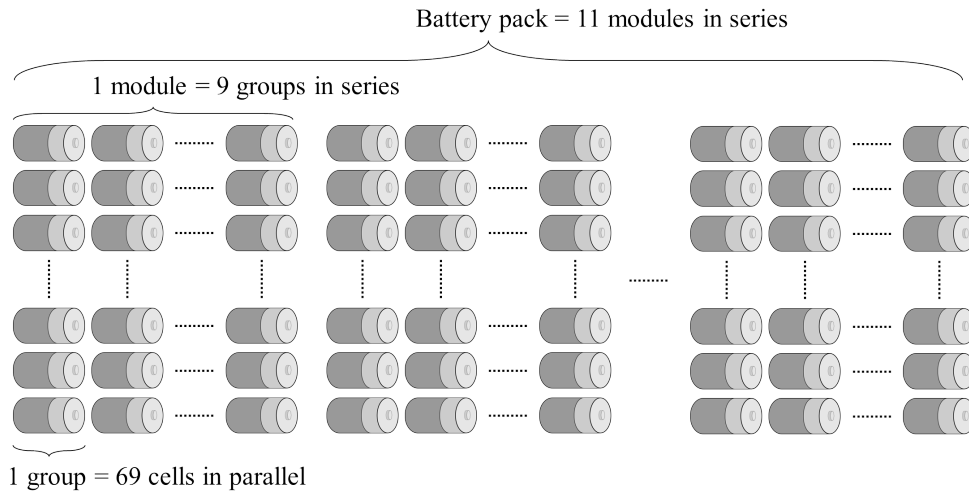


Figure E.4: The 11S 9S 69P configuration

Assuming that the battery pack is consisted of the 18650 Li-Ion battery cells with the characteristics of Table E.2, the battery pack specifications were calculated:

1. Maximum Capacity: $Q_{max_pack} = Q_{max_cell} \cdot 69 = 2.2 \cdot 69 = 151.8Ah$
2. Nominal Capacity: $Q_{nom_pack} = Q_{nom_cell} \cdot 69 = 2.1 \cdot 69 = 144.9Ah$
3. Nominal Voltage: $V_{nom_pack} = V_{nom_cell} \cdot 99 = 3.7 \cdot 99 = 366.3V$
4. Total Impedance: $R_{pack} = R_{cell} \cdot \frac{99}{69} = 0.04 \cdot \frac{99}{69} = 0.05739\Omega$
5. Discharge End Voltage: $V_{min_pack} = V_{min_cell} \cdot 99 = 3.0 \cdot 99 = 297V$
6. Charge Voltage: $V_{c_pack} = V_{c_cell} \cdot 99 = 4.2 \cdot 99 = 415.8V$
7. Charge End Current: $i_{min_pack} = i_{min_cell} \cdot 69 = 22mA \cdot 69 = 1.518A$

For the above calculations a battery cell management system was assumed to be in place to balance the battery cell utilization, and thus the battery pack behaves exactly like a single cell. Based on this assumption, the three points of interest of the discharge characteristic were calculated using the points of the single 18650 Li-Ion battery cell. Solving the system of Equations (E.3)-(E.5) for the new specifications and points, the parameters of Equations (E.1) and (E.2) were recalculated. Table E.3 presents the results for the battery pack:

Table E.3: Parameters of the battery pack

Point 1	V	$4.16 \cdot 99 = 411.84V$
	q	$0Ah$
Point 2	V	$3.67 \cdot 99 = 363.33V$
	q	$1.47 \cdot 69 = 101.43Ah$
Point 3	V	$3.4 \cdot 99 = 366.6V$
	q	$1.9775 \cdot 69 = 136.4475Ah$
A	42.20110765	
B	0.029577048	
K	0.015736639	
E_0	373.9947934	

The discharge characteristics of the battery pack are presented in Figure E.5 for discharge rates of 0.2C, 0.5C, 1C and 2C (30.36A, 75.9A, 151.8A and 303.6A respectively).

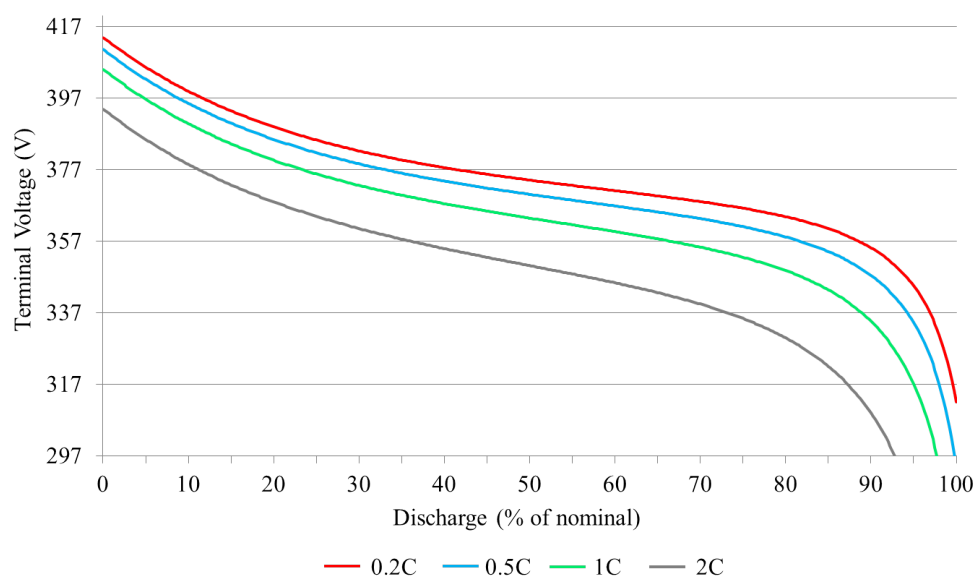


Figure E.5: Generated discharge characteristics for the battery pack

Implementation of the charging / discharging procedure of the EV chargers in SeSAm

This section presents the charging / discharging procedure of the EV chargers in SeSAm.

F.1 The charging/discharging process

The CC-CV charging procedure is described by Equations (F.1) - (F.5). During the CC phase, the current $i(t)$ of the battery pack is constant positive and assumed to be the one at which the EV charger does not exceeds its nominal DC power rating P_{nom}^{DC} when the terminal voltage of the battery pack is maximum. The constant current value was calculated using Equation (F.1).

$$i(t) = i_{cc} = \frac{P_{nom}^{DC}}{V_{c_{pack}}} \quad (F.1)$$

At the end of each minute the charge difference $q_d(t)$, the terminal voltage of the battery pack $V_t(t)$, the SoC of the battery pack $SoC(t)$ and the DC power of the EV charger $P^{DC}(t)$ were calculated using Equations (F.2) - (F.5).

$$q_d(t) = q_d(t - 1) - i(t) \cdot \frac{1}{60} \quad (F.2)$$

$$V_t(t) = E_0 + R \cdot i_t - K \cdot \frac{Q_{max}}{Q_{max} - q_d(t-1)} \cdot q_d(t-1) + K \cdot \frac{Q_{max}}{q_d(t-1)} \cdot i_t + A \cdot e^{-B \cdot q_d(t-1)} \quad (F.3)$$

$$SoC(t) = \frac{Q_{max_pack} - q_d(t)}{Q_{max_pack}} \cdot 100\% \quad (F.4)$$

$$P^{DC}(t) = V_t(t) \cdot i(t) \quad (F.5)$$

When the terminal voltage of the battery pack reaches its maximum value (415.8V), the charging procedure enters the CV phase.

During the CV phase, the terminal voltage of the battery pack is kept constant at its maximum value and the input current $i(t)$ is reduced till it reaches its minimum value (1.518A). At the end of each minute the current $i(t)$, the charge difference $q_d(t)$, the SoC of the battery pack $SoC(t)$ and the DC power of the EV charger $P^{DC}(t)$ were calculated from Equations (F.6) - (F.9).

$$i(t) = \frac{V_t(t) - E_0 + K \cdot \frac{Q_{max}}{Q_{max} - q_d(t-1)} \cdot q_d(t-1) - A \cdot e^{-B \cdot q_d(t-1)}}{R + K \cdot \frac{Q_{max}}{q_d(t-1)}} \quad (F.6)$$

$$q_d(t) = q_d(t-1) - i(t) \cdot \frac{1}{60} \quad (F.7)$$

$$SoC(t) = \frac{Q_{max_pack} - q_d(t)}{Q_{max_pack}} \cdot 100\% \quad (F.8)$$

$$P^{DC}(t) = V_t(t) \cdot i(t) \quad (F.9)$$

When $i(t) = 1.518A$ the charging procedure is over.

If the EV is moving, there is power consumption from its battery. This power consumption $P_{con}(t)$ results in a (negative) discharge current $i(t)$ and a reduction in the

terminal voltage and SoC of the EV battery pack. Equations (F.10) - (F.13) were implemented in SeSAM to calculate the discharge current $i(t)$, the charge difference $q_d(t)$, the terminal voltage $V_t(t)$ and the SoC of the EV battery pack at the end of each minute.

$$i(t) = \frac{P_{con}(t)}{V_t(t-1)} \quad (F.10)$$

$$V_t(t) = E_0 + R \cdot i_t - K \cdot \frac{Q_{max}}{Q_{max} - q_d(t-1)} \cdot (q_d(t-1) - i_t) + A \cdot e^{-B \cdot q_d(t-1)} \quad (F.11)$$

$$q_d(t) = q_d(t-1) - i(t) \cdot \frac{1}{60} \quad (F.12)$$

$$SoC(t) = \frac{Q_{max_{pack}} - q_d(t)}{Q_{max_{pack}}} \cdot 100\% \quad (F.13)$$

When the terminal voltage of the battery pack reaches its minimum value (297V) the EV battery is considered empty, and the EV cannot move any further.

Appendix G

The developed multi-agent simulation model in SeSAm

This section presents screenshots from the developed multi-agent simulation model in SeSAm.

G.1 Screenshots from SeSAm

An example simulation scenario was considered with 10 EV agents in order to demonstrate the user interface and the environment of SeSAm. The structure of the developed model in SeSAm is presented in Figure G.1. Every box corresponds to an entity (agent / resource) with a number of variables. The “world1” entity is a structural entity necessary to initialise the simulation and perform file operations (import / export).

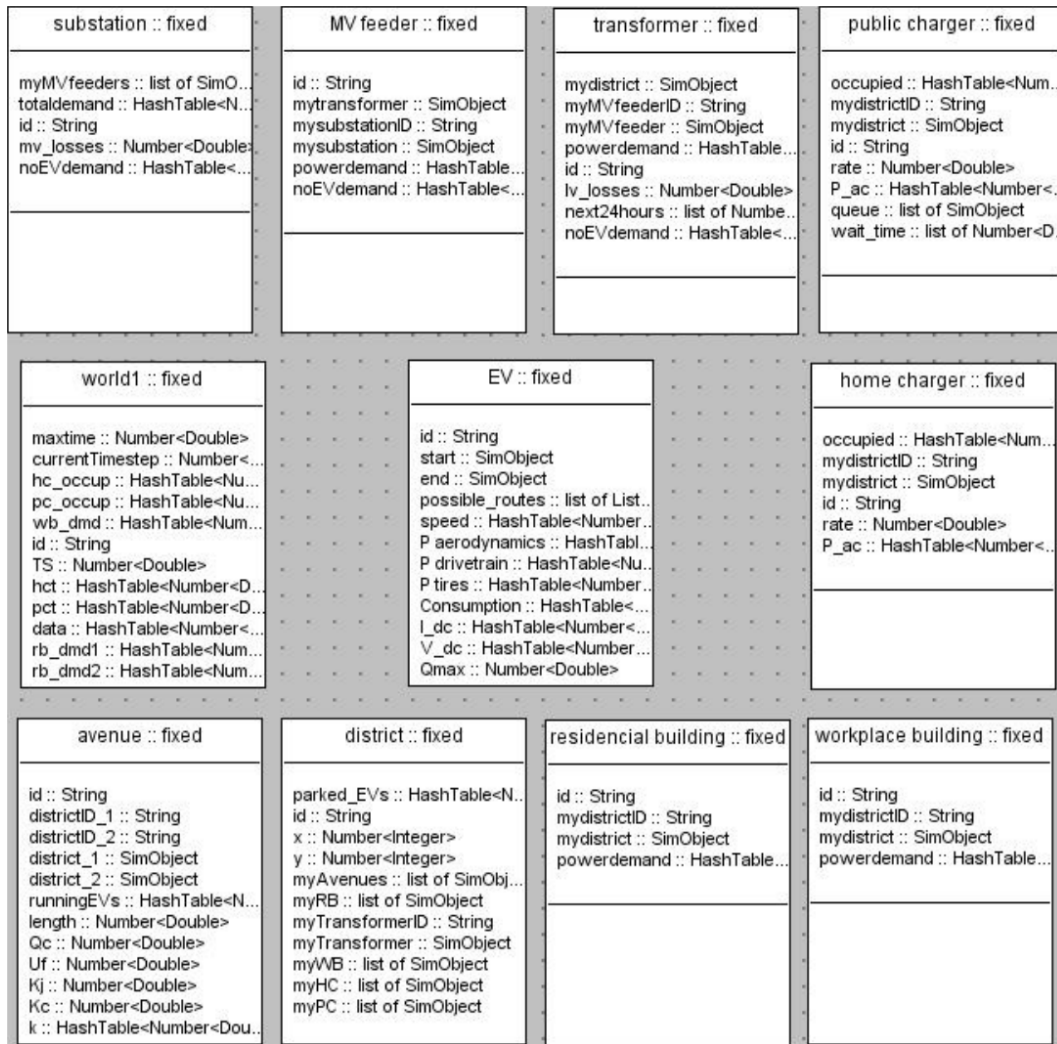


Figure G.1: The structure of the developed model in SeSAM

Figure G.2 presents the reasoning engine of the EV agent. As mentioned in Chapter 5 the EV agent's behaviour was modelled using a state / transition logic, using boxes for the states and arrows for the transitions.

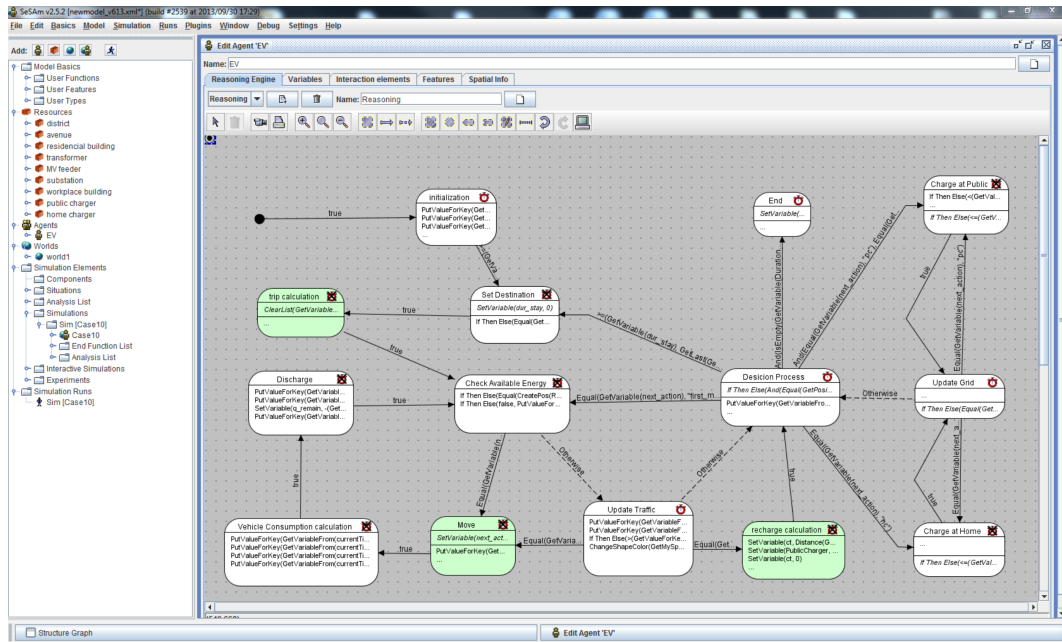


Figure G.2: The reasoning engine of the EV agent in SeSAM

A graphical interface was designed in SeSAM to visualise the EV movements on the road network during the simulation. Different colours were used to describe the EV agent's action (red for discharging, green for charging and black for idle). Figure G.3 presents a snapshot of an example simulation.

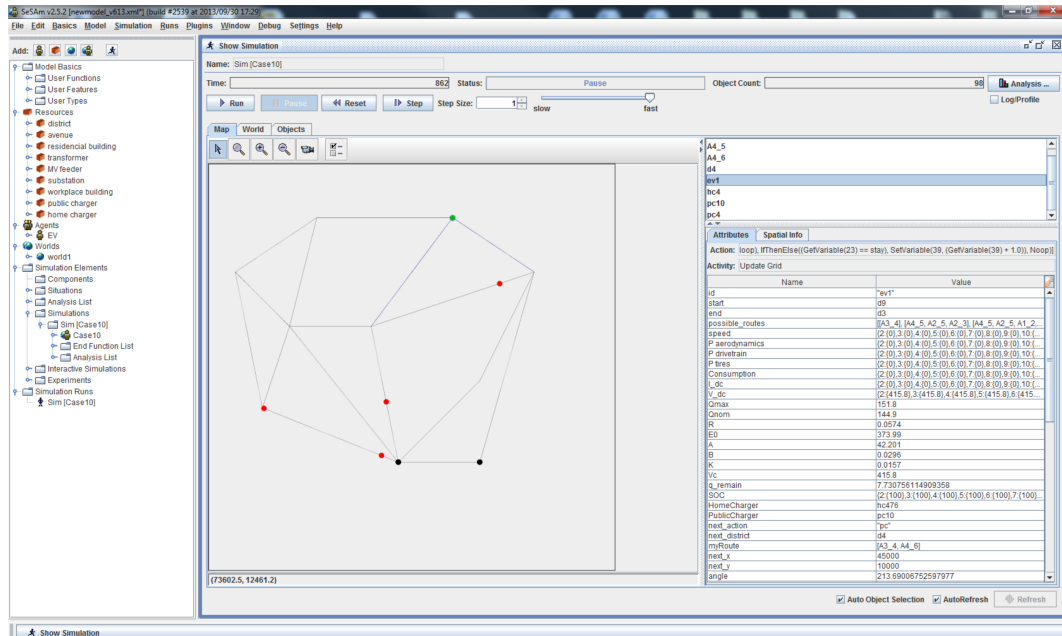


Figure G.3: EV agents on the road network during simulation

Every considered variable of the SeSAM entities was monitored in real time. Figures G.4 and G.5 present the battery characteristics of an EV agent, as well as the power demand from 4 random Public Chargers.

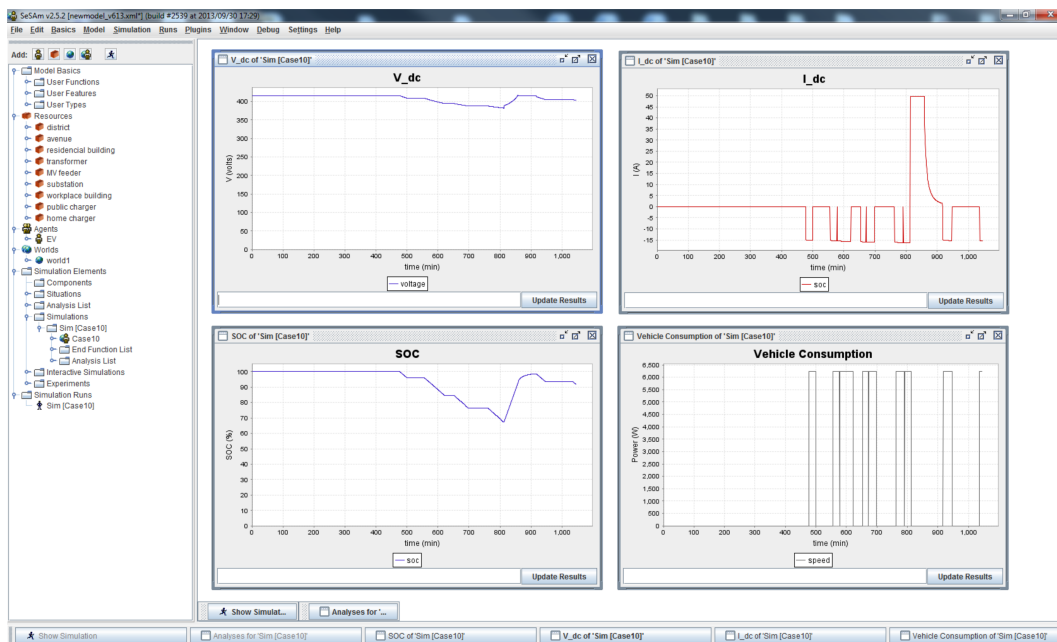


Figure G.4: EV agent characteristics during simulation

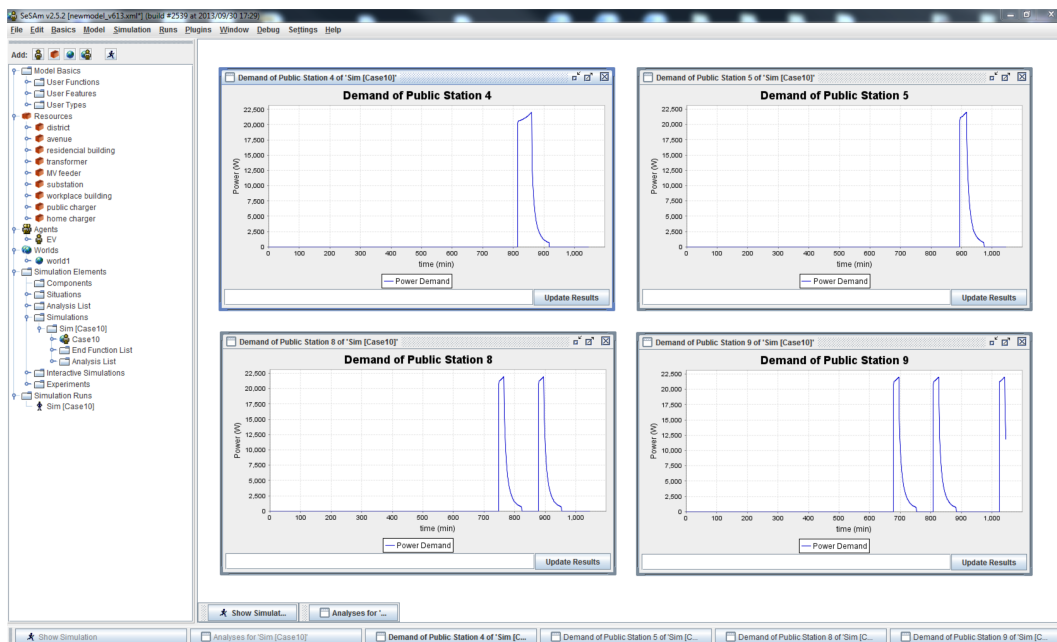


Figure G.5: Power demand from Public Charger entities during simulation

By monitoring the status of the agents' environment, the impact of EV agent beha-

viour was studied. Figures G.6 and G.7 present the transformer demand and the avenue traffic during an example simulation. For visibility purposes, only a sample of Transformers and Avenues is presented here.

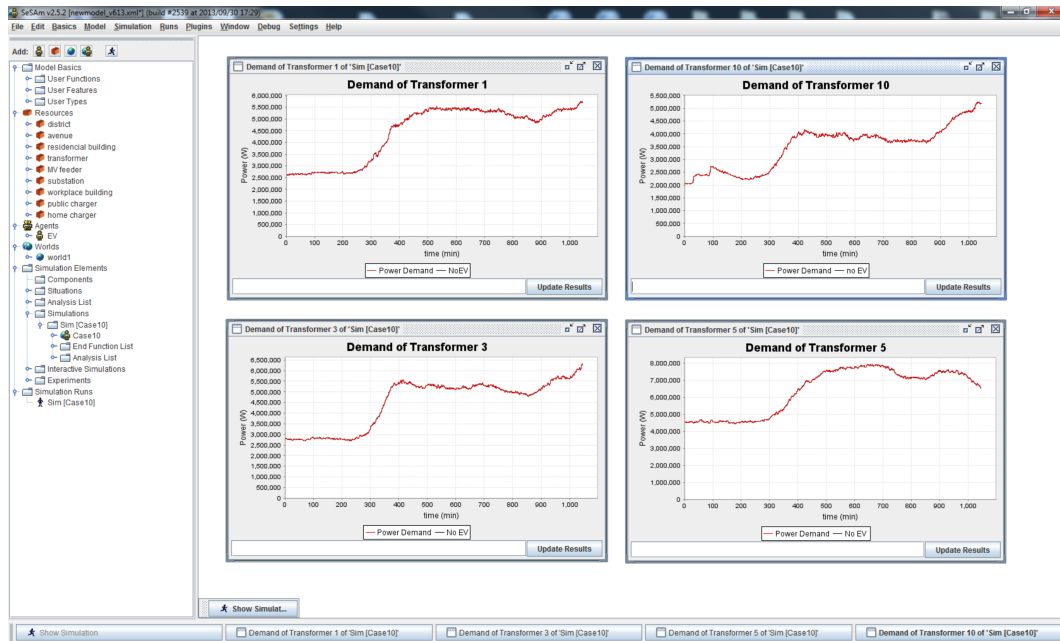


Figure G.6: Power demand from Transformer entities during simulation



Figure G.7: Traffic of Avenue entities during simulation

Bibliography

- [1] "International Energy Agency," 2016.
- [2] Tenergy, "Tenergy 30003 Li-Ion 18650 Cell," tech. rep., 2009.
- [3] C. Yang and R. McCarthy, "Telectricity grid: Impacts of plug-in electric vehicle charging," *Institute of Transportation Studies*, jan 2009.
- [4] P. Papadopoulos, S. Skarvelis-Kazakos, I. Grau, L. M. Cipcigan, and N. Jenkins, "Predicting electric vehicle impacts on residential distribution networks with distributed generation," in *2010 IEEE Vehicle Power and Propulsion Conference*, Institute of Electrical and Electronics Engineers (IEEE), sep 2010.
- [5] P. Papadopoulos, O. Akizu, L. M. Cipcigan, N. Jenkins, and E. Zabala, "Electricity demand with electric cars in 2030: comparing great britain and spain," *Proceedings of the Institution of Mechanical Engineers, Part A: Journal of Power and Energy*, vol. 225, no. 5, pp. 551–566, 2011.
- [6] P. Papadopoulos, S. Skarvelis-Kazakos, I. Grau, L. Cipcigan, and N. Jenkins, "Electric vehicles' impact on British distribution networks," *IET Electr. Syst. Transp.*, vol. 2, no. 3, p. 91, 2012.
- [7] I. C. London, "Smart (and less smart) large-scale integration of ev into european power systems - green emotion deliverable 9.2," 2015.
- [8] Z. Rezvani, J. Jansson, and J. Bodin, "Advances in consumer electric vehicle adoption research: A review and research agenda," *Transportation Research Part D: Transport and Environment*, vol. 34, pp. 122–136, jan 2015.
- [9] C. Mazur, M. Contestabile, G. J. Offer, and N. Brandon, "Assessing and comparing german and UK transition policies for electric mobility," *Environmental Innovation and Societal Transitions*, vol. 14, pp. 84–100, mar 2015.

- [10] M. Tanaka, T. Ida, K. Murakami, and L. Friedman, "Consumers' willingness to pay for alternative fuel vehicles: A comparative discrete choice analysis between the US and Japan," *Transportation Research Part A: Policy and Practice*, vol. 70, pp. 194–209, dec 2014.
- [11] E. Chéron and M. Zins, "Electric vehicle purchasing intentions: The concern over battery charge duration," *Transportation Research Part A: Policy and Practice*, vol. 31, pp. 235–243, may 1997.
- [12] A. Dimitropoulos, P. Rietveld, and J. N. van Ommeren, "Consumer valuation of changes in driving range: A meta-analysis," *Transportation Research Part A: Policy and Practice*, vol. 55, pp. 27–45, sep 2013.
- [13] T. Franke and J. F. Krems, "Interacting with limited mobility resources: Psychological range levels in electric vehicle use," *Transportation Research Part A: Policy and Practice*, vol. 48, pp. 109–122, feb 2013.
- [14] T. Franke and J. F. Krems, "Understanding charging behaviour of electric vehicle users," *Transportation Research Part F: Traffic Psychology and Behaviour*, vol. 21, pp. 75–89, nov 2013.
- [15] A. Kihm and S. Trommer, "The new car market for electric vehicles and the potential for fuel substitution," *Energy Policy*, vol. 73, pp. 147–157, oct 2014.
- [16] Y. Huang and Y. Zhou, "An optimization framework for workplace charging strategies," *Transportation Research Part C: Emerging Technologies*, vol. 52, pp. 144–155, mar 2015.
- [17] J. Neubauer and E. Wood, "The impact of range anxiety and home, workplace, and public charging infrastructure on simulated battery electric vehicle lifetime utility," *Journal of Power Sources*, vol. 257, pp. 12–20, jul 2014.
- [18] "Vehicle technologies office: Workplace charging challenge," 2014.
- [19] "Olev: Grant schemes for electric vehicle charging infrastructure," 2016.
- [20] National Grid, "Introduction to Charging: Which Parties Pay Which Charges?," Tech. Rep. December, 2015.
- [21] B. COYNE, "Triad, capacity costs, CfD and RO: Prepare for increases, warns SmartestEnergy," 2016.

- [22] C. Mullen, P. C. Taylor, V. Thornley, and N. S. Wade, "Use of standby generation for reduction of transmission network charges for half-hourly metered customers," 2014.
- [23] R. J. Flores, B. P. Shaffer, and J. Brouwer, "Electricity costs for an electric vehicle fueling station with level 3 charging," *Applied Energy*, vol. 169, pp. 813–830, may 2016.
- [24] J. Brady and M. O'Mahony, "Modelling charging profiles of electric vehicles based on real-world electric vehicle charging data," *Sustainable Cities and Society*, vol. 26, pp. 203–216, oct 2016.
- [25] E. Liz Waters, Department for Business and I. Strategy, "Energy consumption in the uk," Tech. Rep. November, 2016.
- [26] R. Gough, C. Dickerson, P. Rowley, and C. Walsh, "Vehicle-to-grid feasibility: A techno-economic analysis of EV-based energy storage," *Applied Energy*, vol. 192, pp. 12–23, apr 2017.
- [27] L. Wang, S. Sharkh, and A. Chipperfield, "Optimal coordination of vehicle-to-grid batteries and renewable generators in a distribution system," *Energy*, vol. 113, pp. 1250–1264, oct 2016.
- [28] M. A. Nicholas, G. Tal, and J. Woodjack, "California Statewide Charging Assessment Model for Plug-in Electric Vehicles: Learning from Statewide Travel Surveys." 2013.
- [29] E. Xydas, C. Marmaras, L. M. Cipcigan, N. Jenkins, S. Carroll, and M. Barker, "A data-driven approach for characterising the charging demand of electric vehicles: A UK case study," *Applied Energy*, vol. 162, pp. 763–771, jan 2016.
- [30] National Grid, "Introduction to Triads," tech. rep., 2014.
- [31] D. Pratt, "Saint-Gobain UK & Ireland makes savings from Triad avoidance," 2016.
- [32] N. B. Solutions, "Triad Warning Service," jan 2016.
- [33] S. Custance-baker, "Forecasting triads : The negative feedback problem," tech. rep., British Energy.
- [34] R. F. Engle, C. W. J. Granger, J. Rice, and A. Weiss, "Semiparametric Estimates of the Relation Between Weather and Electricity Sales," *J. Am. Stat. Assoc.*, vol. 81, p. 310, jun 1986.

- [35] D. Bunn, "Forecasting loads and prices in competitive power markets," *Proc. IEEE*, vol. 88, pp. 163–169, feb 2000.
- [36] A. Harvey and S. J. Koopman, "Forecasting Hourly Electricity Demand Using Time-Varying Splines," *J. Am. Stat. Assoc.*, vol. 88, p. 1228, dec 1993.
- [37] A. Pardo, V. Meneu, and E. Valor, "Temperature and seasonality influences on Spanish electricity load," *Energy Econ.*, vol. 24, pp. 55–70, jan 2002.
- [38] N. Amjady, "Short-term hourly load forecasting using time-series modeling with peak load estimation capability," *IEEE Trans. Power Syst.*, vol. 16, no. 4, pp. 798–805, 2001.
- [39] H. Temraz, M. Salama, and V. Quintana, "Application of the decomposition technique for forecasting the load of a large electric power network," *IEE Proc. - Gener. Transm. Distrib.*, vol. 143, no. 1, p. 13, 1996.
- [40] V. A. Levi, "A medium-term probabilistic model for forecasting loads with a small proportion of air conditioners," *Electr. Power Syst. Res.*, vol. 29, pp. 57–67, feb 1994.
- [41] E. Barakat, J. Al-Qassim, and S. Al Rashed, "New model for peak demand forecasting applied to highly complex load characteristics of a fast developing area," *IEE Proc. C Gener. Transm. Distrib.*, vol. 139, no. 2, p. 136, 1992.
- [42] J. W. Taylor, "Short-term electricity demand forecasting using double seasonal exponential smoothing," *J. Oper. Res. Soc.*, vol. 54, pp. 799–805, aug 2003.
- [43] J. V. Ringwood, D. Bofelli, and F. T. Murray, "Forecasting Electricity Demand on Short, Medium and Long Time Scales Using Neural Networks," *J. Intell. Robot. Syst.*, vol. 31, no. 1/3, pp. 129–147, 2001.
- [44] J. Taylor and R. Buizza, "Neural network load forecasting with weather ensemble predictions," *IEEE Trans. Power Syst.*, vol. 17, pp. 626–632, aug 2002.
- [45] H. Morita, T. Kase, Y. Tamura, and S. Iwamoto, "Interval prediction of annual maximum demand using grey dynamic model," *Int. J. Electr. Power Energy Syst.*, vol. 18, pp. 409–413, oct 1996.
- [46] M. Kandil, S. El-Debeiky, and N. Hasanien, "Overview and comparison of long-term forecasting techniques for a fast developing utility: part I," *Electr. Power Syst. Res.*, vol. 58, pp. 11–17, may 2001.

- [47] J. W. Taylor, "Using Weather Ensemble Predictions in Electricity Demand Forecasting," *Int. J. Forecast.*, vol. 19, no. 1, pp. 57–70, 2003.
- [48] A. Douglas, A. Breipohl, F. Lee, and R. Adapa, "The impacts of temperature forecast uncertainty on Bayesian load forecasting," *IEEE Trans. Power Syst.*, vol. 13, no. 4, pp. 1507–1513, 1998.
- [49] M. Smith, "Modeling and Short-Term Forecasting of New South Wales Electricity System Load," *J. Bus. Econ. Stat.*, vol. 18, p. 465, oct 2000.
- [50] P. McSharry, S. Bouwman, and G. Bloemhof, "Probabilistic Forecasts of the Magnitude and Timing of Peak Electricity Demand," *IEEE Trans. Power Syst.*, vol. 20, pp. 1166–1172, may 2005.
- [51] K. Stanton and P. Gupta, "Forecasting Annual or Seasonal Peak Demand in Electric Utility Systems," *IEEE Trans. Power Appar. Syst.*, vol. PAS-89, pp. 951–959, may 1970.
- [52] R. J. Hyndman and S. Fan, "Density Forecasting for Long-Term Peak Electricity Demand," *IEEE Trans. Power Syst.*, vol. 25, pp. 1142–1153, may 2010.
- [53] J. A. Clarke, *Energy Simulation in Building Design*. Butterworth-Heinemann, second ed., 2001.
- [54] U.S. Department of Energy, "Building energy software tools directory."
- [55] F. Lei and P. Hu, "A baseline model for office building energy consumption in hot summer and cold winter region," in *Proc. Int. Conf. Manag. Serv. Sci.*, pp. 1–4, 2009.
- [56] S.-H. Cho, W.-T. Kim, C.-S. Tae, and M. Z. ., "Effect of length of measurement period on accuracy of predicted annual heating energy consumption of buildings," in *Energy Convers. Manag.*, vol. 45, pp. 2867–2878, 2004.
- [57] A. Kimbara, S. Kurosu, R. Endo, K. Kamimura, T. Matsuba, and A. Yamada, "On-line prediction for load profile of an air-conditioning system," in *ASHRAE Trans.*, vol. 101 of 2, pp. 198–207, 1995.
- [58] A. J. Hoffman, "Peak demand control in commercial buildings with target peak adjustment based on load forecasting," in *1998 IEEE Int. Conf. Control Appl.*, vol. 2, pp. 1292–6, 1998.
- [59] G. R. Newsham and B. J. Birt, "Building-level occupancy data to improve ARIMA-based electricity use forecasts," in *Proc. 2nd ACM Work. Embed. Sens.*

- Syst. energy-efficiency Build. BuildSys '10*, (New York, NY, USA), pp. 13–18, ACM, 2010.
- [60] T. Olofsson and S. Andersson, “Long-term energy demand predictions based on short-term measured data,” in *Energy Build.*, vol. 33 of 2, pp. 85–91, 2001.
- [61] P. A. González and J. M. Zamarreno, “Prediction of hourly energy consumption in buildings based on a feedback artificial neural network,” in *Energy Build.*, vol. 37 of 6, pp. 595–601, 2005.
- [62] B. Dong, C. Cao, and S. E. Lee, “Applying support vector machines to predict building energy consumption in tropical region,” in *Energy Build.*, vol. 37 of 5, pp. 545–553, 2005.
- [63] R. Zhang and H. Yang, “Dynamic building energy consumption forecast using weather forecast interpolations,” in *2015 IEEE Int. Conf. Smart Grid Commun.*, pp. 671–676, IEEE, nov 2015.
- [64] F. Oldewurtel, A. Parisio, C. N. Jones, D. Gyalistras, M. Gwerder, V. Stauch, B. Lehmann, and M. Morari, “Use of model predictive control and weather forecasts for energy efficient building climate control,” *Energy Build.*, vol. 45, pp. 15–27, 2012.
- [65] A. J. White and R. Reichmuth, “Simplified method for predicting building energy consumption using average monthly temperatures,” in *Proc. 31st Intersoc. energy Convers. Eng. Conf.*, vol. 3, pp. 1834–1839, 1996.
- [66] M. S. Al-Homoud, “Computer-aided building energy analysis techniques,” in *Build. Environ.*, vol. 36, pp. 421–433, Elsevier Science Ltd, 2001.
- [67] R. Yao and K. Steemers, “A method of formulating energy load profile for domestic buildings in the UK,” *Energy Build.*, vol. 37, pp. 663–671, jun 2005.
- [68] N. S. Javeed and A. Z. Al-Garni, “Forecasting electric energy consumption using neural networks,” in *Energy Policy*, vol. 23 of 12, pp. 1097–1104, 1995.
- [69] F. Lai, F. Magoulès, and F. Lherminier, “Vapnik’s learning theory applied to energy consumption forecasts in residential buildings,” in *Int. J. Comput. Math.*, vol. 85 of 10, pp. 1563–1588, 2008.
- [70] D. Lazos, A. B. Sproul, and M. Kay, “Development of hybrid numerical and statistical short term horizon weather prediction models for building energy management optimisation,” *Building and Environment*, vol. 90, pp. 82–95, aug 2015.

- [71] A. F. Raab and N. Hartmann, "Mobile Energy Resources in Grids of Electricity - Final Recommendations," tech. rep., 2012.
- [72] E. L. Karfopoulos, C. E. Marmaras, and N. Hatziaargyriou, "Charging control model for Electric Vehicle Supplier Aggregator," in *2012 3rd IEEE PES Innov. Smart Grid Technol. Eur. (ISGT Eur.*, pp. 1–7, IEEE, oct 2012.
- [73] K. Clement-Nyns, E. Haesen, and J. Driesen, "The Impact of Charging Plug-In Hybrid Electric Vehicles on a Residential Distribution Grid," *IEEE Trans. Power Syst.*, vol. 25, pp. 371–380, feb 2010.
- [74] L. Pieltain Fernandez, T. Gomez San Roman, R. Cossent, C. Mateo Domingo, and P. Frias, "Assessment of the Impact of Plug-in Electric Vehicles on Distribution Networks," *IEEE Trans. Power Syst.*, vol. 26, pp. 206–213, feb 2011.
- [75] G. Putrus, P. Suwanapingkarl, D. Johnston, E. Bentley, and M. Narayana, "Impact of electric vehicles on power distribution networks," in *2009 IEEE Veh. Power Propuls. Conf.*, pp. 827–831, IEEE, sep 2009.
- [76] J. L. Rodgers and W. A. Nicewander, "Thirteen ways to look at the correlation coefficient," *The American Statistician*, vol. 42, pp. 59–66, feb 1988.
- [77] S. K. Tyagi, "Correlation coefficient of dual hesitant fuzzy sets and its applications," *Applied Mathematical Modelling*, vol. 39, pp. 7082–7092, nov 2015.
- [78] D. Pavanello, W. Zaiman, A. Colli, J. Heiser, and S. Smith, "Statistical functions and relevant correlation coefficients of clearness index," *Journal of Atmospheric and Solar-Terrestrial Physics*, vol. 130-131, pp. 142–150, aug 2015.
- [79] H. Liao, Z. Xu, and X.-J. Zeng, "Novel correlation coefficients between hesitant fuzzy sets and their application in decision making," *Knowledge-Based Systems*, vol. 82, pp. 115–127, jul 2015.
- [80] Y. Kim, T.-H. Kim, and T. Ergün, "The instability of the pearson correlation coefficient in the presence of coincidental outliers," *Finance Research Letters*, vol. 13, pp. 243–257, may 2015.
- [81] M.-T. Puth, M. Neuhäuser, and G. D. Ruxton, "Effective use of pearson's product-moment correlation coefficient," *Animal Behaviour*, vol. 93, pp. 183–189, jul 2014.
- [82] U. of Waikato, "WEKA," jan 2016.

- [83] A. G. Anastasiadis, E. Voreadi, and N. D. Hatziargyriou, "Probabilistic Load Flow methods with high integration of Renewable Energy Sources and Electric Vehicles - case study of Greece," in *2011 IEEE Trondheim PowerTech*, pp. 1–8, IEEE, jun 2011.
- [84] S. Deilami, A. S. Masoum, P. S. Moses, and M. A. S. Masoum, "Voltage profile and THD distortion of residential network with high penetration of Plug-in Electrical Vehicles," in *2010 IEEE PES Innov. Smart Grid Technol. Conf. Eur. (ISGT Eur.*, no. 4, pp. 1–6, IEEE, oct 2010.
- [85] Q. Gong, S. Midlam-Mohler, V. Marano, and G. Rizzoni, "Study of PEV Charging on Residential Distribution Transformer Life," *IEEE Trans. Smart Grid*, vol. 3, pp. 404–412, mar 2012.
- [86] E. L. Karfopoulos and N. D. Hatziargyriou, "A Multi-Agent System for Controlled Charging of a Large Population of Electric Vehicles," *IEEE Trans. Power Syst.*, vol. 28, pp. 1196–1204, may 2013.
- [87] S. Acha, T. C. Green, and N. Shah, "Optimal charging strategies of electric vehicles in the UK power market," in *ISGT 2011*, pp. 1–8, IEEE, jan 2011.
- [88] Y. Cao, S. Tang, C. Li, P. Zhang, Y. Tan, Z. Zhang, and J. Li, "An Optimized EV Charging Model Considering TOU Price and SOC Curve," *IEEE Trans. Smart Grid*, vol. 3, pp. 388–393, mar 2012.
- [89] M. A. Golkar, "USING A MULTIVARIATE DOE METHOD FOR CONGESTION STUDY IN DISTRIBUTION SYSTEMS UNDER IMPACTS OF PLUG-IN ELECTRIC VEHICLES," in *CIREN 21 st Int. Conf. Electr. Distrib.*, no. 0718, pp. 6–9, 2011.
- [90] N. Leemput, J. Van Roy, F. Geth, P. Tant, B. Claessens, and J. Driesen, "Comparative analysis of coordination strategies for electric vehicles," in *2011 2nd IEEE PES Int. Conf. Exhib. Innov. Smart Grid Technol.*, pp. 1–8, IEEE, dec 2011.
- [91] Luonan Chen, H. Suzuki, T. Wachi, and Y. Shimura, "Components of nodal prices for electric power systems," *IEEE Trans. Power Syst.*, vol. 17, no. 1, pp. 41–49, 2002.
- [92] M. A. Ortega-Vazquez, F. Bouffard, and V. Silva, "Electric Vehicle Aggregator/System Operator Coordination for Charging Scheduling and Services Procurement," *IEEE Trans. Power Syst.*, vol. 28, pp. 1806–1815, may 2013.

- [93] N. Rotering and M. Ilic, "Optimal Charge Control of Plug-In Hybrid Electric Vehicles in Deregulated Electricity Markets," *IEEE Trans. Power Syst.*, vol. 26, pp. 1021–1029, aug 2011.
- [94] E. Sortomme, M. M. Hindi, S. D. J. MacPherson, and S. S. Venkata, "Coordinated Charging of Plug-In Hybrid Electric Vehicles to Minimize Distribution System Losses," *IEEE Trans. Smart Grid*, vol. 2, pp. 198–205, mar 2011.
- [95] P. Richardson, D. Flynn, and A. Keane, "Local Versus Centralized Charging Strategies for Electric Vehicles in Low Voltage Distribution Systems," *IEEE Trans. Smart Grid*, vol. 3, pp. 1020–1028, jun 2012.
- [96] W. Su, H. Eichi, W. Zeng, and M.-Y. Chow, "A Survey on the Electrification of Transportation in a Smart Grid Environment," *IEEE Trans. Ind. Informatics*, vol. 8, pp. 1–10, feb 2012.
- [97] C. Jin, J. Tang, and P. Ghosh, "Optimizing Electric Vehicle Charging: A Customer's Perspective," *IEEE Trans. Veh. Technol.*, vol. 62, pp. 2919–2927, sep 2013.
- [98] F. Kennel, D. Gorges, and S. Liu, "Energy Management for Smart Grids With Electric Vehicles Based on Hierarchical MPC," *IEEE Trans. Ind. Informatics*, vol. 9, pp. 1528–1537, aug 2013.
- [99] R. Patil, J. C. Kelly, Z. Filipi, and H. Fathy, "A framework for the integrated optimization of charging and power management in plug-in hybrid electric vehicles," in *2012 Am. Control Conf.*, pp. 1327–1334, IEEE, jun 2012.
- [100] J. Zhao, F. Wen, Z. Y. Dong, Y. Xue, and K. P. Wong, "Optimal Dispatch of Electric Vehicles and Wind Power Using Enhanced Particle Swarm Optimization," *IEEE Trans. Ind. Informatics*, vol. 8, pp. 889–899, nov 2012.
- [101] N. Munier, *A Strategy for Using Multicriteria Analysis in Decision-Making*. Springer Netherlands, 2011.
- [102] D. Ernst, M. Glavic, F. Capitanescu, and L. Wehenkel, "Reinforcement learning versus model predictive control: A comparison on a power system problem," *IEEE Transactions on Systems, Man, and Cybernetics, Part B (Cybernetics)*, vol. 39, pp. 517–529, apr 2009.
- [103] Y. Zhang, S. Wang, and G. Ji, "A comprehensive survey on particle swarm optimization algorithm and its applications," *Mathematical Problems in Engineering*, vol. 2015, pp. 1–38, 2015.

- [104] L. Zhou, F. Li, C. Gu, Z. Hu, and S. Le Blond, "Cost/Benefit Assessment of a Smart Distribution System With Intelligent Electric Vehicle Charging," *IEEE Trans. Smart Grid*, vol. 5, pp. 839–847, mar 2014.
- [105] C.-K. Wen, J.-C. Chen, J.-H. Teng, and P. Ting, "Decentralized Plug-in Electric Vehicle Charging Selection Algorithm in Power Systems," *IEEE Trans. Smart Grid*, vol. 3, pp. 1779–1789, dec 2012.
- [106] L. Gan, U. Topcu, and S. H. Low, "Optimal decentralized protocol for electric vehicle charging," *IEEE Trans. Power Syst.*, vol. 28, pp. 940–951, may 2013.
- [107] J. M. Foster, G. Trevino, M. Kuss, and M. C. Caramanis, "Plug-In Electric Vehicle and Voltage Support for Distributed Solar: Theory and Application," *IEEE Syst. J.*, vol. 7, pp. 881–888, dec 2013.
- [108] P. Papadopoulos, N. Jenkins, L. M. Cipcigan, I. Grau, and E. Zabala, "Coordination of the Charging of Electric Vehicles Using a Multi-Agent System," *IEEE Trans. Smart Grid*, vol. 4, pp. 1802–1809, dec 2013.
- [109] S. Weckx, R. D'Hulst, B. Claessens, and J. Driesensam, "Multiagent Charging of Electric Vehicles Respecting Distribution Transformer Loading and Voltage Limits," *IEEE Trans. Smart Grid*, vol. 5, pp. 2857–2867, nov 2014.
- [110] Y. Xu, "Optimal Distributed Charging Rate Control of Plug-In Electric Vehicles for Demand Management," *IEEE Trans. Power Syst.*, vol. 30, pp. 1536–1545, may 2015.
- [111] Y. Wang, W. Saad, Z. Han, H. V. Poor, and T. Basar, "A Game-Theoretic Approach to Energy Trading in the Smart Grid," *IEEE Trans. Smart Grid*, vol. 5, pp. 1439–1450, may 2014.
- [112] W. Lee, L. Xiang, R. Schober, and V. W. S. Wong, "Electric Vehicle Charging Stations With Renewable Power Generators: A Game Theoretical Analysis," *IEEE Trans. Smart Grid*, vol. 6, pp. 608–617, mar 2015.
- [113] W. Kempton and S. E. Letendre, "Electric vehicles as a new power source for electric utilities," *Transp. Res. Part D Transp. Environ.*, vol. 2, pp. 157–175, sep 1997.
- [114] I. Momber, T. Gomez, G. Venkataramanan, M. Stadler, S. Beer, J. Lai, C. Marnay, and V. Battaglia, "Plug-in electric vehicle interactions with a small office building: An economic analysis using DER-CAM," in *IEEE PES Gen. Meet.*, vol. July, pp. 1–8, IEEE, jul 2010.

- [115] S. Gao, K. T. Chau, C. Liu, D. Wu, and C. C. Chan, "Integrated Energy Management of Plug-in Electric Vehicles in Power Grid With Renewables," *IEEE Trans. Veh. Technol.*, vol. 63, pp. 3019–3027, sep 2014.
- [116] E. L. Karfopoulos and N. D. Hatziargyriou, "Distributed Coordination of Electric Vehicles Providing V2G Services," *IEEE Trans. Power Syst.*, vol. 31, pp. 329–338, jan 2016.
- [117] H. N. T. Nguyen, C. Zhang, and M. A. Mahmud, "Optimal Coordination of G2V and V2G to Support Power Grids With High Penetration of Renewable Energy," *IEEE Trans. Transp. Electrification*, vol. 1, pp. 188–195, aug 2015.
- [118] U. C. Chukwu and S. M. Mahajan, "V2G electric power capacity estimation and ancillary service market evaluation," in *2011 IEEE Power Energy Soc. Gen. Meet.*, pp. 1–8, IEEE, jul 2011.
- [119] T. Ma and O. A. Mohammed, "Economic Analysis of Real-Time Large-Scale PEVs Network Power Flow Control Algorithm With the Consideration of V2G Services," *IEEE Trans. Ind. Appl.*, vol. 50, pp. 4272–4280, nov 2014.
- [120] H. Liu, Z. Hu, Y. Song, and J. Lin, "Decentralized Vehicle-to-Grid Control for Primary Frequency Regulation Considering Charging Demands," *IEEE Trans. Power Syst.*, vol. 28, pp. 3480–3489, aug 2013.
- [121] E. L. Karfopoulos, K. A. Panourgias, and N. D. Hatziargyriou, "Distributed Coordination of Electric Vehicles providing V2G Regulation Services," *IEEE Trans. Power Syst.*, vol. 31, pp. 2834–2846, jul 2016.
- [122] Da Qian Xu, G. Joos, M. Levesque, and M. Maier, "Integrated V2G, G2V, and Renewable Energy Sources Coordination Over a Converged Fiber-Wireless Broadband Access Network," *IEEE Trans. Smart Grid*, vol. 4, pp. 1381–1390, sep 2013.
- [123] J. Lin, K.-C. Leung, and V. O. K. Li, "Optimal Scheduling With Vehicle-to-Grid Regulation Service," *IEEE Internet Things J.*, vol. 1, pp. 556–569, dec 2014.
- [124] M. Ansari, A. T. Al-Awami, E. Sortomme, and M. A. Abido, "Coordinated Bidding of Ancillary Services for Vehicle-to-Grid Using Fuzzy Optimization," *IEEE Trans. Smart Grid*, vol. 6, pp. 261–270, jan 2015.
- [125] S. W. Kim, Y. G. Jin, Y. H. Song, and Y. T. Yoon, "Decentralized Vehicle-to-Grid Design for Frequency Regulation within Price-based Operation," *J. Electr. Eng. Technol.*, vol. 10, pp. 1335–1341, may 2015.

- [126] R. Yu, W. Zhong, S. Xie, C. Yuen, S. Gjessing, and Y. Zhang, "Balancing Power Demand through EV Mobility in Vehicle-to-Grid Mobile Energy Networks," *IEEE Trans. Ind. Informatics*, pp. 1–1, 2015.
- [127] M. Singh, P. Kumar, and I. Kar, "A Multi Charging Station for Electric Vehicles and Its Utilization for Load Management and the Grid Support," *IEEE Trans. Smart Grid*, vol. 4, pp. 1026–1037, jun 2013.
- [128] Y. Ota, H. Taniguchi, T. Nakajima, K. M. Liyanage, J. Baba, and A. Yokoyama, "Autonomous Distributed V2G (Vehicle-to-Grid) Satisfying Scheduled Charging," *IEEE Trans. Smart Grid*, vol. 3, pp. 559–564, mar 2012.
- [129] J. Tan and L. Wang, "Enabling Reliability-Differentiated Service in Residential Distribution Networks With PHEVs: A Hierarchical Game Approach," *IEEE Trans. Smart Grid*, pp. 1–1, 2015.
- [130] A. Schuller, B. Dietz, C. M. Flath, and C. Weinhardt, "Charging Strategies for Battery Electric Vehicles: Economic Benchmark and V2G Potential," *IEEE Trans. Power Syst.*, vol. 29, pp. 2014–2022, sep 2014.
- [131] Ebrahim Saeidi Dehaghani and S. S. Williamson, "On the inefficiency of vehicle-to-grid (V2G) power flow: Potential barriers and possible research directions," in *2012 IEEE Transp. Electrification Conf. Expo*, pp. 1–5, IEEE, jun 2012.
- [132] M. Stadler, I. Momber, O. Mégel, T. Gómez, C. Marnay, S. Beer, J. Lai, and V. Battaglia, "The added economic and environmental value of plug-in electric vehicles connected to commercial building microgrids," in *2nd Eur. Conf. Smart-Grids E-Mobility*, 2010.
- [133] M. C. Bozchalui and R. Sharma, "Analysis of Electric Vehicles as Mobile Energy Storage in commercial buildings: Economic and environmental impacts," *2012 IEEE Power Energy Soc. Gen. Meet.*, pp. 1–8, 2012.
- [134] S. Beer, T. Gómez, S. Member, D. Dallinger, I. Momber, C. Marnay, M. Stadler, and J. Lai, "An Economic Analysis of Used Electric Vehicle Batteries Integrated Into Commercial Building Microgrids," vol. 3, no. 1, pp. 517–525, 2012.
- [135] J. Van Roy, N. Leemput, F. Geth, J. Buscher, R. Salenbien, and J. Driesen, "Electric Vehicle Charging in an Office Building Microgrid With Distributed Energy Resources," *IEEE Trans. Sustain. Energy*, vol. 5, pp. 1389–1396, oct 2014.

- [136] Y.-M. Wi, J.-U. Lee, and S.-K. Joo, "Electric vehicle charging method for smart homes/buildings with a photovoltaic system," *IEEE Trans. Consum. Electron.*, vol. 59, pp. 323–328, may 2013.
- [137] K. Nandha, P. H. Cheah, B. Sivaneasan, P. L. So, and D. Z. W. Wang, "Electric vehicle charging profile prediction for efficient energy management in buildings," *10th Int. Power Energy Conf. IPEC 2012*, pp. 480–485, 2012.
- [138] T. Wei, Q. Zhu, and M. Maasoumy, "Co-scheduling of HVAC control, EV charging and battery usage for building energy efficiency," *2014 IEEE/ACM Int. Conf. Comput. Des.*, pp. 191–196, 2014.
- [139] L. A. Hurtado, A. Syed, P. H. Nguyen, and W. L. Kling, "Multi-agent based electric vehicle charging method for smart grid-smart building energy management," *PowerTech*, 2015.
- [140] H. K. Nguyen and J. B. Song, "Optimal charging and discharging for multiple PHEVs with demand side management in vehicle-to-building," *J. Commun. Networks*, vol. 14, pp. 662–671, dec 2012.
- [141] C. M. Warren, "New working practice and office space density: a comparison of Australia and the UK," *Facilities*, vol. 21, pp. 306–314, dec 2003.
- [142] D. Locke, *Guide to the Wiring Regulations*. Chichester, UK: John Wiley & Sons, Ltd, jan 2008.
- [143] P. Gomm and I. Wengraf, "The Car and the Commute The journey to work in England and Wales," Tech. Rep. December, RAC Foundation, London, 2013.
- [144] Element Energy, "Pathways to high penetration of electric vehicles - Report prepared for Committee on Climate Change," tech. rep., Cambridge, 2013.
- [145] S. Ingram, S. Probert, and K. Jackson, "The impact of small scale embedded generation on the operating parameters of distribution networks," tech. rep., P B Power, 2003.
- [146] E. Xydias, C. Marmaras, and L. M. Cipcigan, "A multi-agent based scheduling algorithm for adaptive electric vehicles charging," *Applied Energy*, vol. 177, pp. 354–365, sep 2016.
- [147] International Energy Agency, "Energy Efficiency," 2016.
- [148] United Nations Environment Programme, "Why Buildings," 2016.

- [149] T. Weng and Y. Agarwal, "From Buildings to Smart Buildings—Sensing and Actuation to Improve Energy Efficiency," *IEEE Des. Test Comput.*, vol. 29, pp. 36–44, aug 2012.
- [150] J. Laustsen, "Energy efficiency Requirements in Building Codes, Energy Efficiency Policies for New Buildings," (Paris), 2008.
- [151] L. Pérez-Lombard, J. Ortiz, and C. Pout, "A review on buildings energy consumption information," *Energy Build.*, vol. 40, pp. 394–398, jan 2008.
- [152] D. Wijayasekara, O. Linda, M. Manic, and C. Rieger, "Mining Building Energy Management System Data Using Fuzzy Anomaly Detection and Linguistic Descriptions," *IEEE Trans. Ind. Informatics*, vol. 10, pp. 1829–1840, aug 2014.
- [153] National Institute of Standards And Technology, "Cyber-Physical Systems," 2016.
- [154] Pacific Northwest National Laboratory, "What is the VOLTTRON platform," 2016.
- [155] F. Kupzog, T. Sauter, and K. Pollhammer, "IT-Enabled Integration of Renewables: A Concept for the Smart Power Grid," *EURASIP J. Embed. Syst.*, vol. 2011, pp. 1–8, 2011.
- [156] National Institute of Standards And Technology, "Building Integration with Smart Grid Project," 2016.
- [157] K. Amarasinghe, D. Wijayasekara, and M. Manic, "Neural Network based downscaling of Building Energy Management System data," in *2014 IEEE 23rd Int. Symp. Ind. Electron.*, pp. 2670–2675, IEEE, jun 2014.
- [158] D. Wijayasekara and M. Manic, "Data-fusion for increasing temporal resolution of building energy management system data," in *IECON 2015 - 41st Annu. Conf. IEEE Ind. Electron. Soc.*, pp. 004550–004555, IEEE, nov 2015.
- [159] M. D. Symans and S. W. Kelly, "Fuzzy logic control of bridge structures using intelligent semi-active seismic isolation systems," *Earthquake Engineering and Structural Dynamics*, vol. 28, no. 1, pp. 37–60, 1999.
- [160] L. Zadeh, "Fuzzy sets," *Information and Control*, vol. 8, pp. 338–353, jun 1965.
- [161] W. Zheng and H. Xu, "Design and application of self-regulating fuzzy controller based on qualitative and quantitative variables," in *Fifth World Congress on Intelligent Control and Automation (IEEE Cat. No.04EX788)*, IEEE.

- [162] M. W. Ahmad, M. Mourshed, B. Yuce, and Y. Rezgui, "Computational intelligence techniques for HVAC systems: A review," *Building Simulation*, vol. 9, pp. 359–398, mar 2016.
- [163] U. JD Bagley, University of Michigan, "The behavior of adaptive systems which employ genetic and correlation algorithms," Tech. Rep. PhD Thesis, 1967.
- [164] J. H. Holland, *Adaptation in Natural and Artificial Systems: An Introductory Analysis with Applications to Biology, Control and Artificial Intelligence*. Cambridge, MA, USA: MIT Press, 1992.
- [165] T. Chow, G. Zhang, Z. Lin, and C. Song, "Global optimization of absorption chiller system by genetic algorithm and neural network," *Energy and Buildings*, vol. 34, pp. 103–109, jan 2002.
- [166] S. A. Kalogirou, "Artificial neural networks and genetic algorithms in energy applications in buildings," *Advances in Building Energy Research*, vol. 3, pp. 83–119, jan 2009.
- [167] P. Ferreira, A. Ruano, S. Silva, and E. Conceição, "Neural networks based predictive control for thermal comfort and energy savings in public buildings," *Energy Build.*, vol. 55, pp. 238–251, dec 2012.
- [168] M. Fardadi, A. Ghafari, and S. Hannani, "PID neural network control of SUT building energy management system," in *Proceedings, 2005 IEEE/ASME Int. Conf. Adv. Intell. Mechatronics.*, pp. 682–686, IEEE, 2005.
- [169] X. Li, C. P. Bowers, and T. Schnier, "Classification of Energy Consumption in Buildings With Outlier Detection," *IEEE Trans. Ind. Electron.*, vol. 57, pp. 3639–3644, nov 2010.
- [170] B. Yuce and Y. Rezgui, "An ANN-GA Semantic Rule-Based System to Reduce the Gap Between Predicted and Actual Energy Consumption in Buildings," *IEEE Trans. Autom. Sci. Eng.*, pp. 1–13, 2015.
- [171] W. Mai, C. Y. Chung, T. Wu, and H. Huang, "Electric load forecasting for large office building based on radial basis function neural network," in *2014 IEEE PES Gen. Meet. | Conf. Expo.*, pp. 1–5, IEEE, jul 2014.
- [172] L. Bu, D. Zhao, Y. Liu, and Q. Guan, "A hierarchical classification algorithm for evaluating energy consumption behaviors," in *2014 Int. Jt. Conf. Neural Networks*, pp. 1461–1466, IEEE, jul 2014.

- [173] M. W. Khan, M. A. Choudhry, and M. Zeeshan, "An efficient design of genetic algorithm based Adaptive Fuzzy Logic Controller for multivariable control of HVAC systems," in *2013 5th Comput. Sci. Electron. Eng. Conf.*, pp. 1–6, IEEE, sep 2013.
- [174] A. I. Dounis and C. Caraiscos, "Advanced control systems engineering for energy and comfort management in a building environment-A review," *Renew. Sustain. Energy Rev.*, vol. 13, no. 6-7, pp. 1246–1261, 2009.
- [175] X. Guan, Z. Xu, and Q.-S. Jia, "Energy-Efficient Buildings Facilitated by Microgrid," *IEEE Trans. Smart Grid*, vol. 1, pp. 243–252, dec 2010.
- [176] J. Li, Z. Wu, S. Zhou, H. Fu, and X.-P. Zhang, "Aggregator service for PV and battery energy storage systems of residential building," *CSEE J. Power Energy Syst.*, vol. 1, pp. 3–11, dec 2015.
- [177] S. X. Chen, H. B. Gooi, and M. Q. Wang, "Sizing of Energy Storage for Microgrids," *IEEE Trans. Smart Grid*, vol. 3, pp. 142–151, mar 2012.
- [178] N. Liu, Q. Chen, J. Liu, X. Lu, P. Li, J. Lei, and J. Zhang, "A Heuristic Operation Strategy for Commercial Building Microgrids Containing EVs and PV System," *IEEE Trans. Ind. Electron.*, vol. 62, pp. 2560–2570, apr 2015.
- [179] R. Bhimasingu and Y. Pavan Kumar, "Review and retrofitted architectures to form reliable smart microgrid networks for urban buildings," *IET Networks*, vol. 4, pp. 338–349, nov 2015.
- [180] M. Pipattanasomporn, M. Kuzlu, and S. Rahman, "An Algorithm for Intelligent Home Energy Management and Demand Response Analysis," *IEEE Trans. Smart Grid*, vol. 3, pp. 2166–2173, dec 2012.
- [181] L. Wang, Z. Wang, and R. Yang, "Intelligent Multiagent Control System for Energy and Comfort Management in Smart and Sustainable Buildings," *IEEE Trans. Smart Grid*, vol. 3, pp. 605–617, jun 2012.
- [182] Z. Wang and L. Wang, "Adaptive Negotiation Agent for Facilitating Bi-Directional Energy Trading Between Smart Building and Utility Grid," *IEEE Trans. Smart Grid*, vol. 4, pp. 702–710, jun 2013.
- [183] D. T. Nguyen and L. B. Le, "Optimal Bidding Strategy for Microgrids Considering Renewable Energy and Building Thermal Dynamics," *IEEE Trans. Smart Grid*, vol. 5, pp. 1608–1620, jul 2014.

- [184] "Communications requirements of smart grid technologies," 2010.
- [185] "Electricity settlement," 2017.
- [186] I. A. Sajjad, G. Chicco, and R. Napoli, "Definitions of demand flexibility for aggregate residential loads," *IEEE Transactions on Smart Grid*, vol. 7, pp. 2633–2643, nov 2016.
- [187] H. Kim and M. Parashar, "CometCloud: An Autonomic Cloud Engine," in *Cloud Comput.*, ch. 10, pp. 275–297, Hoboken, NJ, USA: John Wiley & Sons, Inc., jan 2011.
- [188] I. Momber, T. Gómez, and M. Rivier, "Regulatory Framework and Business Models Integrating EVs in Power Systems," in *Electr. Veh. Integr. into Mod. Power Networks*, pp. 251–271, New York, NY: Springer New York, 2013.
- [189] J.-P. Rodrigue, C. Comtois, and B. Slack, *The geography of transport systems*. Routledge, 2009.
- [190] C. Marmaras, M. Corsaro, E. Xydias, L. M. Cipcigan, and M. A. Pastorelli, "Vehicle-to-building control approach for EV charging," *Proc. Univ. Power Eng. Conf.*, 2014.
- [191] T. Arentze, T. Feng, H. Timmermans, and J. Robbroeks, "Context-dependent influence of road attributes and pricing policies on route choice behavior of truck drivers: results of a conjoint choice experiment," *Transportation (Amst.)*, vol. 39, pp. 1173–1188, nov 2012.
- [192] S. Raveau, J. C. Muñoz, and L. de Grange, "A topological route choice model for metro," *Transp. Res. Part A Policy Pract.*, vol. 45, pp. 138–147, feb 2011.
- [193] C. R. Bhat, "Work travel mode choice and number of non-work commute stops," *Transp. Res. Part B Methodol.*, vol. 31, pp. 41–54, feb 1997.
- [194] A. L. C. Bazzan and F. Klügl, "A review on agent-based technology for traffic and transportation," *Knowl. Eng. Rev.*, vol. 29, no. May, pp. 1–29, 2013.
- [195] M. Balmer, N. Cetin, K. Nagel, and B. Raney, "Towards truly agent-based traffic and mobility simulations," *Proc. Third Int. Jt. Conf. Auton. Agents Multiagent Syst.*, vol. 1, pp. 60–67, 2004.
- [196] A. Doniec, R. Mandiau, S. Piechowiak, and S. Espié, "A behavioral multi-agent model for road traffic simulation," *Eng. Appl. Artif. Intell.*, vol. 21, pp. 1443–1454, dec 2008.

- [197] M. Ghamami, A. Zockaie, and Y. M. Nie, "A general corridor model for designing plug-in electric vehicle charging infrastructure to support intercity travel," *Transp. Res. Part C Emerg. Technol.*, vol. 68, pp. 389–402, jul 2016.
- [198] S. Li, Y. Huang, and S. J. Mason, "A multi-period optimization model for the deployment of public electric vehicle charging stations on network," *Transp. Res. Part C Emerg. Technol.*, vol. 65, pp. 128–143, apr 2016.
- [199] F. He, Y. Yin, and J. Zhou, "Deploying public charging stations for electric vehicles on urban road networks," *Transp. Res. Part C Emerg. Technol.*, vol. 60, pp. 227–240, nov 2015.
- [200] S. Y. He, Y.-H. Kuo, and D. Wu, "Incorporating institutional and spatial factors in the selection of the optimal locations of public electric vehicle charging facilities: A case study of Beijing, China," *Transp. Res. Part C Emerg. Technol.*, vol. 67, pp. 131–148, jun 2016.
- [201] W. Tu, Q. Li, Z. Fang, S.-l. Shaw, B. Zhou, and X. Chang, "Optimizing the locations of electric taxi charging stations: A spatial-temporal demand coverage approach," *Transp. Res. Part C Emerg. Technol.*, vol. 65, pp. 172–189, apr 2016.
- [202] K. Coninx and T. Holvoet, "A Microscopic Traffic Simulation Platform for Coordinated Charging of Electric Vehicles," in *Adv. Pract. Appl. Heterog. Multi-Agent Syst. PAAMS Collect.*, pp. 323–326, 2014.
- [203] S. Bae and A. Kwasinski, "Spatial and temporal model of electric vehicle charging demand," *IEEE Trans. Smart Grid*, vol. 3, no. 1, pp. 394–403, 2012.
- [204] M. D. Galus, R. A. Waraich, F. Noembrini, K. Steurs, G. Georges, K. Boulouchos, K. W. Axhausen, and G. Andersson, "Integrating power systems, transport systems and vehicle technology for electric mobility impact assessment and efficient control," *IEEE Trans. Smart Grid*, vol. 3, no. 2, pp. 934–949, 2012.
- [205] P. Olivella-Rosell, R. Villafafila-Robles, A. Sumper, and J. Bergas-Jané, "Probabilistic agent-based model of electric vehicle charging demand to analyse the impact on distribution networks," *Energies*, vol. 8, no. 5, pp. 4160–4187, 2015.
- [206] J. Soares, B. Canizes, C. Lobo, Z. Vale, and H. Morais, "Electric vehicle scenario simulator tool for smart grid operators," *Energies*, vol. 5, no. 6, pp. 1881–1899, 2012.

- [207] F. Klügl, R. Herrler, and M. Fehler, "SeSAm: Implementation of Agent-Based Simulation Using Visual Programming," *Proc. fifth Int. Jt. Conf. Auton. agents multiagent Syst. - AAMAS '06*, p. 1439, 2006.
- [208] L. Imeers and S. Logghe, "Traffic Flow Theory (Faculty of engineering, Katholieke Universiteit Leuven)," 2002.
- [209] C. Fleischer, W. Waag, H.-M. Heyn, and D. U. Sauer, "On-line adaptive battery impedance parameter and state estimation considering physical principles in reduced order equivalent circuit battery models," *J. Power Sources*, vol. 260, pp. 276–291, aug 2014.
- [210] K. Sun and Q. Shu, "Overview of the types of battery models," in *Proc. 30th Chinese Control Conf.*, pp. 3644–3648, 2011.
- [211] C. M. Shepherd, "Design of Primary and Secondary Cells II: An Equation Describing Battery Discharge," *J. Electrochem. Soc.*, vol. 112, no. 7, pp. 657–664, 1965.
- [212] O. Tremblay and L. a. Dessaint, "Experimental validation of a battery dynamic model for EV applications," *World Electr. Veh. J.*, vol. 3, no. 1, pp. 1–10, 2009.
- [213] G. Berdichevsky, K. Kelty, J. Straubel, and E. Toomre, "The Tesla Roadster Battery System," tech. rep., 2007.
- [214] R. V. Haaren, "Assessment of Electric Cars ' Range Requirements and Usage Patterns based on Driving Behavior recorded in the National Household Travel Survey of 2009," Tech. Rep. 917, 2012.
- [215] TeslaMotors, "Tesla Roadster Features and Specifications."
- [216] Y. Yang, E. Yao, Z. Yang, and R. Zhang, "Modeling the charging and route choice behavior of BEV drivers," *Transportation Research Part C: Emerging Technologies*, vol. 65, pp. 190–204, apr 2016.
- [217] X.-H. Sun, T. Yamamoto, and T. Morikawa, "Fast-charging station choice behavior among battery electric vehicle users," *Transportation Research Part D: Transport and Environment*, vol. 46, pp. 26–39, jul 2016.
- [218] Rivier, Gomez, Cossent, and Momber, "New actors and business models for the integration of electric vehicles," Tech. Rep. Deliverable 5.1, Project MERGE, 2012.
- [219] R. Bi, J. Xiao, V. Viswanathan, and A. Knoll, "Influence of charging behaviour given charging station placement at existing petrol stations and residential car

- park locations in singapore," *Procedia Computer Science*, vol. 80, pp. 335–344, 2016.
- [220] C. Y. Lee, "An algorithm for path connections and its applications," *IEEE Transactions on Electronic Computers*, vol. EC-10, pp. 346–365, sep 1961.
- [221] E. W. Dijkstra, "A note on two problems in connexion with graphs," *Numerische Mathematik*, vol. 1, pp. 269–271, dec 1959.
- [222] V. T. N. Nha, S. Djahel, and J. Murphy, "A comparative study of vehicles' routing algorithms for route planning in smart cities," in *2012 First International Workshop on Vehicular Traffic Management for Smart Cities (VTM)*, IEEE, nov 2012.
- [223] D. Papadaskalopoulos, G. Strbac, P. Mancarella, M. Aunedi, and V. Stanojevic, "Decentralized participation of flexible demand in electricity markets part ii: Application with electric vehicles and heat pump systems," *IEEE Transactions on Power Systems*, vol. 28, pp. 3667–3674, nov 2013.

